

REAR-FACING CHILD SAFETY SEAT PERFORMANCE IN FRONTAL NCAP LEVEL CRASHES

Gary R. Whitman, Arlie V. Hart, III, Larry Sicher, Brian Benda, Louis A. D'Aulerio
ARCCA, Inc
United States
Paper Number 13-0010

ABSTRACT

Objective

To study the performance of Rear-Facing Child Safety Seats (RFCSS) when installed in the center-rear occupant position of vehicles involved in New Car Assessment Program (NCAP) severity level frontal crashes, the authors conducted a series of simulated frontal crash tests using a horizontal accelerator.

Method

The authors conducted two series of simulated frontal crash tests using a horizontal accelerator (sled facility) to assess RFCSSs of different designs. The first used a free-standing bench seat, the second used a sled buck constructed from a small domestic SUV. The tests included infant-only (with and without a base) and convertible CSSs, untethered and tethered.

Results and Data Sources

Without a tether, the RFCSSs experienced severe forward translation and forward and downward rotation. This kinematic resulted in the RFCSSs impacting the front-center console, and the infant dummy experiencing very high head accelerations and Head Injury Criteria (HIC) values, indicating a high risk of serious head injury. The use of a tether, with one end attached to the top portion of the CSS's seat back and the other attached to structure behind the CSS's occupant position, resulted in a significant reduction of the forward and downward rotation of the RFCSS. This prevented impact with the front seats and center console, and resulted in a significant reduction in peak head acceleration and HIC values.

Discussion and Limitations

RFCSSs are very effective in providing crash protection to young children in frontal crashes. Particularly in Europe and Australia, where RFCSS are often prevented from rotating by various devices, including: tethers, floor supports, rigid attachment, and/or by positioning the RFCSS against the vehicle's interior. Without these devices, RFCSS can rotate forward and downward significantly during a

frontal crash. The amount of rotation depends upon the quality of the RFCSS installation and the geometry of the vehicle interior. The rotation and translation of the RFCSS may result in it impacting the vehicle interior, and/or allow the infant to slide up the RFCSS seat back, increasing the potential for head impact. The Federal Motor Vehicle Safety Standard 213 requires that RFCSSs limit their seat back rotation to 70 degrees from vertical when tested in a 48 kph (30 mph) delta-V simulated frontal crash. Real-world crashes are often more severe. This is why adult restraint systems are assessed in the NCAP frontal crash testing at a delta-V of 56 kph (35 mph). The National Highway Traffic and Safety Administration currently includes CSSs in the rear outboard occupant positions of vehicles tested in the NCAP. However, the public is often advised to install CSSs in the center-rear occupant position where head impact risks are different than at the outboard positions.

This study was limited to frontal crashes. Additional testing in other crash directions is needed to identify the potential benefits of anti-rotation devices in those crash scenarios.

Conclusions/Relevance

The use of anti-rotation devices with RFCSSs significantly increases the crash protection provided infants during frontal crashes.

BACKGROUND

Field experience and testing has demonstrated that the best crash protection for infants and young children is provided by rear-facing child safety seats (RFCSS).[1,2,3,4,5,6] This is particularly true in frontal collisions. Frontal collisions are the most frequent type of crash and typically result in the highest delta-Vs and peak accelerations. A primary advantage of the RFCSS in frontal crashes is that the seatback is the main restraint structure for the child. The RFCSS seat back widely distributes the restraining load to the head and torso of the child, and prevents significant movement of the head relative to the torso, thereby minimizing neck loads. CSS manufacturers in the U.S., NHTSA, and other organizations dedicated to child passenger safety, recommend RFCSSs be installed at angles ranging

from 30° to 45° from the vertical. RFCSSs frequently incorporate indicators to show the installer what the manufacturer's recommended installation angle is. Due to the RFCSS seat back's inclined plane, as the child loads the CSS' seat back during a frontal crash, a forward and downward force is applied to the seat back. When the CSS is only secured to the vehicle by the lap belt portion of the seat belt or the lower LATCH (Lower Anchors and Tether for Children) strap, as is the case with the majority of RFCSS in the U.S., the force applied will cause the CSS to rotate forward and downward about the lap belt, compressing into the vehicle seat bottom cushion. This movement increases the potential for the CSS and child's head to impact objects forward of their occupant position, and for the infant to slide up the RFCSS seat back, thus exposing the infant's head to potential impact and the neck to increased loading. Typically, the objects impacted are the front seats and the front center console. These kinematics were observed during Transport Canada frontal crash testing reported by Tylko.[7] To counter this hazard, European and Australian RFCSS incorporate several different means to limit their forward and downward rotation. [8] One approach is the Australian-type tether design. This tether design attaches to the RFCSS at the head end and wraps around the RFCSS toward the rear of the vehicle, over the vehicle seat back, and attaches to the vehicle behind the RFCSS occupant position (Figure 1). During a frontal crash, the tether minimizes forward and downward rotation. Frontal crash sled testing conducted by the University of Michigan Transportation Research Institute indicated that the Australian-type tether reduced RFCSS forward displacement, head and chest acceleration, and neck loading during frontal crash testing. [9] Another method used in Europe to limit RFCSS forward and downward rotation is the leg support. The leg support attaches to the head end of the RFCSS and extends down to the floor of the vehicle (see Figure 2). During a frontal crash, the leg support prevents forward and downward rotation of the RFCSS. Other European RFCSS are positioned more forward on the vehicle's seat so that they are supported by the back of the front seat. In a frontal crash, the back of the front seat prevents forward and downward rotation. In the U.S., a RFCSS must limit the rotation of its seat back to no more than 70 degrees from vertical during the 48 kph (30 mph) delta-V simulated frontal crash sled test required by FMVSS 213. It must do so while only secured by the vehicle's lap belt or lower LATCH strap. While FMVSS 213 does not permit the use of tethers or leg supports to comply with its requirements, it does not prevent manufacturers from providing these devices

as supplements to the lap belt or lower LATCH strap attachment.



Figure 1. RFCSS w/Australian Tether.



Figure 2. RFCSS w/Foot Support.

A real-world crash investigated by the authors involved an infant restrained in an infant only CSS, secured rear facing in the rear center occupant position of a small sport utility vehicle (SUV). The front of the SUV impacted the side of a mid-size pickup truck. The crash resulted in a delta-V of 53-64 kph (33-40 mph). During the crash, the infant sustained a severe head injury. The testing reported in this paper was conducted with a sled buck based on the SUV. The testing confirmed that the infant's injury resulted from impact of the RFCSS and the infant's head directly with the center console between the front seats, and that the injurious impact would have been prevented had the infant been restrained in a tethered RFCSS. Similar testing was also conducted using the freestanding seat specified in FMVSS 213 to compare the performance of the infant seat when installed in an actual vehicle to its performance when installed in the FMVSS 213 seat fixture.

APPROACH

Two series of simulated frontal crash testing were conducted on a horizontal accelerator (sled tests). The first series was conducted using the freestanding FMVSS 213 bench seat fixture (Figure 3), while the second series used a vehicle buck constructed from a small domestic SUV. (Figure 4). The sled pulse used in both test series was based on the NCAP test accelerations measured at the left and right rear cross-member in two tests of the SUV. [10, 11] The resulting pulse produced a delta-V of approximately 66-68 kph (41-42 mph), with a peak acceleration of 45-47 g, and pulse duration of 100 ms (Figure 5).



Figure 3. FMVSS 213 Seat Fixture.



Figure 4. Small SUV Sled Buck.

Three different RFCSSs were selected for testing in both test series—two rear-facing-only (RFO) CSSs, and one rear-facing convertible CSS. The RFO CSSs could be installed with and without an installation base. Table 1 provides a description of each CSS tested. All CSSs tested incorporated energy-attenuating expanded polystyrene foam lining the interior surfaces of the side wings and seat back.

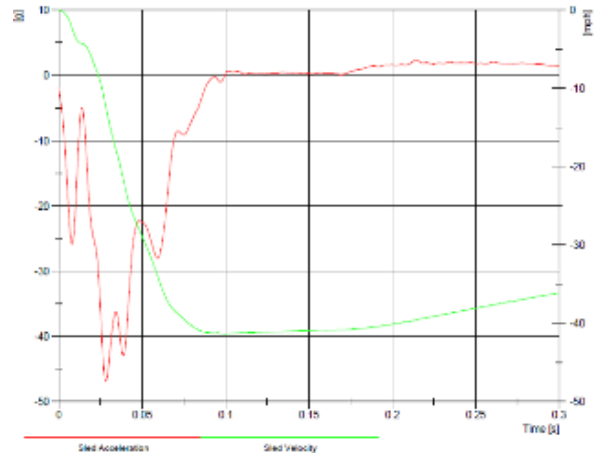


Figure 5. Sled Test Pulse from Series 1, Test 1.

Table 1.
Rear-Facing CSS Tested

CSS A	Infant only CSS, no tether available
CSS B	Infant only CSS, tether compatible
CSS C	Convertible CSS, tether compatible

All tests were conducted with a CRABI 12-month Anthropometric Test Device (ATD) instrumented with tri-axial head and chest accelerometers and upper neck load cells. The ATD was secured in each CSS in accordance with manufacturer's instructions. Each CSS was secured to the vehicle seat in accordance with the CSS instructions. High-speed video cameras were mounted overhead and on each side of the test fixture to record the kinematics of the CSS and ATD. Sled acceleration was measured and recorded.

Test Series 1

In the Test Series 1, the RFCSSs were secured to the FMVSS 213 seat fixture using the LATCH lower anchors, except for Test 1-1, which was secured using a lap belt as that RFCSS configuration was not compatible with LATCH. Table 2 provides the matrix for Test Series 1.

Table 2.
Test Series 1 Matrix

Test No.	Test Unit	Base Used	Tethered	Initial Seat Back Angle (degrees from vertical)
1-1	CSS A	No	No	42
1-2	CSS A	Yes	No	42
1-3	CSS B	Yes	Yes	46
1-4	CSS B	Yes	Yes	45
1-5	CSS C	N/A	Yes	35
1-6	CSS B	Yes	Yes	35

Test Series 2

In Test Series 2, the RFCSS were secured in the center rear occupant position of the SUV sled buck using the vehicle lap-belt-only available at that occupant position. Table 3 provides the matrix for Test Series 2.

Table 3.
Test Series 2 Matrix

Test No.	Test Unit	Base Used	Tethered	Initial Seat Back Angle (degrees from vertical)
2-1	CSS A	Yes	No	42
2-2	CSS B	Yes	Yes	40
2-3	CSS C	N/A	Yes	35

TEST RESULTS

Appendix A provides a summary of all instrumentation data from Test Series 1 and 2.

Test Series 1

Test 1-1. During Test 1-1, CSS A, an RFO CSS installed without its base and untethered slid forward on the test fixture seat and rotated downward until the CSS was almost entirely beyond the front edge of the seat. The CSS also rotated downward to the point that the CSS seat back was nearly horizontal (Figure 6a). The foot-end of the CSS deformed inward severely due to loading by the lap belt (Figure 6b). The HIC15 was 333.



Figure 6a. Test 1-1 Side View.



Figure 6b. Test 1-1 Overhead View.

Figure 6. Test 1-1 Maximum Excursion.

Test 1-2. During Test 1-2, CSS A, an RFO CSS installed with its base, slid forward significantly, but less than in Test 1-1 (Figure 7a). However, the downward rotation of the CSS was greater than that observed in Test 1-1, such that the seat back rotated beyond horizontal (Figure 7b). The HIC15 was 528.



Figure 7a. Test 1-2 Side View.



Figure 7b. Test 1-2 Side View.

Figure 7. Test 1-2 Maximum Excursion.

Test 1-3. During Test 1-3, CSS B, an RFO installed with its base and tethered performed well in spite of deformation to the structure to which the tether was secured, and compression of the top of the test seat's seat back cushion by the tether. The CSS remained entirely on the test fixture's seat bottom, and the seat back rotation was significantly reduced compared to Tests 1-1 and 1-2 (Figure 8). The infant dummy's head, however, still displaced to the top edge of the CSS's seat back. Had the tether anchorage structure not deformed and the vehicle's seat back been configured to be more representative of real-world seats, it is expected that the CSS rotation would have been further reduced, with corresponding reduction in head displacement as well. The HIC15 was 931.



Figure 8a. Test 1-3 Side View.



Figure 8b. Top View.

Figure 8. Test 1-3 Maximum Excursion.

Test 1-4. During Test 1-4, CSS B, an RFO CSS installed with its base and tethered, performed very well in regards to kinematics. The structure to which the tether was secured did not deform. The CSS did not displace significantly forward or rotate downward (Figure 9). Post test, it was determined that several of the ATD's neck data channels failed and consequently the data set is missing some values. The HIC15 was 589.



Figure 9a. Test 1-4 Side View.



Figure 9a. Test 1-4 Top View.

Figure 9. Test 1-4 Maximum Excursion.

Test 1-5. During Test 1-5, CSS C, a rear-facing convertible CSS, performed very well in regards to kinematics. The CSS remained entirely on the test fixture's seat bottom and the CSS did not rotate significantly forward or downward (Figure 10). The HIC15 was 872.



Figure 10a. Test 1-5 Side View.



Figure 10b. Top View.

Figure 10. Test 1-5 Maximum Excursion.

Test 1-6. During Test 1-6, the same model CSS B tested in Test 1-4 was used. During this test, the tether strap failed after being used in two previous tests. As a result, the CSS slid forward and experienced greater downward and forward rotation than during Test 1-4, demonstrating the improved performance provided by an intact tether (Figure 11).



Figure 11a. Side View.



Figure 11b. Top View.

Figure 11. Test 1-6 Maximum Excursion.

The change in the infant seat's seat back angle during the test is provided in Table 4. The instrumentation data is provided in Appendix A.

**Table 4.
Test Series 1 Test Data**

Test No.	Test Unit	Maximum Change in CSS Seat Back Angle (degrees)
1-1	CSS A	27
1-2	CSS A	42
1-3	CSS B (1)	17
1-4	CSS B	1
1-5	CSS C	0
1-6	CSS B (3)	33

(1) Tether anchor deformed forward (2) Neck load cell data acquisition system malfunctioned (3) Tether strap failed

Test Series 2

Test 2-1 During Test 2-1, CSS A, an RFO CSS with its base and untethered was tested. It displaced forward, partially off the front edge of the vehicle seat bottom and rotated downward and forward (Figure 12). The resulting HIC15 was 1653.4. The Neck Tension/Extension Nij was 2.42.



[Note: Top View Camera Malfunctioned.]

Figure 12. Test 2-1 Maximum Excursion.

Test 2-2 During Test 2-2, CSS B, an RFO CSS with base and tethered, performed significantly better in regards to kinematics than CSS A in Test 2-1. CSS B did not displace forward or rotate significantly (Figure 13). There was no impact between the carrier and the front center console. The infant dummy's head did, however, slide above the top of the CSS's seat back. The HIC15 was 970.5. The Neck Tension/Extension Nij was 3.06.



Figure 13a. Test 2-2 Side View.



Figure 13b. Top View.

Figure 13. Test 2-2 Maximum Excursion.

Test 2-3 During Test 2-3, CSS C, a rear-facing convertible CSS with tether, performed very well compared to test 2-1 and 2-2. The bottom of CSS C displaced forward but remained on the vehicle seat bottom, and the CSS did not rotate forward or downward (Figure 14). Due to the forward displacement of the CSS's bottom while the top was tethered, the seat back angle actually became 7 degrees more upright. The HIC15 during the test was 786 and the Neck Tension/Extension Nij was 1.15.



Figure 14a. Test 2-3 Side View.



Figure 14b. Test 2-3 Top View.

Figure 14. Test 2-3 Maximum Excursion.

Test data from Test Series 2 is provided in Table V. Instrumentation data is provided in Appendix A.

Table 5.
Test Series 1 Test Data

Test No.	Test Unit	Maximum Change in CSS Seat Back Angle (degrees)
2-1	CSS A	13
2-2	CSS B	4
2-3	CSS C	-7

DISCUSSION

Kinematics

CSS A

Dummy head displacement was greatest with CSS A. When used without its base, the loading applied by the securing lap belt at the foot-end of the CSS caused the side walls of the CSS to deform inward. This deformation shortened the distance between the two lap belt hooks on the CSS. The shortened distance reduced the length of the lap belt path, creating excess lap belt length. The excess lap belt allowed the CSS to displace forward, sliding nearly off the front edge of the seat. When secured with its base, the belt path was not as severely altered, therefore the forward displacement was less. Due to its lack of tether, however, this CSS rotated severely forward and downward when tested, both with and without its base. In Test Series 2, similar extreme rotation resulted in this CSS impacting the center front console with its head end, and resulted in a very high HIC (1653) and Nij (2.42) values. Similar results were observed during frontal crash testing conducted by Transport Canada, in which untethered rear-facing CSSs were secured in the second row center occupant position.[12] Tytko reported that “Contact with the center console was observed in small and large vehicles and at crash speeds as low as 40 km/h. In all cases, forward excursion of the infant seat was great enough to cause a significant portion of the infant restraint to slide off the front edge of the vehicle seat.”

CSS B

CSS B was very effective in controlling the kinematics of the seat and dummy. Even when the tether was compromised, rotation of this CSS was significantly reduced. When the tether remained intact, there was virtually no rotation of this CSS (1 and 4 degrees). The top of the dummy’s head moved up to the top of the CSS seat back, but even when tested in a vehicle, this motion did not result in the dummy’s head striking anything.

CSS C

The kinematics with CSS C, the tethered rear-facing convertible CSS, were the best overall. There was essentially no forward or downward rotation of the head portion of the CSS in either of the test series. In Test Series 2, the CSS seat back angle actually became more upright due to some forward displacement of the bottom while the top was restrained by the tether. The forward displacement of the CSS bottom was due to approximately 30.5 mm (1.25”) of slippage of the securing vehicle lap belt through its locking latchplate. This slippage was likely due to a compatibility problem between the CSS and the vehicle, as the geometry of the two resulted in an angle between the LATCH strap and its adjuster that compromised the performance of the locking latchplate. The dummy’s head remained well below the top of the CSS seat back and was well-supported. Similar frontal crash sled testing of rear-facing CSS conducted by Sherwood, et al., did not reveal a significant kinematic difference between Australian tethered and untethered RFCSS. [13] That testing was conducted at approximately the FMVSS 213 frontal crash pulse, with a delta-V of 49 kph (30 mph), peak acceleration of 23 G, and a duration of 85 msec, and did not include any infant-only CSSs. The lower severity of the Sherwood tests and the lack of infant-only CSSs likely accounts for the smaller difference between tethered and untethered configurations.

Head Acceleration and HIC15

All but two tests exceeded the HIC15 limit of 390 used in FMVSS 208 for the 12 month CRABI. One CSS that did not exceed the 390 value was CSS A in Test 1-1, which reported a HIC15 of 333, but that CSS nearly slid off the front edge of the vehicle seat. The excessive forward displacement and forward and downward rotation of the CSS extended the time and distance over which the infant dummy’s head was accelerated. This reduced the loading of the head into the CSS’s seat back, likely resulting in the lower HIC15, and there was no structure forward of the CSS for the exposed head to strike. However, this CSS showed very dangerous kinematics. The other CSS that did not exceed the 390 HIC15 value was CSS B, when its tether failed in Test 1-6. The tether failure allowed more forward and downward rotation, which likely also reduced the extent to which the dummy head loaded the CSS seat back. An unlimited HIC level of 1000 was exceeded in four tests, those being Test 1-3 with CSS B during Test Series 1, and all of the tests in Series 2. Only CSS A exceeded an unlimited HIC of 2000. This occurred during Test 2-

1, where the HIC15 was 1653. These extremely high HIC values were caused by the forward displacement and forward and downward rotation of the CSS, causing the head-end of the CSS to impact the center console. All other tests resulted in HIC15 values between 390 and 1000.

Similarly high head accelerations were observed in frontal crash testing by Transport Canada.[14] Tylko reported that “Elevated dummy head accelerations were observed in 10 of the 24 tests conducted with the infant seat installed in the center seating position of the second row (location 15). The elevated head accelerations were the result of interaction between the back of the infant seat and the center console...”

Frontal crash sled testing conducted by Abdelilah et al.,[15] at 48 kph (30 mph) delta-V and with RFCSS rigidly supported to prevent any forward displacement or forward and downward rotation, and with the dummy’s head positioned against the CSS seat back, revealed that, under those conditions, the RFCSS sufficiently limited HIC without the need for energy attenuating foam.[16] In those tests, however, there was no opportunity for the CSS to impact the vehicle’s interior. The testing reported by Tylko and in this paper clearly demonstrate that, in more severe frontal crashes where there is contact with the vehicle’s interior, dangerously high HIC values occur. It must be noted that in actual use, children and infants may also not always position the head against the seat back. As such, any gap between the CSS seat back and the child’s head would result in the child’s head developing a relative velocity to the CSS seat back during a frontal crash. As a result, when the head impacts the seat, the head accelerations experienced will be amplified, causing higher head acceleration and HIC values. Limiting RFCSS movement through the use of an Australian tether or leg support during a frontal crash will eliminate impacts with the vehicle interior, but these tests also show the need for energy attenuation in higher crash severities due to the potential of a gap between the child’s head and CSS seat back.

Neck Loads

In spite of very little visually discernable neck extension, the tension/extension Nij threshold values used in FMVSS 208 for the 12 month CRABI ATD were exceeded in all of the tests conducted in both test series. Four tests exceeded an Nij of 2. These four tests were with the CSS A and B, the infant-only CSSs. These CSSs have significantly lower seat back heights and their seat backs are more flexible toward the top when compared to convertible CSSs. CSS C, the convertible CSS, had the lowest Nij values. This

is likely because of its more effective seat back, due to its greater height and rigidity, combined with its effective tether. The tether prevented the CSS from tipping, which prevents the cervical spine from aligning with the crash pulse vector, and the more rigid seat back provides more effective support to the head and torso, thus minimizing the amount of neck extension. Even with CSS C, however, the neck tension/extension Nij values exceeded the FMVSS 208 threshold in both test series, with an Nij of 1.89 in Test Series 1 and Nij of 1.15 in Test Series 2. At the present time, Nij requirements have not been incorporated into FMVSS 213. According to the National Highway Traffic Safety Administration (NHTSA), one of the reasons is that the use of Nij appears to over predict the likelihood of neck injuries. Investigations of real world frontal crashes show that neck injury to children restrained in CSSs is rare when head impact is not involved.[17] Sherwood, et al., found similar test results during their testing of rear-facing CSS at 48 kph (30 mph), approximately the same as the FMVSS 213 frontal crash pulse.[18] The authors concluded that, “The high values are due to the fact that the dummy neck is likely stiffer than the child and has no range of free motion on either side of the neutral position (Crandall et al., 1999; Janssen et al., 1991). In a child, it would be expected that the minimal changes in kinematics which occur while the head and thorax are supported by the child restraint would result in negligible increase in neck joint stiffness. In the dummy, even small changes result in rapidly increasing stiffness values.”[19] The NASS CDS database, created and maintained by NHTSA, was queried for real-world cases involving infants (0-1 year) in rear-facing CSS, exposed to frontal crashes of 48 kph (30 mph) delta-V or greater. Twenty-eight such cases were identified. None of the infants in these crashes sustained a cervical injury. This suggests that the high Nij values measured in the subject tests over predict the risk of neck injury and should only be used for comparative analyses. Previous epidemiology studies have found that neck injuries to infants in frontal crashes are extremely rare, and that head impact injuries are by far the most frequent mechanism of serious injuries.[20,21,22] Therefore, minimizing head excursion and the associated potential for head impact should be the top priority for rear-facing CSSs, as it is for all CSSs. Fortunately, as demonstrated by the subject testing involving CSS C, the rear-facing CSS that best minimized head excursion and the potential for head impact also resulted in the lowest risk of neck injury.

The American Academy of Pediatrics now recommends children traveling in motor vehicles

remain in a rear-facing CSS until at least two years of age and as long as possible.[23] This is resulting in heavier and taller children traveling in RFCSS. In a crash, the larger child will apply a greater inertial load to the CSS and the load will be applied higher due the child's higher center of gravity. This will result in greater forward translation and greater forward and downward rotation of the CSS. The taller seat height also increases the risk of head impact and neck injury. To counter these factors, Australian tethers, support legs, or other equally effective technologies, should be used to minimize RFCSS forward translation and forward and downward rotation.

Out of concern for the frequently high head accelerations observed during frontal crashes with RFCSS positioned in the second row center position and a center console forward of that position, Tytko recommended that parents and caregivers "...avoid installing rear facing infant seats in the center second row if the vehicle is equipped with a center front console." [24] The authors of this paper agree with her concern, but there are other risks that must also be considered. Such a practice would position children in outboard occupant positions where they are at greater risk of injury from vehicle intrusion during side impacts. Side impacts are known to be a leading cause of serious injury, especially to outboard occupants seated adjacent to the impact, due to the risks created by intrusion and occupant impact with the vehicle's side interior. Therefore, we recommend that parents and caregivers position their infants and young children rear-facing in the second row center occupant position whenever possible and use a RFCSS equipped with an Australian type tether or leg support. RFCSS with Australian type tethers are currently available in the U.S. from several manufacturers, and U.S. motor vehicles have been equipped with ready-to-use tether anchorages since the early 2000s. We urge other CSS manufacturers to incorporate Australian tethers or leg supports into their RFCSS as soon as possible, and also recommend that NHTSA implement a more limited RFCSS rotation requirement into FMVSS 213 to further stimulate their adoption.

Chest Acceleration

The peak chest acceleration sustained over a 3 msec duration exceeded the FMVSS 213 limit of 60 G in all the testing conducted. Chest acceleration was consistently greater with those CSSs that best limited head and torso displacement. This is likely because the chest is decelerated over a shorter distance and time duration due to the reduced CSS displacement

and rotation. Real world data from Australia, where all rear-facing CSS are tethered, does not indicate a greater frequency of chest injury. Therefore, limiting CSS forward displacement and rotation does not appear to introduce a significant chest injury risk.

Real-world crash Investigation

One of the stimuli for the research testing discussed in this paper was the investigation of a real-world crash conducted by the authors. The crash involved a small domestic SUV that impacted the passenger side of a full-size pickup truck (Figure 15). A 5-month-old, 9 kg (20 lbs), 68 cm (26.8 inches) infant was restrained in the same make and model CSS as CSS A, and located in the center rear occupant position of the Ford Escape at the time of the crash. The infant carrier was secured to the vehicle using the lower LATCH strap (Figure 16). There was no intrusion into the center rear occupant position of the SUV (Figure 17).



Figure 15. Ford Escape Post Crash.

During the crash, the head end of the CSS impacted with the front center console and the child sustained severe brain injuries, including:

- an extensive post-traumatic subarachnoid hemorrhage,
- intra-ventricular hemorrhage,
- a severe brainstem injury including approximately $\frac{3}{4}$ of the pons,
- bilateral femur fractures

An accident reconstruction analysis determined that the Delta-V for the SUV was 53-64 kph (33-40 mph), with peak acceleration levels comparable to the NCAP level testing for that vehicle. The PDOF of the crash was slightly to the left of center, at -10 to -20 degrees.



Figure 16. Exemplar CSS A Installed In Center Rear of an exemplar SUV.



Figure 17. Center rear occupant position of Ford Escape.

The testing conducted during Test Series 1 and 2 identified the mechanism of the child’s head injuries as impact of the head end of the infant seat with the front center console, and the resulting accelerations applied to the infant’s head. Test Series 1 and 2 also determined that had the infant been restrained by a RFCSS with an Australian type tether that the injury mechanism would have been eliminated.

NHTSA conducted NCAP testing on the same model SUV as represented in Test Series 2, with the same model CSS in the right rear occupant position as CSS A, with a 12 month CRABI ATD installed.[25] The kinematics of the CSS were substantially similar to those observed in Test 2-1, except that since there was no console forward of the right rear occupant position, and the right front seat back rotated forward, the infant safety seat did not impact any object during the test. As a result, the HIC36 measured was 907, less than half the 2031 HIC36

measured during Test 2-1. Comparison of the infant safety seats’ maximum forward excursion during Test 2-1 and the SUV NCAP test are provided in Figure 18 and 19. This comparison demonstrates that without effective limitation of forward and downward rotation of rear-facing CSSs, the same frontal crash, with the same CSS, in the same row, without intrusion into the occupant space, can result in much different risks of head injury simply by using a different occupant position.



Figure 18. Test 2-1 Maximum forward excursion.



Figure 19. Ford Escape maximum forward excursion.

Leg Support for Rear-Facing Child Safety Seats

In Europe, motor vehicles are assessed for occupant crash protection in a program referred to as the Euro-NCAP. One test conducted as part of that program is an offset frontal impact into a deformable barrier at 64 kph (40 mph).[26] As part of that test, a forward-facing and a rear-facing CSS, recommended by the vehicle manufacturer, are installed in the outboard occupant positions and their dynamic performance is assessed. An 18-month infant dummy is secured in the rear-facing CSS. Review of European frontal crash NCAP testing with a RFCSS incorporating a leg support indicates that a leg

support is very effective in limiting forward displacement and forward and downward rotation of the RFCSS. Frontal crash sled testing conducted by Sherwood indicates that a leg support provides increased frontal crash protection to children in RFCSS by limiting forward displacement and forward and downward rotation and maximizing crash ride down.[27]

CONCLUSIONS

The testing and crash investigation reported in this paper indicate that, in order to optimize the crash protection of children exposed to frontal crashes while restrained in a RFCSS, the RFCSS's tendency to displace forward and rotate forward and downward must be limited. This testing also indicates that an Australian type tether significantly improves the performance of RFCSS in NCAP-level frontal crashes by limiting the forward displacement and forward and downward rotation that can result in severe head impact and neck loading. Prior research and Euro-NCAP testing indicates that a foot support also effectively limits forward displacement and forward and downward rotation, and maximizes crash ride down. The use of the Australian type tether or a leg support with a RFCSS increases the effectiveness of RFCSS and reduces the potential for serious injuries and fatalities. These features also compensate for installation errors and vehicle compatibility problems, such as a loosely secured lap belt or lower LATCH strap, and vehicle buckle/latchplate incompatibility with the CSS belt path. Because head impact is the leading mechanism of serious injury, priority should be given to minimizing head impacts. This can be accomplished by the use of the Australian type tether or a leg support.

FMVSS 213 permits the seat back of an infant seat to rotate up to 70 degrees from vertical. In an actual motor vehicle, this degree of rotation will often result in the head end of the infant seat impacting a seat or center console forward of the RFCSS, as occurred in Test 2-1 and during the real-world crash discussed earlier. In the late 1990s, NHTSA realized that an 813 mm (32") head excursion limit requirement for forward-facing child safety seats was inadequate to ensure that children in such CSS would not strike their head in real-world crashes due to the limited clearance in motor vehicles. NHTSA, therefore, implemented a new a 721 mm (28") head excursion limit requirement and permitted the use of a tether in order to comply. The authors strongly recommend an analogous requirement for rear-facing CSS to further limit RFCSS rotation, and to allow the use of tethers

or leg supports to comply with this additional requirement.

The findings of this study also indicate that infants are better protected when the head is well below the top of the CSS seat back. The authors recommend that, once infants properly fit a convertible CSS with its higher seat back than an infant only CSS and can maintain their head up under the more upright orientation of the convertible CSS, those infants should be transitioned to a rear-facing convertible CSS, so that they can be afforded the protective benefits of the higher seat back, more upright orientation, and likely larger side wings.

LIMITATIONS

The limited neck biofidelity of the CRABI 12 month ATD, combined with the limited knowledge pertaining to child neck injury tolerance, limits the use of the neck load data to comparisons only.

The testing conducted did not include RFCSS incorporating leg supports, and limited resources constrained the number of tests conducted in this study. Additional tests of both untethered, tethered, and leg supported rear-facing CSS is recommended to further study their performance during NCAP level frontal crash conditions.

ACKNOWLEDGMENTS

The authors would like to thank Mr. Dennis Cathy and Mr. David Sleppy for their funding and support of this research.

-
- [1] Weber, K. (2000). "Crash Protection for Child Passengers." UMTRI Research Review **31**(3)..
 - [2] Kamren, B., et al., (1993) The Protective Effects of Rearward Facing CRS: An Overview of Possibilities and Problems Associated with Child Restraints for Children Aged 0- 3 Years, (SAE 933093)
 - [3] Carlsson, G. et al., "Rearward-Facing Child Seats – The Safest Car Restraint for Children?" *Accident Analysis & Prevention* Vol. 23 1991
 - [4] Isaksson, I. et al., "Trends and Effects of Child Restraint Systems Based on Volvo's Swedish Accident Database" SAE 973299
 - [5] Henary, B., et al., "Car Safety Seats for Children: Rear Facing for Best Protection" *Injury Prevention* 2007;13:398-402, doi:

-
- 10.1136/ip.2006.015115, 28 August 2007
- [6] Jakobsson, L., et al., "Safety for the Growing Child – Experiences from Swedish Accident Data" 19th International Technical Conference on the Enhanced Safety of Vehicles, Paper Number 05-0330, June 2005
- [7] Tylko S., Transport Canada "Interactions of Rear-Facing Child Restraints with the Vehicle Interior during Frontal Crash Tests" 22nd International Technical Conference on the Enhanced Safety of Vehicles, Washington, DC, June 13-16, 2011, Paper Number 11-0406
- [8] Australian/New Zealand Standard ASNZS 1754:2004 Child Restraints Systems for use in Motor Vehicles
- [9] Manary M. A., et al. "The Effects of Tethering Rear-Facing Child Restraint Systems on ATD Responses" 50th Annual Proceedings Association for the Advancement of Automotive Medicine, October 16-18, 2006
- [10] New Car Assessment Program, Frontal Barrier Impact Test, Report Number NCAP-MGA-2001-016, March 16, 2001
- [11] New Car Assessment Program, Frontal Barrier Impact Test, Report Number 5FEM-MGA-2001-026, April 20, 2001
- [12] Tylko S., op cit. (2011)
- [13] Sherwood, et al., op cit. (2004)
- [14] Tylko S., op cit. (2011)
- [15] Abdelilah, Y., "The Effects of Head Padding in Rear Facing Child Restraints" SAE 2005-01-1839
- [16] Abdelilah, Y., op cit (2005)
- [17] Department of Transportation, NHTSA, 49 CFR Part 571 [Docket No. NHTSA-03015351] Federal Motor Vehicle Safety Standards; Child Restraint Systems Final Rule, Federal Register/Vol 68, No. 121, June, 24, 2003
- [18] Sherwood, et al., "The Performance of Various Rear Facing Child Restraint Systems in a Frontal Crash" 48th Annual Proceedings, Association for the Advancement of Automotive Medicine, September 13-15, 2004
- [19] Sherwood, et al., op cit. (2004)
- [20] Carlsson, G., et al., "Rearward-Facing Child Seats – The Safest Car Restraint for Children?" Accident Analysis & Prevention, Vol. 23. Nos 2'3, pp 175-182. 1991
- [21] Henary, B., et al., "Car Safety Seats for Children: Rear Facing for Best Protection: Injur Prevention 2007;13:398-402. doi: 10.1135/ip.2006015115
- [22] Jakobsson, L., et al., "Safety for the Growing Child – Experiences from Swedish Accident Datas" Paper Number 05-0330, Proceedings 19th International Technical Conference on the Enhanced Safety of Vehicles, June 2005
- [23] American Academy of Pediatrics, Policy Statement Child Passenger Safety, DOI: 10.1542/peds.2011-0213, *Pediatrics* published online Mar 21, 2011;
- [24] Tylko S., op cit. (2011)
- [25] NHTSA New Car Assessment Program, Frontla Barrier Crash Test, 2008 Ford Escape, Report Number: CAL-07-12, March 1, 2007
- [26] Hobbs, C. A., McDonough, P.J., "Development of the European New Car Assessment Programme (Euro NCAP), Paper Number 98-S11-O-06
- [27] Sherwood, et al., op cit. (2004)
-

APPENDIX A. TEST SERIES 1 AND 2 INSTRUMENTATION DATA

Test No.	Test Unit	Shed Delta-V (mph) / Accel (G)	Resultant Head Accel. (G)	HIC	HIC36	HIC15	Chest Accel 3ms (G)	Neck Tortion (N)	Upper Neck Compression (N)	Upper Neck Shear (N)	Upper Neck Flexion (N-M)	Upper Neck Extension (N-M)	MTF	NTE	NCF	NCE
1-1	C88 A	41.87/49.69	111.74	919.0	997.1	398.1	94.1	1492	1070	630 ⁽¹⁾ 219	10	19	.89	1.74	1.1	.69
1-2	C88 A	41.93/49.71	77.94	961.6	997.9	627.9	90.4	2376	409	680 ⁽¹⁾ 287	12	14	.81	2.44	.22	.28
1-3	C88 B	40.77/49.31	98.8	1369.8	1369.8	930.7	701	1899	291	960 ⁽¹⁾ 68	0	26	.26	2.73	.27	.32
1-4	C88 B	42.47/46.11	76.67	830.2	830.2	689.3	72	1678	660	960 ⁽¹⁾ 130	(1)	(1)	(1)	(1)	(1)	(1)
1-5	C88 C	41.84/46	67.61	976.7	976.7	671.7	72	1820	834	960 ⁽¹⁾ 137	6	13	.29	1.89	.16	.62
1-6	C88 B	41.99/46.34	70.02	894.8	499	382.8	82.1	1677	499	960 ⁽¹⁾ 280	15	12	.69	1.69	.46	.42
2-1	C88 A	41.27/46.4	189.83	2081	2081	1669.4	87.6	2107	368	778 ⁽¹⁾ 149	4	18	1.37	2.42	.12	.31
2-2	C88 B	42.07/46.74	94.67	1166.7	1166.7	970.6	71.8	2369	301	1120 ⁽¹⁾ 160	0	26	.24	3.09	.08	.48
2-3	C88 C	41.73/46.16	68.48	1029.1	1029.1	789.1	76.2	962	189	294 ⁽¹⁾ 249	15	9	.37	1.16	.39	.19

(1) Instrumentation failure resulted in data not being recorded

MINIMIZING THE RISK OF LAP/SHOULDER BELTED CHILDREN SUBMARINING THE LAP BELT IN FRONTAL CRASHES

Gary R. Whitman, Arlie V. Hart, III, Larry Sicher, Brian Benda, Louis A. D'Aulerio
ARCCA, Inc
United States
Paper Number 13-0041

ABSTRACT

The objective of the study presented by this paper was to determine whether belt-positioning-booster seats incorporate seat bottom design features, identified by previous research, to minimize the risk of submarining. The booster seats were evaluated through inspection and testing. The geometry of the BPB's seat bottom was measured and recorded. The comparative restraining ability of the BPB's seat bottom ramp was tested. The compressibility of the BPB while seated on a vehicle seat was tested. The compressibility of the BPB alone was also tested using the test specified in the Canadian and Australian/New Zealand standards.

The inspection and load testing of various BPBs, as reported in this paper, reveals that BPB seat bottom designs vary significantly. Some BPBs incorporate significant seat ramp geometry and have very little compressibility. Others have no seat ramp at all and have very high compressibility. It is critical that BPB manufacturers understand the importance of anti-submarining seat bottom ramps and low compressibility of the seating surface, and incorporate these features into all BPBs. To ensure this and do so in a manner that is consistently compatible with vehicle seats and seat belts, the authors recommend that NHTSA develop and incorporate requirements into FMVSS 213 specifying the BPB's seating surface geometry and compressibility characteristics, including the seating surface compressibility requirement specified in the Canadian and Australian/New Zealand standards. In lieu of such requirements, the manufacturers of BPBs and automobiles must work together to ensure that the BPB component integrates properly with the seats and seat belt systems at all automobile occupant positions that can be used by a child to ensure that submarining is prevented.

BACKGROUND

After the introduction of seat belts for adults, occupants frequently sustained severe abdominal and lumbar spine injuries during frontal crashes due to the lap belt slipping off the iliac spines of the pelvis and loading into the soft abdominal region.[1,2,3] This kinematic pattern is referred to as "submarining"

the lap belt, and the resulting injury is generally referred to as "seat belt syndrome." [4,5] Research has identified several design attributes of the seat belt and vehicle seat that are critical to prevent occupant submarining when using a continuous loop lap/shoulder seat belt. These attributes are:

- A lap belt geometry with an angle greater than 45 degrees from horizontal
- Maximization of the distance of the lap/shoulder belt junction to the centerline of the occupant's body
- Minimization of downward and forward displacement of the pelvis by limiting the compressibility of the seat bottom cushion and incorporating an anti-submarining seat bottom ramp [6,7,8,9,10,11,12,13,14,15,16,17]
- Countering of the force and moment applied to the pelvis by the lap belt that tends to rotate the top of the pelvis rearward by applying a load to the bottom of the pelvis from a structural anti-submarining ramp in the seat bottom. [18,19,20, 21,22,23,24,25,26]

Figure 1 provides an example of a vehicle seat that incorporates an anti-submarining ramp or beam to minimize the potential of submarining.



Figure 1. 2001 Volvo S60 Right Front Seat Bottom Ramp.

Children, when they outgrow child safety seats with integrated harnesses, are too small to properly fit an adult lap/shoulder belt. Additionally, a child's body is not as compatible with a lap/shoulder belt restraint as the adult body. First, the child's pelvis is not fully developed. The anatomical features of the adult pelvis that engage with the lap belt are the anterior

superior iliac spines (ASIS).[27,28] Their shape helps to keep the lap belt engaged with the pelvis. The ASIS of the child's pelvis are not well defined. Therefore, the potential for the lap belt to slip off the pelvis onto the abdomen is much greater. [29,30,31,32] The risk of adult occupants submarining is reduced by their knees and feet often loading against vehicle structure forward of their occupant position during frontal crashes. Because of their shorter legs, such loading will not typically occur with children, which further increases their potential for submarining.

To improve the fit of adult lap/shoulder belts used by children, BPB seats are required.[33,34] The BPB raises the seated shoulder height of the child. This improves the positioning of the shoulder belt, resulting in it being farther from the neck and more centered on the shoulder. It also raises the child's pelvis, thus allowing the lap belt to assume a more vertical orientation, and increases the distance from the lap/shoulder belt junction to the centerline of the child's body. Both of these factors help to maintain the lap belt on the pelvis of the child. The BPB seating surface also has a shorter fore/aft dimension compared to the vehicle seat. This allows the child to sit more comfortably by enabling the knees to bend in a more natural manner than when the child sits directly on the vehicle seat. This decreases the child's tendency to slump in order to allow the knees to bend. Slumping tips the pelvis back, further increasing the potential for the lap belt to slip off the pelvis. After introduction of BPBs in the 1970s,[35] there was not the expected reduction in abdominal injuries in children. Investigators found that the BPB itself typically did not incorporate the countermeasures required by a seating system to prevent submarining of the lap belt. Many of the BPBs' seating surfaces were highly compressible, did not incorporate anti-submarining seat ramps and/or seat belt guides.[36,37,38] In response to the hazard created by highly compressible seating surfaces, Canada and Australia/New Zealand adopted requirements in their standards that limited the compressibility of BPB seating surfaces to 25 and 32 mm (1 and 1¼ inches), respectively, when a 2250 N (~506 lbs) force is applied.[39,40] Researchers also determined that BPBs needed lap belt guide hooks to resist the lap belt moving upward off the pelvis. Because of these realizations and requirements, the majority of BPBs incorporated anti-submarining ramps, low compressibility seat bottom seating surfaces, and lap belt guide hooks. This resulted in a reduction in the frequency of the abdominal and spinal injuries by children restrained by adult lap/shoulder seat belts when using a BPB. [41,42]

There are no requirements in NHTSA's Federal Motor Vehicle Safety Standard (FVMSS) 213 - Child Restraint Systems directly pertaining to the design and performance of BPB with regard to submarining. [43] There is a 915 mm (36 inch) limit on knee excursion limit on all forward-facing child restraint systems when tested in accordance with 48 km/h (30 mph) frontal crash sled test. However, this requirement was incorporated before the introduction of BPBs, with the hope that a child safety seat that allowed submarining would fail the knee excursion requirement. However, with a BPB, the child dummy's knees are typically positioned farther back, because the booster has a thinner, or no, seat back. As a result, the dummy can submarine the lap belt without failing the knee excursion limit. Also, research has found that the current state of the art child dummy is ineffective at revealing a risk of submarining, due to non-biofidelic high stiffness in the lumbar spine.⁴⁴

METHODOLOGY

Four different studies (Studies A, B, C, and D) were conducted to assess the anti-submarining seat bottom ramp and seat bottom compressibility of several different BPBs. The methodology of each study is provided below.

A: BPB Seating Surface Geometry Comparison

The contour of each BPB seating surface was examined and documented using a contour gauge. The angle of the seating surface from horizontal was also measured at 152, 203, 254, and 305 mm (6, 8, 10, and 12 inches) from the rear edge of the booster seat or the booster seat's seat bight, when it incorporated a seat back.

B: BPB Seating Surface Pelvic Restraint Test

The objective of the BPB's Seating Surface Pelvic Restraint Test was to determine the ability of the BPB's seating surface structure to apply a restraining load to the bottom of a child's pelvis. The test methodology, developed by researcher Svensson, [45] was conducted as follows:

1. The upholstery covering the seat bottom of the BPB was removed prior to testing to allow observation of the BPB seat bottom structure during the test. Each BPB was secured to a hydraulic ram fixture. The orientation of the BPB bottom was flat relative to the horizontal travel of the ram. The lower torso/buttocks of a Hybrid III 6-year-old child dummy was attached to the end of the ram. The end

of the ram was positioned on the BPB seating surface where a child would normally sit (Appendix A). The travel of the ram was limited to horizontal displacement only. The loads applied to the lower torso of the dummy were measured by the dummy's triaxial lumbar load cell. Horizontal displacement of the ram was measured by a string potentiometer. Pre-test still photographs of the test article and test set-up were taken.

2. The ram was slowly pulled horizontally toward the front edge of the BPB until it reached the front edge. Load, displacement, and time data were measured concurrently and recorded by a data acquisition system. Each test was video recorded.

3. Post-test photographs were taken of each test article prior to and after removal from the test fixture.

C: BPB/Vehicle Seat Bottom Compressibility Test

The objective of this testing was to determine the capability of BPBs' seat bottom structures to minimize downward displacement of the child's pelvis during a frontal crash.

The test methodology used was a variant to the Svensson methodology.[46] The protocol for the compressibility testing was as follows:

Samples of various Belt-Positioning-Boosters (BPB) were acquired. Each was subjected to seat bottom compression testing. The testing was conducted as follows:

1. The upholstery covering the seat bottom of the BPB was removed prior to testing to allow observation of the BPB's seat bottom structure during the test. The BPB was placed on a vehicle seat bottom and secured to the seat by a lap belt. The fixture oriented the bottom of the vehicle seat bottom to an angle of 25 degrees (front edge up) such that the hydraulic ram applied a forward and downward load to the BPB's seating surface (Appendix B). The loading surface of the ram incorporated the lower torso/buttocks region of a Hybrid III 6-year-old child dummy. The movement of the ram was limited to horizontal. Pre-test still photographs were taken of the test article and test set-up.

2. The load applied was increased during the test as required to maintain the slow forward travel of the ram. The loads applied were measured via the triaxial lumbar load cell within the child dummy's lower torso. Displacement of the ram was measured via a string potentiometer attached to the end of the ram. The data was recorded by a data acquisition system that recorded the load data relative to time and displacement. The test was video recorded.

3. The load maintained slow forward travel of the ram until the dummy's buttocks reached the forward edge of the booster or a vertical or longitudinal force of 4448 N (1000 lbs) to the lumbar load cell was exceeded.

4. Post-test photographs were taken of the test article prior to and after removal from the test fixture.

D: Belt-Positioning-Booster Compressibility Test

This testing was conducted in accordance with Canadian Motor Vehicle Safety Standard (CMVSS) 213, Section 408, which states: "After the application of a preload of 175 N to the booster seat, the booster seat, including any padding or covering, must not deflect more than 25 mm under the application of a vertical force of 2250 N applied anywhere on the upper seating surface of the booster seat through the apparatus described in section 17 of ASTM D3574-08, *Standard Test Methods for Flexible Cellular Materials — Slab, Bonded, and Molded Urethane Foams*, published by ASTM International." ASTM D3574-08 specifies that the indenter that loads the booster seat be a flat circular foot 200 mm +3/-0 mm (8 inches) in diameter.

TEST AND EVALUATION RESULTS

Belt-Positioning-Booster Seating Surface Geometry Comparison

The contours of the seating surfaces of eighteen BPBs were measured and recorded. Plots of the contours are provided in Appendix C. The angles of each BPB's seating surface were measured at multiple locations along the longitudinal centerline and are provided in Appendix D. The complete front edge contour was not always acquired due to the limits of the contour gauge.

The fore/aft depth of the BPBs seat bottom ranged from 289 to 400 mm (11 3/8 to 15 3/4 inches). The maximum angle of the seat bottom surface of the BPBs ranged from 3 to 19 degrees from horizontal. The average maximum seating surface angle was 12.4 degrees. Only one BPB had a maximum a seat surface angle of less than 5 degrees. That BPB had a maximum angle of only 3 degrees 6 inches from its rear edge, and was actual a negative angle of -1 degree at 203 and 254 mm (8 and 10 inches) from its rear edge. Four BPBs had a maximum seating surface angle between 5 and 10 degrees. The remaining thirteen BPBs all had seating surface angles that equaled or exceeded 10 degrees.

Belt-Positioning Booster Seating Surface Pelvic Restraint

The force required to push the dummy pelvis from the normal seating position to the front edge of the BPB without allowing it to move upward was measured. The results are provided in Appendix E. Due to limited test assets, only 15 BPBs were subjected to this test series.

The force application by the hydraulic ram was stopped after either the vertical (z) or longitudinal (x) lumbar loads exceeded 4448 N (1000 lbs), even if the front edge of the BPB had not been reached. Due to both human and hydraulic ram response times, however, the force applied to the booster exceeded that level in several tests. Three BPBs generated a resultant force of less 2224 N (500 lbs) resisting the movement of the pelvis. One of those only generated 173 N (38.9 lbs) of force. Six BPBs generated a resultant force between 2224 and 4448 (500 and 1000 lbs), and six exceeded 4448 N (1000 pounds).

BPB Seat Bottom & Vehicle Seat Compressibility

The force-deflection results acquired during the BPB seat bottom/Vehicle Seat compressibility testing is provided in Appendix F.

At six inches of displacement, the all of BPBs generated a force ranging between 200 lb and 2224 N (500 lbs), except for the Harmony Youth Booster. At 6 inches of displacement, it only generated approximately 150 lbs. and it never exceeded 200 lbs. whereas all of the other BPB exceeded 1200 lbs. The force-deflection characteristics of the various BPBs while, positioned on a vehicle rear seat (2005 Dodge Stratus) varied widely amongst the units tested. When compared at 2224 N (500 lbs) of resultant force the combined deflection of the vehicle seat bottom and BPBs ranged from approximately 165 to 216 mm (6.5 to 8.5 inches), except for one BPB. That BPB did not reach a resultant force of 2224 N (500 lbs), however it did experienced nearly 381 mm (15 inches) of combined deflection.

Canadian/Australian BPB Compressibility Test

The results of the testing conducted in accordance with the Canadian and Australian/New Zealand child restraint standards are provide in Appendix G and H. Prior to this testing, the authors became aware of a unique inflatable BPB called the “Bubble Bum.” This BPB was added to the units tested. Those BPBs that exceeded the Canadian 25 mm (1 inch) deflection requirement were tested a second time to confirm the result. Due to a significant difference between the

first two tests of the Harmony Youth BPB, three additional tests of that BPB were conducted. All but two BPBs complied with the Canadian 25 mm (1 inch) deflection limit. The two BPBs that failed are shown in Figures 2 and 3, while subjected to the 2250 N (506 lbs) force. One other BPB deflected to the limit. Subsequent to this testing, the authors learned that the Harmony Youth Booster sold in Canada incorporated thicker walls than the U.S. version. Therefore, Canadian Harmony Youth Boosters were subsequently acquired and tested.



Figure 2. Harmony Youth BPB.



Figure 3. Bubble Bum BPB.

Figure 4 shows one of the BPBs that complied with the Canadian requirement.



Figure 4. Volvo BPB.

DISCUSSION

Before the introduction of BPBs, children who outgrew child safety seats would sit directly on the vehicle seat and use the adult seat belts for crash restraint. These adult seat belts, however, did not properly fit children and frequently caused serious injury, particularly abdominal and lower spinal injuries from loading by the lap belt. Belt-positioning-boosters (BPB) seats were introduced to improve the fit of the adult lap/shoulder seat belt when used by children. After introduction of BPBs, however, it was observed that their use did not reduce the frequency of abdominal injuries.[47] Many of these early BPBs had highly compressible seating surfaces lacked structural anti-submarining seat ramps and lap belt guide hooks. The evaluation and testing of BPBs conducted by the authors indicates that since then, the majority of BPBs introduced incorporate seating surfaces with low compressibility and anti-submarining seat ramps. The majority also incorporate lap belt guide hooks. These features combine to minimize the potential for submarining by limiting forward and downward movement of the pelvis and providing a restraining force to the bottom of the pelvis that counters the lap belt force applied to the top of the pelvis. Two of the BPBs evaluated, however, had very little or no seat ramp and, therefore, did not provide any significant restraining load to the pelvis. One of those two BPBs, the Harmony Youth, also had an extremely compressible seating surface. Previous research indicates that these deficiencies significantly increase the potential for submarining.[48,49,50,51,52,53,54,55,56]The Bubble Bum, which was discovered late in the study and therefore only subjected to the Canadian Compression testing was also highly compressible and lacked a seat ramp structure.

One BPB evaluated and tested, the Britax Parkway, in addition to incorporating an anti-submarining seat bottom ramp and low compressibility incorporated an Anti-Submarining Clip (ASC). The ASC attaches to a strap secured to the center of the BPB seat bottom. After a child occupies the BPB and secures the lap/shoulder belt, the clip is attached to the center of the lap belt and adjusted snug. The ASC acts as a crotch strap to hold the lap belt down on the pelvis. Brown reported that during frontal crash sled testing, "These crotch strap-like devices held the lap belt down throughout the impact." [57] The Bubble Bum BPB incorporates lap belt hooks on the outboard sides of the booster to hold the lap belt down, similar to lap belt guide hooks. As with the Britax Parkway's ASC, one of these belt hooks would have to be

attached and detached each time the child donned and doffed the seat belt, making it highly likely that these hooks will often not be used. With the Britax Parkway, the ASC is supplemental to the passive anti-submarining features that the Parkway incorporates, i.e., seat ramp, low compressibility, and lap belt guide hooks. The Bubble Bum does not incorporate these features and is totally reliant on the belt hooks to be used to prevent submarining.

Modern rear seat automotive restraint systems consist of a lap/shoulder belt and seat and are often supplemented with side impact protective inflatable devices. To work effectively and avoid submarining injuries, the seat belt and seat must be designed to work together to balance the forces applied to the occupant's pelvis. For the adult occupant, this can be readily accomplished because the vehicle manufacturer has complete control over the both the seat belt and seat design. For a child who has outgrown a conventional child safety seat and is using the adult lap/shoulder belt with an add-on BPB seat, the vehicle manufacturer has no control over the design of the BPB. There are no requirements pertaining to the design or performance of the BPB seat bottom relative to its restraining the pelvis. Therefore, the ability of BPBs to balance the forces applied to the pelvis varies significantly. Requirements need to be incorporated into FMVSS 213 that will enable vehicle manufacturers to rely on the BPB to complement the seat and seat belt to ensure that submarining is avoided.

Hybrid III (HIII) dummies have been found to be too stiff in the lumbar region. This stiffness prevents pelvic rotation and therefore prevents the dummy from submarining under circumstances that a human child would.⁵⁸ Therefore, dynamic testing with the HIII dummy cannot be relied upon to determine if a system allows submarining.

Due to children's immature anatomy and tendency to get out-of-position, it is recommended that children remain in forward-facing CSS incorporating five-point harnesses for as long as possible. Fortunately, there are now such CSSs readily available for children up to 36.3 kg (80 lbs) and 1346 mm (53 inches). For children transitioned to a BPB, BPBs incorporating an anti-submarining clip appears to be an effective countermeasure to ensure submarining is prevented.

To maximize the effectiveness of the seat ramp, the ramp must remain in position during the crash. The majority of BPB on the market do not attach to the vehicle. Some BPBs incorporate high friction material on the bottom to minimize movement. A few BPBs incorporate the ability to secure to the vehicle

using the lower LATCH anchorages. This feature ensures the BPB remains in proper position, not only during frontal crashes, but also in all crash modes, including rollover. During a rollover crash, an unattached booster could get out of position or come out from under the child completely, compromising the fit and performance of the lap/shoulder belt. In side impacts, researchers have found that an unattached BPB will move more readily, reducing the effectiveness of any side wing restraint provided with the BPB and that it is feasible to develop a BPB incorporating rigid LATCH anchorages that significantly improves the BPB's side impact protection.[59]

CONCLUSIONS

Published epidemiology studies indicate that BPBs generally reduce the rate of injury to children in crashes compared to children using only the adult seat belt. However, children continue to sustain "seat belt syndrome" injuries. Research has determined that seat design is critical to avoiding submarining the lap belt and preventing seat belt syndrome injuries. Children are especially vulnerable to submarining the lap belt. Yet, there are no requirements to ensure that BPBs incorporate features that have been identified as critical to avoid submarining the lap belt during frontal crashes. These features include anti-submarining seat bottom ramps, low compressibility seating surfaces, and effective lap belt guide hooks. There are BPBs on the market in the U.S. that fail to incorporate an anti-submarining design. Their high seating surface compressibility, lack of ramp, and lack of effective lap belt guide hooks promote submarining of the lap belt. BPB manufacturers, automobile manufacturers, and NHTSA must work together to establish requirements that will ensure that the BPB will work properly with motor vehicle seat belts to prevent submarining and its associated injuries.

STUDY LIMITATIONS

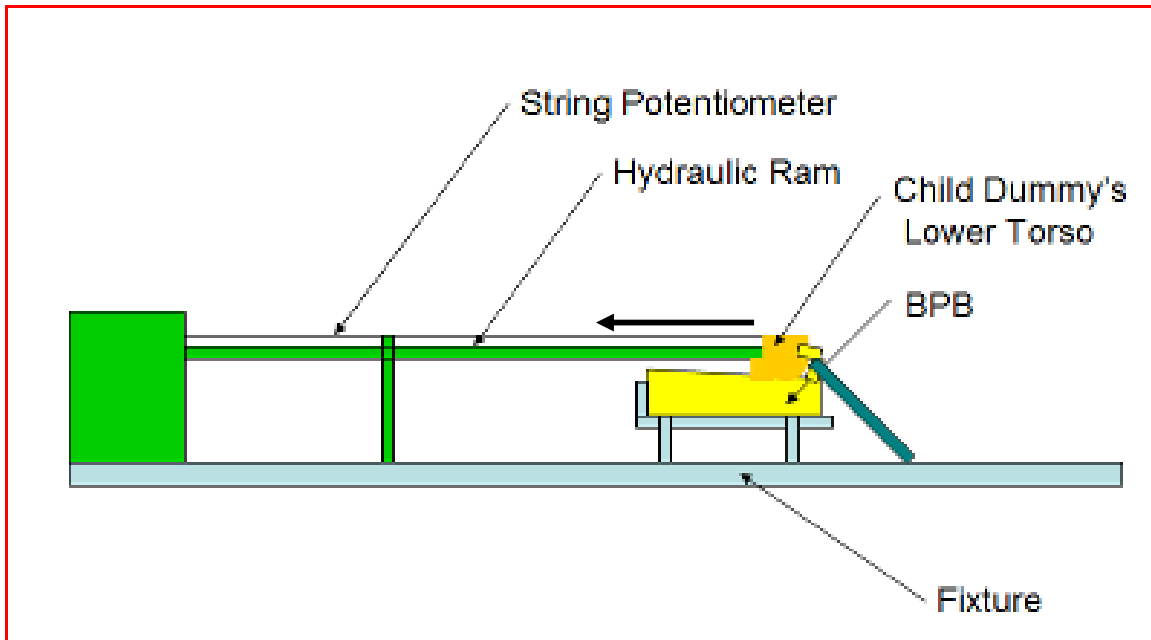
This study evaluated a sampling of BPBs on the U.S. market since the 1980s. It did not include all BPBs currently available in U.S.

REFERENCES

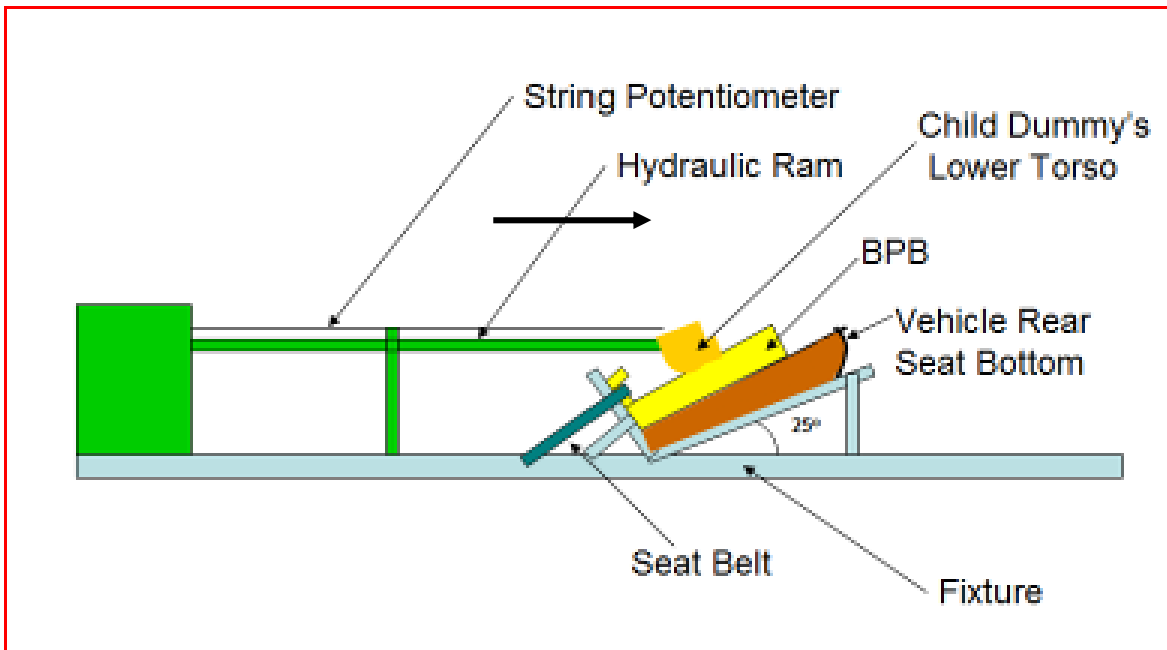
-
- [1] Stalnaker RL. "Tests of Current and Experimental Child Restraint Systems" SAE 740045
- [2] Adomeit D. and Heger A. Motion Sequence Criteria and Design Proposals for Restraint Devices in Order to Avoid Unfavorable Biomechanic Conditions and Submarining SAE 751146
- [3] Svensson LG. Means for Effective Improvement of the Three-Point Seat Belt in Frontal Crashes SAE 780898
- [4] Brown, J., Bilston, L., "Spinal Injuries in Rear Seated Child Occupants Aged 8 – 16 Years" Prince of Wales Medical Research Institute, UNSW, Australia Paper No 07-0461
- [5] Tarriere C. *Children Are Not Miniature Adults*. pp. Proc. of Int. Conf. on the Biomechanics of Impacts (IRCOBI), 1995:15–27
- [6] Stalnaker RL. op cit. (1974)
- [7] Adomeit D. and Heger A., op cit. (1975)
- [8] Svensson LG., op cit., (1978)
- [9] Adomeit D. Seat Design-A Significant Factor for Seat Belt Effectiveness SAE 791004
- [10] States JD. "Safety Belts and Seat Design – An Insight From Racing" October 1980
- [11] Lundell B., et al. "Safety Performance of a Rear Seat Belt System with Optimized Seat Cushion Design" SAE 810796
- [12] Leung YC., et al. Submarining Injuries of 3 Pt. Belted Occupants in Frontal Collisions – Description, Mechanisms and Protection
- [13] General Motors "Belt Restraint Systems Design Considerations and Performance Considerations" 1984
- [14] Haberi J., et al. "New Rear Safety Belt Geometry – A contribution to Increase Belt Usage and Restraint Effectiveness" SAE 870488
- [15] Horsch JD., et al. "A Kinematic Analysis of Lap-Belt Submarining for Test Dummies" SAE 892441
- [16] Nilson G., et al. "The Potential Injury-Reducing Benefits of a Well Designed Car Seat" S-41 2 96
- [17] ARCCA, Inc, Department of the Army, "Occupant Crash Protection Handbook for Tactical Ground Vehicles", November 15, 2000
- [18] Adomeit D. and Heger, op cit. (1975)
- [19] Svensson LG., op cit. (1978)
- [20] Adomeit D., op cit. (1979)
- [21] States JD. "Safety Belts and Seat Design – An Insight From Racing" October 1980
- [22] General Motors, op cit., (1984)
- [23] Haberi J., et al., op cit. (1987)
- [24] Horsch JD., et al. op cit. (1989)
- [25] Nilson G., et al., op cit. , (1996)
- [26] ARCCA, Inc, Department of the Army, "Occupant Crash Protection Handbook for Tactical Ground Vehicles", November 15, 2000
- [27] Burdi, A. R., et. al. (1969). Infants and Children in the Adult World of Automobile Safety Design: Pediatric and Anatomical considerations For Design of Child Restraints. ASME Third

- Biomechanical and Human Factors Division Conference, June 12-13, 1969. University of Michigan, Ann Arbor.
- [28] Agran, P., et al., "Child Occupant Protection In Motor Vehicles" *Pediatrics in Review* Vol. 18 No. 12 December 1997
- [29] Herbert DC, et al., Traffic Accident Research Unit, Dept of Motor Transport New South Wales, Australia Evaluation of Australian Child Restraint SAE 730972
- [30] Stalnaker, R.L., Highway Safety Research Institute, "Dynamic Performance of Child Restraint System" 10/5/73.
- [31] Stalnaker RL., op cit. (1974)
- [32] Tarriere C. *Children Are Not Miniature Adults*. pp. Proc. of Int. Conf. on the Biomechanics of Impacts (IRCOBI), 1995:15-27
- [33] Policy Statement, Child Passenger Safety COMMITTEE ON INJURY, VIOLENCE, AND POISON PREVENTION *Pediatrics* published online Mar 21, 2011; DOI: 10.1542/peds.2011-0213
- [34] Tarriere C., op cit. (1995)
- [35] Weber K. (2000) "Crash Protection for Child Passengers: A Review of Best Practice" *UMTRI Research Review*, Vol. 31, pp. 1-28.
- [36] Stalnaker, RL, "Inconsistencies in State Laws and Federal Regulations Regarding Child Restraint Use in Automobiles" SAE 933087
- [37] Brown J., Griffiths M., Paine M. "Effectiveness of Child Restraints The Australian Experience" Research Report RR 06/02, For Australian New Car Assessment Program, June 2002
- [38] Griffiths M., Brown J., Paine M., "Safety Innovations for Australian Child Restraints" Public Policy Department, Royal Automobile Club of Victoria Ltd, June 2004
- [39] Griffiths, M., Brown, J., Kelly, P., "Child Restraint System Development in Australia" 94S 10 015 Fourteenth International Technical Conference on the Enhanced Safety of Vehicles, Munich, May 1994
- [40] AS/NZS 1754:2004 Australian/New Zealand Standard Child Restraint Systems for use in Motor Vehicles
- [41] Jermakian, J., at al., "Abdominal Injury Risk for Children Seated in Belt Positioning Booster Seats" Paper Number 07-0441, 20th International Technical Conference on the Enhanced Safety of Vehicles, June 2007
- [42] Arbogast, K., et al., "Effectiveness of Belt Positioning Booster Seats: An Updated Assessment" *Pediatrics* 2009;124;1281-1286; originally published online Oct 19, 2009; DOI: 10.1542/peds.2009-0908
- [43] Federal Motor Vehicle Safety Standard 213 Child Restraint Systems
- [44] S. Couturier, et al., "Procedure to Assess Submarining in Frontal Impact" Paper Number 07-0481 The 20th International Technical Conference on the Enhanced Safety of Vehicles Conference (ESV) in Lyon, France, June 18-21, 2007
- [45] Svensson, L., op cit. , (1978)
- [46] Svensson, L., op cit. (1978)
- [47] Trossielle, X., et al., "Abdominal Injury Risk To Children and its Prevention" IRCOBI Conference, Hannover, September 1997
- [48] Adomeit D. and Heger A., op cit. (1975)
- [49] Svensson LG., op cit. (1978)
- [50] Adomeit D., op cit., (1979)
- [51] States JD., op cit., 1980
- [52] General Motors, op cit., (1984)
- [53] Haberi J., et al., op cit., (1987)
- [54] Horsch JD., op cit. , 1989
- [55] Nilson G., et al., op cit., (1996)
- [56] ARCCA, Inc, op cit. (2000)
- [57] Brown J., et al., "The Need for Enhanced Protocols for Assessing the Dynamic Performance of Booster Seats in Frontal Impacts" *Traffic Injury Prevention*, 10:58-69, 2009
- [58] S. Couturier, et al., "Procedure to Assess Submarining in Frontal Impact" Paper Number 07-0481 The 20th International Technical Conference on the Enhanced Safety of Vehicles Conference (ESV) in Lyon, France, June 18-21, 2007
- [59] Huot, M., et al., "Design and Sled Testing of a High Back Booster Seat Prototype Offering Improved Side Impact Protection" *IJCrash* 2005 Vol. 10 No. 4 pp. 359-370

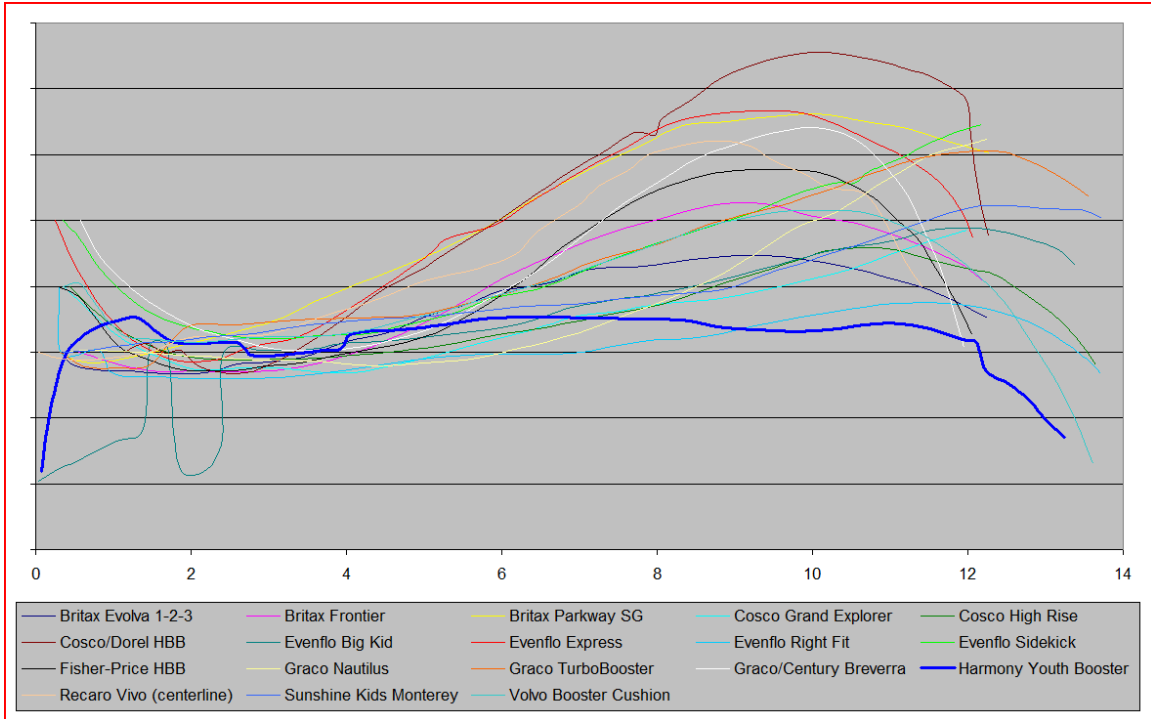
APPENDICES



Appendix A. BPB Seat Surface Pelvic Restraint Test Set-up.



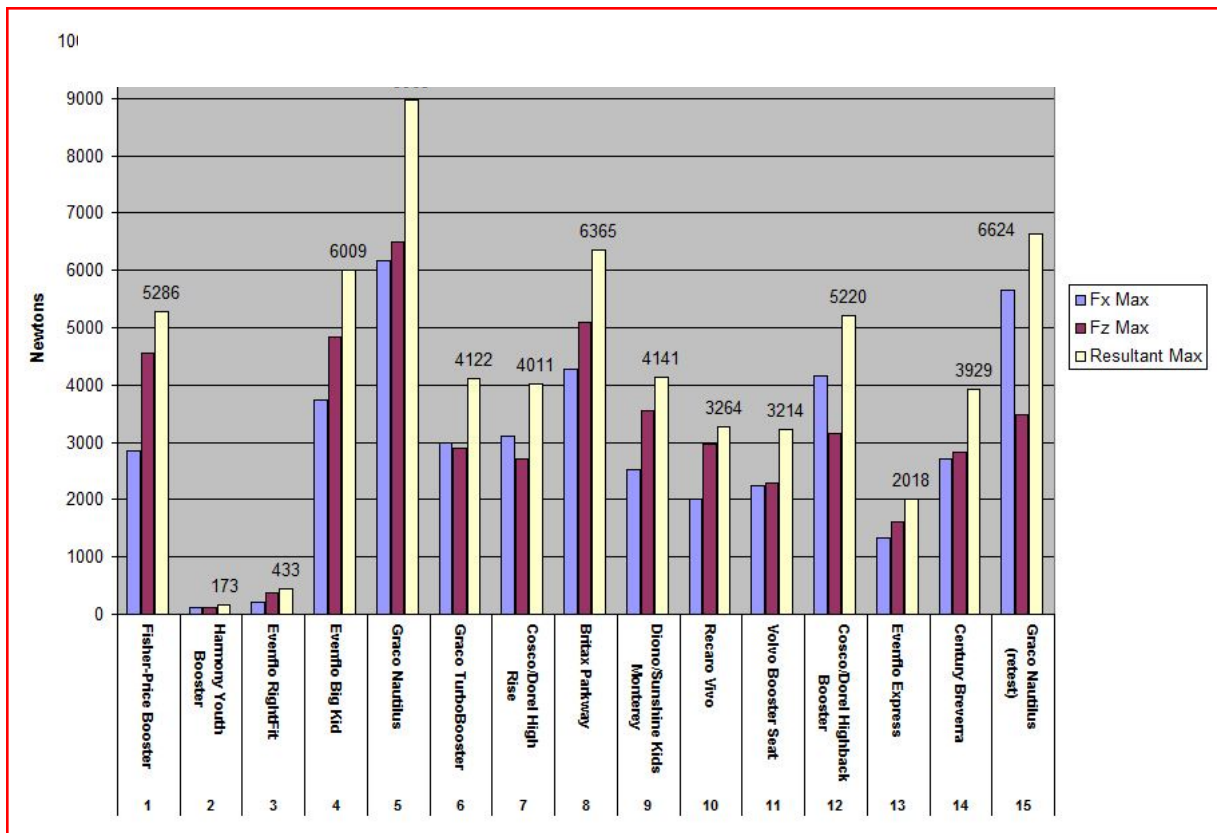
Appendix B. BPB Seat Bottom Compression Test Set-up.



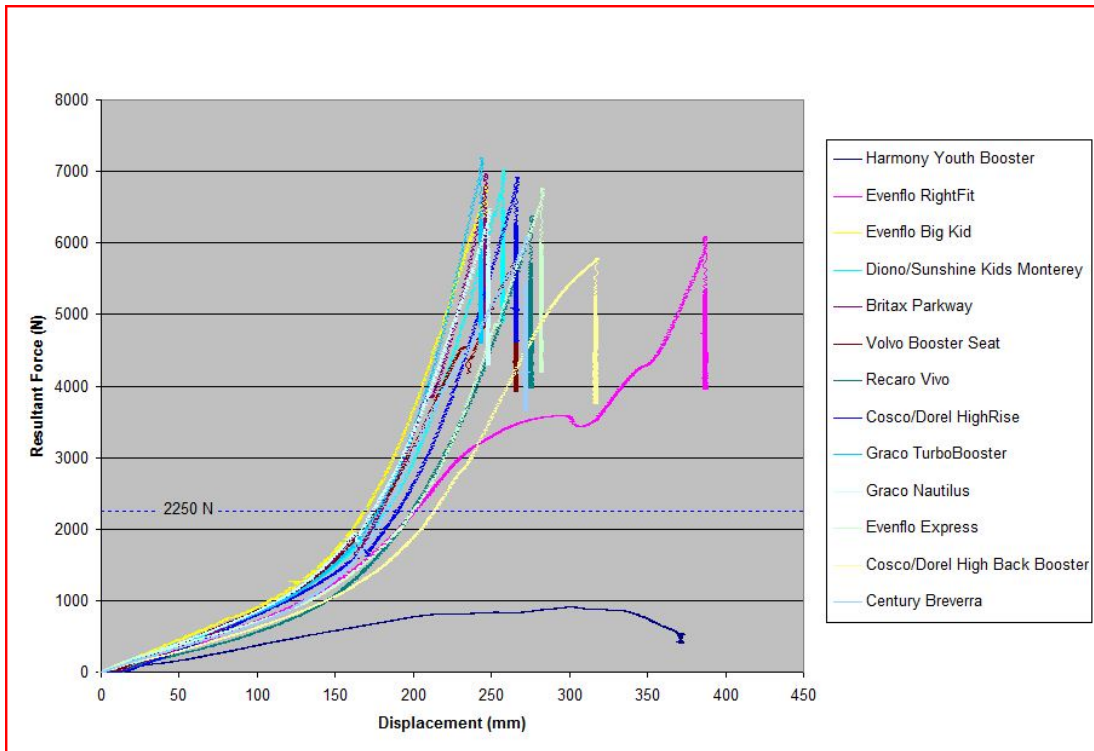
Appendix C. BPB Seat Surface Contours.

BPB Make/Model	Seat Bottom Fore/Aft Depth, (mm)	Angle at 152 mm (6") (degrees)	Angle at 203 mm (8") (degrees)	Angle at 254 mm (10") (degrees)	Angle at 305 mm (12") (degrees)	Maximum Angle
Volvo Booster Cushion	362 (14¼")	10	12	0	-27	12
Evenflo Sidekick	400 (15¾")	9	11	11	12	12
Cosco Grand Explorer	400 (15¾")	7	6	8	8	8
Graco/Century Breverra	363 (14¼")	12	16	0	-	16
Evenflo Right Fit	363 (14¼")	3	4	6	-5	6
Fisher Price Safe Embrace	381 (15")	18	12	-12	-	18
Dorel/Cosco Highback	381 (15")	19	16	3	-28	19
Evenflo Express	289 (11-3/8")	17	10	-7	-	17
Dorel Highrise	394 (15½")	6	8	11	-14	11
Graco Turbo Booster	394 (15½")	7	10	9	2	10
Evenflo Big Kid	362 (14¼")	6	7	8	1	8
Britax Parkway	356 (14")	13	15	18	-2	18
Graco Nautilus	311 (12¼")	8	14	18	12	18
Recaro Vivo	311 (12¼")	7	6	3	-	7
Sunshine Kids Monterey	324 (12¾")	6	8	12	14	14
Britax Frontier	305 (12")	15	5	-5	-19	15
Britax Evolva	356 (14")	12	8	-4	-15	12
Harmony Youth	368 (14½")	3	-1	-1	-16	3
Average	356 (14")	9.9	9.3	4.3	-5.5	12.4

Appendix D. BPB Seating Surface Angle along the Longitudinal Centerline (at various points from the back edge of the BPB).



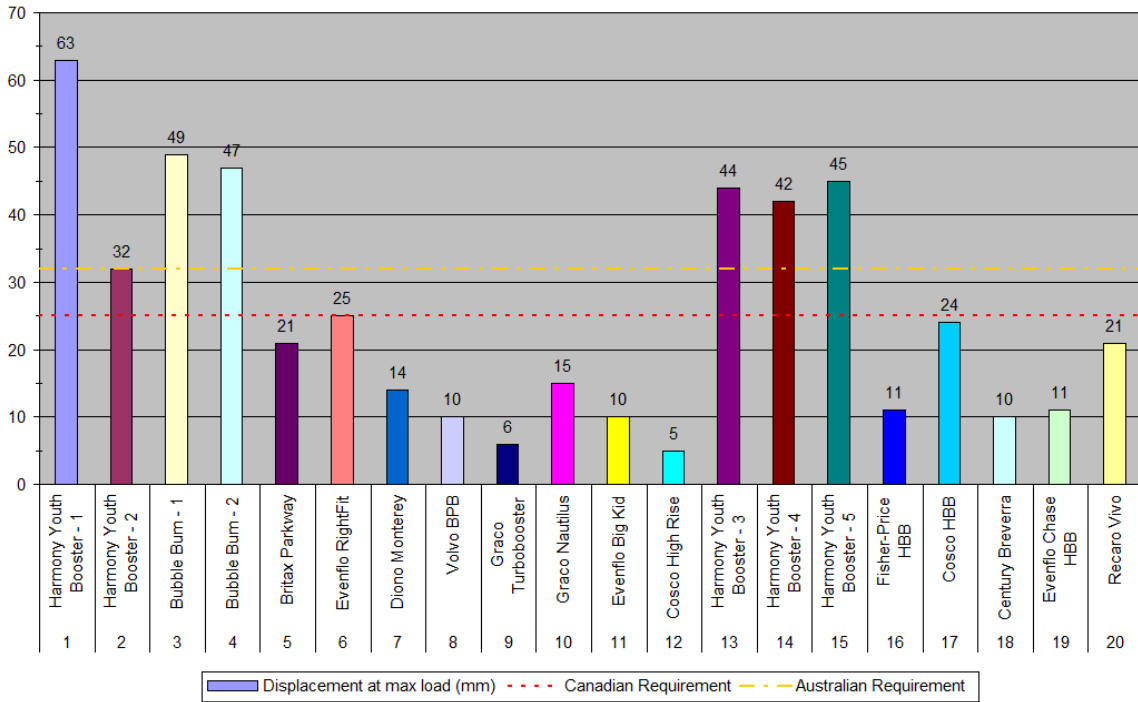
Appendix E. Maximum Load Generated During Seat Bottom Pelvic Restraint Testing.



Appendix F. BPB Seat Bottom Compressibility Testing Force-Deflection Curves.

Test No.	Make/Model	Model Number	Date of Manufacture	Test Result (mm)	Pass/Fail (>25mm)
1	U.S. Harmony/Youth	0304003LRW	09/06/10	63 (2.5")	Fail
2	U.S. Harmony/Youth	0304003LRW	09/06/10	32 (1.25")	Fail
3	Bubble Bum/Booster	BB001US	11/30/11	48 (1.9")	Fail
4	Bubble Bum/Booster	BB001US	11/30/11	46 (1.8")	Fail
5	Britax/Parkway	E9LA869	7/11	21 (0.8")	Pass
6	Evenflo/Right Fit	2451184	08/14/01	25 (1")	Pass
7	Diono/Monterrey	US15000	10/11	14 (0.55")	Pass
8	Volvo/Booster	9451523	98	10 (0.4")	Pass
9	Graco/Turbo Booster	1747302	6/10/11	6 (0.25")	Pass
10	Graco Nautilus	1757842	08/01/09	15 (0.6")	Pass
11	Evenflo Big Kid	3091982A	07/13/10	10 (0.39")	Pass
12	Cosco High Rise	22297-A06	1/11/11	5 (0.20")	Pass
13	U.S. Harmony Youth	0304003HCM	03/27/12	44 (1.75")	Fail
14	U.S. Harmony Youth	0304003WPK	07/19/10	42 (1.65")	Fail
15	U.S. Harmony Youth	0304003CCE	09/01/11	46 (1.8")	Fail
16	Fisher Price	79750	11/30/97	11 (0.43")	Pass
17	Cosco High Back	023377	03/22/10	24 (0.94")	Pass
18	Century Breverra	4865ABN	12/07/98	10 (0.39")	Pass
19	Evenflo Chase	32911113	04/04/12	11 (0.43")	Pass
20	Recaro Vivo	351.00.ME19	03/26/12	21 (0.83")	Pass
21	Canadian Harmony Youth	0304004LRC	05/19/12	25.3 (1.00)	Fail
22	Canadian Harmony Youth	0304004LRC	05/19/12	27 (1.06)	Fail
23	Canadian Harmony Youth	0304004LRC	02/10/12	20 (0.87)	Pass
24	Canadian Harmony Youth	0304004LRC	05/19/12	26 (1.02)	Fail

Appendix G. CMVSS Seat Surface Compressibility Testing.



Appendix H. CMVSS Seat Surface Compressibility Test Results.

TOWARDS A WORLD-WIDE HARMONIZED PEDESTRIAN LEGFORM TO VEHICLE BUMPER TEST PROCEDURE

Oliver Zander

Claus Pastor

Federal Highway Research Institute (BASt)

Germany

Peter Leßmann

Dirk-Uwe Gehring

BGS Böhme & Gehring GmbH

Germany

Paper Number 13-0175

ABSTRACT

A biofidelic flexible pedestrian legform impactor (FlexPLI) has been developed from the year 2000 onwards and evaluated by a technical evaluation group (Flex-TEG) of UN-ECE GRSP. A recently established UN-ECE GRSP Informal Group on GTR9 Phase 2 is aiming at introducing the FlexPLI within world-wide regulations on pedestrian safety (Phase 2 of GTR No. 9 as well as the new UN regulation 127 on pedestrian safety) as a test tool for the assessment of lower extremity injuries in lateral vehicle-to-pedestrian accidents. Besides, the FlexPLI has already been introduced within JNCAP and is on the Euro NCAP roadmap for 2014.

Despite of the biofidelic properties in the knee and tibia sections, several open issues related to the FlexPLI, like the estimation of the cost benefit, the feasibility of vehicle compliance with the threshold values, the robustness of the impactor and of the test results, the comparability between prototype and production level and the finalization of certification corridors still needed to be solved. Furthermore, discussions with stakeholders about a harmonized lower legform to bumper test area are still going on.

This paper describes several studies carried out by the Federal Highway Research Institute (BASt) regarding the benefit due to the introduction of the FlexPLI within legislation for type approval, the robustness of test results, the establishment of new assembly certification corridors and a proposal for a harmonized legform to bumper test area. Furthermore, a report on vehicle tests that previously had been carried out with three prototype legforms and were now being repeated using legforms with serial production status, is given.

Finally, the paper gives a status report on the ongoing simulation and testing activities with respect to the development and evaluation of an

improved test procedure with upper body mass for assessing pedestrian femur injuries.

INTRODUCTION

A biofidelic flexible pedestrian legform impactor (FlexPLI) is foreseen for being implemented within world-wide regulations on pedestrian safety as well as consumer test programmes as a test tool for the assessment of knee and tibia injuries caused within lateral vehicle-to-pedestrian accidents.

After the evaluation by a technical evaluation group (Flex-TEG) of GRSP in 2010, the FlexPLI was rated as not yet being ready for legislation. Thus, a new Informal Group on GTR9 Phase 2 was established under the umbrella of GRSP, dealing with the remaining open issues related to the introduction of the FlexPLI. The current timeline foresees the submission of a final draft of phase 2 of GTR9 to the December 2013 meeting of GRSP and an adoption of the draft by WP.29 in June 2014. The application of the FlexPLI for type approval testing could then be expected as from 2016 on.

The tasks that IG GTR9-PH2 was mandated by GRSP to cover were related to the Flex-TEG activities, the FlexPLI biofidelity, the benefit and the costs, the technical specifications (drawings) and PADI, the durability, the test procedure itself, the certification tests, a review and exchange of test results, the reproducibility and repeatability, the injury criteria and threshold values, the vehicle countermeasures, and to the development of a draft proposal to amend UN GTR No. 9 as well as a complementary draft proposal to amend the UN Regulation on pedestrian safety.

In this paper, several studies of the Federal Highway Research Institute (BASt) as contributions to the work to be covered by the IG GTR9-PH2 are described. A benefit study aims at an estimation of the cost reduction due to the introduction of the FlexPLI within legislation. A robustness study gives an overview of the long term performance of test results with the FlexPLI.

New assembly certification corridors for both the inverse and the pendulum certification test were drafted and proposed by BAST to the Informal Group. Furthermore, a proposal for a modification of the lower legform to bumper test area to address the development of vehicle front shapes with extraordinary small test areas was submitted to the Task Force Bumper Test Area (TF-BTA) chaired by the European Commission. Finally, BAST investigated the change in overall performance between the first prototype legs of the build level GTR and the first serial production legs, based on vehicle tests, and thus concluded modified impactor threshold values.

Besides the IG activities, the paper reports about the latest status of the evaluation of an upper body mass (UBM) to be applied to the FlexPLI for the assessment of femur injuries as a possible replacement of the current upper legform to bonnet leading edge test.

ESTIMATION OF COST REDUCTION

Accident data from the German In Depth Accident Study (GIDAS) was processed and transferred to data from the German national accident statistics to estimate a reduction of costs in Germany due to the introduction of vehicles with a pedestrian friendly bumper design. From the national dataset, accidents occurring during the years 2009 until 2011 with two road users, namely one passenger car and one pedestrian involved, were considered. In total, 65.843 accidents resulted in annually averaged 323 fatally injured, 5.774 seriously injured and 15.785 slightly injured road users in Germany, see figure 1.

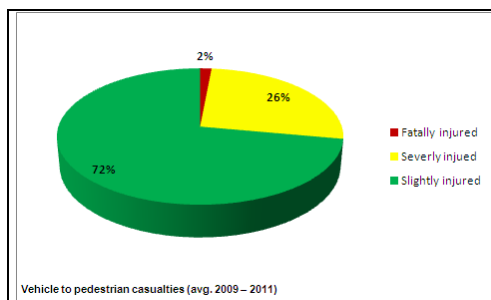


Figure 1. Vehicle to pedestrian casualties in Germany 2009 – 2011.

From the GIDAS dataset (1999 - 2011), only accidents with one pedestrian and one passenger car involved were taken into account. From the 1.925 recorded accidents 1.760 were found as being complete in terms of relevant information as e.g. type of injury, impact location and injury causing vehicle parts and could thus be used for the calculation of a change in MAIS injury distribution due to the introduction of a pedestrian friendly

bumper design. Furthermore, only laterally impacted pedestrians with the impact location at 8-10 o'clock and 2-4 o'clock with the injury causing parts on the vehicle front (without bonnet leading edge) were analyzed. To estimate the cost reduction due to the introduction of the FlexPLI the assumption was made that the severity of the detected AIS 1-3 injuries could be shifted downwards by AIS-1 in case of the vehicle being equipped with a pedestrian friendly bumper. Thus, by downwards shifting of AIS-1 an open tibia fracture would e.g. result in a closed tibia fracture, and a closed tibia fracture would result in bruises. When considering all injury types of tibia, fibula, knee, ligaments and subtalar joint, in total 498 vehicle-to-pedestrian accidents in the GIDAS database were affected by the AIS-1 downwards shift. The MAIS injury distribution of all complete pedestrian casualties in the original and the shifted dataset is shown in figure 2:

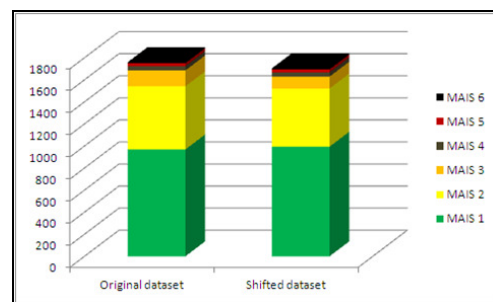


Figure 2. MAIS injury distribution of pedestrian casualties before and after AIS-1 shifting.

Thus, pedestrian casualties with an MAIS 3 were reduced by 25 percent, pedestrian casualties with an MAIS 2 were reduced by approx. 8 percent and consequently MAIS 1 casualties had a slight increase of 2,6 percent. MAIS 4-6 casualties were not affected by the downwards shift of AIS 1-3 lower extremity injuries because afterwards they still remained at their previous MAIS level.

Figure 3 provides the MAIS injury distribution of the fatally, severely and slightly injured pedestrians reported within GIDAS:

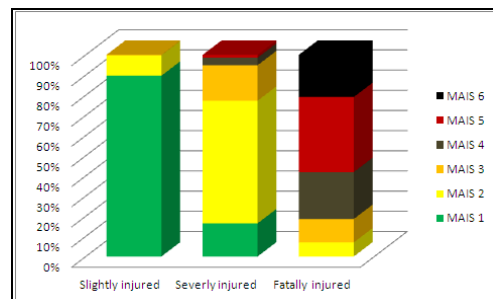


Figure 3. MAIS injury distribution of fatally, severely and slightly injured pedestrians before AIS-1 shifting.

A shifting of AIS-1 then leads to the reduction of fatally injured pedestrians by 3,5 percent, the reduction of severely injured pedestrians by 8,8 percent and the increase of slightly injured pedestrians by 1,5 percent. Figure 4 shows the casualties in absolute numbers:

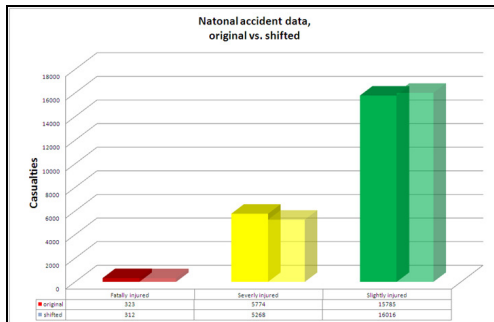


Figure 4. Shifting of fatally, severely and slightly injured pedestrians in national accident database due to AIS-1 shifting.

Under consideration of the corresponding costs per case the maximum annual cost reduction in Germany due to vehicles designed with pedestrian friendly bumper (AIS-1 shifting) is estimated at 63.725.349,- €, as shown in Table 1:

Table 1.
Estimated maximum annual cost reduction.

	original	shifted	Diff. [abs]	costs per case [€]	Reduction [€]
Fatally injured	323	312	11	1018065	11.364.027
Severely injured	5774	5268	506	105477	53.355.492
Slightly injured	15785	16016	-231	4305	-994.170
Σ					63.725.349

When taking into account the injury risk coverage rate of 70% realized due to the introduction of the FlexPLI, the annual cost reduction in Germany is estimated at 44.607.744,- €.

ROBUSTNESS OF TEST RESULTS

At the first meeting of the Informal Group GTR9 Phase 2, OICA (2011) reported about the long term durability of a FlexPLI prototype impactor. In total, more than 300 tests had been carried out with FlexPLI SN02, whose physical damages apparently had no significant effect on the vehicle test results. However, BAST further investigated the robustness of the FlexPLI test results. Basis of the comparative study were the inverse certification test results obtained with two different prototype impactors, one of them containing the formerly used polyester bone core material (SN02), while the other one was equipped with the currently used vinylester bone cores (SN04).

Long term performance of SN02

Inverse certification tests with FlexPLI prototype SN02 were performed at BAST during a time period of approximately three years. During this time period, except the replacement of the string potentiometers in January 2010 and the replacement of the short by long rubber material (as decided during the 8th meeting of the FlexPLI Technical Evaluation Group in May 2009), neither major exchange of parts nor calibration of particular sensors was undertaken. In total, 20 inverse certification tests using three different honeycomb materials according to the draft GTR9 specifications were carried out between January 2009 and November 2011, tests #1-12 using the FlexPLI with short rubber material and tests #13-20 with long rubber material and after the replacement of the string potentiometers. The last test was performed after a complete disassembly and reassembly of the impactor. An overview of the tibia test results is given in figure 5:

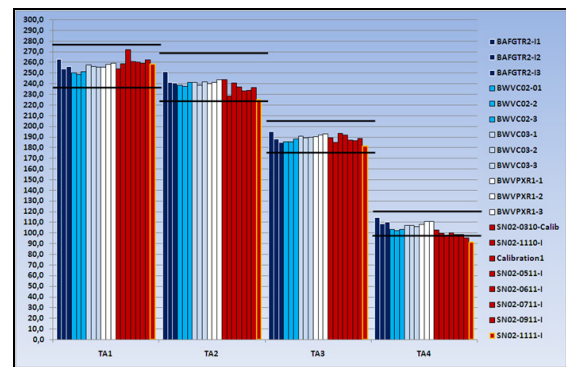


Figure 5. Tibia bending moment test results of inverse certification tests with SN02.

Almost all tibia results fulfilled the first draft inverse certification corridors. Only segment tibia 4 did not meet the draft corridor during the last two tests. Here, the exchange of the string potentiometers and the extension of the rubber material led to a noticeable decrease of the peak bending moments. A further significant decrease was also noted after the disassembly and reassembly of the impactor.

Figure 6 shows the knee ligament test results:

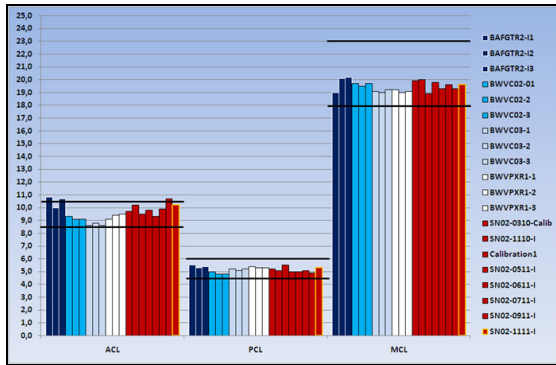


Figure 6. Knee ligament elongation test results of inverse certification tests with SN02.

All elongation results of the medial collateral and the posterior cruciate ligament met the draft inverse certification corridors. Only with the anterior cruciate ligament a few issues were detected in the course of the test series when the corridor was not met during three tests. An influence of the string potentiometer replacement, the rubber extension and the impactor disassembly and reassembly at BAST on test results was not noticed.

Table 2 demonstrates the comparatively low scatter of tests results with SN02 regardless the exchange of string potentiometers, extension of the rubber sheets and the disassembly and reassembly during the test series. While tibia segments 1-3 as well as MCL had a good repeatability with coefficients of variation below 3%, the repeatability of the remaining segments was still acceptable (CVs at or below 7%)

Table 2. Repeatability of SN02 test results.

	T1	T2	T3	T4	ACL	PCL	MCL
MV	257,53	238,70	188,78	103,90	9,62	5,17	19,46
SD	5,10	5,69	3,40	5,99	0,67	0,21	0,40
CV [%]	1,98	2,38	1,80	5,77	6,96	4,06	2,08
Max	271,80	251,30	194,90	114,50	10,80	5,50	20,20
Dev. from MV [%]	5,54	5,28	3,24	10,20	12,32	6,40	3,80
Min	248,50	224,90	181,10	91,00	8,60	4,80	18,90
Dev. From MV [%]	3,51	5,78	4,07	12,42	10,56	7,14	2,88
Max. dev. From MV	14,27	13,80	7,68	12,90	1,19	0,37	0,74
Max. dev. From MV [%]	5,54	5,78	4,07	12,42	12,32	7,14	3,80
Range	23,30	26,40	13,80	23,50	2,20	0,70	1,30

For a more detailed analysis of the test results, the time history curves of four of the inverse tests were investigated. Test #2 was performed with the FlexPLI in baseline condition, test #13 approximately one year later and after the replacement of the string potentiometers and extension of the rubber material, test #15 another year later and test #20 after the complete disassembly and reassembly of SN02. Figure 7 illustrates the time history curves for the tibia 2 results of the four tests:

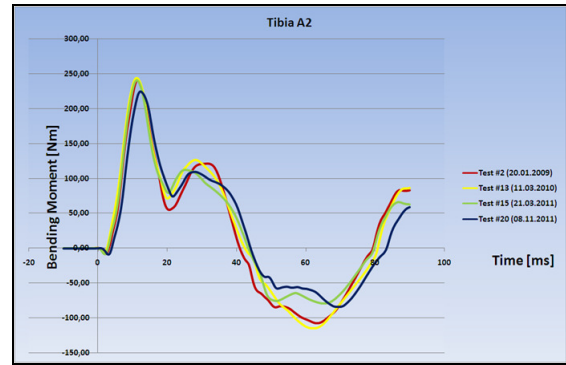


Figure 7. Tibia 2 time history curves of four inverse tests with SN02 at different build levels.

As observed for all SN02 segments, the repeatability during the primary impact phase was quite good. On the other hand, test #2 always showed the highest decay after the first peak. The test performed after the disassembly and reassembly procedure showed for most of the segments a slightly different behavior especially after reaching the maximum value.

The time history curves of the remaining segments can be found in the appendix.

Analysis

During a time period of approximately three years 20 inverse certification tests with SN02 were carried out at BAST. Four (out of seven) segments showed a good repeatability at least during the main impact phase. The repeatability of the ACL/PCL results was naturally lower than for most of the other segments. After the replacement of the string potentiometers and the rubber extension a decrease of the tibia 4 results was observed.

After the disassembly and reassembly of the impactor a decrease of the tibia results and slight change of the time history curves was noticed. From test #13 on the tibia 4 results constantly decreased. Altogether, no major influence of the physical damages reported by OICA on the test results was detected.

Long term performance of SN04

Inverse certification tests with FlexPLI prototype SN04 were performed at BAST during a time period of approximately 2,5 years. Before the start of the test series, the optional sensors including the aluminium brackets were removed. No further major exchange of parts nor calibration of particular sensors was observed. During the entire test period, SN04 was equipped with vinylester bone core material. All inverse certification tests at BAST were performed with long rubber material. Altogether, 14 inverse certification tests with SN04

were carried out between July 2009 and February 2012. Figure 8 presents the test results of the tibia segments:

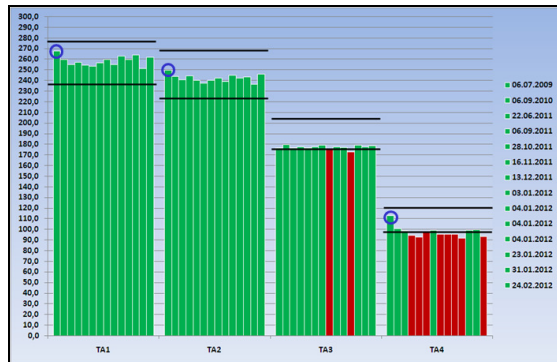


Figure 8. Tibia bending moment test results of inverse certification tests with SN04.

Nearly all tibia 1-3 test results met the first draft inverse certification corridors. On the other hand, the broad majority of the maximum loadings of tibia 3 and 4 was at the lower end or outside the draft corridors. Furthermore, test #1 provided the maximum results for three of the segments.

In terms of the ligament elongation results, all MCL and the majority of PCL results met the draft corridors while most of the ACL results were at the upper end or outside the corridor, as demonstrated in figure 9. Again, test #1 provided the maximum results for two of the elongations.

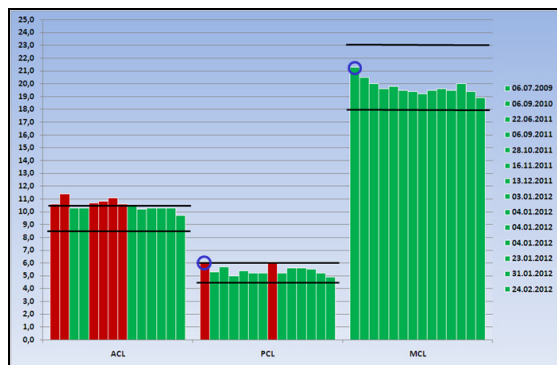


Figure 9. Knee ligament elongation test results of inverse certification tests with SN04.

Regarding the repeatability of test results, the observations made for SN02 were confirmed with SN04. Table 3 shows a good repeatability of the test results of tibia segments 1-3 and MCL. For the remaining segments, the coefficients of variation were still acceptable (CVs \leq 7%).

Table 3.
Repeatability of SN04 test results.

	T1	T2	T3	T4	ACL	PCL	MCL
MV	258,45	242,08	177,16	97,44	10,51	5,43	19,73
SD	4,65	3,50	1,82	5,28	0,42	0,36	0,59
CV [%]	1,80	1,45	1,03	5,42	3,96	6,72	3,01
Max	267,90	249,40	179,70	112,90	11,40	6,10	21,30
Dev. from MV [%]	3,66	3,02	1,43	15,86	8,50	12,37	7,97
Min	251,50	236,20	172,60	91,40	9,70	4,90	18,90
Dev. From MV [%]	2,69	2,43	2,58	6,20	7,68	9,74	4,20
Max. dev. From MV	9,45	7,32	4,56	15,46	0,89	0,67	1,57
Max. dev. From MV [%]	3,66	3,02	2,58	15,86	8,50	12,37	7,97
Range	16,40	13,20	7,10	21,50	1,70	1,20	2,40

For a further investigation of the robustness of test results, again the time history curves of four different tests were analyzed in detail and compared to those of SN02. Here, test #1 was chosen as it provided outliers for five segments. Tests #2 and #4 were carried out one year later each. Test #13 was the fourth test chosen.

Figure 10 shows the time history curves for the PCL elongation of SN04 during the four tests and gives a comparison to those of SN02.

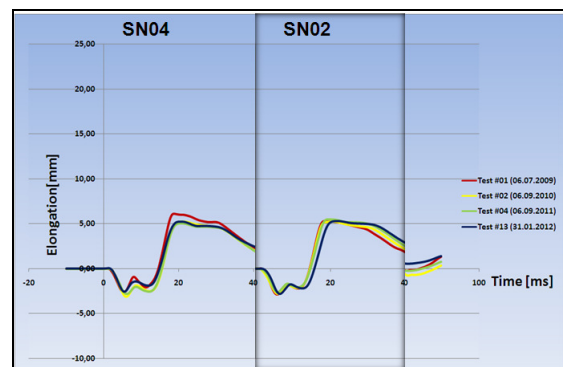


Figure 10. PCL time history curves of four inverse tests with SN04 and comparison to SN02.

As for most of the other segments, the SN04 curve characteristics showed a repeatable behavior and were quite alike to those of SN02 during the impact phase. However, test #1 contributed with the maximum result in many cases to an increase of scatter.

As for SN02, all other time history curves of SN04 are listed in the appendix.

Analysis

14 inverse certification tests with SN04 were carried out at BAST during approx. 2,5 years. As with SN02, the same four (out of seven) segments showed a good repeatability. The repeatability of ACL/PCL results was naturally lower than with most of the other segments.

Test #1, providing the maximum result for five (out of seven) segments and signing responsible for a significant repeatability decrease of Tibia A4, PCL and MCL, could be considered to some extent as being an outlier. This is of further importance because test #1 described the SN04 impactor condition before vehicle tests with different legforms carried out by OICA in August 2009 and reported within OICA (2012), showing lower curve levels and peak values of SN04 than of other impactors.

Altogether, all SN04 curve characteristics were comparable to those of SN02 during the primary impact phase.

REFINEMENT OF FULL ASSEMBLY CERTIFICATION CORRIDORS

Draft inverse and pendulum certification corridors had been proposed by the Japanese Automobile Research Institute (Konosu, 2009) and BAST (Zander, 2009-2) to and agreed by the Technical Evaluation Group (Flex-TEG) of GRSP using prototype legform impactors of the final build level GTR. After the issue of the first serial production legforms it has been found that the test performance of the impactors partly differed between the prototype and serial production build level, latter ones in various cases not fulfilling the draft certification corridors anymore. Thus, a subgroup of the IG GTR9-PH2 was tasked with the review and a possible update of the dynamic assembly certification corridors. Based on test results with three master legforms representing the latest serial production build level and tested in three experienced test houses, BAST undertook a recalculation of the first draft inverse and pendulum certification corridors.

Methodology

As impactors for the tests, two completely overhauled legforms (SN01 and SN03) as well as a new engineering leg (E-Leg) were chosen. The results of the tests in three different test houses were validated against the first draft corridors, which were, if necessary, re-calculated afterwards. The method used for updating the corridors was the procedure proposed by BAST to and agreed by Flex-TEG (Zander, 2009-2). First, based on the actual test results, reproducibility corridors were defined by picking the segments of all impactors having coefficients of variation (CVs) below 5%. From those, the pooled means for all segments were calculated and the reproducibility corridors were defined, considering a scatter of +/- 10% to the particular pooled means. Subsequently, the maxima and minima of all test results of each segment meeting the reproducibility corridors were

determined. Finally, the limits of the certification corridors were defined under consideration of scatter by adding 5% to the particular maxima and subtracting 5% from the corresponding minima.

Inverse certification test

Three completely overhauled or brand new serial production impactors were tested three times each in three experienced test labs. Altogether, 15 out of 189 segment results did not pass their corresponding first draft inverse certification corridor, most of them in section tibia 3, with borderline results at the lower end of the corridor for tibia 4 as well. On the other hand, the results for tibia 1-2 as well as the ligament elongations still looked promising, meeting those corridors in most of the cases (figures 11 and 12).

Table 4 illustrates that most of the segments delivered repeatable results with CVs below 5%. Only five out of 27 segments could not be used for the calculation of reproducibility corridors.

Table 4.
Repeatability of inverse test results with master legforms.

Segment	Tibia A1	Tibia A2	Tibia A3	Tibia A4	ACL	PCL	MCL
Setup 1							
Setup 2							
Setup 3							
Setup 4							
Setup 5							
Setup 6							
Setup 7							
Setup 8							
Setup 9							

After deleting the segments with insufficient repeatability, the remaining results were used for the definition of the reproducibility corridors, applying +/-10% to the pooled means of the particular segments:

Table 5.
Definition of reproducibility corridors for inverse certification test.

Segment	Tibia A1	Tibia A2	Tibia A3	Tibia A4	ACL	PCL	MCL
Setups for Reproducibility Corridor (CV < 5%)	15	15	15	15	123/173	123/173	123/173
Pooled Means with CV < 5%	243.93	220.47	177.61	100.74	8.95	4.91	19.09
Upper Limit	273.89	253.52	195.37	110.81	9.84	5.41	21.00
Lower Limit	224.08	207.42	159.85	90.67	8.05	4.42	17.18

All setups and segments with reproducible test results were then used for the definition of the inverse certification corridors by determination of their individual maxima and minima and consideration of scatter, adding 5% to their maxima and subtracting 5% from their minima:

Table 6.
Definition of certification corridors for inverse certification test.

Test #	Tibia A1	Tibia A2	Tibia A3	Tibia A4	ACL	PCL	MCL
Setup 1							
Setup 2							
Setup 3							
Setup 4							
Setup 5							
Setup 6							
Setup 7							
Setup 8							
Setup 9							
Maximum	259.98	240.13	183.73	193.27	9.60	5.49	20.20
Minimum	241.68	220.47	173.98	187.69	8.40	4.45	18.26
Max + 1.0% (consideration of scatter)	272.98	252.14	192.92	198.44	10.00	5.52	21.21
Min - 0.5% (consideration of scatter)	239.65	209.45	182.21	192.55	7.80	4.23	17.95
Certification Corridor Upper Limit	272	252	192	198	10	5	21
Certification Corridor Lower Limit	239	209	182	192	8	4	18

Figures 11 and 12 show the inverse test results with the three master legforms and their fitment within the first draft corridors (black) and the new corridors (green).

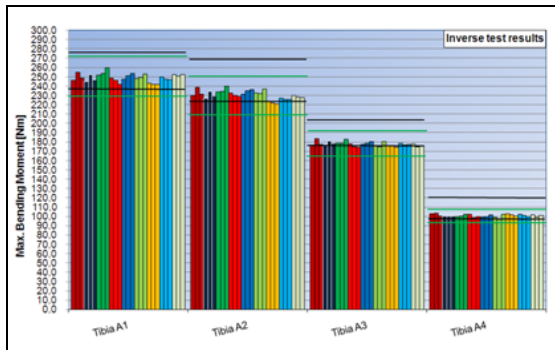


Figure 11. Tibia results of inverse certification tests with master legforms.

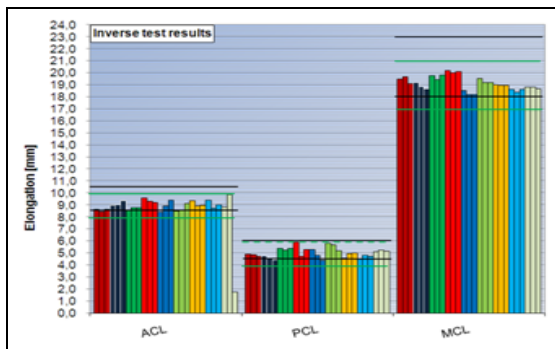


Figure 12. Ligament results of inverse certification tests with master legforms.

All regular certification test results passed well the new inverse corridors. Only one test failed due to an ACL potentiometer failure.

Pendulum certification test

As with the inverse test, three completely overhauled or brand new serial production impactors were pendulum tested three times each in three experienced test labs. In total, 35 out of the 189 segment results, most of them MCL

elongations and some ACL/PCL elongations did not pass their corresponding first draft pendulum certification corridor. While most tibia results were located well in the middle or the upper half of the corridors, most ligament results were borderline at the lower end or out of the corresponding corridor (figures 13 and 14).

As it can be seen in table 7, all segments performed well in terms of repeatability with CVs below 5% and could thus be used for the definition of the pendulum reproducibility corridors:

Table 7.
Repeatability of pendulum test results with master legforms.

Segment	Tibia A1	Tibia A2	Tibia A3	Tibia A4	ACL	PCL	MCL
Setup 1							
Setup 2							
Setup 3							
Setup 4							
Setup 5							
Setup 6							
Setup 7							
Setup 8							
Setup 9							

The reproducibility corridors, that were again calculated by drafting a 10% variance around the pooled means, are given in table 8:

Table 8.
Definition of reproducibility corridors for pendulum certification test.

Segment	Tibia A1	Tibia A2	Tibia A3	Tibia A4	ACL	PCL	MCL
Setup for Reproducibility Corridor (CV < 5%)	19	19	19	19	19	19	19
Pooled Mean with CV < 5%	253.34	203.09	153.32	102.63	9.38	4.20	22.40
Upper Limit	278.67	223.40	168.65	112.89	10.32	4.62	24.64
Lower Limit	228.00	182.78	137.99	92.36	8.44	3.78	20.16

Those setups and segments with reproducible test results were then again taken into account for the definition of the pendulum certification corridors, determining their individual maxima and minima and considering a scatter of 5%, added to their maxima and subtracted from their minima:

Table 9.
Definition of certification corridors for pendulum certification test.

Test #	Tibia A1	Tibia A2	Tibia A3	Tibia A4	ACL	PCL	MCL
Setup 1							
Setup 2							
Setup 3							
Setup 4							
Setup 5							
Setup 6							
Setup 7							
Setup 8							
Setup 9							
Maximum	259.94	208.81	158.31	106.09	9.99	4.51	23.59
Minimum	247.26	199.80	148.18	99.49	8.76	3.84	21.08
Max + 1.0% (consideration of scatter)	272.94	219.25	165.22	111.73	10.40	4.84	24.26
Min - 0.5% (consideration of scatter)	234.94	198.01	139.80	97.47	8.31	3.41	20.50
Certification Corridor Upper Limit	272	219	165	111	10.5	5	24
Certification Corridor Lower Limit	235	198	140	98	8	3.5	20.5

Figures 13 and 14 show all pendulum test results with the three master legforms and their fitment within the first draft corridors (black) and the new corridors (blue).

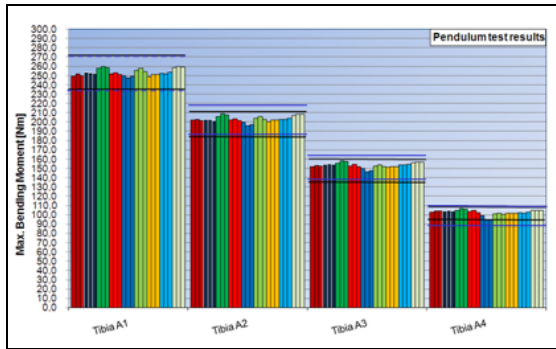


Figure 13. Tibia results of pendulum certification tests with master legforms.

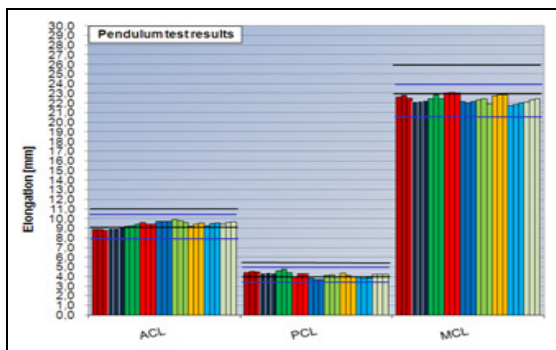


Figure 14. Ligament results of pendulum certification tests with master legforms.

All certification tests with the master legforms passed the new pendulum corridors.

Analysis

The inverse and pendulum certification corridors have been revised, taking into account the test data from three completely overhauled or brand-new legform impactors (master legforms). As a method of updating the corridors, the established method as agreed by the Flex-TEG was used.

Based on the available test data, the first draft inverse corridors have been further tightened for four segments and slightly widened for two segments for the establishment of the new inverse corridors. One corridor width remained unchanged. Furthermore, the first draft pendulum corridors have been widened for six segments in order to define the new pendulum corridors. One segment remained unchanged.

The inverse mid corridor for all segments was shifted downwards (between 2,3 and 7,8 percent), while the pendulum mid corridor for all ligaments was shifted downwards (between 7,5 and 9,5 percent), for two tibia segments upwards (2,5 and 3,4 percent), and for two tibia segments it remained almost unchanged. In order to comply with the latest requirements, a detailed check-up and, where

necessary, update of all previously built impactors is strongly recommended.

HARMONIZATION OF LOWER LEGFORM TO BUMPER TEST AREA

At the 1st meeting of the Informal Group GTR9-PH2 a request of the European Commission to amend the terms of reference of the IG was discussed. It was requested that this amendment would contain re-assessment of the legform test zone to counteract manufacturer's practice of making the bumper test area as narrow as possible by using different vehicle design means. There was consensus within the IG that no amendment of the terms of reference was needed as those already covered the general possibility of modifying the pedestrian test procedures for the legform impact. BAST detailed a proposal on how possibly modifying the legform test area.

Background

Within the current GTR9 test procedure, the bumper test area is defined as the "frontal surface of the bumper limited by two longitudinal vertical planes intersecting the corners of the bumper and moved 66 mm parallel and inboard of the corners of the bumpers" (UNECE, 2009). Several years ago the manufacturer's practice to keep the bumper test area narrow using means of design, resulting in possibly hard structures outside the bumper test area being unassessed, was already noted by Euro NCAP.

In order to also enable tests to and assessments of structures outboard of the bumper corners that are likely to be more injurious than in the adjacent inboard area, this problem was addressed by Euro NCAP (2012) by widening the bumper test area to either the ends of the bumper cross beam or the bumper corners, eliminating the 66 mm inboard distance, whatever area is larger, see figure 15:

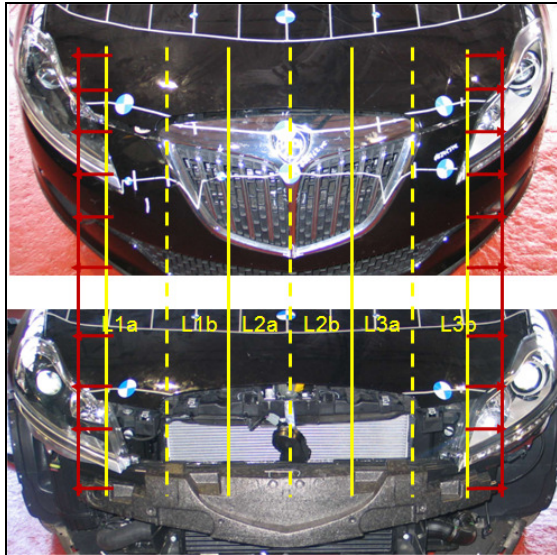


Figure 15. Bumper test area limited by bumper corners according to current GTR9 and former Euro NCAP Protocol (yellow limitations) and according to current Euro NCAP protocol (red limitations).

Though the current practice of Euro NCAP was a step into the right direction, the premature limitation of the bumper test area still needs to be investigated. An early draft of a bumper test procedure (1985) defined the corners of the bumper by the vehicle's point of contact with a straight edge which makes an angle of 45° with the vertical longitudinal plane of the vehicle and is tangential to the outer bumper surface. Within a draft proposal for a European Council Directive a change of the angle to 60° was implemented (EC, 1992). In 2002, the British Transport Research Laboratory (TRL) found an actual vehicle with very small bumper test width, just between the inner ends of the headlights, and therefore proposed to Working Group 17 of the European Enhanced Vehicle-safety Committee (EEVC WG 17) to change the angle back to 45° . However, WG 17 (2002) found that further research would be necessary and for the time being decided to keep the 60° .

Proposal for lower legform to bumper test area

A premature limitation of the width of the test area has been found to exclude potentially injurious structures on the vehicle front from being tested and assessed accordingly. Without in depth accident investigations the assumption has to be made that vehicle-to-pedestrian accidents addressed by the EEVC WG 17 procedures are equally distributed over the whole vehicle width; therefore the vehicle should be assessed accordingly. If legislation aimed at the limitation of the legform test zone e.g. by its definition by structural elements like cross beams, longitudinal beams etc.,

detailed information on impactor validation would be needed.

The aim of appropriately defining the bumper test area should be enabling the test lab to always test the most injurious impact locations. Therefore, as test area the whole width of the vehicle excluding the mirrors is proposed. For European Regulation, the test area is then to be subdivided into three equal parts:

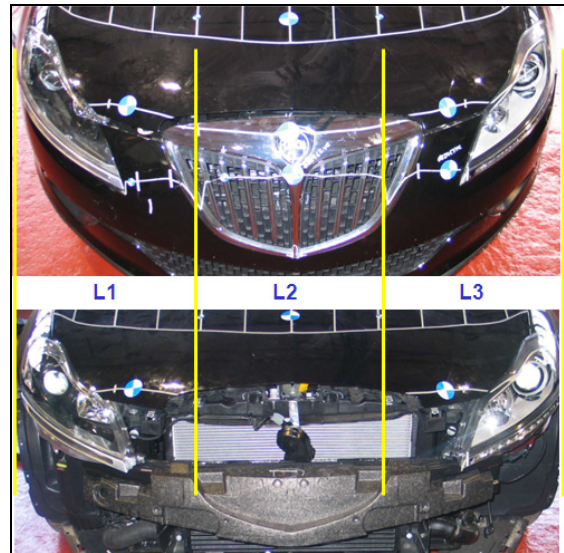


Figure 16. Bumper test area defined by the entire vehicle width (without mirrors).

Analysis of extended test area

During the latest discussions, a concern has been expressed that the legform impactors are unlikely to be appropriate test tools for application outside the bumper corners because high impactor rotation outside the current GTR test area could occur in case of the bumper being impacted at an angle smaller than 60° .

On the other hand, the bumper corners limiting the GTR9 legform test area are described in the EEVC WG 10 report already; here no indications with respect to impactor validation for selected impact angles are given. Up to now there is no proof for testing outside the current GTR test area necessarily providing unacceptable impactor rotation. Tests even outside the bumper corners were proven to sometimes provide higher or at least equal test results, as shown in figure 17:

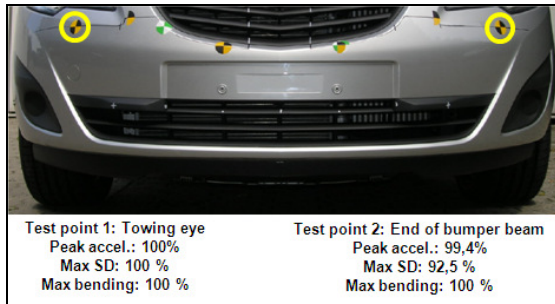


Figure 17. Testing outside bumper corners.

Furthermore, the bumper corners are defined using the outer bumper surface which is not relevant for the feasibility of tests. Altogether, no evidence for the inappropriateness of the extension is given.

As the proposal foresees tests to be performed on potentially injurious test points only, no further problems are expected. On test points with possibly high rotation of the impactor no tests should be conducted. Therefore, as before, the test lab is supposed to always check the structures behind the bumper cover / surface and thus to remove the bumper cover in order to decide whether a test makes sense or not.

COMPARATIVE VEHICLE TESTS

After the issue of the first serial production legforms it has been found that the performance between the prototypes used for the Technical Evaluation Group activities and the serial build level differed to some extent. To get a better understanding of the difference of real world performance within FlexPLI to bumper impacts, tests on vehicles formerly tested with the FlexPLI prototypes (Zander, 2009) have been repeated by BASt with the serial production legforms that were used for the establishment of the certification corridors.

Test overview

An overview of the tests is shown in figure 18:

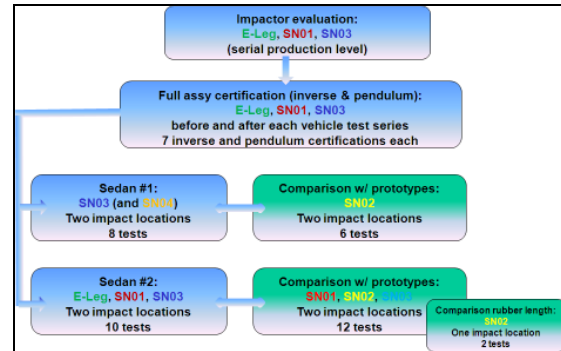


Figure 18. Vehicle tests with master legforms at BASt and comparison to prototype results.

Before and after each vehicle test series, a full assembly inverse as well as pendulum certification test was performed with each impactor. While the first vehicle (Sedan #1) was tested with the SN03 master leg three times each on two impact locations, the second vehicle (Sedan #2) was tested with all three master legforms three times each on the first impact location and one time with SN03 on a second impact location. The test series was amended by two tests with prototype SN04 against Sedan #1. The test results were then compared to those obtained with the FlexPLI prototypes SN01-SN03. In addition, the influence of long and short rubber sheets was investigated, using SN02 prototype at Sedan #2.

Full assembly certification tests.

All three master legforms used for the comparative study were inverse and pendulum certified before and after each test series. For the inverse certification tests, all impactors met the new corridors. However, it was noted that the results for tibia 4 were partly low to borderline. For the pendulum test, all impactor results for all segments except one tibia 4 and two PCL results were well within the new certification corridors. Altogether, the new corridors were entirely met by all impactors during every test.

Sedan #1 test results

Figures 19 and 20 show the tibia and knee test results on Sedan #1 that was tested on two different impact locations three times each with prototype impactor SN02 as well as with master leg SN03. Besides, one additional test was performed with prototype SN04 on both impact locations.

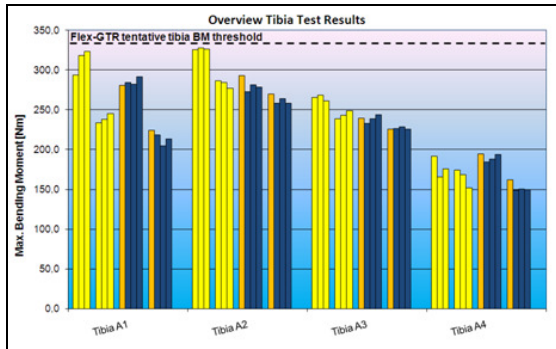


Figure 19. Tibia results of Sedan #1 tests with SN02 prototype (Y), SN03 master leg (B) and SN04 prototype (O) on two impact locations.

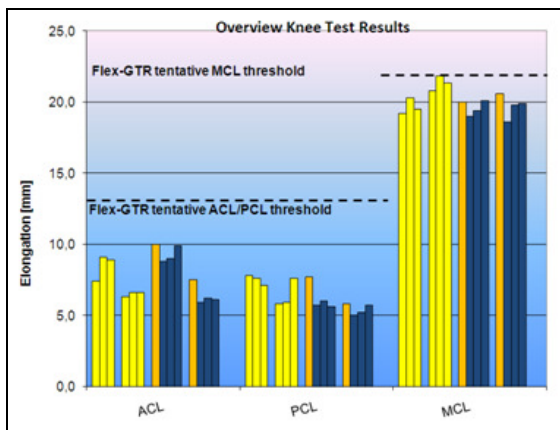


Figure 20. Knee results of Sedan #1 tests with SN02 prototype (Y), SN03 master leg (B) and SN04 prototype (O) on two impact locations.

It can be seen that all FlexPLI threshold values as proposed by the Flex-TEG were met in all tests with Sedan #1. A comparison of the test results on impact location #1 shows that the tibia 1-3 and PCL results were lower while tibia 4 as well as ACL gave higher results with the serial production leg. For MCL, no significant difference between prototype and master leg could be observed, see table 10:

Table 10.
Deviation of mean values of SN03 serial production leg from SN02 prototype – impact location #1.

	Tibia A1	Tibia A2	Tibia A3	Tibia A4	ACL	PCL	MCL
MY SN02	311.83	326.33	264.87	177.50	8.47	7.50	19.67
MV SN03	285.97	377.47	238.63	188.87	9.23	5.77	19.50
Dev. (%)	8.30	-14.57	9.30	6.40	9.86	23.11	-0.85

Tests on impact location #2 consistently showed lower results of the master legform SN03:

Table 11.
Deviation of mean values of SN03 serial production leg from SN02 prototype – impact location #2.

	Tibia A1	Tibia A2	Tibia A3	Tibia A4	ACL	PCL	MCL
MY SN02	238.07	282.27	243.50	164.97	6.50	6.43	21.30
MV SN03	212.20	260.00	227.03	149.77	6.07	5.30	19.43
Dev. (%)	-11.24	-7.89	-6.76	-9.21	-6.67	-17.62	-8.76

Furthermore, a slight tendency of SN04 to produce higher results than SN03 could be noted in most cases.

Table 12 demonstrates the repeatability of the SN02 prototype test results being partly marginal (CV > 7%) or unacceptable (CV > 10%):

Table 12.
Coefficients of Variation of SN02 prototype and SN03 master leg on Sedan #1.

Setup	Tibia 1	Tibia 2	Tibia 3	Tibia 4	ACL	PCL	MCL
Sedan #1 P1 SN02 Proto	5.05	0.34	1.43	7.43	10.97	4.81	2.89
Sedan #1 P2 SN02 Proto	2.45	1.75	2.10	7.08	2.66	15.72	2.35
Sedan #1 P1 SN03 Serial	1.76	1.55	2.24	2.51	6.35	3.61	2.86
Sedan #1 P2 SN03 Serial	3.28	1.33	0.69	0.44	2.52	6.80	3.72

The serial production leg SN03 shows an improved repeatability with all coefficients of variation in at least an acceptable range (CV ≤ 7%).

Sedan #2 test results

The results of the Sedan #2 tests are shown in figures 21 and 22:

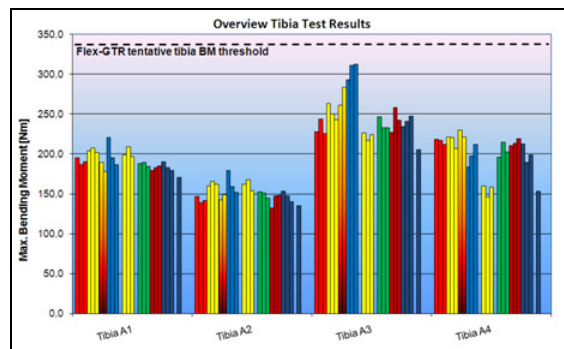


Figure 21. Tibia results of Sedan #2 tests with SN01 prototype + masterleg (R+DR), SN03 prototype + master leg (B+DB), SN02 prototype (Y), E-Leg masterleg (G) and SN02 prototype with long rubber (O) on two impact locations.

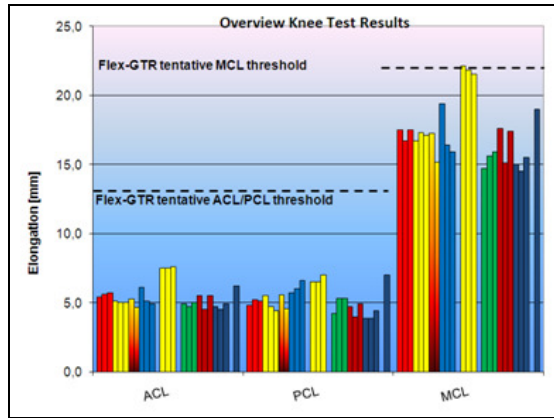


Figure 22. Knee results of Sedan #2 tests with SN01 prototype + masterleg (R+DR), SN03 prototype + master leg (B+DB), SN02 prototype (Y), E-Leg masterleg (G) and SN02 prototype with long rubber (O) on two impact locations.

All but one test passed on Sedan #2 the TEG tentative tibia and knee threshold values. Only the MCL requirement was failed once with the SN02 prototype. On impact location #1 the tests performed with the serial production legforms resulted in generally lower values than those with the prototype impactors, as it can be seen in table 13:

Table 13.
Deviation of mean values of serial production legs from prototypes – impact location #1.

	Tibia A1	Tibia A2	Tibia A3	Tibia A4	ACL	PCL	MCL
INV SN03 SN03	198.59	156.21	263.31	209.01	5.32	5.32	17.17
INV E-Leg SN01 SN03	184.56	146.40	240.29	206.29	4.91	4.91	15.70
Dev. [%]	-7.01	-6.28	-8.74	-1.98	-7.72	-15.42	-8.54

On impact location #2, most results (except PCL) were again lower with the serial production impactor SN03 (table 14), however, the statistical significance of this comparison is limited because only one test was performed with SN03.

Table 14.
Deviation of SN03 serial production leg results from mean values of SN02 prototype – impact location #2.

	Tibia A1	Tibia A2	Tibia A3	Tibia A4	ACL	PCL	MCL
INV SN02	201.40	161.37	222.57	154.07	7.53	6.67	21.00
Single Feet SN03	170.20	125.40	205.20	153.00	6.20	7.00	16.00
Dev. [%]	-15.44	-16.09	-7.00	-1.00	-17.70	5.00	-12.04

Table 15 shows the repeatability of the prototype against serial production legform test results. While the scatter of the cruciate ligament elongations sometimes remains unacceptable ($CV > 10\%$), the tibia repeatability is improved, having all CVs in an acceptable range ($\leq 7\%$). The scatter of the knee results has partly increased.

Table 15.
Coefficients of Variation of prototypes and master legs on Sedan #2.

Setup	Tibia 1	Tibia 2	Tibia 3	Tibia 4	ACL	PCL	MCL
Sedan #2 P1 SN01 Proto	2.18	2.78	4.18	1.59	2.74	4.14	2.68
Sedan #2 P1 SN02 Proto	1.40	1.82	4.01	3.69	1.15	11.68	1.79
Sedan #2 P1 SN03 Proto	8.74	8.83	3.57	7.09	11.98	7.51	10.99
Sedan #2 P2 SN02 Proto	3.36	4.23	2.38	4.87	0.77	4.33	1.38
Sedan #2 P1 Eleg Serial	1.28	2.78	3.36	4.64	3.14	12.37	4.06
Sedan #2 P1 SN01 Serial	1.74	6.33	6.45	2.10	11.17	10.42	8.32
Sedan #2 P1 SN03 Serial	2.99	4.47	2.64	5.83	4.26	7.10	3.33

The influence of the rubber length evaluated with SN04 shows inconsistent results, depending on the location of the particular vehicle load paths:

Table 16.
Deviation of results with impactor SN02 with long rubber sheets to those with short rubber sheets – impact location #1.

	Tibia A1	Tibia A2	Tibia A3	Tibia A4	ACL	PCL	MCL
INV SN02 SR	204.47	162.67	252.20	215.10	5.03	4.87	17.03
INV SN02 LR	184.3	146.0	272.8	225.1	5.0	5.1	16.3
Dev. [%]	-9.89	-10.25	8.17	4.60	-0.66	4.79	-4.60

Analysis

18 impactor tests with three different serial production impactors (E-Leg, SN01 and SN03) and SN04 on two different vehicles were carried out at BASt.

The master legforms have been successfully inverse and pendulum certified according to the TF-RUCC corridor proposal before and after each vehicle test series. All test results entirely met the tentative FlexPLI thresholds for tibia bending moments as well as ligament elongations.

A comparison of the serial production impactor test results with prototype results on identical impact locations shows that the serial production impactors are producing in most cases lower output values than the prototypes. This observation is in line with the inverse certification tests presented in this study.

The repeatability of vehicle test results shows an improvement regarding the tibia segments while the scatter in the knee has partly even increased.

The influence of the length of the rubber sheets on the test results is inconsistent and seems to depend on the location of the particularly impacted load paths.

STATUS OF DEVELOPMENT AND EVALUATION OF AN UPPER BODY MASS FOR THE FLEX-PLI

Though the FlexPLI has been proven to have biofidelic properties for an improved assessment of knee and tibia injuries in lateral vehicle-to-pedestrian accidents, the biofidelity of the femur section still needs to be improved, reason why the output of the femur strain gauges is not yet being considered for the assessment of femur injuries.

Thus, an upper body mass (UBM) for the FlexPLI that had been developed in a first step within the FP6 project APROSYS by Bovenkerk et al. (2009), was validated in a second step within tests of different car front shapes and against full scale vehicle to dummy tests with applied FlexPLI by Zander et al. (2009 and 2011). In latter study it was found that the maximum loadings of most of the segments were comparable in component tests with UBM and full scale tests, but that the characteristics of the corresponding time history traces were not always fully alike. While tests against further vehicle frontend shapes should amend the data basis, an optimization of the kinematics and impactor response could be done by vertical and longitudinal UBM alignment, based on additional simulations and component tests. In a third step, an FE model of the UBM was developed on the LS DYNA platform by BAST (Methner, 2012) and applied to the FlexPLI FE model. Simulations with the FlexPLI-UBM against a generic car frontend with adjustable load paths were carried out within the FP 7 project IMVITER by Eggers et al. (2012):

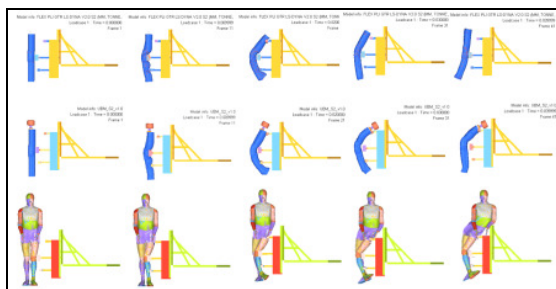


Figure 23. Simulations with baseline FlexPLI, FlexPLI-UBM and THUMS against test rig.

Those simulations were then compared to impactor tests with applied upper body mass against a validation rig:

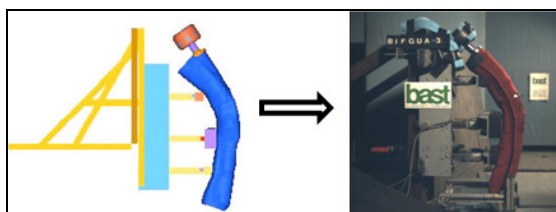


Figure 24. FlexPLI-UBM simulations and impactor tests against test rig.

As already indicated within previous studies, for the sedan and SUV frontend, the FlexPLI with upper body mass showed a much better kinematic correlation with full human body simulation model than the baseline impactor. On the other hand, impactor tests with applied UBM had to be conducted at comparatively low impact speeds. The

generic car frontend needs appropriate modifications so that tests at impact speeds around 40 kph will be possible.

In the long run, the bumper test with baseline FlexGTR and the test of the bonnet leading edge with upper legform impactor which is still carried out within European Legislation as well as the Euro NCAP test programme should be replaced by a unique test with FlexPLI-UBM to appropriately assess tibia, knee as well as femur injuries. Further research in this context is needed and should focus on the correlation between the impactor threshold values and the underlying injuries predicted by human models.

DISCUSSION

The flexible pedestrian legform impactor FlexPLI has been evaluated by a Technical Evaluation Group of GRSP from 2005 to 2010. Aim was the introduction of the FlexPLI within the UN global technical regulation on pedestrian safety (UN-GTR9). However, GRSP found that the FlexPLI was at that stage not ready for legislation and therefore mandated an informal group to address all open issues related to the FlexPLI for being implemented within a second phase of the GTR. This paper presents several studies carried out by the German Federal Highway Research Institute BAST as contribution to the work of the IG. An investigation of the estimated cost reduction in Germany due to the introduction of the FlexPLI results in around 44 Mio € to be annually saved.

A long term study proves the test results with both the FlexPLI at prototype status with polyester bone core material as well as equipped with vinylester bone cores, despite some physical wearing, as being very robust. However, the overall performance between the latest prototype build level and the serial production status have been found to differ to some extent. Therefore, BAST drafted new assembly certification corridors for both the dynamic inverse as well as the pendulum certification test. The FlexPLI serial production legform having a lower output than the prototype was confirmed in a comparative study with tests against vehicles that had been previously tested with FlexPLI prototypes. Thus, a downwards shift of the current draft FlexPLI impactor thresholds (UNECE, 2012) according to the actual performance within the inverse certification tests, as already proposed by BAST to the IG (Zander, 2012-6), seems reasonable.

A modified definition of the assessment area for lower legform to bumper tests has been proposed by BAST to address manufacturer's practice to reduce its width by design elements. The proposal that foresees to also test points outside the area limited by the bumper corners is expected to be

feasible for both, the EEVC WG 17 legform impactor described in the current GTR9 as well as the new FlexPLI for GTR9-PH2.

An improved injury assessment ability of the femur section of the FlexPLI will be addressed with the introduction of an upper body mass representing the pedestrian's torso. Evaluation activities are still ongoing by amending the data basis and developing corresponding correlations between human body models and the FlexPLI with applied upper body mass.

CONCLUSIONS

The FlexPLI prototype build level that has been evaluated and subsequently proposed by the Flex-TEG for the implementation within global technical regulation on pedestrian safety was not ready for legislation at that stage.

The remaining open issues are being addressed by the GRSP Informal Group on GTR9 Phase 2. After the finalization of the work of the informal group, the GTR-PH2 is expected to be adopted by GRSP in December 2013 and subsequently voted by WP.29 in June 2014.

Ideally, a modified bumper test area will be implemented from the start. However, the progress of the Task Force Bumper Test Area won't delay the finalization of the work of the informal group.

The evaluation of the FlexPLI with applied upper body mass requires further research and thus needs to be addressed within a third phase of the global technical regulation on pedestrian safety.

REFERENCES

Bovenkerk J., Zander O. 2009. "Evaluation of the extended scope for FlexPLI obtained by adding an upper body mass." Deliverable D333H of the European FP6 research project on Advanced Protection Systems (APROSYS).

Commission of the European Communities. 1992. "Draft proposal for a Council Directive adapting to technical progress Council Directive 74/483/EEC relating to the external projections of motor vehicles including their effect on pedestrians." Document III/4025-92. Brussels, April 1992.

Eggers A., Schwedhelm H., Zander O., Puppini R., Puleo G., Mayer C., Kumar N., Jacob C., Beaugonin M. 2012. "Analysis of new simulation technologies for pedestrian safety. Potential of VT to fully substitute RT for this purpose." Deliverable D6.1 of the European FP7 research project on Implementation of Virtual Testing in Safety Regulations (IMVITER).

European Enhanced Vehicle-safety Committee. 2002. "EEVC WG 17 11th meeting minutes." EEVC WG 17 Doc 197R1. May 2002.

European New Car Assessment Programme (Euro NCAP). 2012. "Pedestrian Testing Protocol Version 6.2" December 2012

Konosu A. (JARI). 2009. "Requirement Corridor (BASt-Method) for Pendulum Type (Type 3) Dynamic Calibration Test Method." Doc TEG-120 of 10th Meeting of the GRSP Flex PLI Technical Evaluation Group. Bergisch Gladbach, Germany, December 1st – 2nd 2009.

Methner F. 2012. "Development of an Upper Body Mass (UBM) simulation model for the Flexible Pedestrian Legform Impactor (FLEX-PLI-GTR)". Internal report of BASt. January 2012.

OICA. 2011. "FlexPLI Version GTR Prototype SN-02 - Durability Assessment." Doc GTR9-1-04 of 1st Meeting of the GRSP IG GTR9-PH2. Geneva, Switzerland, December 1st-2nd 2011.

OICA. 2012. "FlexPLI Comparison - Revision 1." Doc GTR9-2-10-r1 of 3rd Meeting of the GRSP IG GTR9-PH2. Paris, France, May 29th-30th 2012.

Transport Research Laboratory. 2002. "Suggestions for EEVC WG 17 test procedures and for EC draft directive." EEVC WG 17 Doc 186. May 2002.

United Nations Economic Commission for Europe. 2009. "Addendum to global registry, created on 18 November 2004, pursuant to Article 6 of the agreement concerning the establishing of global technical regulations for wheeled vehicles, equipment and parts which can be fitted and/or be used on wheeled vehicles (ECE/TRANS/132 and Corr.1). Done at Geneva on 25 June 1988: Global technical regulation No. 9 Pedestrian Safety (Established in the Global Registry on 12 November 2008)."

United Nations Economic Commission for Europe. 2012. "Economic Commission for Europe, Inland Transport Committee, World Forum for Harmonization of Vehicle Regulations, Working Party on Passive Safety Fifty-second session Geneva, 11–14 December 2012 Item 4(a) of the provisional agenda Global technical regulation No. 9 (Pedestrian safety) – Phase 2 of the global technical regulation Proposal for Amendment 2 (DRAFT-ver.121206) Submitted by the chairperson of informal working group on Global technical regulation No. 9 (Pedestrian safety)-Phase 2*." Doc GTR9-5-29 of 5th Meeting of the GRSP IG GTR9-PH2. Bergisch Gladbach, Germany, December 6th-7th 2012.

Zander O., Gehring D., Leßmann P., Bovenkerk J. 2009. "Evaluation of a flexible pedestrian legform impactor (FlexPLI) for the implementation within legislation on pedestrian protection." Paper no. 09-0277 of 21st ESV conference proceedings.

Zander O. 2009-2. "Finalisation of Impact and Assessment Conditions for Inverse Certification Test." Doc TEG-119 of 10th Meeting of the GRSP Flex PLI Technical Evaluation Group. Bergisch Gladbach, Germany, December 1st – 2nd 2009.

Zander O., Gehring D., Leßmann P. 2011. "Improved assessment methods of lower extremity injuries in vehicle-to-pedestrian accidents using impactor tests and full scale dummy tests." Paper no. 11-0079 of 22nd ESV conference proceedings.

Zander O. 2012. "Proposal for a Modification of the Bumper Test Area for Lower and Upper Legform to Bumper Tests." Doc GTR9-2-03 of 2nd Meeting of the GRSP IG GTR9-PH2. Osaka, Japan, March 28th-29th 2012.

Zander O. 2012-2. "Robustness of SN02 prototype test results - Revision 1." Doc GTR9-2-04r1 of 2nd Meeting of the GRSP IG GTR9-PH2. Osaka, Japan, March 28th-29th 2012.

Zander O. 2012-3. "Robustness of SN04 prototype test results." Doc GTR9-3-05 of 3rd Meeting of the GRSP IG GTR9-PH2. Paris, France, May 29th-30th 2012.

Zander O. 2012-4. "Comparison of FlexPLI Performance in Vehicle Tests with Prototype and Series Production Legforms." Doc GTR9-4-14 of 4th Meeting of the GRSP IG GTR9-PH2. Washington, United States of America, September 17th-19th 2012.

Zander O. 2012-5. "Refinement of Corridors for FlexPLI Dynamic Assembly Certification Tests." Doc TF-RUCC-4-04 of the 4th Meeting of the Task Force Review and Update Certification Corridors (TF-RUCC) of the IG GTR9-PH2. June 18th, 2012.

Zander O. 2012-6. "Verification of Draft FlexPLI prototype impactor limits and application to FlexPLI serial production level." Doc GTR9-5-20 of 5th Meeting of the GRSP IG GTR9-PH2. Bergisch Gladbach, Germany, December 6th-7th 2012.

Zander O., Pastor C. 2012. "Estimation of Cost Reduction due to Introduction of FlexPLI within GTR9." Doc GTR9-5-19 of 5th Meeting of the GRSP IG GTR9-PH2. Bergisch Gladbach, Germany, December 6th-7th 2012.

APPENDIX

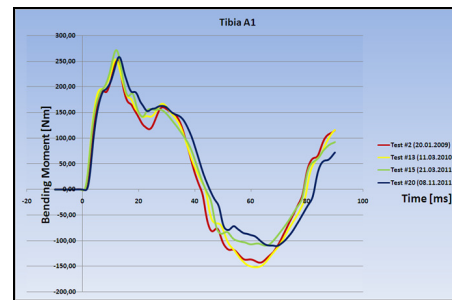


Figure 25. Tibia 1 time history curves of four inverse tests with SN02 at different build levels.

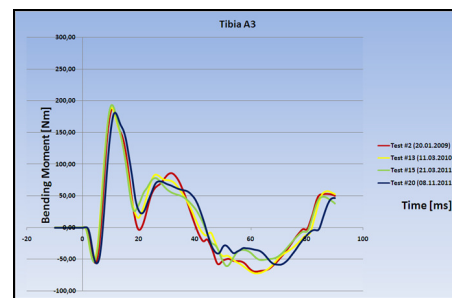


Figure 26. Tibia 3 time history curves of four inverse tests with SN02 at different build levels.

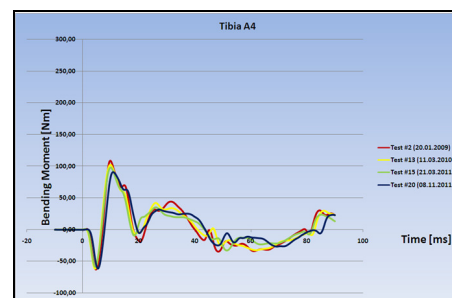


Figure 27. Tibia 4 time history curves of four inverse tests with SN02 at different build levels.

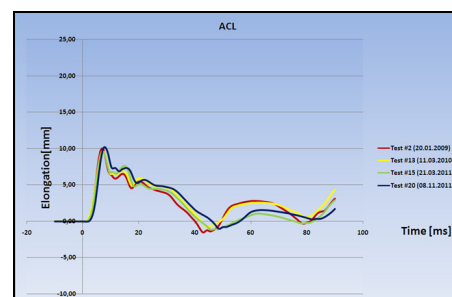


Figure 28. ACL time history curves of four inverse tests with SN02 at different build levels.

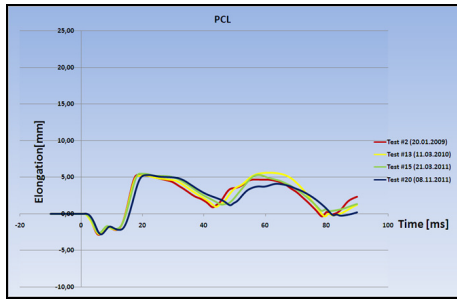


Figure 29. PCL time history curves of four inverse tests with SN02 at different build levels.

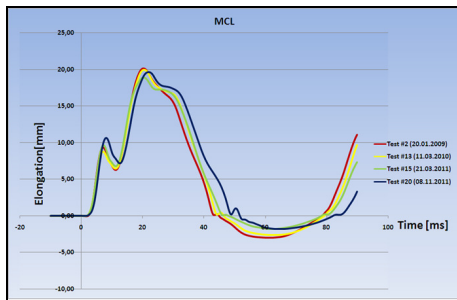


Figure 30. MCL time history curves of four inverse tests with SN02 at different build levels.

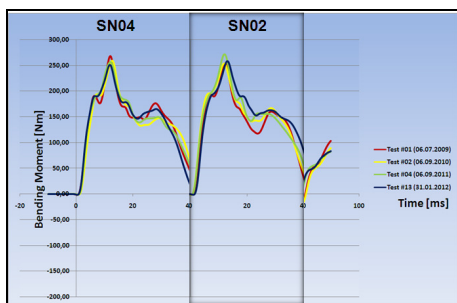


Figure 31. Tibia 1 time history curves of four inverse tests with SN04 and comparison with SN02.

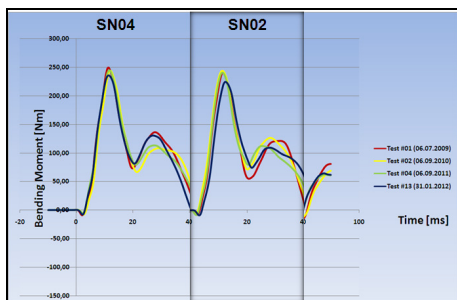


Figure 32. Tibia 2 time history curves of four inverse tests with SN04 and comparison with SN02.

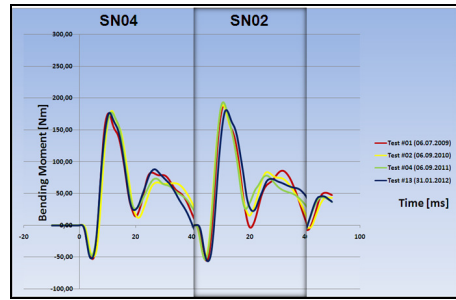


Figure 33. Tibia 3 time history curves of four inverse tests with SN04 and comparison with SN02.

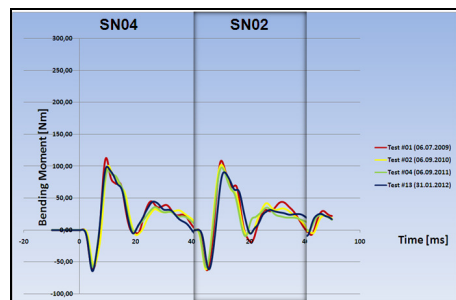


Figure 34. Tibia 4 time history curves of four inverse tests with SN04 and comparison with SN02.

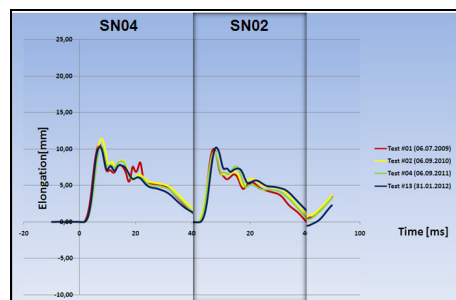


Figure 35. ACL time history curves of four inverse tests with SN04 and comparison with SN02.

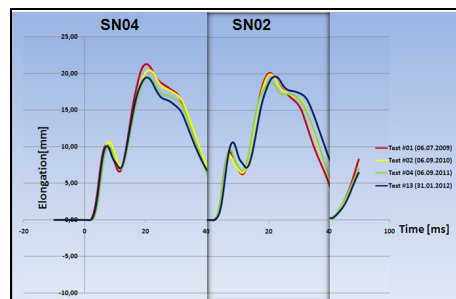


Figure 36. MCL time history curves of four inverse tests with SN04 and comparison with SN02.

IMPROVED SAFETY OF BICYCLISTS IN THE EVENT OF A COLLISION WITH MOTOR VEHICLES AND DURING SINGLE ACCIDENTS

Oliver Zander

Federal Highway Research Institute (BASt)
Germany

Dirk-Uwe Gehring

Peter Leßmann

BGS Böhme & Gehring GmbH
Germany
Paper Number 13-0180

ABSTRACT

Recent accident statistics from the German national database state bicyclists being the second endangered group of vulnerable road users besides pedestrians. With 399 fatalities, more than 14.000 seriously injured and more than 61.000 slightly injured persons on German roads in the year 2011, the group of bicyclists is ranked second of all road user groups (Statistisches Bundesamt, 2012). While the overall bicycle helmet usage frequency in Germany is very low, evidence is given that its usage leads to a significant reduction of severe head injuries.

After an estimation of the benefit of bicycle helmet usage as well as an appropriate test procedure for bicyclists, this paper describes two different approaches for the improvement of bicyclist safety. While the first one is focusing on the assessment of the vehicle based protection potential for bicyclists, the second one is concentrating on the safety assessment of bicycle helmets.

Within the first part of the study the possible revision of the existing pedestrian testing protocols is being examined, using in depth accident data, full scale simulation and hardware testing.

Within the second part of the study, the results of tests according to supplemental test procedures for the safety assessment of bicycle helmets developed by the German Federal Highway Research Institute (BASt) are presented.

An additional full scale test performed at reduced impact speed proves that measures of active vehicle safety as e.g. braking before the collision event do not necessarily always lead to a reduction of injury severity.

INTRODUCTION

Almost one out of ten fatally injured road users in Germany in 2011 was a bicyclist. Altogether, 76.750 bicyclists have been injured, thereof 399 fatally and 14.437 seriously (Statistisches

Bundesamt, 2012). Despite this huge number of fatally and seriously injured bicyclists on German roads the average helmet usage frequency is at 6 percent only, whereas the helmet usage frequency of those bicyclists aged 10 years or younger is at 53 percent and thus significantly higher than the helmet usage frequency of the bicyclists aged 17 years or older (between 2 and 4 percent only) (Otte et al., 2008). Despite these facts, when using a bicycle helmet, the head injury severity can be reduced significantly.

After estimating the potential benefit of wearing a bicycle helmet as well as of introducing a test procedure for evaluating the passive cyclist safety potential of vehicle frontends, two different approaches for the improvement of the safety of bicyclists in the event of a collision with a motor vehicle are presented.

An additional full scale test at reduced impact speed is used for the investigation of the impact of vehicle braking before the collision event on the risk of head injuries.

BENEFIT ESTIMATION

Bicycle usage benefit estimation

Figure 1 gives an overview of the distribution of the AIS head injury severity of bicyclists suffered due to a collision with a motor vehicle in Germany:

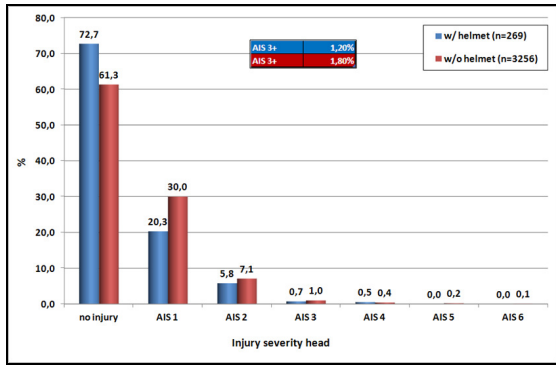


Figure 1. AIS distribution of bicyclist head injuries in Germany (Otte et al., 2008)

It can be seen that the proportion of bicyclists involved in accidents with motor vehicles not suffering any heard injury is significantly higher when wearing a helmet. Besides, the helmet usage leads to approx. 33 % reduction of the portion of AIS 3+ head injuries. Those facts indicate that bicyclists benefit in terms of both, less as well as more severe head injuries when wearing a bicycle helmet.

Test procedure benefit estimation

An investigation of the German In-Depth Accident Study (GIDAS, 2012) resulted in 3804 bicyclists involved in collisions with motor vehicles, thereof 3104 not wearing a helmet. Altogether, 9133 injuries were recorded, thereof 2451 injuries (27 percent) within vehicle zones addressed to a certain extent by the current pedestrian test procedure according to Euro NCAP (2013), and to another portion by a lateral and longitudinal extension of this test zone, having the first contact of the cyclist between -85 and +85 cm along the lateral vertical vehicle plane as shown in figure 2.

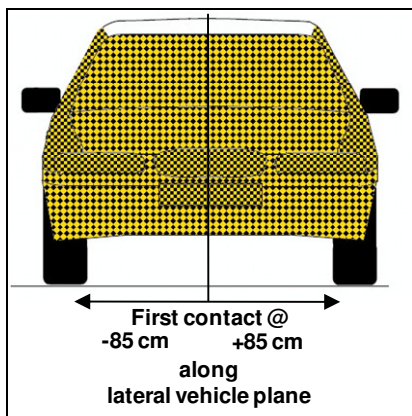


Figure 2. Definition of addressed zones on vehicle front.

442 of the detected injuries were head injuries (18 percent), thereof 424 (96 percent) suffered while the head of the cyclist being unprotected (figure 3).

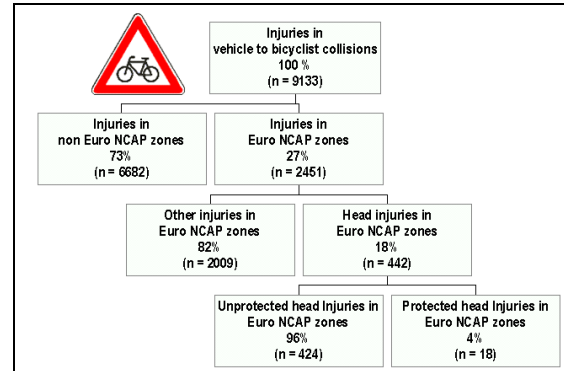


Figure 3. Portion of bicyclist head injuries covered by Euro NCAP pedestrian test zones.

Figure 4 demonstrates that 50 percent or more of all AIS 3 and AIS 4 bicyclist head injuries where the head being unprotected occurred within zones addressed by the described extended Euro NCAP testing protocol.

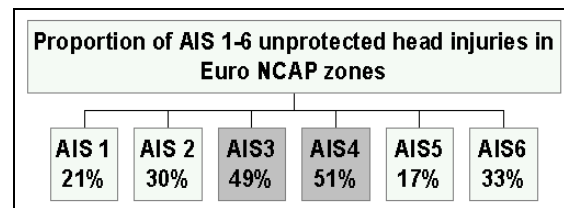


Figure 4. Portion of bicyclist head injuries covered by Euro NCAP pedestrian test zones.

APPROACHES FOR THE IMPROVEMENT OF BICYCLIST SAFETY

Within the following chapter two different approaches towards an improvement of the safety of bicyclists in the event of a collision with a motor vehicle are described. While the first one is based on the assessment of the protection potential of vehicle frontends, the second one is dealing with an enhanced safety assessment of bicycle helmets.

Vehicle based safety assessment

As a starting point for a possible introduction of a test procedure for the assessment of the safety of vehicle frontends, a comparison of pedestrian and cyclist accidents should figure out the principal differences in the impact behavior of those two groups of vulnerable road users. This can be done by means of in-depth accident data, human modeling and virtual testing as well as within full scale tests.

In-depth accident data The investigated GIDAS sample (2012) consists of 1414 pedestrian accidents and 2262 cyclist accidents with motor vehicles having the first contact between -85 and +85 cm along the lateral vertical vehicle plane. Figure 5 illustrates the cumulative wrap around distances (WAD) for the pedestrian and cyclist head impacts at all collision speeds.

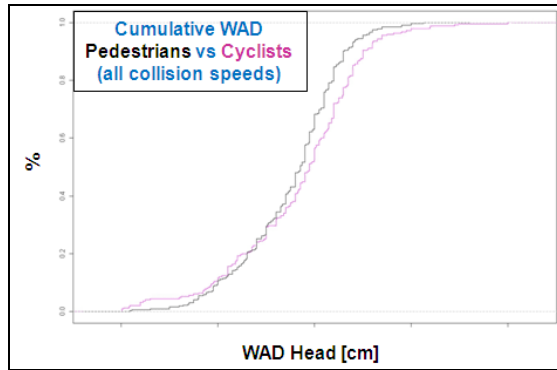


Figure 5. Cumulative wrap around distances (WAD) of pedestrians and cyclists head impacts at all collision speeds.

It can be seen that the head of the cyclists tends to generally impact the vehicle front rearwards of the pedestrian head.

Figure 6 is focusing on accidents at a collision speed of 40 kph or lower. 1032 pedestrian accidents and 1699 cyclist accidents with motor vehicles having the first contact between -85 and +85 cm along the lateral vertical vehicle plane emphasize the observation of pedestrian heads impacting more rearwards on the vehicle front than those of cyclists.

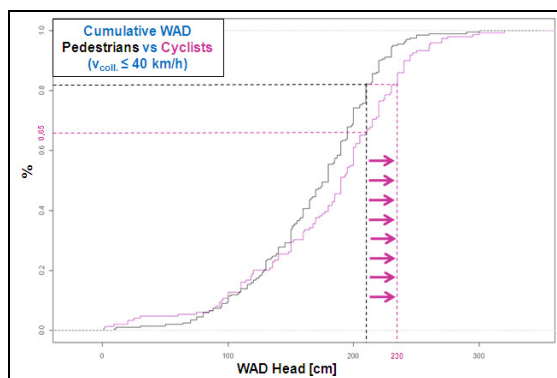


Figure 6. Cumulative Wrap around distances (WAD) of pedestrians and cyclists head impacts at collision speeds up to 40 kph.

Here, WAD 2100 covers approx. 80 % of all pedestrian but only 65 % of all cyclist head impacts. Equal effectiveness for cyclists, i.e. coverage of 80% of all cyclist head impacts, could

be expected by a rearward extension of the head impact area to WAD 2300. Although the definition of the wrap around distances taken from GIDAS and used within this dataset differs from the one according to the pedestrian test procedures (Euro NCAP, 2012), the trend of cyclist head impacts generally taking place rearward of the pedestrian head impacts is obvious.

Human modeling and virtual testing Within the FP6 project APROSYS (Advanced Protection Systems) funded by the European Commission, the impact conditions of pedestrians and cyclists have been studied in detail, using human model simulations and virtual test methods. Here, it has been found that independent from the vehicle shape the cyclist head impact is generally located further back on a vehicle, often beyond WAD 2100 (figure 7).

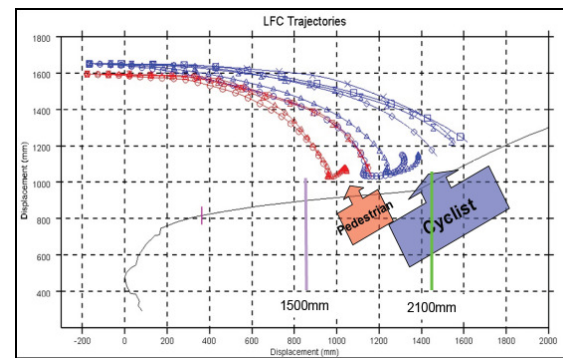


Figure 7. Head impact locations of cyclists vs. pedestrians on large family cars derived from human model simulations (Watson et al., 2009).

On the other hand, large bonnet leading edge heights tend to prevent cyclists sliding up the bonnet so that the corresponding head impact locations are more frequently within the current pedestrian head impact zones (Watson et al., 2009).

In terms of head impact angles, partly significant differences between pedestrian and cyclist head impacts were found. For multi-purpose vehicles, supermini vehicles and large family cars the cyclist head impact angles were found being shallower than those of the pedestrian. The fourth vehicle category, sports utility vehicles, produced the highest head impact angles for both, pedestrians and cyclists (figure 8):

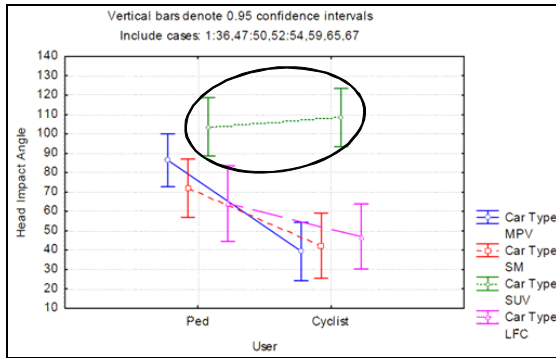


Figure 8. Head impact angles of cyclists vs. pedestrians on four different vehicle categories derived from human model simulations (Watson et al., 2009).

APROSYS also investigated possible modifications of currently available pedestrian impactors for the purpose of improving the pedestrian test procedures towards a consideration of the protection of cyclists. The current pedestrian head impactors were seen as a suitable basis for cyclist safety enhancement, but it was also stressed that the partly greater rotational motion of the cyclist head needs to be taken into account (Deck et al., 2008). Thus, new criteria for the risk of diffuse axonal injuries (DAI), subdural haematomas (SDH) and skull fractures were proposed by Deck et al. and modified head impactors, such as shown in figure 9, were developed by Brüll et al. (2009), considering amongst others the rotational aspects of head impacts of pedestrians as well as of cyclists.

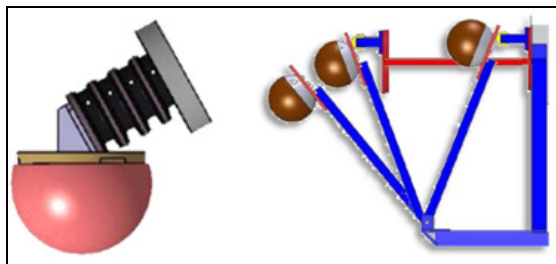


Figure 9. Head neck impactor and pendulum impactor (Brüll et al., 2009)

Full scale tests A series of five full scale tests with a sedan shaped car against an adult and a child dummy seated on an adult bicycle was carried out at BASt. While the head of the Hybrid II 50th percentile adult dummy placed on the bicycle seat was unprotected, the three years old Q3 child dummy in the child seat was wearing a bicycle helmet during all tests. Five different bicycles of different frame and wheel sizes as well as two different child seats were used. The repeatability of the test setup in terms of upmost points of the HII dummy head and the bicycle helmet was acceptable, as can be seen in figure 10. The vehicle

speed was 40 kph in all tests, the aimed first point of contact of the adult dummy was at vehicle longitudinal centerline.

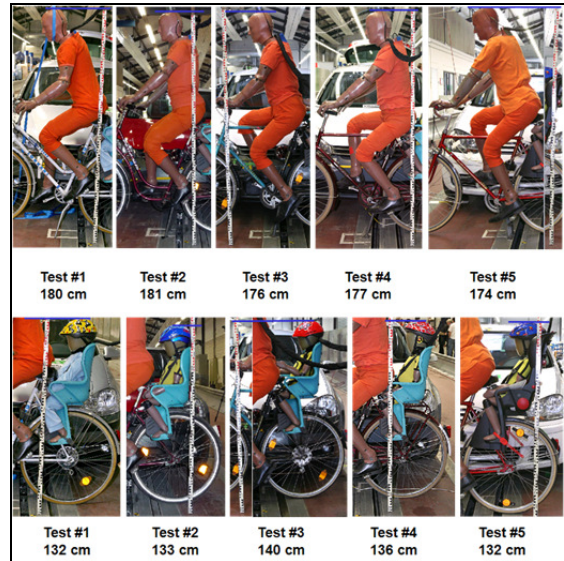


Figure 10. Test setups and HII head and Q3 helmet upmost points.

While the impact of the HII adult dummy took place on the windscreen, the Q3 child dummy impacted the car always on the bonnet (figure 11).

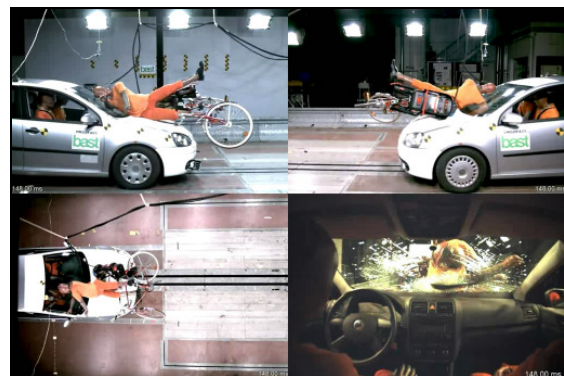


Figure 11. Different views and timing of the head impact of HII and Q3 dummy on windscreen and bonnet.

The tests showed that the 50th percentile male head impact is only partly covered by the currently defined adult head impact area. Figure 12 demonstrates that in two cases the impact locations of the adult head were significantly beyond WAD 2100. Only in one test WAD 2100 covered the adult head impact completely.



Figure 12. Head impact location of HII dummy on the vehicle front.

While WAD 2100 was shown as not being the appropriate rearward limitation for the adult head impact of bicyclists, the impact of the Q3 head occurred in four cases below WAD 1500 which was used within previous test protocols as the rearward limitation for the child head impact. In the fifth case, the child head impact was covered by WAD 1700 which is the current rearward limitation:

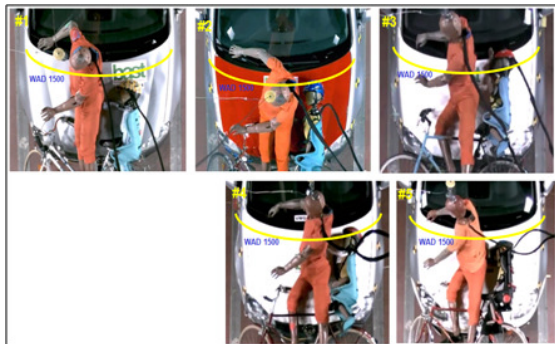


Figure 13. Head impact location of Q3 dummy on the vehicle front.

Thus, in terms of the 3 YO child, a rearward extension of the child head test area seems not necessary. On the other hand, further information on the impact conditions of other statures such as a 6YO bicyclist is needed.

Summary of vehicle based assessment In depth accident data, virtual testing with human body models as well as full scale dummy tests indicate that in case of a collision with a motor vehicle the bicyclist head impacting the vehicle front rearwards of the pedestrian. Furthermore, the head impact angles between bicyclists and pedestrians partly differ significantly.

Safety assessment of bicycle helmets

For the purpose of assessing the protection potential of bicycle helmets, corresponding test procedures are described amongst others within the European Standard EN 1078 (CEN, 2006-2). Modified procedures as well as more stringent requirements can be found within consumer test programmes as e.g. from ADAC (2010), Stiftung Warentest (2005) or Öko Test (2010). Supplemental test procedures, representing more realistic impact conditions, have been developed by BAST.

European Standard EN 1078 The European Standard EN 1078 “Helmets for pedal cyclists and for users of skateboards and roller skates” contains requirements and test methods for bicycle helmets regarding their

- material
- helmet construction
- field of vision
- shock absorbing properties
- durability
- retention system properties
- labelling
- manual / information

Obviously of highest interest for the protection of cyclists in the event of a collision is the assessment of the shock absorbing properties. For that purpose, a pre-conditioned bicycle helmet impacts under a guided free fall a flat as well as a kerbstone test anvil at test speeds of 5,42 m/s and 4,57 m/s respectively, see figure 14:

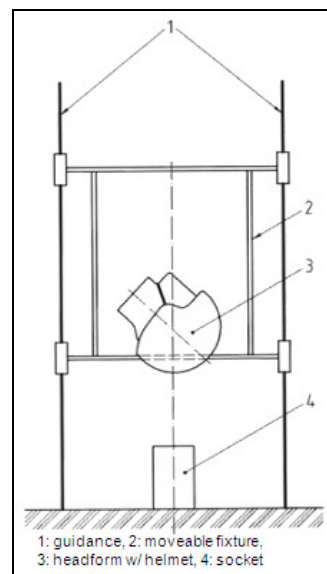


Figure 14. Test setup for the assessment of shock absorbing properties (CEN, 2006-2).

The acquired maximum peak acceleration of the headform to be used within these tests according to the European Standard EN 960 (CEN, 2006-1) must not exceed 250 g.

Consumer testing Various consumer test programmes for the assessment of bicycle helmets contain a broader variety and also more stringent requirements than the European Standard. Amongst others, within the tests according to ADAC the raised impact speed for the kerbstone test (5,42 m/s instead of 4,57 m/s) leads to higher loadings on the helmet during the test. When just fulfilling the requirement for the maximum acceleration of the headform according to the European Standard, the helmet is ranked comparatively poor within the assessment of ADAC. In order to score full points in that category, the maximum acceleration must not exceed 120 g.

Supplemental test procedures Aim of the development of additional test procedures for the safety assessment of bicycle helmets based on more stringent requirements than those described in the European Standard and consumer test programmes was the definition of more realistic accident situations of bicyclists during collisions with motor vehicles and during single accidents. Impactor tests based on the current pedestrian test procedures were carried out against a sedan shaped vehicle front. During lateral upset tests a 6YO HIII child dummy seated on a bicycle impacted with his head a simulation of road surface and kerbstone. Pendulum tests were performed as means of simulation of an overturn over the handlebar and subsequent head impact against the road surface or an obstacle. Full scale tests were performed to validate the results of the impactor tests on the one hand and to simulate a real situation as it can be actually found during vehicle to cyclist collisions. Altogether, 16 comparative tests were performed with and without applied bicycle helmet. An overview of the tests and corresponding setups is given in table 1.

Table 1.
Overview of tests according to supplemental test procedures.

# Test	Test No.	Description	Vehicle
1 Pos 1	BVGFH-C1C	Ped Pro Component Test Pos 1	Sedan
2 Pos 1 - Helmet	BVGFH-C1C-H	Ped Pro Component Test Pos 1 - Helmet	Sedan
3 Pos 2	BVGFH-C2A	Ped Pro Component Test Pos 2	Sedan
4 Pos 2 - Helmet	BVGFH-C2A-H	Ped Pro Component Test Pos 2 - Helmet	Sedan
5 Pos 3	BVGFH-C4B	Ped Pro Component Test Pos 3	Sedan
6 Pos 3 - Helmet	BVGFH-C4B-H	Ped Pro Component Test Pos 3 - Helmet	Sedan
7 Road Surface	UV6YH3F1	Lateral Upset Road surface	
8 Road Surface - Helmet	UV6YH3F2	Lateral Upset Road surface - Helmet	
9 Kerbstone	UV6YH3F3	Lateral Upset Kerbstone	
10 Kerbstone - Helmet	UV6YH3F5	Lateral Upset Kerbstone - Helmet	
11 Pendulum upright	PV6YH3-1	Overturn upright	
12 Pendulum upright - Helmet	PV6YH3-2	Overturn upright - Helmet	
13 Pendulum declined	PV6YH3-3	Overturn declined	
14 Pendulum declined - Helmet	PV6YH3-4	Overturn declined - Helmet	
15 Bonnet	GV6YH3F3	Full Scale Test Bonnet Impact	Sedan modified
16 Bonnet - Helmet	GV6YH3F4	Full Scale Test Bonnet Impact - Helmet	Sedan modified
15 Road Surface	GV6YH3F3	Full Scale Test Secondary Impact	Sedan
16 Road Surface - Helmet	GV6YH3F4	Full Scale Test Secondary Impact - Helmet	Sedan

Prior to the comparative study the following expectations were defined:

- 1) An increasing protection potential of bicycle helmets with increasing impact severity
- 2) A decreasing protection potential of bicycle helmets in combination with already improved, “vulnerable road user friendly” vehicle frontends

Impactor tests The assessment of the potential of pedestrian head protection is currently based on tests with the adult and the child/small adult head impactor described within various test procedures as e.g. the European Legislation on Pedestrian Safety (European Commission, 2009) and the Euro NCAP Pedestrian Testing Protocol (2012). Comparative tests under identical impact conditions were performed with the child/small adult head impactor with and without bicycle helmet against three different impact locations on a pedestrian three star rated vehicle according to a previous version of the Euro NCAP assessment protocol (2004):

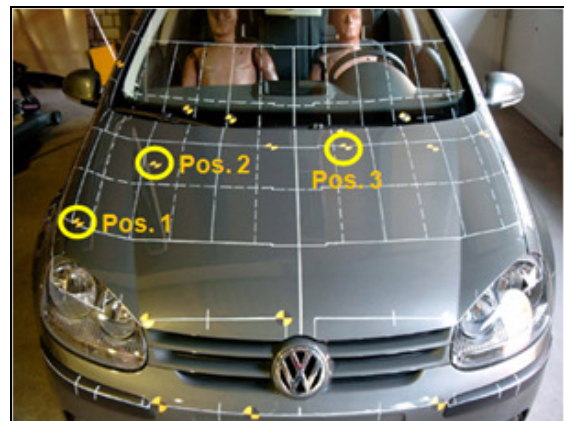


Figure 15. Impact locations for headform testing.

The tested structures were

- Position 1: bonnet support
- Position 2: gas spring support
- Position 3: fire wall

In total, six headform tests were performed so that each location was impacted with the child/small adult headform without and with applied bicycle helmet.

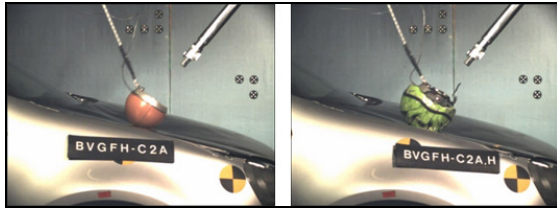


Figure 16. Headform testing without and with helmet.

The test results in terms of the resultant peak acceleration are shown in figure 17, the Head Performance Criteria (HPC) results are given in figure 18:

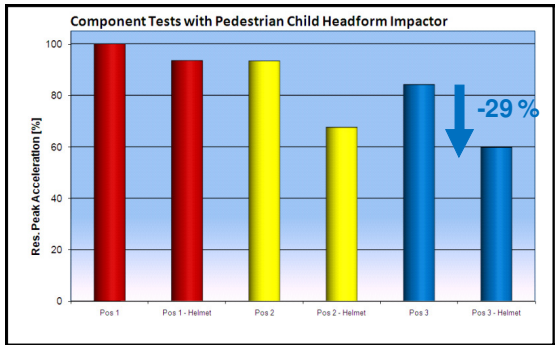


Figure 17. Peak acceleration results of component tests with child/small adult head impactor.

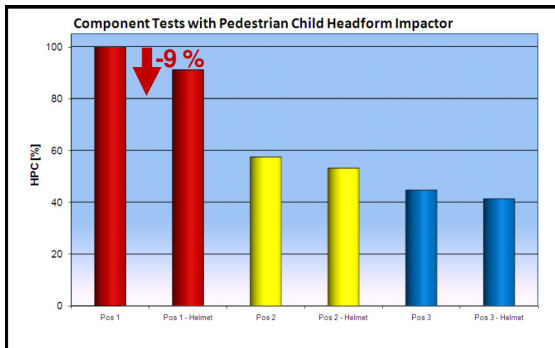


Figure 18. HPC results of component tests with child/small adult head impactor.

The diagrams demonstrate that the bicycle helmet used for these tests provided a reduction of the resultant peak acceleration up to 29 % related to the unprotected headform. The calculated HPC of the headform equipped with bicycle helmet could be reduced up to 9 % related to the HPC of unprotected headform.

The following time history curves (figure 19) show that the resultant peak acceleration was mainly derived from the acceleration in z-direction, latter one distributed more homogeneously along the entire duration of the impact in the tests with bicycle helmet:

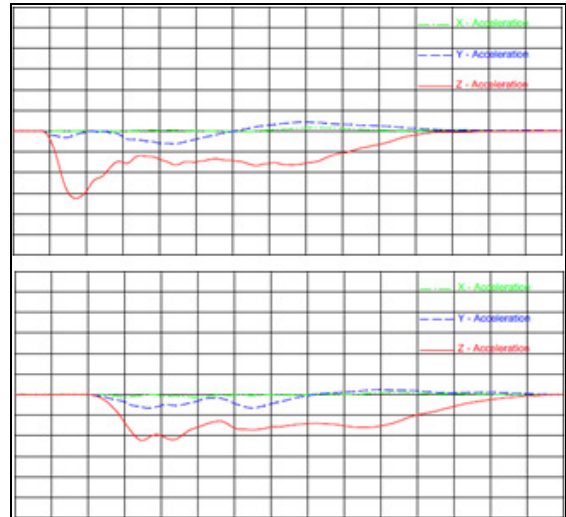


Figure 19. Acceleration time history curves of unprotected (top) and protected (bottom) headform in component tests against impact position #3.

Lateral upset Lateral upset tests were conducted as simulation of a bicyclist ground impact against the road surface and a kerbstone. The tests were performed with a 6 YO HIII dummy positioned on a bicycle with a rim size of 20 inches, with its head being protected with a bicycle helmet and also unprotected (figure 20).



Figure 20. Test setups for lateral upset tests.

The test setup was chosen in a way providing the first ground contact of the dummy with its head (figure 21).

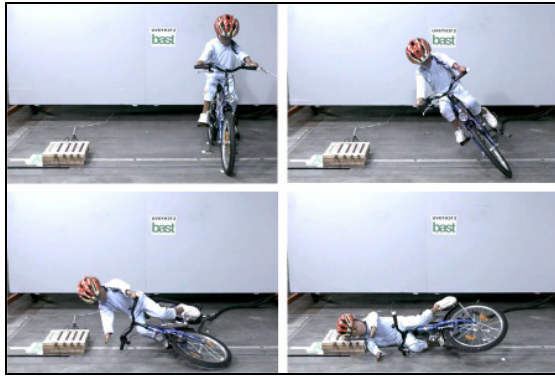


Figure 21. Dummy trajectory within lateral upset tests.

Figures 22 and 23 show the test results in terms of HPC and peak head acceleration during the impact tests against the road surface and kerbstone simulation with protected and unprotected head.

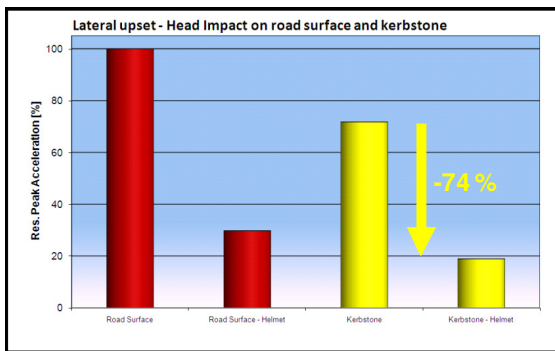


Figure 22. Peak acceleration results of lateral upset tests with HII 6YO dummy.

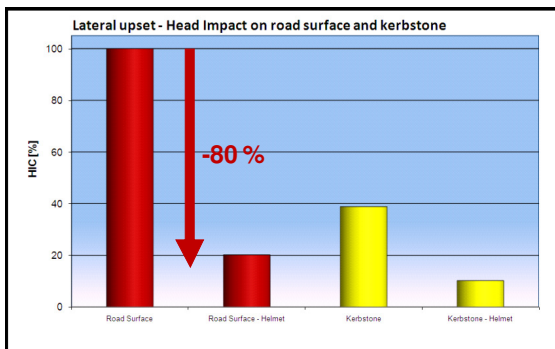


Figure 23. HPC results of lateral upset tests with HII 6YO dummy.

The comparative tests on both impact locations demonstrate the high protection potential of the bicycle helmet. According to the lateral upset tests, when impacting the kerbstone simulation, the helmet provided a maximum reduction of the resultant peak acceleration of 74 % compared to unprotected dummy head. A maximum HPC reduction of 80 % compared to the HPC value of

the unprotected head is achieved during the road surface impact.

Handlebar overturn The simulation of an overturn over the bicycle handlebar and subsequent impact against the road surface or a rigid obstacle was simulated during pendulum tests. Those tests were again performed with a 6 YO HII dummy with protected and unprotected head in upright and declined position (figures 24 and 25).

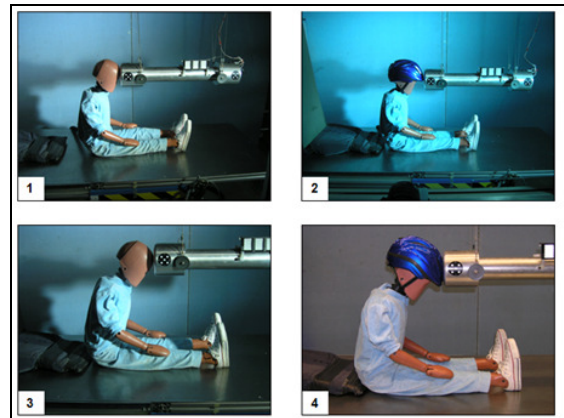


Figure 24. Test setups for pendulum tests.



Figure 25. Pendulum tests – example declined and protected head.

As during the lateral upset tests, the high protection potential of the bicycle helmet is underlined also within the handlebar overturn tests (figures 26 and 27).

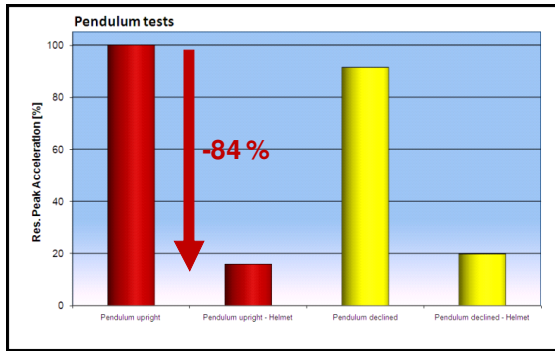


Figure 26. Peak acceleration results of handlebar overturn tests with HII 6YO dummy.

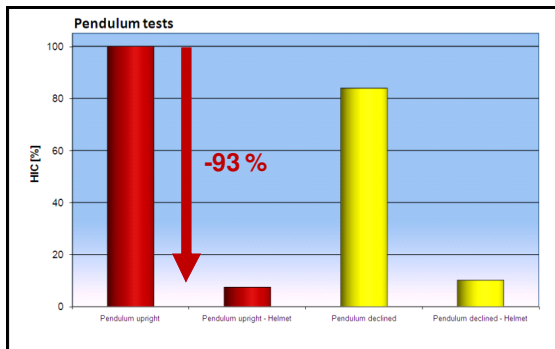


Figure 27. HPC results of handlebar overturn tests with HII 6YO dummy.

While the maximum acceleration could be reduced by up to 84 % when using a bicycle helmet during the accident, the calculated HPC was reduced by up to 93 % compared to the HPC of the unprotected head.

Full scale vehicle to dummy tests In addition to the impactor tests according to the procedures described within legislation and consumer test programmes and the lateral upset and handlebar overturn simulations, two full scale vehicle to dummy tests were performed. The 6YO HII dummy positioned on a bicycle with a rim size of 20 inches was impacted by a modified sedan shaped vehicle with bonnet reinforcements at an impact speed of 40 kph. The aimed impact location was at the longitudinal vehicle centre plane. Besides the loadings of the head during the primary impact on the bonnet, those due to the secondary ground impact were recorded and assessed as well (figure 28).

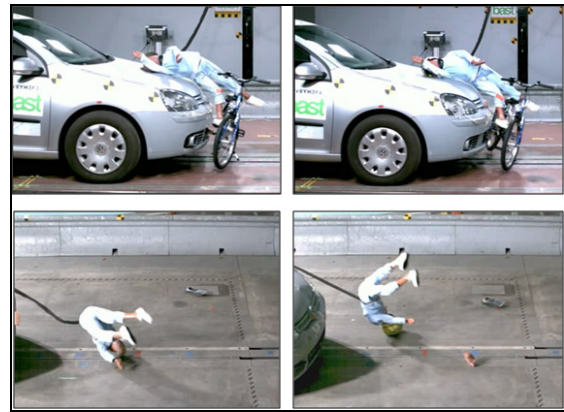


Figure 28. HII 6YO dummies primary impact on the vehicle front and secondary impact on the ground.

The comparative tests were performed with protected and unprotected dummy head. Wrap around distances of 1280 mm and 1260 mm respectively and lateral impact positions at 60 mm and 150 mm provided an acceptable repeatability of test and impact conditions for full scale vehicle to dummy tests.

Once again, the comparative tests demonstrated the high potential of the bicycle helmet especially when impacting rigid structures. Figure 29 shows a reduction of the resultant peak acceleration provided by the helmet at 40 % on the bonnet and at 90 % during the secondary impact, compared to the unprotected dummy head:

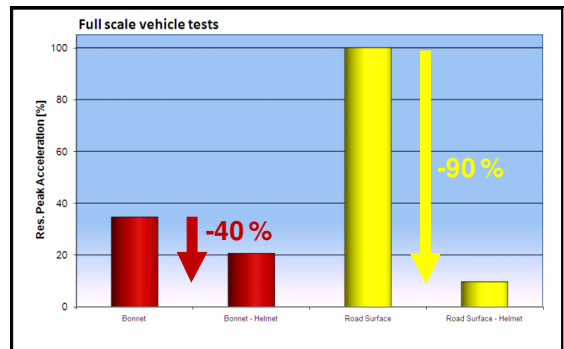


Figure 29. Peak acceleration results of full scale vehicle to HII 6YO dummy tests.

In terms of HPC, the reduction was at 15 % during the bonnet impact and at 98 % during the secondary impact compared to HPC value of the unprotected child head (figure 30):

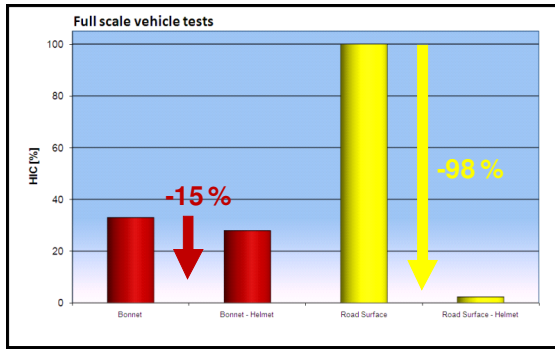


Figure 30. HPC results of full scale vehicle to HII 6YO dummy tests.

Contribution of active vehicle safety

An additionally performed full scale test at reduced impact speed was aimed for assessing measures of active vehicle safety as e.g. braking before the collision event towards injury mitigation. Therefore, the 6 YO HIII child dummy with unprotected head and positioned on the 20 inch rim sized bicycle was impacted at a reduced impact speed of 30 kph.

The reduced impact speed did not show any significant effect on the wrap around distance of the head impact, which was this time at 1290 mm and thus even further rearwards than during the tests at 40 kph. Besides, a secondary impact was noted on the bonnet.

Figure 31 shows the peak resultant head acceleration, HPC and 3 ms cumulative value of the unprotected 6 YO head during the tests at 40 kph and 30 kph.

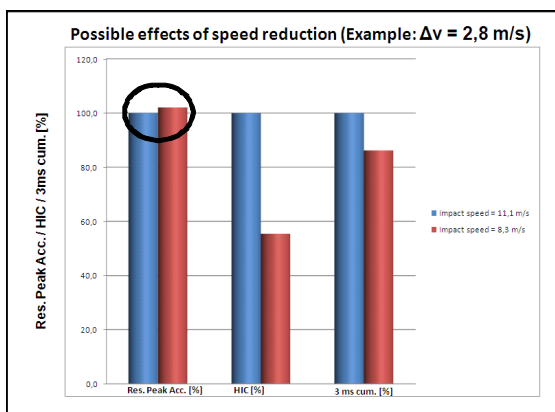


Figure 31. Influence of impact speed reduction.

As it could be expected, the calculated HPC was significantly higher within the test at higher impact speed. The 3 ms value was higher at 40 kph, too. On the other hand, a slightly higher peak resultant head acceleration at lower impact speed indicated that a different structure must have been impacted

in the test at lower impact speed. This leads to the assumption that within tests at reduced impact speed the benefit of speed reduction might partly be compensated due to the different impact location and thus possibly harder structure.

DISCUSSION

Real world accident investigations result in the group of bicyclists being on rank 2 of casualties considering all injury severities in Germany. Bicycle helmets have been proved to always providing head protection in different accident scenarios. The supplemental tests beyond EN 1078 presented in this study demonstrated an increasing protection potential of bicycle helmets with increasing impact severity. In combination with optimized, i.e. „VRU friendly“ vehicle frontends the protection potential of bicycle helmets has been found to decrease, but still being significant. Amongst other things, the helmet usage leads to approx. 33 % reduction of the portion of AIS 3+ head injuries. On the other hand, the overall bicycle helmet usage frequency has been found at 6% only in Germany.

A comparison of in depth cyclist and pedestrian accident data as well as simulation and test data suggested a rearward extension of the head impact area for the assessment of passive safety systems. A further investigation of the German In-Depth Accident Study (GIDAS) showed that another 50 percent or more of all AIS 3 and AIS 4 bicyclist head injuries where the head being unprotected occur within zones that could be addressed by an extended Euro NCAP testing protocol.

An additional full scale test performed at reduced impact speed proved that measures of active vehicle safety as e.g. braking before the collision event do not necessarily always lead to a reduction of injury severity.

CONCLUSIONS

Improvement of bicyclist protection is suggested by either an enhancement of passive, active or integrated vehicle based cyclist protection, leading to accident avoidance or injury mitigation, or by cyclist self protection using a bicycle helmet, always focusing on mitigation only.

Within Euro NCAP, active safety will be initially implemented from the year 2014 on. Active pedestrian safety will follow two years later, introducing the assessment of AEB systems on top of state-of-the-art passive pedestrian safety. Bicyclists are expected to follow in a later stage. However, active safety is expected to never be able to target all accidents.

REFERENCES

Allgemeiner Deutscher Automobilclub ADAC e.V.. 2012. „Test 2010: Fahrradhelme für Kinder – Methodik und Hintergrund.“ Report available at <http://www.adac.de/infotestrat/tests/fahrrad-zubehoer-sport/kinderfahrradhelme/default.aspx?tabid=tab4>.

Brüll S., Bovenkerk J. 2009. “New and improved test methods to address head impacts.” Deliverable 333C of the European FP6 research project on Advanced Protection Systems (APROSYS).

CEN (European Committee for Standardization). 2006-1. „Headforms for use in the testing of protective helmets.” European Standard EN 960:2006 D. 2006.

CEN (European Committee for Standardization). 2006-2. „Helmets for pedal cyclists and for users of skateboards and roller skates.” European Standard EN 1078:1997 + A1:2005 D.

European Commission. 2009. “ COMMISSION REGULATION (EC) No 631/2009 of 22 July 2009 laying down detailed rules for the implementation of Annex I to Regulation (EC) No 78/2009 of the European Parliament and of the Council on the type-approval of motor vehicles with regard to the protection of pedestrians and other vulnerable road users, amending Directive 2007/46/EC and repealing Directives 2003/102/EC and 2005/66/EC.” Official Journal of the European Union L 195/1, 25.07.2009.

European New Car Assessment Programme (Euro NCAP). 2008. “Assessment Protocol and Biomechanical Limits - Version 4.1.” Euro NCAP, 2004.

European New Car Assessment Programme (Euro NCAP). 2013. “Pedestrian Testing Protocol - Version 6.2.” www.euroncap.com.

Öko-Test. 2010. „Kinder-Fahrradhelme.“ Öko-Test Issue March 2010.

Otte D., Haasper C., Wiese B. 2008. „Wirksamkeit von Fahrradhelmen bei Verkehrsunfällen von Radfahrern auf Kopfverletzungshäufigkeit und Verletzungsschwere.“ VKU Verkehrsunfall und Fahrzeugtechnik, Ausgabe Oktober 2008.

Statistisches Bundesamt. 2012. “Verkehrsunfälle 2011. Fachserie 8, Reihe 7.” Wiesbaden, 2012.

Stiftung Warentest. 2005. “Auf Spartour. Fahrradhelme für Kinder und Erwachsene.” Test Issue 4/2005.

Watson J., Hardy R. 2009. “Additional/alternate test methods for cyclists.” Deliverable 333E of the European FP6 research project on Advanced Protection Systems (APROSYS).

AN EQUATION FOR GENERALISING FROM IMPACT TEST PERFORMANCE TO REAL-WORLD CRASHES

T. P. Hutchinson
R. W. G. Anderson
D. J. Searson

Centre for Automotive Safety Research, University of Adelaide
Australia
Paper Number 13-0355

ABSTRACT

Research Question / Objective: Instrumented headforms are projected at the fronts of cars to assess pedestrian safety. Better information would be obtained from these and other types of impact tests if performance over the range of expected impact conditions in the field were taken into account. That is, some means is needed to convert from performance in tightly-specified test conditions to what happens in the real-world. *Method:* Pedestrian impact safety performance of a car is affected by speed, head mass, and the distribution of impact locations over the front of the car. The effects are complicated because bottoming out may occur, that is, the hood or other surface structure may fail to absorb sufficient energy to prevent contact with much stiffer structures beneath it. In turn, the locations are affected by the geometry of the car, the impact speed, and the pedestrian's stature. The relative frequencies of different speeds, masses, and so on are important inputs to the calculation of an average. *Results:* The principal result is a theory. This has three steps. The first is to convert the test quantity (e.g., HIC, the Head Injury Criterion) observed in test conditions to what would be observed if (for example) speed or mass were different. The second is to convert the test quantity to something that can be meaningfully averaged --- for example, average dollar cost of HIC or the probability of death corresponding to a given HIC. The third is to obtain the average cost, or average probability of death, by integration over the quantities that vary from crash to crash: speed, head mass, stature, and impact location. *Discussion and Limitations:* The theory that is developed may be used to calculate, for example, the changes that result if test performance is improved, or the probabilities of different conditions change. With appropriate modification, the theory is applicable to many other forms of testing also. The chief limitation is that good information is required on such things as the dependence of HIC on speed and mass, the dependence of cost on HIC, and the relative frequencies of speeds, masses, and so on. Such information is difficult to obtain. *Conclusions:* Better representation of the effect of impact conditions on severity is required if a test

regime is to provide appropriate incentives for improvement in vehicle design. This paper identifies what information is needed, and shows how it can be used to estimate average real-world performance starting from what is observed in an impact test.

INTRODUCTION

As part of testing of new cars by consumer organisations, an approximate sphere with an accelerometer inside it is projected at the front of a car. The speed and other conditions of the impact are specified. However, real pedestrian impacts are at a wide range of speeds. We have recently described a method of calculating average performance across a range of impact speeds, and across a range of effective head masses (Hutchinson et al., 2012a). Lubbe et al. (2012) discussed our method and other literature on this, and gave attention to variation in other factors as well as speed. They were most concerned with the distribution of pedestrian impact points over the front of the car. In turn, this distribution is affected by the geometry of the car, the impact speed, and the pedestrian's stature. Lubbe et al. also make passing mention of pedestrian gender and age as factors that vary. Further, a review by Hu and Klinich (2012) particularly emphasised (a) the need to keep in mind the special characteristics of older pedestrians, and (b) bottoming out as a danger to pedestrians (this term refers to the hood deforming so much that very stiff structures underneath it are contacted, with consequent great increase of the severity of the impact). Both of these issues imply the need for information beyond a test result.

This paper proposes an equation that will integrate over the range of pedestrian head masses, the range of pedestrian statures, and the range of impact locations on the car, as well as over the range of speeds. To some extent, then, this paper is a response to Lubbe et al. and to Hu and Klinich. Geometry of the car is not a random variable, and frailty of the pedestrian affects injury and its consequences rather than what is measured in an impact test, and these are discussed separately. Our arguments are made in the context of (and with reference to the specifics of) pedestrian headform

testing, but are of broad applicability in impact testing.

At present, the purpose of impact testing appears to be the measurement of safety in particular conditions of impact. Impact testing will be more valuable if it measures safety averaged over a wide range of real-world impact scenarios. Perhaps “estimation” would be a better word than “measurement”, as to the variability in test results is added uncertainty about how to generalise from the particular conditions of the test to real-world crashes. In referring to conditions of impact, we mean the speed of the headform, its mass, the locations on the front of the car that are tested, and so on. The specifics which are laid down in the test protocol seem to be intended to be representative of, or typical of, pedestrian impacts. Performance in other conditions is also important. Performance will be different if conditions change --- the impact will be more severe if the speed is higher --- and the effects are likely to be complicated.

- Low speed impacts are very important numerically. Some authors have argued that the test speeds that are used are consequently unrepresentative.
- If bottoming out did not occur at the test speed, it may do at some higher speed that is still within the realistic range. If bottoming out did occur at the test speed, it may not at some lower speed that is still within the realistic range. In either case, there is a great change from what happens in the test.
- The A pillars are usually not tested. They are typically very stiff and receive a default fail result.
- The windscreen is usually not tested. It is typically sufficiently soft to receive a default pass result.
- Pedestrians of different statures will impact the car in different places: the taller they are, the further from the front of the car will be the impact.
- Speed will affect not only the severity of the impact at a given location, but also the location that is struck.
- A change of the effective head mass is likely to have different results at different speeds and different locations. An increase of effective head mass will lead to acceleration taking place over a longer distance. At low speed and with plenty of clearance distance under the hood, that will mean lower accelerations. But at high speed and with little clearance distance under the hood, the increased distance will make bottoming out more likely, and hence a great increase in severity.

- New technology such as forward-looking radar or improved tyres may substantially reduce impact speeds. Lubbe et al. (2012) note that passive and active safety systems cannot be assessed by a straightforward combination of distinct methods as the benefits “are measured in different units: e.g., impact speed reduction for active safety systems and injury criteria measurements for the passive safety system component test”.

As already mentioned, our method was described in Hutchinson et al. (2012a). There is relevant previous literature that we built upon, notably by Searle et al. (1978), Horsch (1987), Viano (1988), and Korner (1989). Other aspects are discussed in Anderson et al. (2012), Hutchinson et al. (2012b), and Searson et al. (2012a,b,c).

DERIVATION OF REAL-WORLD CONSEQUENCES FROM A TEST RESULT

Notation

Notation is given below. It is consistent with that of Hutchinson et al. (2012a).

- x : speed of impact of the car with the pedestrian (it is assumed this is the same as the speed with which the head hits the car)
- m : effective mass of the pedestrian's head
- s : stature of pedestrian
- i : location on the car (this is a categorical variable, a name rather than a number)
- u : distance of the head impact point from the front of the car
- w : distance of the head impact point from the side of the car, laterally across the car
- h : HIC, the Head Injury Criterion
- $p(h)$: cost of h (or, rather, the average cost, as the injuries and outcomes will vary)
- $f(x)$: probability density function of speed x
- $g(m, s)$: joint probability distribution of head mass m and stature s
- z : frailty

In pedestrian headform tests, HIC is used to characterise the test result. This is not essential, though, and h could instead be the maximum acceleration or some other summary.

Overview of Calculation

The calculation has three steps. The first is to convert the test quantity (e.g., HIC, the Head Injury Criterion) observed in test conditions to what would be observed if (for example) speed or mass were different. The second is to convert the test

quantity to something that can be meaningfully averaged --- for example, average dollar cost of HIC or the probability of death corresponding to a given HIC. The third is to obtain the average cost, or average probability of death, by integration over the quantities that vary from crash to crash. Hutchinson et al. (2012a) were chiefly concerned with the effect of speed, and had the expression $p(h(x, i)).f(x)$ for the cost corresponding to speed x and location i . (Notice that it is assumed that h alone determines p : the other variables have their effects on p because they affect h .) Hutchinson et al. obtained the following equation for average cost (their equation 3).

$$Av(p_i) = \int p(h(x, i)).f(x).dx$$

The above equation refers to location i on the car. Locations differ in how safe or unsafe they are. HIC at a location is converted to a number of points at that location, and points are summed to get a score for the car. For these reasons, Hutchinson et al. regarded the location on the car as being the basic unit to analyse. But Lubbe et al. (2012) are quite correct to say that averaging over the whole car is important (this is particularly so because change to the distribution of speeds will change the distribution of impact locations), and so is averaging over pedestrian head mass and stature. A generalised expression of similar form will be obtained below that applies to the car as a whole.

Conditions that Vary

Quantities that vary in the real world, and over which the cost should be averaged, are listed below, with a short description of how they have their effects.

- Speed of impact. Firstly, at any given location on the car, HIC increases with increasing speed. Secondly, the impact location of the head will be further from the front of the car, the higher the speed is.
- Mass of pedestrian's head. HIC depends on mass as well as on speed.
- Stature of pedestrian. The impact location of the head will be further from the front of the car, the taller the pedestrian is.
- Impact location on the car. Each location on the car may be different in respect of both the surface (e.g., the hood) and what is underneath (e.g., the engine). The distance u of the head impact point from the front of the car is not random, being determined by impact speed and pedestrian stature, but the distance w of the head impact point from the side of the car is a random variable. Possibly impact angle should be included also, but this will not be considered below.

These effects are represented in mathematical notation as follows (the symbols are as listed earlier).

- Speed. Firstly, $h(x)$. Secondly, $u(x)$.
- Mass. h depends on m as well as on x : $h(x, m)$.
- Stature. u depends on s as well as on x : $u(x, s)$.
- Impact location. h depends on location: $h(x, m, i)$.

Expression for the Average of p

As already noted, Hutchinson et al. (2012a) wrote $p(h(x, i))$ to show that x affects h and this in turn affects p , and multiplied this by $f(x)$. To include the extra variables, this may be generalised as below.

Firstly, $p(h(x, m, i))$ shows that mass affects h and hence p .

Secondly, i is defined by the distances u and w , along and across the car. Thus p becomes $p(h(x, m, i(u, w)))$.

Thirdly, u is determined by x and s . Thus p becomes $p(h(x, m, i(u(x, s), w)))$.

Fourthly, this will need to be multiplied by the probabilities with which x , m , and s occur: $p(h(x, m, i(u(x, s), w))).f(x).g(m, s)$.

Finally, average p is obtained by integrating over the four quantities x , m , s , w . The equation (below), in contrast to our earlier paper, applies to the car as a whole.

$$Av(p) = \iiint \int p(h(x, m, i(u(x, s), w))).f(x).g(m, s).dx.dm.ds.dw. \quad (\text{Equation 1})$$

Comments

Four comments on Equation (1) are worth making.

- Different probabilities of different w are not shown in Equation (1). It would be necessary to do so if some locations across the width of the car are struck more frequently than others. (In addition, it may be the case that narrow cars miss some pedestrians that wider cars would hit. It is probably more convenient to take account of this via reduced impact frequency rather than by setting h to 0 for impacts that are avoided.)
- The effective head mass m and the pedestrian's stature s may not be independent, in which case $g(m, s)$ will be a complicated bivariate probability density, but lack of information may mean the use of the product of probability densities of m and of s , $g_1(m).g_2(s)$.

- The name of the impact location, i , could be omitted from the equation. The expression would then be $p(h(x, m, u(x, s), w))$. There is nothing wrong with this, but the disadvantage is that it may mislead us into thinking that h is a simple function of the distances u and w . That is unlikely: h is quite a different function of x and m for all the various locations that might be struck.
- The dependence of cost on h could be split into several stages --- for example, injury at a given h , outcome of a given injury, and cost of a given outcome. But at present this seems unnecessary.

DISCUSSION

Data Requirements

The expression $p(h(x, i)).f(x)$ (Hutchinson et al., 2012a) requires good data on the functions $h(x)$ and $p(h)$ and on the probability density $f(x)$ if the result is to be accurate in absolute terms. What Lubbe et al. (2012) call for, and we have tried to provide in Equation (1), requires in addition good data on the dependence of h on m , the dependence of u on x and s , and the bivariate probability density $g(m, s)$. These are severe demands, but are not out of the question. This is so especially since improvement in the comparability of vehicles and usefulness of impact test results may occur even if the numerical magnitude of $\Delta v(p)$ is not accurate in absolute terms.

Frailty

Injuries, outcomes, and therefore costs vary from person to person, even if they are of the same stature and effective head mass, and strike the same location on the car at the same speed and angle. This may be ascribed to differences in frailty. "Frailty" here may have a limited meaning (bone strength, resistance to infection, and so on), or may be a catch-all term referring to any aspect of a person's reaction to applied physical force. Frailty is not recorded in road crash statistics, but perhaps age could be used instead. It should also be noted that in the present context, frailty is something other than stature and head mass, as these are already included in the expression given.

Variability in frailty is not treated in Equation (1) in the same way as variability in speed, stature, and head mass. The reason is that variability in frailty is presumed to be taken account of by using an average cost function $p(h)$. That is, frailty does not affect HIC, or whatever other summary of the physical aspects of the impact is being used. Rather, frailty affects the human's reaction to HIC:

with z being frailty, h is still $h(x, m, i)$, not $h(x, m, i, z)$, and frailty would be introduced by writing $p(h, z)$. Expressed in other words, an impact location that is safer than another for one level of frailty is expected to also be safer for all other levels of frailty; the same cannot be said about speed or stature or head mass. Furthermore, if the distributions of x , m , and s are independent of z , it is sufficient to use $p(h)$, with this having been averaged over z . If the distributions of x , m , and s are different for people of different frailties, then the product of cost and its probability should be shown as $p(h, z).f(x, z).g(m, s, z)$. But this is impracticable --- it is far too demanding of data.

Car Geometry

Cars differ in their geometry, including hood height, hood length, hood angle, and various other characteristics. This is not a random variable, and is not treated as x , m , and s are. But car geometry will, with speed and pedestrian stature, affect where on the car the pedestrian will strike, and perhaps also affect the speed and angle of the impact. Referring to Equation (1), either the distance $u(x, s)$ will depend on car geometry or this quantity will need re-interpretation dependent on car geometry (perhaps as a wrap-around distance).

Crash Configuration

The characteristics of the car (that is, the dependence of h on i and other variables) may be relevant to more than one type of crash. For example, some locations on the car may be capable of striking a pedestrian who was in front of the car or a pedestrian who walks into the side of the car. This would require separate equations of the form of Equation (1) for the different crash types.

Overview

Equation (3) of Hutchinson et al. (2012a) and Equation (1) of the present paper show the principles of the necessary calculation.

Benefits from the calculation will include estimation of the effects of making changes --- changing the design or material of the hood so as to reduce the HIC observed in the test, increasing the underhood clearance distance, reducing the speeds at impact (e.g., by use of active safety systems, or improved brakes and tyres), and so on.

The considerable obstacles to using Equation (1) should be recognised. These include inferring the dependence of h on x and m from HIC measured at specific x and m , knowing the empirical dependence of p on h , and knowing the empirical relative frequencies of different speeds, effective

head masses, and pedestrian statures (i.e., $f(x)$ and $g(m, s)$).

ACKNOWLEDGEMENTS

The Centre for Automotive Safety Research (CASR) receives core funding from both the South Australian Department for Planning, Transport and Infrastructure and the South Australian Motor Accident Commission. CASR performs pedestrian impact tests for the Australasian New Car Assessment Program. The views expressed are those of the authors and do not necessarily represent those of the University of Adelaide, ANCAP, or CASR's other funding organisations.

REFERENCES

- Anderson, R.W.G., D.J. Searson, and T.P. Hutchinson. 2012a. "Integrating the Assessment of Pedestrian Safety in Vehicles with Collision Detection and Mitigation Systems." Presented at the IRCOBI (International Research Committee on the Biokinetics of Impacts) Conference, held in Dublin. Available at <http://www.ircobi.org/downloads/irc12/default.htm>
- Horsch, J.D. 1987. "Evaluation of Occupant Protection from Responses Measured in Laboratory Tests." SAE Technical Paper 870222. Society of Automotive Engineers, Warrendale, PA.
- Hu, J. and K.D. Klinich. 2012. "Toward Designing Pedestrian-Friendly Vehicles." Report No. UMTRI-2012-19, Transportation Research Institute, University of Michigan, Ann Arbor.
- Hutchinson, T.P., R.W.G. Anderson, and D.J. Searson. 2012a. "Pedestrian Headform Testing: Inferring Performance at Impact Speeds and for Headform Masses Not Tested, and Estimating Average Performance in a Range of Real-World Conditions." *Traffic Injury Prevention*, 13, 402-411.
- Hutchinson, T.P., R.W.G. Anderson, and D.J. Searson. 2012b. "Testing in Order to Measure the Protection Against Impact of People, Manufactured Items, and Agricultural Produce: How to Consider All Severities of Shock." In A. Kolousov, R. Das, and S. Wildy (Editors), *Proceedings of the 7th Australasian Congress on Applied Mechanics*, pp. 925-932. Engineers Australia (National Committee on Applied Mechanics), Barton, ACT. (ISBN of USB: 9781922107619.)
- Korner, J. 1989. "A Method for Evaluating Occupant Protection by Correlating Accident Data with Laboratory Test Data." SAE Technical Paper 890747. Society of Automotive Engineers, Warrendale, PA.
- Lubbe, N., M. Edwards, and M. Wisch. 2012. "Towards an Integrated Pedestrian Safety Assessment Method." Presented at the IRCOBI (International Research Committee on the Biokinetics of Impacts) Conference, held in Dublin. Available at <http://www.ircobi.org/downloads/irc12/default.htm>
- Searle, J.A., J. Bethell, and G. Baggaley. 1978. "The Variation of Human Tolerance to Impact and its Effect on the Design and Testing of Automotive Impact Performance." SAE Technical Paper 780885. Society of Automotive Engineers, Warrendale, PA.
- Searson, D.J., R.W.G. Anderson, and T.P. Hutchinson. 2012a. "The Effect of Impact Speed on the HIC Obtained in Pedestrian Headform Tests." *International Journal of Crashworthiness*, 17, 562-570.
- Searson, D.J., R.W.G. Anderson, and T.P. Hutchinson. 2012b. "Use of a Damped Hertz Contact Model to Represent Head Impact Safety Tests." In A. Kolousov, R. Das, and S. Wildy (Editors), *Proceedings of the 7th Australasian Congress on Applied Mechanics*, pp. 230-239. Engineers Australia (National Committee on Applied Mechanics), Barton, ACT. (ISBN of USB: 9781922107619.)
- Searson, D.J., T.P. Hutchinson, and R.W.G. Anderson. 2012c. "From Crash Test Speed to Performance in Real World Conditions: A Conceptual Model and its Application to Underhood Clearance in Pedestrian Head Tests." *Stapp Car Crash Journal*, 56, 485-496.
- Viano, D.C. 1988. "Limits and Challenges of Crash Protection." *Accident Analysis and Prevention*, 20, 421-429.

IMPACT OF CORRELATED COLOR TEMPERATURE OF HEADLAMPS ON VISIBILITY

Ronald B. Gibbons, Ph.D.

Jason Meyer

Virginia Tech Transportation Institute

United States of America

Paul S. Rau, Ph.D., CPE

Markus L. Price

National Highway Traffic Safety Administration

United States of America

Paper Number 13-0136

ABSTRACT

The purpose of this project was to provide an initial investigation into the effects of different light source correlated color temperatures (CCT) on detection and color recognition of roadway objects and pedestrians. This project included an investigation of both the light source spectrum from the overhead lighting spectrums as well as correlated color temperature from vehicle headlamps.

The detection of pedestrians and small objects along the roadway edge was measured on the Virginia Smart Road. Here the objects were located at specific points along the roadway and participant drivers performed a detection task. The point of first detection was recorded and the detection distance calculated. The objects appeared under high-pressure sodium (HPS) and light-emitting diode (LED) overhead lighting systems, as well as headlamps filtered to resemble LED and the amber overhead HPS sources.

The primary results from this investigation indicate that: 1) There is not a significant difference in terms of pedestrian detection and targets located immediately alongside the roadway between the correlated color temperature of the vehicle headlamps within the range selected ; 2) Overhead lighting is a significant factor in the detection and color recognition of pedestrian clothing, but results indicate that it is the intensity – not necessarily the color – of the lighting that makes it a significant factor;

The tasks considered in this investigation were primarily foveal, meaning that pedestrians were within the line of sight of the driver. However, most spectral impact is expected to be in the periphery of the visual field. Part of this investigation considered the extent to which peripheral vision plays a role in object detection for a driver. Further investigation using a more extensive peripheral detection component is required to more fully explore the impact of the light source to the periphery.

As light sources transition to new technologies, light source spectrum is becoming a significant safety aspect of the roadway environment. The impact of the correlated color temperature of the headlamp is not significant in the foveal detection of pedestrians and objects within the range investigated. Further investigation of the peripheral impact of these light sources on pedestrian and driver safety is ongoing.

INTRODUCTION

While traditional roadway lighting utilizes high-pressure sodium (HPS) light sources, the source provides an amber color that does not allow object color to appear correctly. The light source spectral output (i.e., the wavelength by wavelength emission of the light source) is heavily weighted in the yellow and red portions of the spectrum of visual light. With the advent of applying light-emitting diode (LED) technology to roadway lighting, the concept of a more broad spectral distribution of light potentially provides additional benefits to the driver. Recent research has shown a benefit of broad-spectrum light in the detection of objects along the side of a roadway when compared to traditional narrow-

spectrum light sources (Lewis, 1999). The potential benefit is such that a lower light level may provide the same visual performance under a broad spectrum source (such as LED) as compared to a higher light level under a narrow band source (such as HPS). Lower lighting level will reduce energy usage and the potential number of luminaires required for a roadway lighting scene. Further benefits might also include better object color recognition and higher visual comfort. This project provides an initial investigation of these effects.

In addition to overhead lighting, vehicle headlamp technology has also significantly changed in recent years. With the advent of new light source technologies, such as LED headlamps, the same considerations of possible benefits must be made in terms of spectral output.

PURPOSE AND SCOPE

The purpose of this project was to identify the impact, if any, of different spectral distributions and their intensities on the detection and color recognition of objects in the roadway. Based on the results of the current study, future phases will incorporate factors such as detection and color recognition of objects and pedestrians located peripherally to the driver.

METHODS

Experimental Design

The experimental design used in this project consisted of a 2x2x5x4 mixed-factors design. The factors and the levels are described below.

- Participant Age (2 levels): Younger (25-35 years old) and Older (65 years old and above). The younger and older age groups were selected to investigate the changes in vision and perception that may occur with increasing age.
- Roadway Type (2 levels): High speed roadway (55mph) and Low speed roadway (35mph). A low speed roadway condition is instrumental in applications of street lighting where pedestrians are most often to be encountered. A high speed condition was selected for application on highways.
- Overhead Lighting (5 levels): 2700 Kelvin HPS luminaires (150W) and 6000 Kelvin LED luminaires (the CCT was measured to verify the performance). Both types of luminaires were dimmable, adding an additional level, such that participants experienced LED High and LED Low, as well as HPS High and HPS Low. The High levels for both luminaires resulted in an average roadway illuminance of approximately 4 lux. The Low levels for both luminaires resulted in an average roadway illuminance of approximately 1 lux. A fifth condition of no overhead lighting was also included in the study.
- Headlamp Type (4 levels): White/blue-filtered headlamps and white/yellow-filtered headlamps. The basic high-intensity discharge (HID) headlamp was filtered to emit both the white/blue and white/yellow colors. The white/blue color was used to create the correlated color temperature similar to an LED headlamp, while white/yellow was used to simulate halogen output. In addition to this, filters were designated as High and Low in terms of their transmittance level.

Dependent Variables As a measure of the visibility, the distances at which participants could see pedestrians and wooden targets were recorded. When a participant could first see a pedestrian or target, he/she would verbally identify it by saying “pedestrians” or “target” depending on the object presented. The in-vehicle experimenter would press a button when the participant identified the object correctly and again when the participant verbally identified the color of the object correctly. Finally, the in-vehicle experimenter would press a button when the vehicle reached the object presented. These buttons flagged the data so, during later analyses, the distance traveled between these points could be determined. These distances were called the Detection Distance and the Color Recognition Distance for those particular instances.

Participants

Thirty-two participants were selected to participate in this study. Participants were selected from two age categories: younger (25-35 years old) and older (65+). Sixteen participants from each age group performed the study. Each group of participants consisted of an even number of males and females. Virginia Tech Institutional Review Board (IRB)

approval was obtained prior to recruiting subjects. Subjects were paid \$30/hr. and were allowed to withdraw at any point in time, with compensation adjusted accordingly.

Facilities and Equipment

Virginia Smart Road The experiment took place at the Virginia Tech Transportation Institute (VTTI) and on the Virginia Smart Road in Blacksburg, VA. The Smart Road is a 2.2-mile two-lane controlled access road. The Smart Road is equipped with a 0.75 mile long variable overhead lighting system. There are three luminaires on each lighting pole that can be individually turned on and dimmed. The lighting poles can be spaced at 40, 60, 80 and 120 meters and can be varied in height between 11 and 15 meters.

Participants drove the entire road, through both lighted and unlighted sections of the road.

Pedestrians and Targets Pedestrians were clothed in scrubs of blue, gray, black, or red depending on the order of the experimental design. Targets were 18cm by 18cm wooden objects painted blue, gray, green, or red and also presented based on the order of the experimental design. Pedestrians and targets were stationary and positioned 60cm outside the white line of the vehicle’s travel lane. The experimental design also included an off-axis pedestrian located approximately 18 meters off the roadway, also clothed in the blue, gray, black, or red clothing (depending on the experimental design).

Overhead Lighting 150 Watt HPS and 6000K LED luminaires installed on the Smart Road were equipped with dimming mechanisms. The luminaires were mounted at 15 meters high and spaced at 80 meters. The HPS and LED overhead luminaires were characterized using a mobile measurement system developed by VTTI. The dim levels for each of the lighting conditions were established so that the average illuminance on the roadway was equivalent between the two lighting systems. Target and pedestrian locations were carefully selected throughout the test area in order to ensure equal illuminance under both the HPS and LED luminaires.

Test Vehicles Participants drove one of two 1999 or 2000 Ford Explorers with four HID low beams capable of being filtered to output white/blue or white/yellow light. Lee-brand filters were selected and combinations of filters with headlamps were classified as either “High” or “Low.” The High filter level along with the four HID low beams resulted in approximately the same amount of light as one would see with a typical two-headlamp system. The Low filter level resulted in an approximately 30% reduction in light level. Levels of transmittance, correlated color temperatures (CCT), and specific filter identification number combinations used are shown below in Table 1.

Table 1.
Headlamp Filter Specifications

Color	Intensity	Transmittance	CCT	Filters
White/Yellow	High	0.4883	2926	205 223 298
White/Yellow	Low	0.3821	2910	205 223 209
White/Blue	High	0.4367	5357	202 218
White/Blue	Low	0.3130	5120	202 218 298

An in-vehicle experimenter rode in the passenger seat for the duration of the study. The vehicle was equipped with a Data Acquisition System (DAS) which recorded vehicle network data and four camera views inside and around the vehicle. The DAS recorded the driving distance and the button presses for the Detection Distance calculations. The DAS also recorded information entered by the experimenter such as the participant’s age, subject number, and button presses. In addition, each vehicle was equipped with a luminance camera system which took specialized photos throughout the study. These photos allowed for the measurement of the luminance of any object captured in the forward view of the vehicle. These photos also allowed for a post-hoc analysis of object contrast.

Experimental Procedure

Participants were initially screened over the telephone, followed by an initial in-person screening visit. This initial visit included participants reading the Informed Consent form and completing vision-related tests. These vision tests included an evaluation of useful field of view (UFOV), visual acuity, color vision, and contrast sensitivity. If

eligible for the study, a time was scheduled for testing. Participants were instructed to meet an experimenter at VTTI in Blacksburg, VA. Participants were scheduled in pairs. Upon arriving at VTTI, each participant was asked to re-read and sign the Informed Consent form, and fill out a W-9 tax form, a health questionnaire, and a pre-drive questionnaire.

Once all forms and vision tests were complete, the experimenter would orient the participant to the study. Experimenters would explain to participants what was meant by the detection and color recognition of objects, and what participants were to say at such instances.

Once participants had been oriented to the study, each in-vehicle experimenter would escort his/her assigned participant to the experimental vehicle. The in-vehicle experimenter would familiarize the participant with the vehicle controls, such as seat and mirror adjustments. When the participant and computer systems in each vehicle were ready, the experimenters would instruct the participants to exit the parking lot and drive to the Smart Road.

Participants drove a practice lap in order to become familiar with the vehicle and the route they would be driving on the Smart Road. In addition, the in-vehicle experimenters would answer any questions the participants had. No pedestrians or targets were presented during the practice lap, and participants were not asked to identify any objects.

After the practice lap was complete, the test laps began. Each participant drove eight test laps during which they identified pedestrians, targets, and their respective colors. Participants then drove an additional eight laps on a following night, in order to decrease the impact of fatigue. Participants were asked to drive at 35 mph or 55 mph depending on the order of the experimental design for the evening. Participants would pause and park the vehicle in turnaround sections of the road in order to complete questionnaires. This would also allow experimenters the opportunity to change overhead lighting and headlamp configurations based on the experimental design for the evening.

Once all laps were completed, participants were instructed to exit the Smart Road and return to the VTTI parking lot. From there, the experimenters escorted each participant back inside. Participants were then given a copy of the informed consent form and a receipt showing their time of participation and how much compensation they would receive. Participants earned \$30 per hour, and were paid with cash following their final night of participation.

Data Analysis

Recorded data were reduced using VTTI's Data Analysis & Reduction Tool (DART) in order to isolate distances associated with participant detections and color recognitions of objects. Images recorded at the moments of detection and recognition through the luminance camera system were also analyzed, resulting in luminance and contrast data for pedestrians and targets.

RESULTS

Pedestrians – Detection (Overhead Lighting Present) The Detection Distance was considered in an Analysis of Covariance (ANCOVA) considering all of the experimental design parameters. The actual speed of the vehicles was considered a covariate as it was a continuous variable that was controlled for, capable of influencing detection and recognition distances. In order to determine the relationships only when overhead lighting was present, results do not take into account data collected from the dark or un-illuminated section of the road. The results from this ANCOVA (a significance level of 95% ($\alpha=0.05$)) are summarized in Table 2. The significant factors are denoted by an asterisk and the associated F values are shown.

Table 2.
ANCOVA Results for Pedestrian Detection Distance

Source	F Value	Pr > F
Age	7.78	0.0092*
Headlamps	0.57	0.5674
Age*Headlamps	0.64	0.5329
Pedestrian Clothing Color	4.27	0.0073*

Age*Pedestrian Clothing Color	0.71	0.5494
Headlamp Color and Intensity*Pedestrian Clothing Color	0.44	0.8513
Age*Headlamp Color and Intensity*Pedestrian Clothing Color	2.09	0.0573
Overhead Lighting Color and Intensity	5.55	0.0023*
Age*Overhead Lighting Color and Intensity	1.13	0.3461
Headlamp Color and Intensity*Overhead Lighting Color and Intensity	0.42	0.8648
Age*Headlamp Color and Intensity*Overhead Lighting Color and Intensity	1.58	0.1741
Pedestrian Clothing Color*Overhead Lighting Color and Intensity	2.1	0.0327*
Age*Pedestrian Clothing Color*Overhead Lighting Color and Intensity	0.55	0.8371
Headlamp Color and Intensity*Pedestrian Clothing Color*Overhead Lighting Color and Intensity	0.77	0.7131
Age*Headlamp Color and Intensity*Pedestrian Clothing Color*Overhead Lighting Color and Intensity	0.75	0.7041
<i>p < .05 significant</i>		

Within this analysis, participant age, pedestrian clothing color, overhead lighting color and intensity, and the interaction of pedestrian clothing color and overhead lighting color and intensity were found to be significant. It is to be expected that there would be a significant difference between the ages of participants due to the differences in visual acuity between the ages. This difference is shown in Figure 1 with younger participants significantly detecting pedestrians from further away than did older participants.

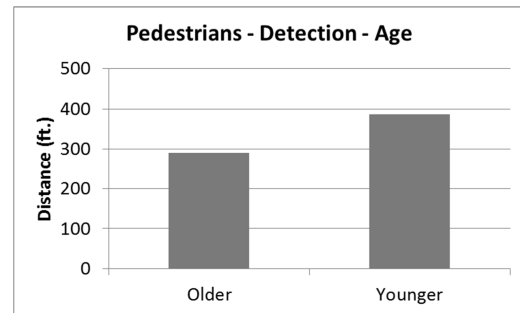


Figure 1. Mean detection distance of pedestrians by age.

The other significant effects are detailed along with the results of pedestrian color recognition.

Pedestrians – Color Recognition (Overhead Lighting Present) The Color Recognition Distance of pedestrians was also considered in an ANCOVA with the vehicle speed as a covariate. The results from this ANCOVA (a significance level of 95% ($\alpha=0.05$)) are summarized in Table 3.

Table 3.
ANCOVA Results for Pedestrian Color Recognition Distance

Source	F Value	Pr > F
Age	7.42	0.0108*
Headlamp Color and Intensity	1.22	0.3016
Age*Headlamp Color and Intensity	0.68	0.5131
Pedestrian Clothing Color	28.67	<.0001*
Age*Pedestrian Clothing Color	2.02	0.1172
Headlamp Color and Intensity*Pedestrian Clothing Color	1.62	0.1464
Age*Headlamp Color and Intensity*Pedestrian Clothing Color	1.45	0.2004
Overhead Lighting Color and Intensity	1.62	0.1963
Age*Overhead Lighting Color and Intensity	1.13	0.3453
Headlamp Color and Intensity*Overhead Lighting	0.83	0.5532

Color and Intensity		
Age*Headlamp Color and Intensity*Overhead Lighting Color and Intensity	1.74	0.1385
Pedestrian Clothing Color*Overhead Lighting Color and Intensity	2.06	0.0379*
Age*Pedestrian Clothing Color*Overhead Lighting Color and Intensity	0.36	0.9535
Headlamp Color and Intensity*Pedestrian Clothing Color*Overhead Lighting Color and Intensity	0.43	0.9549
Age*Headlamp Color and Intensity*Pedestrian Clothing Color*Overhead Lighting Color and Intensity	0.46	0.9161
<i>p < .05 significant</i>		

Similar to the results of the pedestrian detection, participant age, pedestrian clothing color, and the

interaction of pedestrian clothing color and overhead lighting color and intensity were statistically significant. However, in contrast to pedestrian detection results, overhead lighting color and intensity was not a significant factor in pedestrian color recognition. Regarding the significance of participant age, this may be expected as the lens of the human eye undergoes a physical yellowing with increased age (Coren and Gergus, 1972).

With the interaction of pedestrian clothing color and overhead lighting color and intensity being significant in terms of both detection and color recognition of pedestrians, a focus on these factors is displayed in Figure 2. Here, the impact of overhead lighting color on each pedestrian clothing color is similar between lighting types. In general, all of the pedestrians were more visible under the HPS light source with the gray-clothed pedestrians performing at the highest detection distance. The red-clothed pedestrian was less visible under the HPS than under the LED and took a more substantial decrement than did the other object types.

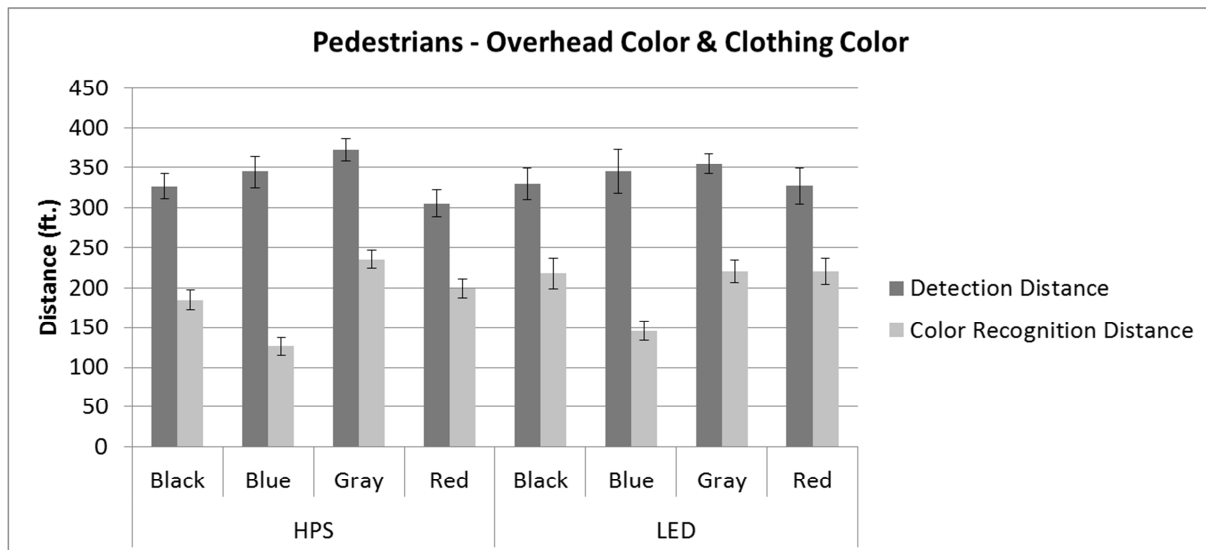


Figure 2. Mean detection and color recognition distances of pedestrians by clothing color and overhead lighting color.

In terms of the interaction between lighting source type and lighting level and light source, participants both detected and recognized pedestrian clothing color from further away when under the LED lighting than they did when under the HPS, but only for the higher intensity condition. As the factor of overhead

lighting color and intensity was a pooled factor, and seeing the similarity between lighting types in Figure 2, this leads one to believe that the significance of this factor in the resulting ANCOVA table is due more to the intensity aspect than the color aspect. In other words, any differences in participants' ability to

detect or recognize pedestrian clothing color are more likely due to the differences in intensities between LED and HPS and not necessarily their differences in spectral color output. In order to highlight the role that intensity is playing in the significant effects of overhead lighting, Figure 3 shows the interaction where it can be seen that the LED outperformed the

HPS at the high intensity level but HPS performed at a higher level in the low intensity condition. This inversion in performance of overhead light source as the intensity is decreased remains an area for future research. It is also noteworthy that this was only evident for the detection distance.

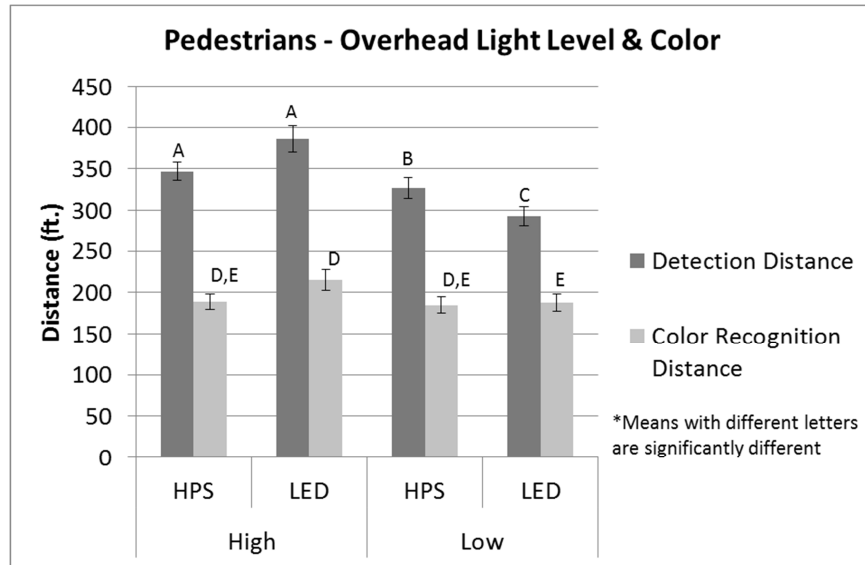


Figure 3. Mean detection and color recognition distance of pedestrians by overhead light.

Off-Axis Pedestrians – Detection and Color Recognition The Detection Distance and Color Recognition Distance of pedestrians located in an off-axis position were considered in an ANCOVA considering all of the experimental design parameters. However, participant detections and color recognitions of the off-axis pedestrians resulted in a small subset of the data collected. Final results indicate that participants failed to detect off-axis pedestrians 77% of the time and failed to recognize pedestrian clothing color 82% of the time. While no meaningful statistically significant conclusions can be drawn from this sample of data, mean distances were compared and are shown in Figure 4.

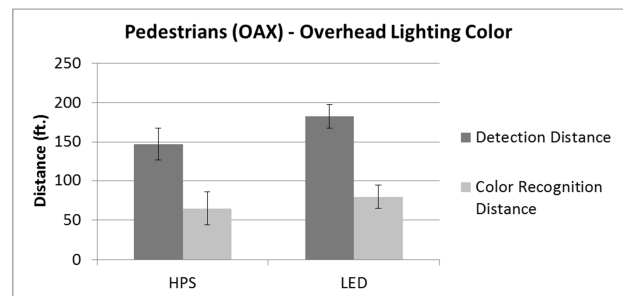


Figure 4. Mean detection and color recognition distance of off-axis (OAX) pedestrians by overhead light.

Pedestrians located peripherally off the roadway were detected from a further distance, on average, when under the LED lighting than when under HPS. This also applied to distances at which color of pedestrian clothing was recognized. While not significantly different, there may be a spectral aspect related to these differences in performance. This would be consistent with expectations of the human eye in conditions of the bluer light of the LED as compared

to the yellow light of HPS. The eye is more sensitive to the blue light of the LED in such mesopic and scotopic driving conditions as this. With the location of these pedestrians in the periphery there is more of a contribution by rods than cones in detection and color recognition. As rods and cones have different response functions to light, the contribution of rods changes the maximum light wavelength sensitivity of the human eye. In a daylight – photopic – scenario the eye would be most sensitive to green light at 555nm. However, in this nighttime scenario, the contribution of rods makes the eye most sensitive to the bluer color of 505nm; therefore, more sensitive to the bluer LED color than the higher yellow wavelength of HPS (CIE, 1951). This might allow those pedestrians located in the periphery under the

bluer LED light to be detected from slightly further away than they are when under the yellow HPS light.

Targets – Detection (Overhead Lighting Present) The Detection Distance of targets was considered in an ANCOVA. Similar to the analysis of the pedestrians, only data recorded from the overhead illuminated section of the road are included in this analysis of targets. The results from this ANCOVA (a significance level of 95% ($\alpha=0.05$)) showed that the main effect of Target Color ($F=12.35$, $p<0.0001$) was significant.

The specific differences among the target colors are discussed in conjunction with the color recognition of targets in Figure 5.

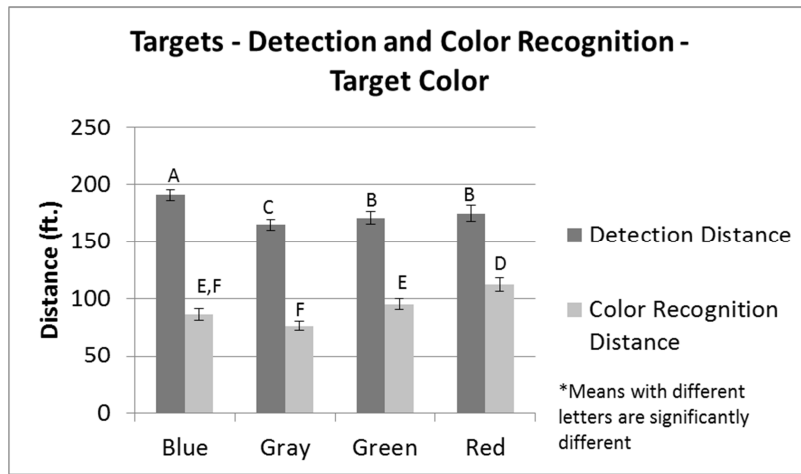


Figure 5. Mean detection and color recognition distances of targets by target color.

Targets – Color Recognition (Overhead Lighting Present) The Color Recognition Distance of targets was considered in an ANCOVA. The results from this ANCOVA (a significance level of 95% ($\alpha=0.05$)) showed that the Main effect of Target Color ($F=3.6$, $p=0.0169$) and the interactions of Target Color, Overhead Lighting Color, and Intensity ($F=3.5$, $p=0.0018$) are significant.

Figure 5 shows the detailed comparison between specific target colors due to the significant impact of target color in both detection and color recognition.

The blue target was detected from significantly further away than were any of the other target colors, with the gray-colored targets having a significantly

shorter detection distance than any other target color. In terms of color recognition, the red target had a significantly greater detection distance than did other targets. Similar to its short detection distance, the gray target had the shortest color recognition distance.

In the case of the significant interaction of Target Color and Overhead Lighting Color and Intensity, Figure 6 shows how the different target colors were recognized under each overhead lighting color.

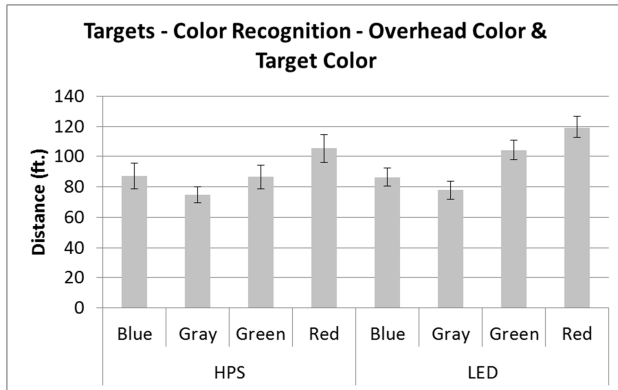


Figure 6. Mean color recognition distance of targets by overhead lighting color and target color.

In general, all of the targets were slightly more visible under the LED light source, with the Red target performing at the highest color recognition distance.

Summary

The combination of color and intensity of the overhead lighting was found to have an impact on the participants' ability to detect pedestrians, but not on their ability to recognize their clothing color. The significant interaction of pedestrian clothing color and overhead lighting on participants' ability to detect pedestrians may be related more to the intensity of the overhead lighting than to the color of

the overhead lighting. In the cases of pedestrians located off-axis or in the periphery, while not statistically significant, results indicate that color of the overhead lighting may also play a major role in determining when they are detected and when their clothing color is recognized. In general, based on statistical findings, the results show that headlamp color within the range tested had a minimal impact on the detection and color recognition of pedestrians and targets when such objects were located along the roadway with overhead lighting present.

In the case of targets, the combination of color and intensity of the overhead lighting was found to have an impact on the participants' ability to recognize the color of targets, but not on their ability to initially detect the targets. Finally, target colors were recognized from further away under the LED overhead lighting than under the HPS (particularly the lower intensity of LED lighting).

DISCUSSION

Off-Axis Pedestrian Color Recognition

In a comparison between pedestrians located along the roadway and those in the driver's peripheral vision (shown in Figure 7), overhead lighting color seemed to have a minimal impact on pedestrians located along the roadway.

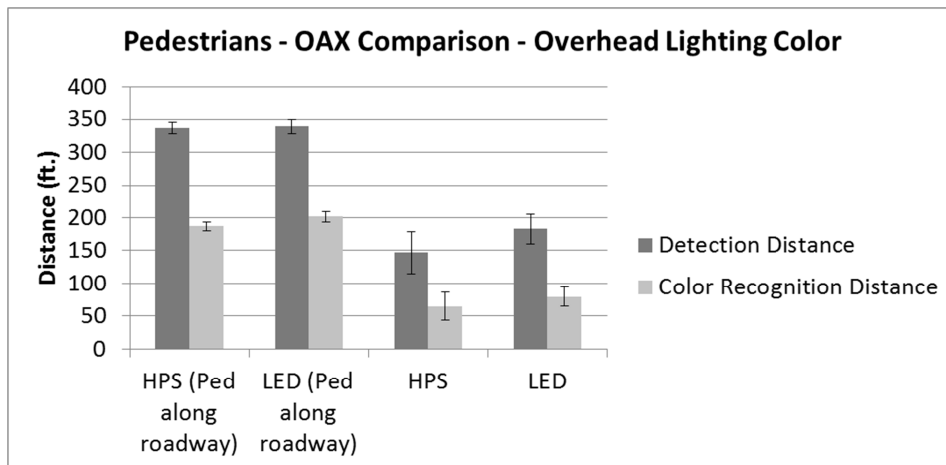


Figure 7. Comparison of pedestrians by location and overhead lighting color.

However, in the case of off-axis pedestrians located in the driver’s peripheral vision, while not statistically significant, the LED overhead lighting allowed a greater detection and color recognition distance than did the HPS overhead source. This

indicates a possible spectral component in how pedestrians located in the periphery are detected and recognized. This is consistent with the results when comparing pedestrian locations, taking into account the color of their clothing, as shown in Figure 8.

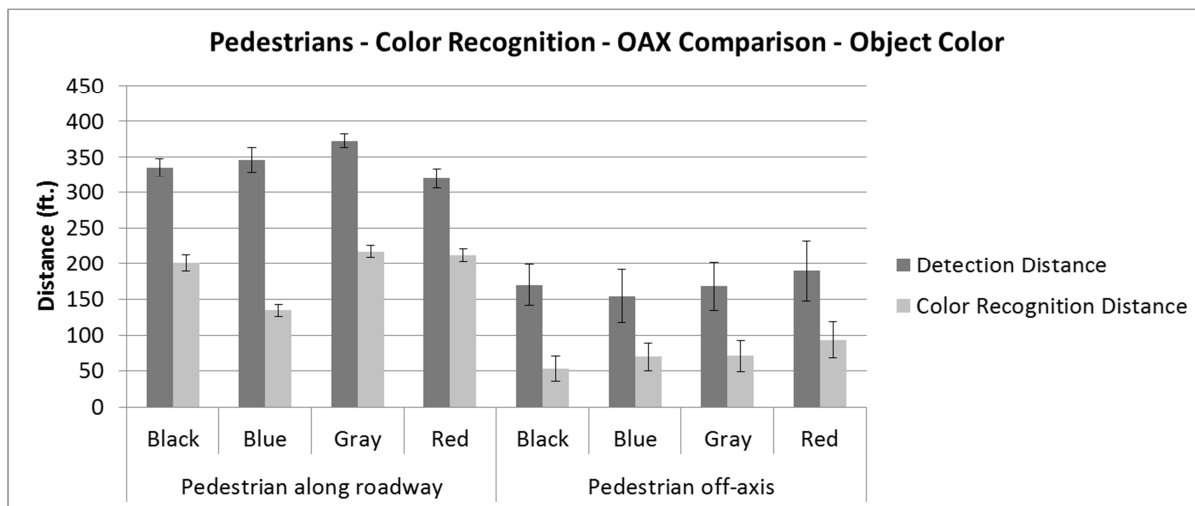


Figure 8. Comparison of pedestrians by location and clothing color.

Particularly worth noting is the significantly lower color recognition of the blue-clothed pedestrian when the pedestrian is located along the roadway. When the pedestrian location is changed to that of an off-axis location, the color recognition of this blue-clothed pedestrian is similar to that of any of the other clothing colors in the off-axis location. This is to be expected as human eyes become more sensitive to this blue color when in lower levels of light (the scotopic and mesopic lighting that comprises most night driving) and the rod-dominated areas of the periphery.

CONCLUSIONS

The conclusions from this investigation indicate that:

- Overhead lighting is a significant factor in the detection and color recognition of pedestrian clothing, but results indicate that it is the intensity, not necessarily the color, of the lighting that makes it a significant factor.

- Pedestrian clothing color plays a significant role in pedestrians being detected and their clothing color recognized.
- Target color plays a significant role in targets being detected and their colors recognized.
- Headlamp color within the range tested appears to have a minimal impact on detection and color recognition of pedestrians and targets in situations with overhead lighting present.
- The CCT of overhead lighting may play a much more significant role when pedestrians are located peripherally, as compared to pedestrians along the roadway.

ACKNOWLEDGMENTS

The authors wish to acknowledge the Federal Highway Administration for its support of this project. Thanks to Mike Flannagan of UMTRI for assistance in selecting headlamp filter materials and measurement data. Thanks also to Alan Lewis for assistance in selecting vision testing equipment and evaluation of protocol.

REFERENCES

CIE Proceedings. 1951. 1, Sec. 4; 3, p. 37; Bureau Central de la CIE, Paris.

Coren, S. and J.S. Girgus. 1972. "Density of Human Lens Pigmentation: In Vivo Measurements Over an Extended Age Range." *Vision Research*, Vol. 12, 343.

Lewis, A.L. 1999. "Visual Performance as a Function of Spectral Power Distribution of Light Sources used for General Outdoor Lighting." *Journal of the Illuminating Engineering Society*, Vol. 28, 37-42.

PEDESTRIAN KINEMATICS – A DETAILED STUDY FROM THE ASPECSS PROJECT

- PRELIMINARY RELEASED -

Rodarius, Carmen

Hair, Stefanie de

TNO

The Netherlands

Mottola, Ernesto

Toyota Motor Europe

Belgium

Schaub, Swen

TRW Automotive GmbH

Germany

Paper Number 13-0410

ABSTRACT

This study aims at providing insight on pedestrian kinematics during vehicle impact for the following variables: pedestrian size, position and posture as well as vehicle related variables like shape, speed and pre-crash braking. It is part of the work conducted within work package 3 “Injury assessment: data for construction of injury risk curves” of the European project “Assessment methodologies for forward looking Integrated Pedestrian and further extension to Cyclists Safety Systems” (AsPeCSS). The results of this subtask are used within the project to adapt current testing procedures towards more realistic approaches based on changes introduced into accident circumstances by today's smarter car designs.

First, a trend study was carried out using simplified vehicle models based on “Advanced PROtection SYStems” (APROSYS) work in MADYMO using the MADYMO ellipsoid human body models. In a second step, different detailed finite element (FE) and multi body (MB) vehicle models of recent cars were investigated using MADYMO and the MADYMO facet pedestrian model as well as LS-Dyna and the “Total Human Model for Safety” (THUMS) human body models.

Approximately 1700 different simulations were done to study the general effect on head impact speed, angle and wrap around distance (WAD) when varying input parameters like vehicle shape and speed but also pedestrian size, postures and orientations towards the car.

The second study confirmed the trends found with the simplified car models and provided more detailed information on the head and upper leg impact conditions. Moreover, some general effects introduced by simplified models were evaluated and corrected using the results of the detailed vehicle studies. Additional parameter variations as

pitching and braking of the car for different initial speeds or lateral impact position provide a complete picture of pedestrian impact kinematics. It was found, that not only vehicle speed and pedestrian size determined how and where the head of the pedestrian hits the car but also differences in posture or vehicle pitching due to pre-crash braking are influencing the kinematics, the impact conditions as well as the potential injury risk significantly. A running child can hence for example hit a car differently than a walking one. Also, significant differences were found depending on whether the head impact occurs on a bonnet top or the windscreen area.

Combining all three simulation studies the influence of active safety systems on the pedestrian kinematics during car to pedestrian impacts has been estimated. The combined use of generic and actual car models leads to results that are valid for the current and future vehicle fleet. Information on pedestrian kinematics is needed to propose updates to current pedestrian regulations and consumer tests in line with the development of integrated safety systems.

INTRODUCTION

The objective of the AsPeCSS project is to contribute towards improving the protection of vulnerable road users (VRU), in particular pedestrians and cyclists by developing harmonized test and assessment procedures for forward looking integrated VRU safety systems. The outcome of the project will be a suite of test and assessment methods as input to future regulatory procedures and consumer rating protocols. Implementation of such procedures / protocols will enforce widespread introduction of such systems in the vehicle fleet, resulting in a significant reduction of fatalities and seriously injured among these VRUs.

The work presented in this paper was conducted within the AsPeCSS work package 3 “Injury assessment: data for construction of injury risk curves”. This WP conducts simulation and testing activities generating input data required for the construction of injury risk functions. Pedestrian impact kinematics were studied using human body models (THUMS and MADYMO models) to generate impactor test conditions for the upper legform and head impactor tests. Using these conditions an extensive test program (including virtual testing) will be performed in a next step generating impactor test results representing pedestrian impacts for a range of speeds and conditions for cars with different passive safety protection levels and different types of cars. The data from these impactor tests will then be transformed into injury risk using injury risk functions available in the literature.

SIMULATION MODELS

Human body models (HBMs): For the simulations, 3 different kinds of human body models were used depending on the vehicle models investigated:

- MADYMO ellipsoid pedestrians of different sizes [4] [8] (see *Figure 1*) for the trend study
- MADYMO facet 50th percentile male pedestrian [10] [8] (see *Figure 1*) for the study using a detailed MADYMO car model
- THUMS 6 years old child and THUMS 50th percentile male [12][13][14] (see *Figure 2*) for the study using detailed LS-Dyna FE car models

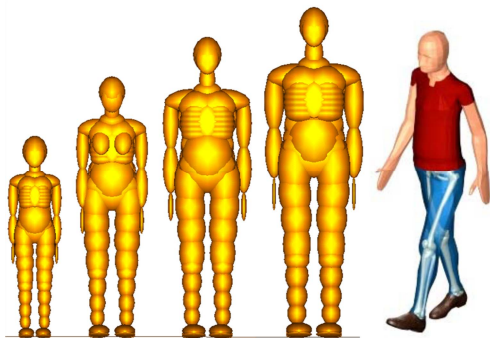


Figure 1. MADYMO ellipsoid pedestrian models. From left to right: 6 year old child, 5th female, 50th male, 95th male. And MADYMO facet pedestrian model in walking position



Figure 2. THUMS FE pedestrian models: 50th male in walking position and 6 year old child in running position

Vehicle models – Trend study: The vehicle models used for the trend study are simplified models (see *Figure 3*) that consist of 8 different planes representing the most important structures of a vehicle front. These models were initially developed within the European 6th framework project APROSYS [2] and further adapted within [11].

The stiffness of the vehicle front and bonnet has been based on the average force - deflection profiles as developed within [2]. The windscreen stiffness has been estimated and adapted based on windscreen impact tests performed at TNO as presented in [11]. All stiffness's are kept the same for all investigated car fronts so the results will not be influenced by a combination of change in geometry and stiffness's, but by change in geometry only. Also no braking or pitching was used. The mass of all vehicle models was set to 1300 kg based on findings from [1] [2].

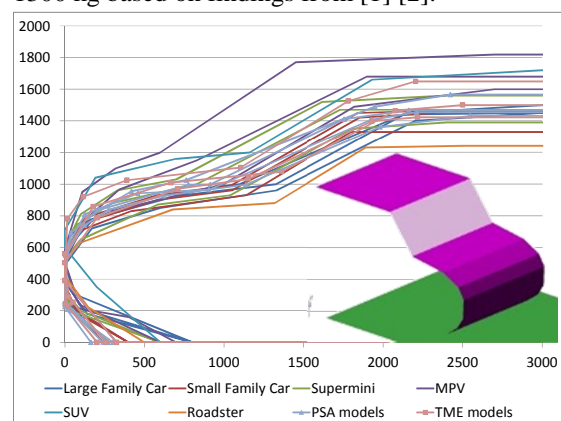


Figure 3: Vehicle contours based on [1], [2] and [11] (left) and example of resulting MADYMO model (right)

In total, 18 vehicle contours were defined for the simulations. These 18 contours define upper and lower boundary as well as median contour of the following vehicle classes:

- Large Family Car (LFC)
- Small Family Car (SFC)
- Supermini (SM)
- Multi-Purpose Vehicle (MPV)
- Sports Utility Vehicle (SUV)
- Roadster (RS)

No RS is used for the detailed model studies. Therefore, the results from these RS profiles are merged together with the SM profile results when being compared to findings from the detailed vehicle model studies. The production year of the car fronts chosen from APROSYS varies from 1994 to 2004 with most cars from 1999 / 2000.

Concerns were raised at the beginning of the project, that these car fronts might be too old to be able to cover the current car fleet on the road properly. Therefore, the centerline of several new car fronts from the different vehicle classes from 2 participating OEMs were checked against the chosen profiles. It was found, that those new car fronts matched the ones based on [2] still reasonably well. It can hence be assumed that the models chosen for this trend study do still cover a wide range of not only older but also recent realistic car fronts.

Vehicle models – detailed study: Two studies were conducted using detailed vehicle models. Study 1 used a facet vehicle model build in MADYMO representing an LFC, whereas in Study 2 simulations were carried out against 3 vehicle models representing an SFC, SM/RS and SUV built in LS-Dyna. All vehicles models used within these two studies were well validated for pedestrian impact and representing actual recent car models.

SIMULATION MATRIX

The parameters chosen for variation as well as their range were based on input retrieved from WP1 “accident analysis” as well as pragmatic considerations like speed limits or availability of models. Within WP1 several sources of accident data to define accident scenarios which are statistically more relevant in EU were analyzed. The most relevant accidents can be characterized as follows:

- Situations where pedestrian was struck by vehicle when crossing road

- Vehicle classes: most representative by European accident data (1. SFC, 2. SM, 3. LFC, 4. SUV and MPV)
- Walking adult and running child pedestrians
- Vehicle speed: covering a range of impact speed, at least from 25 to 40 kph.

Not all these parameters can be described in a statistically meaningful way by investigations conducted in WP1, and some of them cannot be practically addressed by available simulation technology (for example, both driver and vehicle reaction to forthcoming impact).

Some choices were made in terms of parameters setup in T3.1 simulation plan. First of all, the vehicle was assumed to proceed on a straight trajectory with constant speed or constant deceleration at impact, and no driver reaction is following the impact. As for the pedestrian, only standard body types were considered (6YO, AF05, AM50, AM95).

The general simulation set-up and overall parameter variation is presented in *Figure 4*.

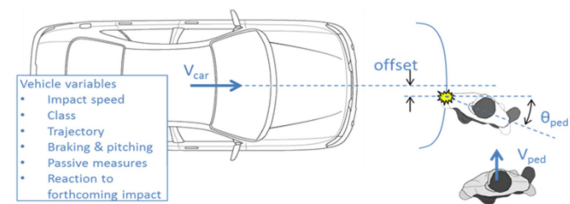


Figure 4: General simulation set-up and overall parameter variation

Trend study: The trend study was conducted in 3 steps with different parameter sets for variation. Due to the simplicity of the car models, runtime for the simulations was low allowing for a large number of simulations. The following parameter variations were considered within the different steps:

Step A: different pedestrian sizes

- 4 pedestrian models (6YO child, 5th female, 50th and 95th male)
- 18 simplified car models (based on [2] and [11])
- 5 car velocities (20 / 30 / 40 / 50 / 60 km/h) and 3 additional car velocities for 6YO child and 50th male (25 / 35 / 80 km/h)
- 1 pedestrian stance (left leg front)
- 1 pedestrian to car orientation (0 degrees = perpendicular to car)

Step B: 50th percentile male

- 1 pedestrian model (50th percentile male)

- 18 simplified car models (based on [2] and [11])
- 5 car velocities (20 / 30 / 40 / 50 / 60 km/h)
- 2 walking pedestrian stances (left leg front / right leg front)
- 3 pedestrian to car orientations (-15 / 0 / 15 degrees)

Step C: 6 year old child

- 1 pedestrian model (6YO child)
- 18 simplified car models (based on [2] and [11])
- 5 car velocities (20 / 30 / 40 / 50 / 60 km/h)
- 3 pedestrian stances (left leg front / right leg front / running)
- 3 pedestrian to car orientations (-15 / 0 / 15 degrees)

This matrix resulted in a total of 1710 simulation runs, of which 1683 could be used for further analysis. The remaining simulations aborted due to numerical instabilities and were neglected for the analysis. The posture used for the running child (see also *Figure 2*) was established based on visual examples of running children found on the internet as no standardized “running child posture” exists so far.

Detailed vehicle model study 1: In this study, only one pedestrian model (MADYMO 50th percentile facet male) and one car model representing a LFC were investigated. The following parameters were varied for a full factorial simulation matrix resulting in 32 simulations:

- Walking stance 50th male pedestrian (struck (left) or non-struck (right) leg front)
- Lateral position of pedestrian (centerline or corner impact)
- Vehicle speed (20 or 40 km/h)
- Vehicle braking (0 or 1g)
- Vehicle pitch (0 or 3deg)

Detailed vehicle model study 2: In this study, two pedestrian models (THUMS 50th percentile male and 6 year old child) and three car models were investigated, based on the priorities from WP1 and the findings from the trend study (e.g. pedestrian orientation not affecting pedestrian kinematics as much as leg positioning). The orientation of the pedestrian towards the car was kept perpendicular and the impact assumed to occur on the centerline of the car for 96 simulations within this study:

- Walking stance 50th male pedestrian (struck (left) or non-struck (right) leg front)
- Running stance 6 year old child (struck (left) or non-struck (right) leg front)
- Vehicle class (Mini / SFC / SUV)

- Vehicle speed (20/30/40/60 km/h)
- Vehicle in constant speed or full braking and pitching conditions

The vehicles chosen for the study account for three clearly different front end shapes. Height of BLE ranges from 710mm in case of SFC, to 757mm of SM, to 854mm of SUV.

RESULTS

Output parameters that were investigated within all three studies related to the pedestrian kinematics were as follows:

- Head WAD / impact location
- Head impact angle
- Head impact speed

In addition to that, also information on the upper leg impact angle as well as speed was gathered for the detailed vehicle study 2.

In general it could be found, that for the head output parameters besides the choice of pedestrian the vehicle speed is most influential parameter.

Trend study: For all pedestrians the head impact location (WAD) rose with increasing vehicle speed. No general influence of the pedestrian orientation towards the car could be found.

The 6 year old child head always hit the bonnet of the car, never the windscreen. The 95th percentile male hit the bonnet in approximately 6% of all simulated conditions but only if the initial speed of the car was 30km/h or less. Two cases were found where this pedestrian hit its head on the car roof, in all other cases the first impact was located on the windscreen.

The 50th percentile male hit a car either on the windscreen, or on the upper bonnet plane. The 5th female results were in-between those of the 50th male and the 6 year old child. As expected it could be seen, that the taller the pedestrian, the higher the head impacted on a car (under similar boundary conditions).

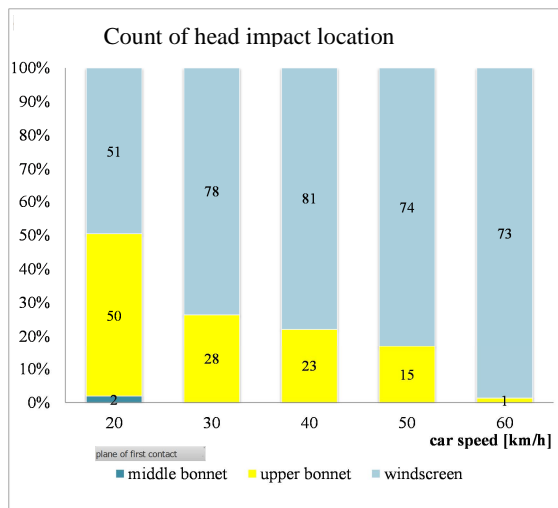


Figure 5: 50th male – head impact location over vehicle speed (Step B results)

When checking the influence of the impact speed on the head impact location for the 50th percentile male, it could be seen that there is a significant increase of impacts on the windscreen when increasing the car speed from 20 to 30 km/h (simulations considered from all vehicle shapes, see Figure 5). When increasing the car speed even further, the portion of hits to the bonnet diminished almost to zero. This indicates that hits on the bonnet are mainly found on the upper most part of the bonnet and proceed over the windscreen base towards the middle of windscreen with increasing speed.

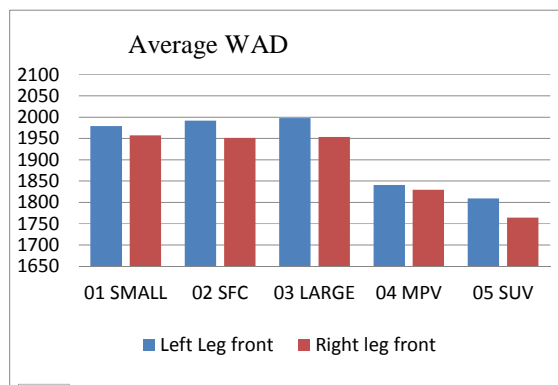


Figure 6: 50th male – influence of stance on average WAD per vehicle class

Though the orientation of the pedestrian towards the car was not found to influence the head impact location significantly, an influence of the pedestrian stance could be found for the 50th percentile male (see Figure 6). If the struck-side (left) leg was positioned to the front, an increase of the average WAD could be seen throughout all defined vehicle classes. Only for the MPV the difference was negligible. For the 6 year old child no influence is found for different walking stances, only for changing the walking to a running stance.

It was found, that a running child would generally hit the bonnet lower than a walking one.

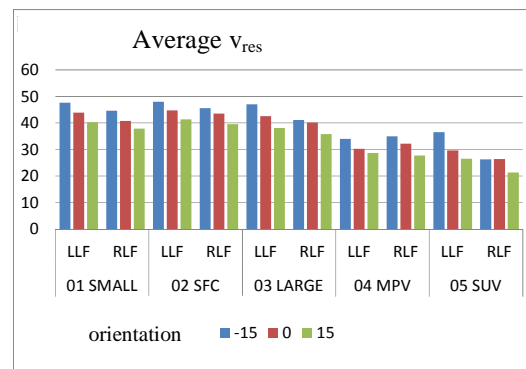


Figure 7: 50th male – influence of stance and orientation on average head impact velocity per vehicle class (Step B results)

The head impact speed is highly influenced by the car speed. The higher the speed of the car, the higher the head impact speed. Also, an influence of the orientation of the pedestrian can be seen when looking at the average resultant head impact speed. From Figure 7 several conclusions can be drawn for the average head impact speed (for the 50th percentile male pedestrian):

- It is higher for small cars compared to larger cars
- It is higher for left (struck-side) leg front compared to right leg front
- It is for both stances highest if the pedestrian is heading under 15 degrees towards the car and lowest if the pedestrian is heading under 15 degrees away from the car.

The difference between the vehicle classes is less significant for the 6 year old child. Also, the average head impact speed is lower for the child compared to the average male.

No head impact below WAD 1000 was observed for any of the car shapes. No child head impact was established above WAD 1500 and no 50th percentile male head impact below WAD 1500. For the 6 year old child and the 50th percentile male pedestrian the current Euro NCAP WADs hence match very well. The 5th female results form a good transition between both pedestrian sizes, though most hits are established in the adult rather than the child area.

The only pedestrians that hit their head higher on a car than WAD 2100 are the 95th percentile male in general and the 50th percentile male for a few cases when the car speed rises above 40 km/h. It can be concluded, that pedestrians up to a size of a 50th

percentile male are well covered within the current Euro NCAP pedestrian test protocol [3] by the chosen WADs.

For the 95th percentile male, only 23% of all head impacts fall below WAD 2100. If the speed of the car is 30 km/h or higher, the head of this pedestrian is likely to hit the car at more than WAD 2100. It could hence be argued, that in order to cover also pedestrians taller than average, an increase of the maximum WAD beyond WAD 2100 could be beneficial.

From the step A simulations which considered all pedestrian sizes head impact speeds were gathered. From *Figure 8* it can be seen, that for car speeds up to and including 50km/h a head impact speed of 40 km/h covers 92% of the impacts for the 6 year old child. For all adults, the coverage is however much lower (60 to 70%). When looking into this issue in more detail it can be seen, that for the 6 year old child the head impact speed hardly ever rises above the initial car speed. Also, the first contact between head and car is always established on the bonnet for this pedestrian. This is much different for the adult pedestrians which are also able to hit the windscreen.

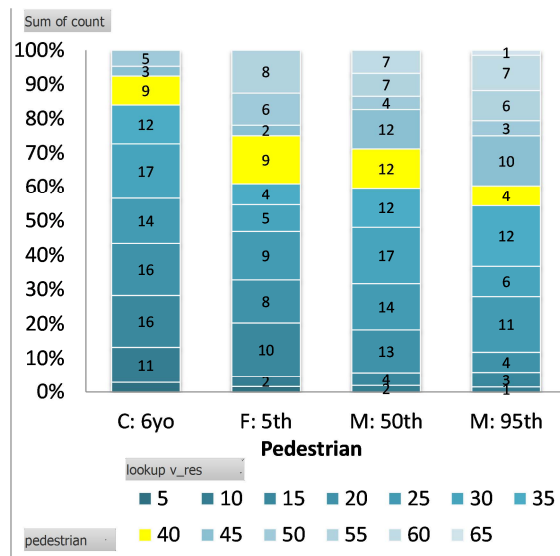


Figure 8: head impact speed distribution per pedestrian, only car speeds up to 50 km/h considered

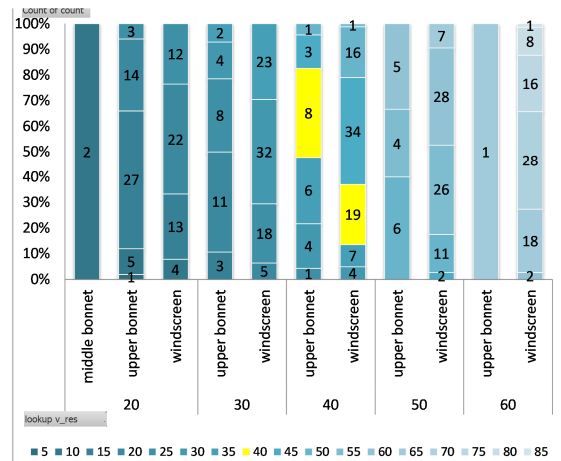


Figure 9: head impact speed [km/h] of 50th percentile male (Step B simulations) over initial car speed [km/h] and first plane contacted by head

Figure 9 shows the head impact speed distribution for the 50th percentile male over the initial car speed. Additionally, the car speeds are split by first head impact location. The following conclusions can be drawn:

- The higher the car speed:
 - the more likely the head impact speed is higher than the car speed
 - the more likely the head hits the windscreen rather than the bonnet
- head impact speeds are higher on the windscreen compared to on the bonnet
- head impacts on the bonnet are well covered with an impact speed of 40 km/h – 99 out of 119 hit the bonnet with an impact speed not higher than 40 km/h. Considering only car speeds up to 40 km/h, a head impact speed to the bonnet of 40 km/h covers even up to 96% of the occurring impacts.
- To achieve similar coverage as for bonnet impacts, head impacts on the windscreen should be conducted with a higher impact speed. Only 45% (159 out of 357) head impacts occur with a speed lower or equal to 40 km/h. Raising the head impact speed on the windscreen to 50 km/h would increase the coverage to 62% (all car speeds considered). Considering only car speeds up to 40 km/h, a head impact speed to the windscreen of 40 km/h and 50 km/h covers up to 75% and 99%, respectively.

In literature similar trends can be found for PMHS tests with crash conditions representing a centerline pedestrian impact at 40 km/h. [6], [7] and [9] found that the head impact speed ranged from 68% to 146%, with a tendency for lower values for bonnet impacts compared to windscreen impacts. The hypothesis that was set up in these studies is that an higher angle of the windscreen results in a higher

head impact speed as the neck cannot limit the head motion to the same extend as in a bonnet impact.

Detailed vehicle model studies: From the detailed vehicle studies no results were obtained that were contradicting to what was found in the trend study. For detailed study 1 pitching was investigated separately from braking, i.e. all vehicles in the field will automatically show pitching due to braking, but depending on vehicle suspension stiffness (and other vehicle parameters) the observed level of pitching can vary from car to car. Furthermore, the effect of braking is higher for lower speeds than for higher speeds, whereas pitching is simply changing the vehicle “geometry” for impact independent from speed. By separating the effects of braking and pitching, it can be analyzed whether braking or pitching effect is bigger and how the two compensate each other.

Starting the analysis WAD, the overall picture for different velocities was a bit fuzzy. Especially the effects of braking and pitching were not homogeneous. So, isolated analysis for different speed levels was performed.

Starting at 20 km/h, *Figure 10* shows the pareto chart for WAD at 20 km/h. Only braking, pitching, pedestrian position and pedestrian stance have significant influence on WAD. Comparing decreases with braking and pitching influence at 20km/h it is obvious, that braking is more significant in this case.

In *Figure 10* the influence of the selected input parameters (vehicle braking, pitching, lateral pedestrian position and pedestrian stance) on the WAD of the 50th percentile pedestrian is shown for 20 km/h. It can be seen, that WAD decreases with braking, but increases with pitching. However, for the 20km/h simulations and for the given pitch angle of 3° braking has more influence than pitching. Therefore, the combined braking+pitching is decreasing WAD. Looking to the other parameters, WAD increases for corner position and for left leg rear (LLR).

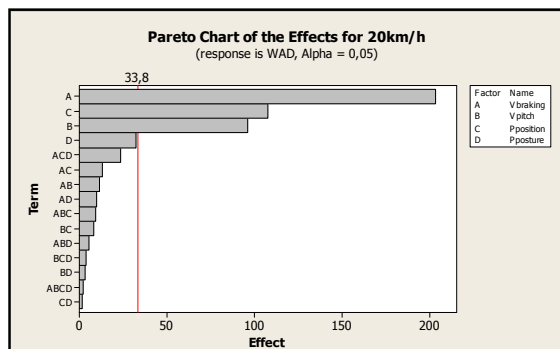


Figure 10: Pareto chart for 50th percentile male head WAD at 20 km/h

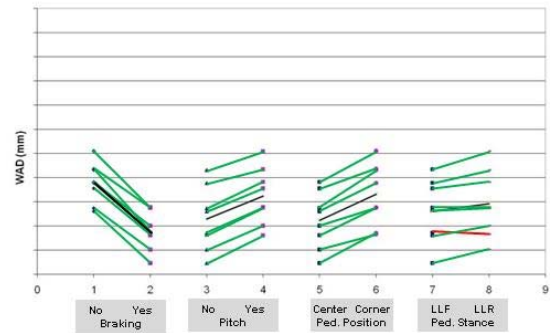


Figure 11: Influence of selected input parameters on 50th percentile male head WAD at 20 km/h

The same analysis for the 40kph simulations shows some significant differences. *Figure 12* shows the pareto chart for 40 km/h, pitching, pedestrian stance, pedestrian position and braking have significant influence on WAD. It is obvious, that the pitching effect is significantly higher than braking here.

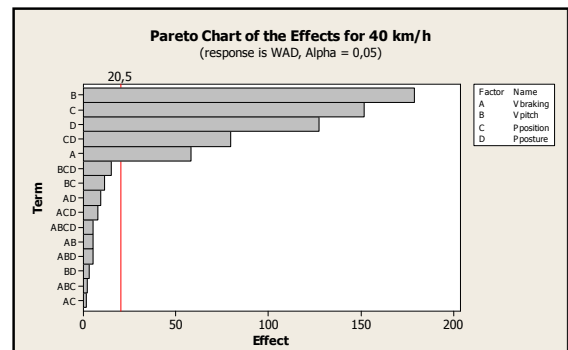


Figure 12: Pareto chart for 50th percentile male head WAD at 40 km/h

Looking to the individual effects in *Figure 13* it can be seen that braking is decreasing WAD whereas pitching is increasing WAD to a higher extend. So, for 40 km/h pitching is more dominant and therefore the overall effect of braking combined with pitching is increasing WAD. Looking to the other parameters in *Figure 13* corner position and LLR are also increasing WAD.

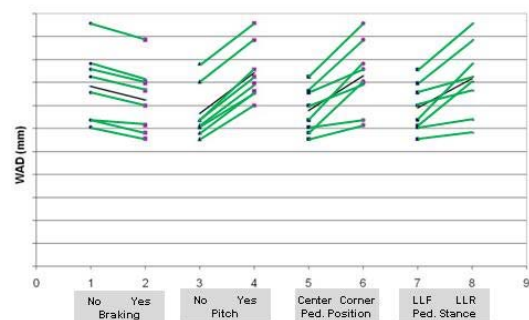


Figure 13: Influence of selected input parameters on 50th percentile male head WAD at 40 km/h

Similar analysis was done for head impact angle and head impact velocity. The general trends as observed in the WAD analysis could also be found there. Besides the impact speed itself, braking and pitching are the most influencing parameters, with pitching being more dominant for increasing speeds.

As the number of simulations conducted in detailed studies is limited and not sufficient to use for statistical trend analysis, the kinematics of pedestrians in detailed models can be used further to confirm the validity of the results from the trend study presented above.

As an example, the kinematics of AM50 impacting small family car (SFC) at 40kph with left leg forward was compared in Figure 14.

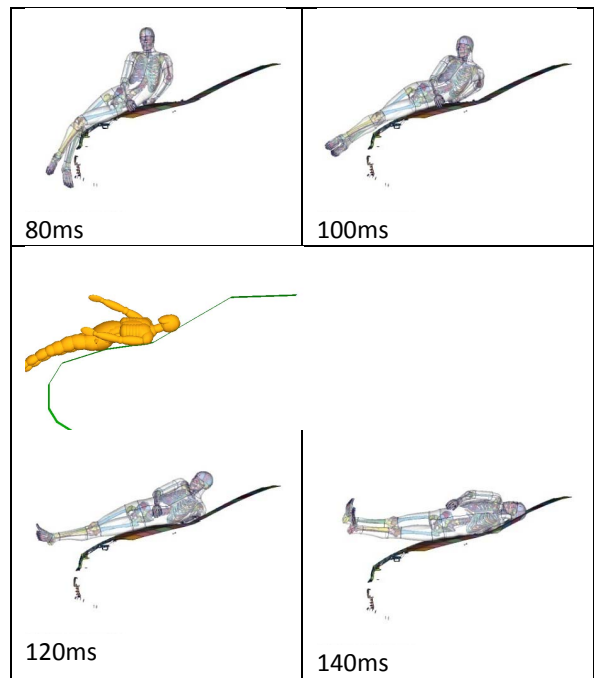
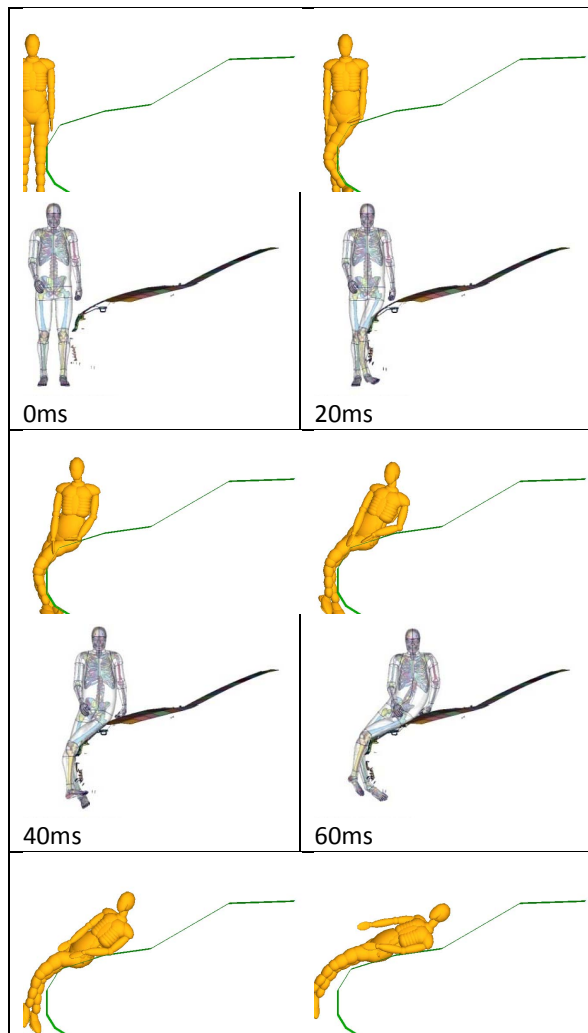


Figure 14 Kinematics of AM50 adult impacting a Lower medium class (SFC) vehicle at 40kph; comparison of simplified (upper) and detailed (lower) simulation

At the very beginning of the impact, the leg on the struck side is contacting the bumper and the femur starts to rotate to follow the shape of the car (time 0-30ms); this behavior is described in similar manner by simplified and detailed models. At around 40ms, the hip starts contacting the bonnet leading edge area, providing a higher force to the torso, which also starts to move (time 40-60ms); some differences start to appear at this point due to the simplified representation of hood shape and stiffness for the simplified model, which results in a different sliding of the hip over the bonnet compared to the detailed model. As a consequence, the torso of the simplified model rotates more and causes earlier impact of the head to the windshield (time 70-120ms). For the detailed model, the smooth shape of the hood and its realistic deformation allow the legs and hip to slide, which causes later torso rotation and head contact. With this mechanism, the head impact point is occurring at a more rearward position (cf. knee location at 100ms). This difference is expected to be mostly due to the characteristics of the simplified vehicle model, which has a simplified stiffness response and does not change its shape during the impact; the simplified model can be therefore considered as causing a systematic error on the trends which had to be accounted for when summarizing results.

Harmonization of the head impact results In order to identify the best set of input parameters for the impactor simulations and physical tests to be

conducted in the next step, the results of the trend study were combined with the results of the detailed vehicle studies. For this purpose, corridors were established from the trend study for different vehicle speeds evaluating trends by means of weighted averages of the simulation results.

Probability corridors for maximum and minimum values were based on linear fitting of representative maximum and minimum results. These trends were then adjusted with the results from the detailed vehicle studies to account for systematic effect induced by simplified vehicle models.

In *Figure 15* and *Figure 16* the respective corridors can be found for the 50th percentile male as well as for the 6 year old child.

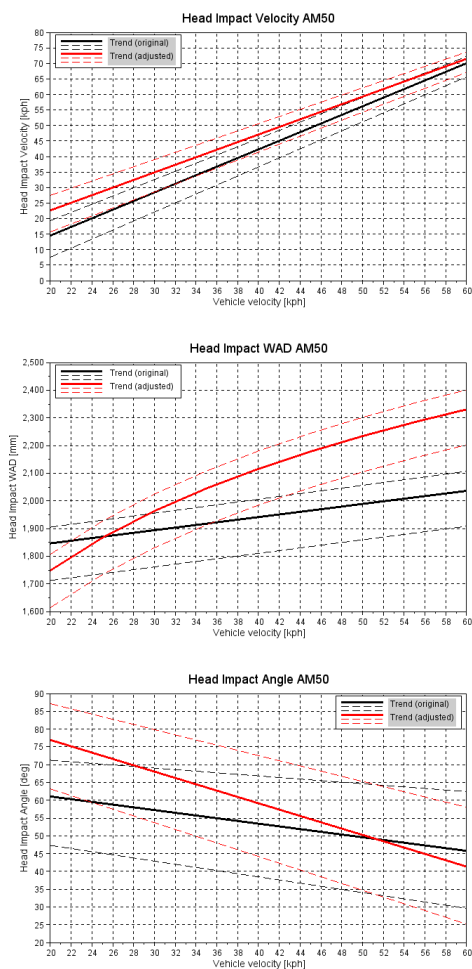


Figure 15: Probability corridors for head WAD, velocity and impact angle from the trend study (black) and adjusted by the detailed studies (red) for the 50th percentile male pedestrian.

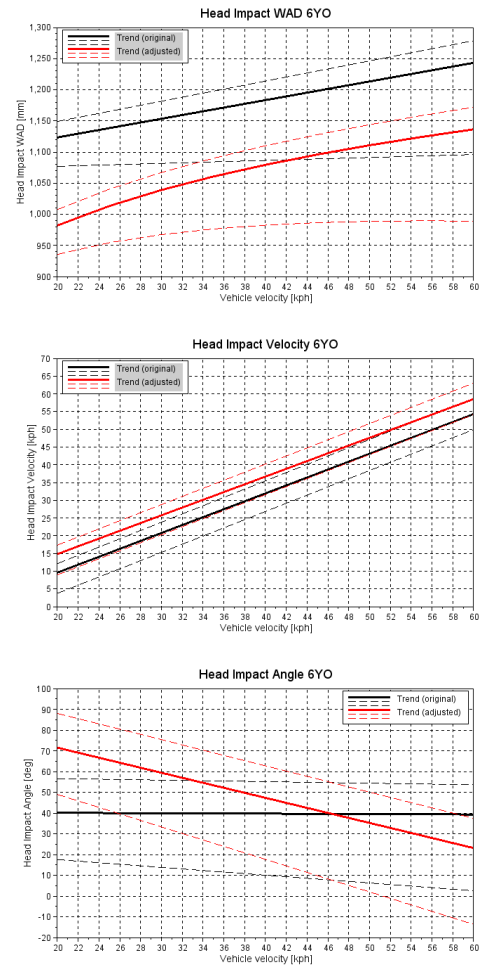


Figure 16: Probability corridors for head WAD, velocity and impact angle from the trend study (black) and adjusted by the detailed studies (red) for the 6 year old child pedestrian.

Main differences were found in **WAD evaluation**, where simplified models seem to underestimate the AM50 impact location for speeds greater than 25kph, when vehicle deformation tends to be significant. This mechanism has been explained above. The opposite effect was found in case of 6YO, but it should be remarked that detailed simulations were only considering running posture. The simplified 6YO simulations results are averaged with those from child pedestrians in walking conditions which were found to result in higher WAD. Moreover, in case of WAD, a significant improvement of trend fitting was observed when using logarithmic fitting rather than linear (R^2 correlation increased from 68.7% to 79.6% in case of AM50 results); that fitting suggests a tendency of head impact location to change much more at lower than higher impact speed.

Some difference can also be found for the trends of the head impact angle for the 6 year old child. The adjusted corridors are much more defined compared to the corridors from the trend study which are quite wide and basically showing not much influence of the vehicle speed at all. This can be explained when looking into the vehicle shapes. For the trend study 18 different contours were considered compared to 3 for the detailed vehicle studies.

From the trend study it can be seen, that the contour of the vehicle can have a major influence on the **head impact angle**. For vehicles with a high car front the impact angle can be almost 90 degrees as the head is not yet bending towards the car upon impact. For cars with a lower car front trends are similar as for an adult, though the absolute head impact angles are in general more shallow as can be seen exemplarily in *Figure 17*. This effect results in less pronounced corridors for the trend study and is much less apparent in the detailed study due to the limited amount in variation of the car fronts.

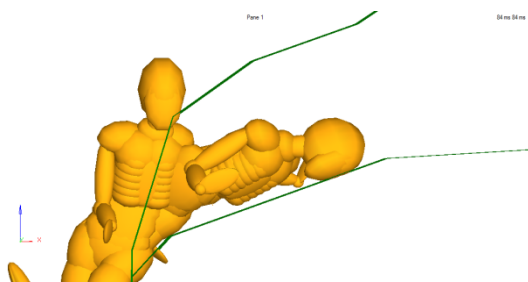


Figure 17: Example of the position of the head for a 6 year old child on different car fronts under similar boundary conditions

Trends found for **impact velocity** are quite consistent between simplified and detailed simulations, considering that the average results from detailed simulations almost fall in the probability corridors evaluated in the trend study.

Upper leg impact conditions Results for upper leg impact conditions were extracted from detailed study 2 only, therefore there was no need for harmonization; on the other hand, they depend on the actual vehicle used, and it is difficult to use them to define general trends. Setting impactor conditions equivalent to results from human body model simulation is not trivial due to femur configuration which is changing during the impact, see *Figure 18* and *Figure 19*. BLE impactor, on the other hand, has fixed impact location and angle, depending on vehicle BLE height and bumper lead [3].

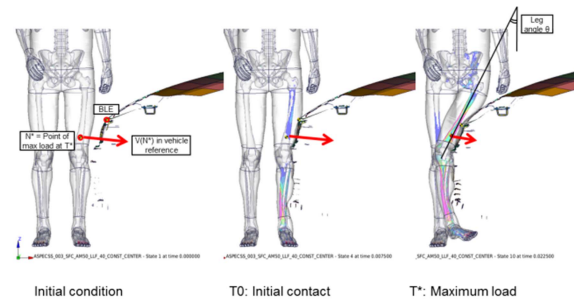


Figure 18 Upper leg impact kinematics; N^* is the point on femur subject to highest load; T_0 is time of first contact of N^* to the vehicle; T^* is time when N^* reaches maximum load.

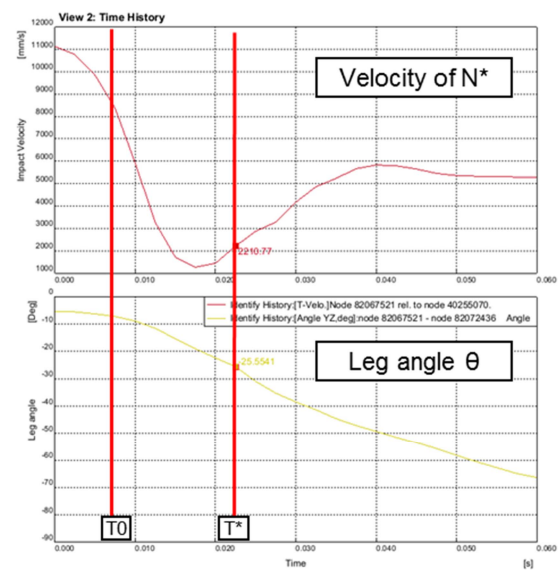


Figure 19 Time-histories of velocity of femur point with maximum load N^* (in vehicle reference) and femur angle θ

Taking into account the suggestions from [12] and [15], the criteria set to analyze parameters effect were:

- Velocity, which is set at initial impact conditions at time T_0
- Angle, which is set at femur maximum load
- Position, which should depend on vehicle geometry and location of maximum load on the femur

Setting equivalent impactor mass over the speed and impact conditions considered is still an issue. Euro NCAP suggests some energy criterion, which is based on 40kph impact speed [11]. On the other hand, some authors suggest to use just a fixed equivalent mass of 7.5 kg for the femur [12].

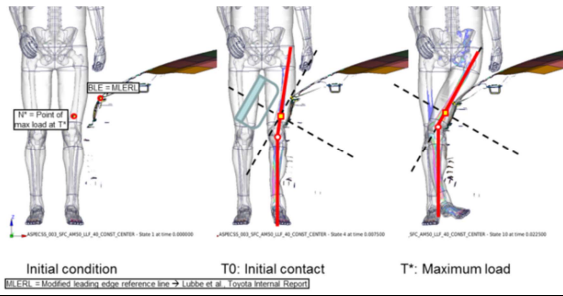


Figure 20 Proposed conditions for upper leg impactor setup in case of AM50 impacting SFC at 40kph.

As it can be observed from the sample case of AM50 impacted by SFC at 40kph (Figure 20), the location of most severe load might be quite different from BLE. That is a purely geometric descriptor, and it does not consider the actual properties of the vehicle front end. The proposed equivalent setup for the BLE impactor is summarized in Figure 21, where 511mm is the distance between knee and ground in THUMS 50th percentile adult model.

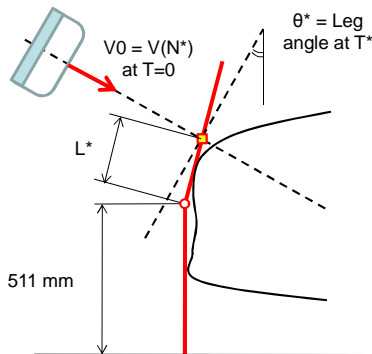


Figure 21 Proposed impactor setup

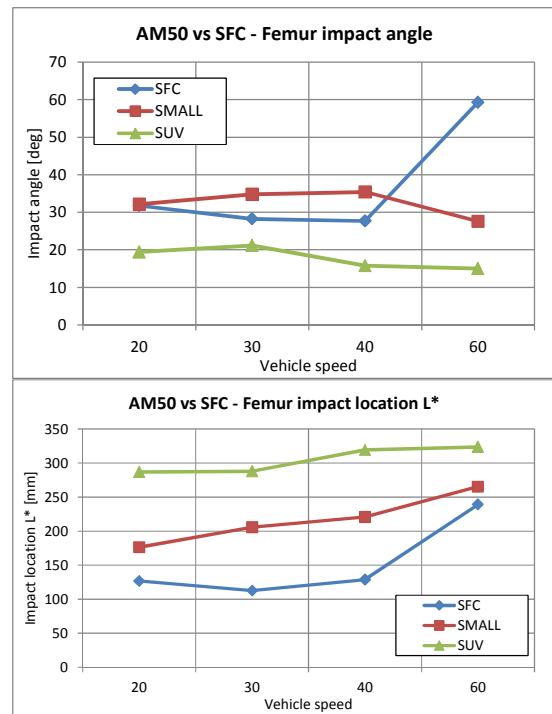
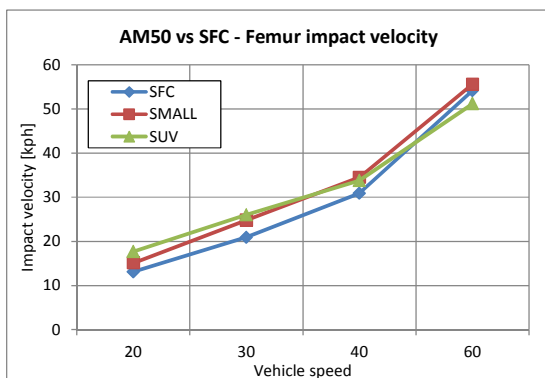


Figure 22 Upper leg impact conditions: impact velocity, angle and location of point N*

The results obtained from detailed simulations with AM50 model were summarized in Figure 22. Charts show a clear trend for impact velocity, but do not show clear trends for impact angle and location with vehicle velocity. The impact location seems to depend on BLE height, but the impact angle is not proportional to this geometrical descriptor, due to femur loading being dependent on actual front end stiffness. An interesting result comes from the case of SFC at 60kph: impact angle and location seem changing completely from results at 40kph and lower impact speeds. This effect can be explained by the actual vehicle behavior: bonnet deforms enough at 60kph to cause femur to contact a hard point in the car (Figure 23, condition 2) at a different location than the bumper in 40kph impact (Figure 23, condition 1).

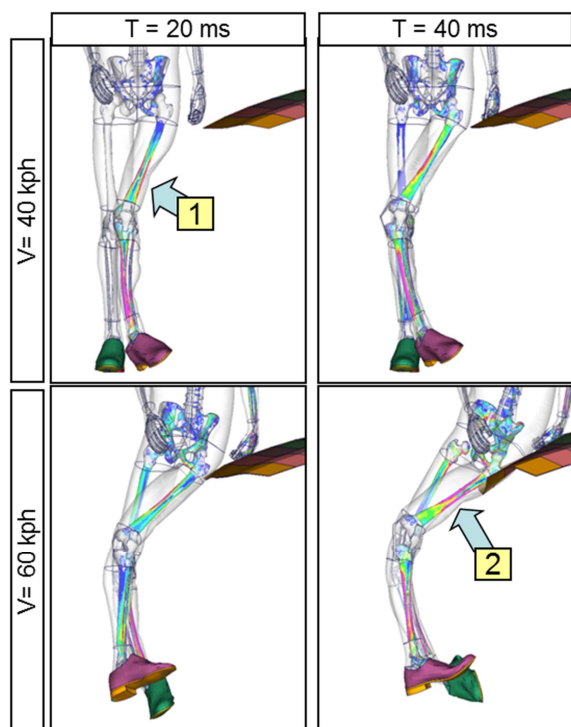


Figure 23 Different mechanism causing maximum load on the femur when impacting SFC at 40kph and 60kph (actual vehicle structure not shown).

CONCLUSIONS

This study addressed the need to investigate impact conditions for a range of vehicle types, impact speed and pedestrian types, while considering the scatter caused by other parameters, such as the pedestrian posture or the vehicle braking.

A large number of parameters was studied by combining a trend study with simplified models and detailed studies with detailed vehicle models to confirm the trends. Results harmonization was also established by means of a comparison of the pedestrian kinematics to confirm a systematic effect from assumptions in the simplified models on the head impact conditions.

With regards to 50th percentile male and 6 year old child, the results for the head impact conditions also confirm the general validity of the current Euro NCAP setup, which is based solely on a vehicle impact speed of 40kph.

The results from this study will be utilized in a next step with in the AsPeCSS project to set up impactor tests addressing a range of impact speeds and representing conditions due to vehicles involved in pedestrian accidents in Europe, also considering new active and passive safety measures for VRU.

ACKNOWLEDGEMENT

This paper summarizes the latest results corresponding to pedestrian kinematics of the European project AsPeCSS (Assessment

methodologies for forward looking Integrated Pedestrian and further extension of Cyclist Safety Systems) no. 285106

REFERENCES

- [1] AP-SP33-022R, "Concepts for a hybrid test procedure", Integrated Project APROSYS 6th framework program, 2006
- [2] AP-SP31-009R, "Stiffness corridors for the current European Fleet", Integrated Project APROSYS 6th framework program, 2008
- [3] Euro NCAP, "Pedestrian Testing Protocol" v6.2, December 2012
- [4] Hoof, J. van, Lange, R. de, Wismans, J., "Improving Pedestrian safety using Numerical Human Models", STAPP Conference Proceedings, 2003
- [5] Janssen, E.G., Nieboer, J.J., "Protection of vulnerable road users in the event of a collision with a passenger car, part 1 – Computer simulations", TNO report No: 75405002/I December 1, Delft, 1990
- [6] Kerrigan, J., Arregui, C., Crandall, J., "Pedestrian head impact dynamics: comparison of dummy and PMHS in small sedan and large SUV impacts", ESV 2009
- [7] Kerrigan, J., Crandall, J., Deng, B., "A comparative analysis of pedestrian injury risk predicted by mechanical impactors and post mortem human surrogates", Stapp Car Crash J. 2008
- [8] MADYMO Human Models Manual, Release 7.4, November 2011
- [9] Masson, C., Serre, T., Cesari, D., "Pedestrian-Vehicle accident: analysis of 4 full scale test with PMHS", ESV 2007
- [10] Meijer, R., Hassel, E. van, Broos, J. et al, "Development of a Multi-Body Human Model that Predicts Active and Passive Human Behaviour", IRC-12-70, IRCOBI conference 2012
- [11] Rodarius, C., Mordaka, J., Versmissen, T., "Bicycle safety in bicycle to car accidents", TNO report TNO-033-HM-2008-00354, 2008
- [12] Snedeker, J., Walz, F., Muser, M., Lanz, C., "Assessing femur and pelvis injury risk in car-pedestrian collisions: comparison of full body PMTO impacts, and a human body finite element model", ESV 2005
- [13] Yasuki, T., Yamamae, Y., "Validation of kinematics and lower extremity injuries estimated by total human model for safety in SUV to pedestrian impact test", Journal of biomechanical science and engineering, Vol15, 2010
- [14] Watanabe, R., Katsuhara, T., Miyazaki, H., Kitagawa, Y., Yauki, T., "Research of the

Relationship of Pedestrian Injury to Collision Speed, Car-type, Impact Location and Pedestrian Sizes using Human FE model (THUMS Version 4)", Stapp Car Crash J., 2012

[15] Lubbe, N., "Proposal for an updated setup for upper leg impactor test", Toyota Motor Europe internal report.

EFFECT OF VISIBILITY AND PEDESTRIAN PROTECTION PERFORMANCE ON PEDESTRIAN ACCIDENTS

Shigeru Ogawa

Mazda Motor Corporation
Japan

Qiang Chen

China Automotive Technology & Research Center
China

Kenji Kawaguchi

Takahiro Narikawa

Mie Yoshimura

Mazda Motor Corporation
Japan

Song Lihua

Mazda Motor (China) Co., Ltd.
China
Paper Number 13-0365

ABSTRACT

The pedestrian accident is an important accident type that should be studied to reduce the number of accidents worldwide. The factors in pedestrian accidents should be quantitatively clarified in order to get clues to reduce the number of pedestrian accidents. In an effort to address this issue, two vehicle-related areas: visibility around A-pillar and pedestrian head protection performance, were analyzed to clarify their influences on the number of pedestrian accidents with the fatality or the injured for each vehicle model in this study. Macro accident data based on the police data from the year of 2008 through 2011 was compiled by ITARDA (Institute for Traffic Accident Research and Data Analysis) in Japan for around 24,000 pedestrian accidents on 39 vehicle models. The number of pedestrian accidents with fatal/serious/minor injury per 10,000 registered vehicles for each vehicle model was utilized as objective variables to determine the probability of the accidents. The relationships between each of the vehicle-related factors described above and the objective variables were carefully scrutinized with use of scatter charts, correlation analyses and multiple regression analyses. It was successfully clarified that the pedestrian accident would be more likely to occur when the angle of hindrance due to A-pillar is larger. It was also captured that the larger horizontal angle of view through the windshield would reduce the occurrence of pedestrian accident. Furthermore, it was clarified that the influence of visibility on the occurrence of pedestrian accident was different among the straight going maneuver, the right-turn maneuver, etc. It was possible to predict the number of fatality or injured in the pedestrian accidents to a certain degree of probability, with use of the combination of visibility indices. In addition, it was clearly captured that the better pedestrian head protection score in the JNCAP test would lead to the

decrease in the number of pedestrian accidents with the fatality or the injured.

Furthermore, the combination of visibility indices and pedestrian head protection score in the JNCAP test successfully provided much better prediction of the number of fatality or injured in the pedestrian accidents. In other words, it was clarified that the optimization of parameters in visibility indices and pedestrian head protection could lead to the decrease in the number of pedestrian accident.

The effects of the pedestrian head protection score in the JNCAP test on the number of pedestrian accidents with the fatality or the injured were elaborately scrutinized from the viewpoint of danger-cognitive velocity and vehicle maneuver, i.e., straight-going, right-turn and left-turn. The results demonstrated that the pedestrian head protection score in the JNCAP test is highly correlated with the pedestrian accident especially in the case of pedestrian's being impacted by vehicle body not a tire nor road, and furthermore in the straight going maneuver at over 40km/h of danger-cognitive velocity.

In-depth accident analysis with data of ITARDA and CIDAS (China In-depth Accident Study) was conducted in Japan and China. The result showed that JNCAP would be effective especially in the crash velocity range of 31-50km/h, which accounts for as much as 40% of total 115 occurred in five major cities in China.

INTRODUCTION

As to fatalities in traffic accidents in Japan, the number of pedestrian has exceeded that of vehicle occupants, consisting of more than 35% of all fatalities [1].

It was said that the number of fatalities of pedestrian in China was 9,891 in 2011, which was equivalent to 16% of all fatalities, 62,387 [2].

A lot of NCAP operations around the world have been introducing pedestrian protection performance tests first on the head, and then on the lower extremities in order to reduce the injury in the pedestrian accidents [3] [4] [5] [6] [7].

Some car manufacturers started to introduce the pop-up hood and the external pedestrian airbags. On the other hand, from the viewpoint of active safety, some automatic emergency braking systems for pedestrians have been promoted by EuroNCAP, etc. [8].

In the present study, the factors in pedestrian accidents should be quantitatively clarified in order to get clues to reduce the number of pedestrian accidents in accordance with the following steps.

1. Visibility performance for each vehicle model was examined in comparison with pedestrian accidents because better visibility seems to be one of the most important factors for avoiding pedestrian accidents.
2. The correlation between pedestrian head protection performance and pedestrian accidents was examined.
3. The combination of visibility and pedestrian head protection performance was studied for good prediction of the number of injured pedestrians. This can be said as the unified theory of visibility and pedestrian head protection performance.
4. Effect of the pedestrian head protection score in the JNCAP test on pedestrian accidents was elaborately scrutinized from the three viewpoints: injuring objects, danger-cognitive velocity and vehicle maneuver, i.e., straight-going, right-turn and left-turn.
5. In-depth Accident Data in China and Japan was employed for the purpose of clarifying the characteristics of pedestrian accidents.

DATASET

Visibility parameters

Figure1 and 2 indicate the definitions of visibility parameters discussed in this study. There are four parameters: Angle of Hindrance at Driver's side (AHD), Angle of View at Driver's side (AVD), Angle of Hindrance at Passenger's side (AHP) and Angle of View at Passenger's side (AVP). The eye points were defined based on American Anthropomorphic Male 50 percentile dummy (AM50).

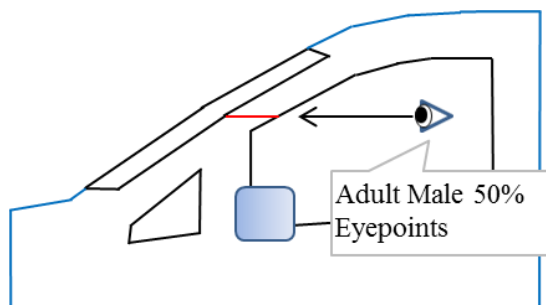


Figure1. Definitions of visibility parameters (side view).

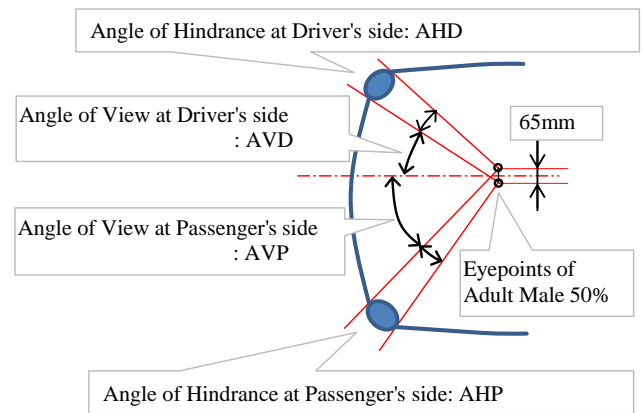


Figure2. Definitions of visibility parameters (top view).

Pedestrian Head Protection Performance

The score of pedestrian head protection performance evaluated by JNCAP was utilized as a parameter of passive safety performance. The projecting speed of the head impactor is 35km/h, and the equivalent velocity of vehicle was 44km/h. HIC, or head injury criteria, was measured. The integrated final score is converted to “0” through “4” [9].

Pedestrian Accident Data

Macro Accident Data in Japan Macro pedestrian accident data based on the police data was compiled by ITARDA (Institute for Traffic Accident Research and Data Analysis) in Japan. The following parameters were categorized in the present study.

Accident investigated period: the year of 2008 through 2011
 Injury severity: Minor, Serious, Fatal
 Danger-cognitive velocity: 20km/h or less, 20-40km/h, more than 40km/h
 Injuring objects: Vehicle body, Tire, Road, Others

Here, the fatal injury is defined as death within 24hours after the accident, and the serious injury is defined as the one which needs the treatment more than 30 days before the recovery. Macro accident data based on the police data from the year of 2008 through 2011 were compiled by ITARDA in Japan for 24,086 pedestrian accidents on 39 vehicle models. The number of pedestrian accidents with fatal/serious/minor injury per 10,000 registered vehicles for each vehicle model was utilized as objective variables to determine the probability of the accidents.

When the relationships among visibility, pedestrian head protection performance and pedestrian accident was analyzed, the vehicle models with the registered number more than 300,000 in four years were selected because the vehicles with the low volume have the wide confidence interval and could lead to fallible conclusions.

As to the 19 models of these focused vehicle models, the visibility parameters were available. As to the 29 models of them, the pedestrian head protection score in the JNCAP test was available. As to the 14 models of them, both parameters were available.

The registered numbers of each vehicle model utilized as a denominator was calculated based on sales volume in each month. The contribution rate for the sale year and the vehicle survival rate were taken into consideration.

The numbers of pedestrian accidents with fatal/serious/minor injury per 10,000 registered vehicles for each vehicle model, which was obtained by dividing the number of accidents during four years by the number of registered vehicles during four years, was adopted as objective variables to determine the probability of accidents per year.

In-depth Accident Data in Japan and China For Japan, the data collected by ITARDA through investigation on accidents around Tsukuba City, Ibaraki Prefecture was used. This data includes three body types: sedans, SUVs, and station wagons, and three driving maneuvers: straight-going, turning right or turning left. The data was collected for about 19 years from 1993 through 2011.

On the other hand, for China, the data collected by CIDAS through investigation on pedestrian accidents in Beijing, Ningbo, Changsha, Weihai and Foshan. The same body types and vehicle maneuvers as these of ITARDA's are covered. The data was collected for about 2 years from 2011 to 2012.

METHODOLOGY

The relationships among each of the vehicle-related factors described above and the objective variables were carefully scrutinized with use of scatter charts, correlation analyses and multiple regression analyses.

RESULTS

Big Pictures of Pedestrian Accidents

The distribution of casualties classified as a vehicle maneuver for each degree of injuries is depicted in Figure 3. Minor injury is a major part of injured pedestrian accidents with injuries. A lot of accidents occur in the straight-going maneuver and the right-turn maneuver, in contrast with the left-turn maneuver.

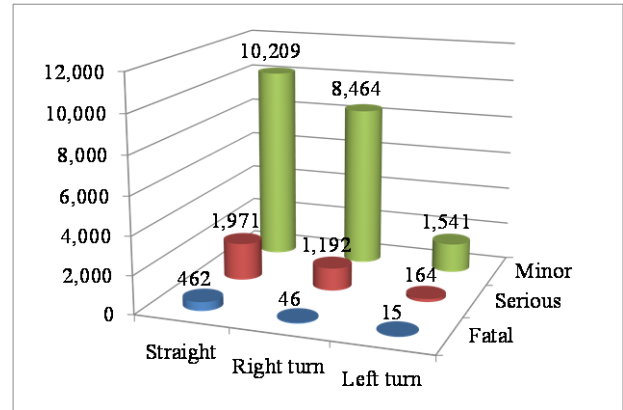


Figure3. Pedestrian accident for vehicle maneuver and degree of injury.

Figure4 demonstrated the percentages of straight-going, right-turn and left-turn for each degree of injuries. The percentage of straight-going in fatal accidents was as high as around 90%. On the other hand, however, the percentage of right-turn for each of serious injury and minor injury was around 30%, 40%, respectively, whereas the percentage of left- turn remained small for each degree of injuries.

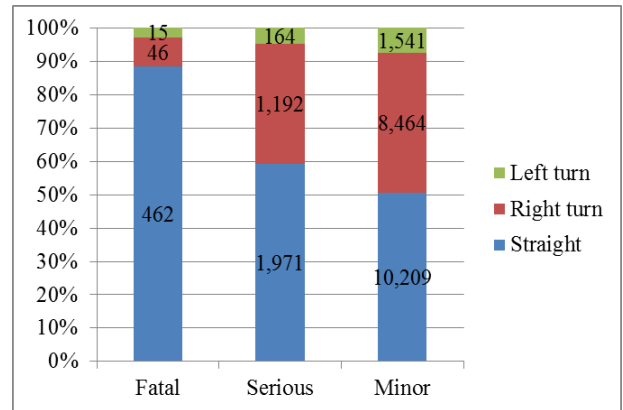


Figure4. Rates of vehicle maneuver for each degree of injuries.

Visibility Effects on Pedestrian Accident

The result of relationship between visibility and the number of all (fatal/serious/minor) injured pedestrians per 10,000 registered vehicles in the right-turn maneuver is illustrated in Figure 5. The horizontal axis indicates the angle of hindrance at driver's side (AHD) as defined in Figure 2, described above. It was clarified that the more the AHD is, the more likely it is for the injured accident to occur in the right-turn maneuver.

There were two points around 11 degrees of angle of hindrance at driver's side in Figure 5. The number of injured pedestrians for one model was more than 7, but the number for the other model was less than 3. One of the factors for this difference was considered to be another visibility parameter; angle of view at the driver's side. In fact, the former model had a relatively small angle of view at driver's side; 21 degrees, and the latter model had a large angle; 25 degrees (See in Figure 6).

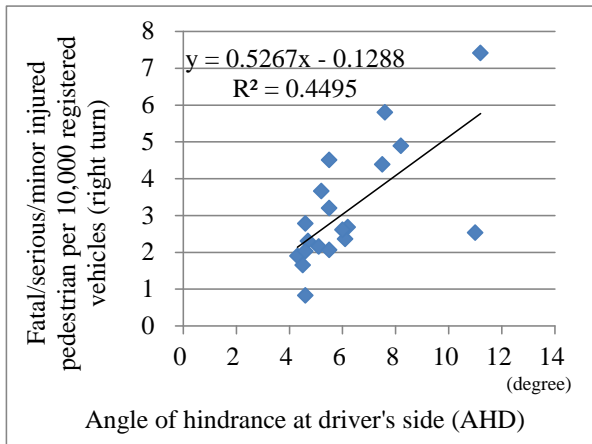


Figure 5. Relationship between the number of fatal/serious/minor injured pedestrians per 10,000 registered vehicles and angle of hindrance at driver's side in the right-turn maneuver.

Another visibility parameter, i.e. angle of view at driver's side (AVD) is adopted as horizontal axis in Figure 6. It depicted that the more the AVD is, the less the number of injured pedestrians is in the right-turn maneuver.

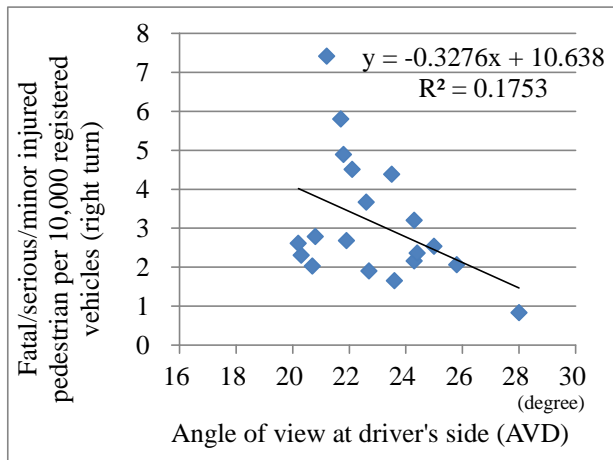


Figure 6. Relationship between the number of fatal/serious/minor injured pedestrians per 10,000 registered vehicles and angle of view at driver's side at right turn.

Correlation coefficients, which are defined to be square root of coefficients of determination and have plus and minus, for relationships among the number of fatal/serious/minor injured pedestrians and four visibility parameters were summarized in Figure 7.

This detailed examination provided different results about effects of visibility in each case of the straight-going maneuver and the right-turn maneuver.

Angle of view at passenger's side (AVP) was also found to be important in the straight-going maneuver because a larger AVP would provide a wider horizontal view through windshield.

Angle of hindrance at driver's side (AHD) and angle of view at driver's side are crucial in the right-turn maneuver as described before. AHP showed relationship to some extent, but this was because AHP had relationship with AHD.

Angles of view at both sides (AVD, AVP) were also found to be important even in the total case because a larger angle of view would provide a wider horizontal view through windshield.

In short, it can be said that the pedestrian accident would be more likely to occur when the angle of hindrance due to A-pillar is larger, and also when the angle of view is small. These results seemed to be reasonable when driving scene was imagined.

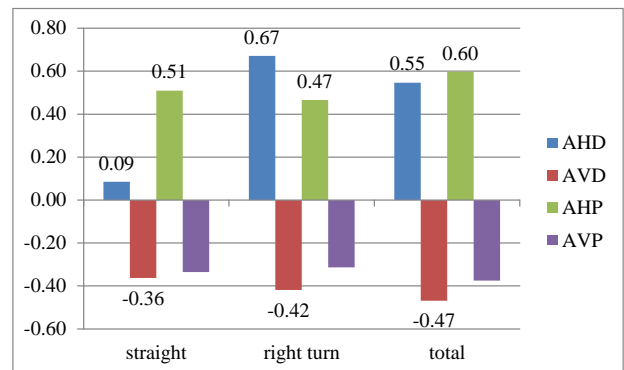


Figure 7. Correlation coefficients for relationships among the numbers of fatal/serious/minor injured pedestrians per 10,000 registered vehicles and visibility indices for each driver's maneuver.

Combination of Visibility indices: AHD and AVP

The number of all (fatal/serious/minor) injured pedestrian per 10,000 registered vehicles including three vehicle maneuver: straight-going, right-turn and left-turn was estimated by combination of visibility indices.

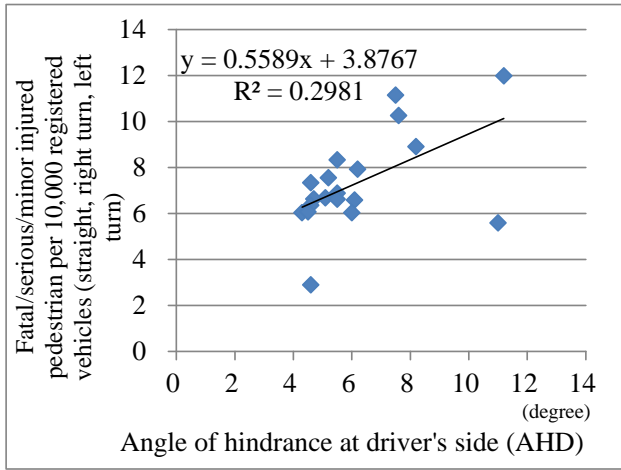


Figure8. Relationship between the number of fatal/serious/minor injured pedestrian per 10,000 registered vehicles and angle of hindrance at driver's side in straight going, right turn, and left turn.

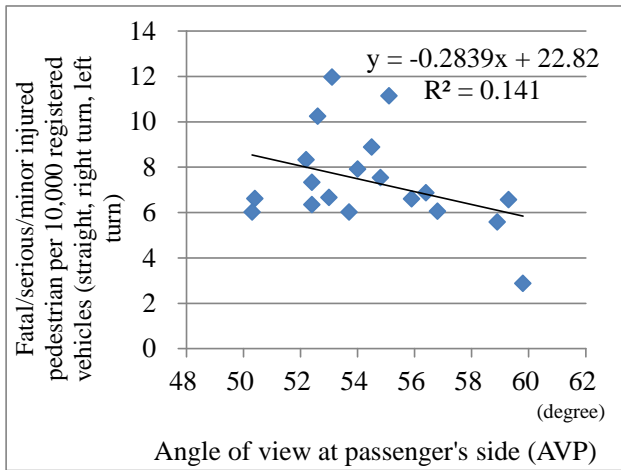


Figure9. Relationship between the number of fatal/serious/minor injured pedestrian per 10,000 registered vehicles and angle of hindrance at driver's side in straight going, right turn, and left turn.

Four visibility parameters were taken into consideration at first, and then backward elimination method was utilized in order to determine the best combination of visibility parameters. As a result, the combination of AHD and AVP was selected. Before describing the result of the combination, the relationships between the number of injured pedestrians and AHD, and the relationship between the number of injured pedestrians and AVP were depicted in Figure8 and Figure9, respectively. Some correlations were found, but there were some unexpected plots.

The result of multiple regression analysis utilizing AHD, AVP was shown in Figure 10. The multiple regression equation was obtained as follow (Equation 1):

$$\text{Estimated values} = 0.6298 \cdot \text{AHD} - 0.3530 \cdot \text{AVP} + 22.676 \quad (1).$$

P values were 0.0031, 0.0178 for AHD, AVP respectively, which were less than 0.05. F value of the equation was 0.003256. Hence, this analysis could be said to be significant. Standard regression coefficients for AHD, AVP were 0.62, -0.47, respectively. AHD had a little greater effect than AVP. The coefficient of determination could indicate to account for the numbers of accidents to around 50 percent degree. It was captured that visibility has significant relationships with pedestrian accidents. The knowledge like this result could be a clue to decrease the number of pedestrian accidents.

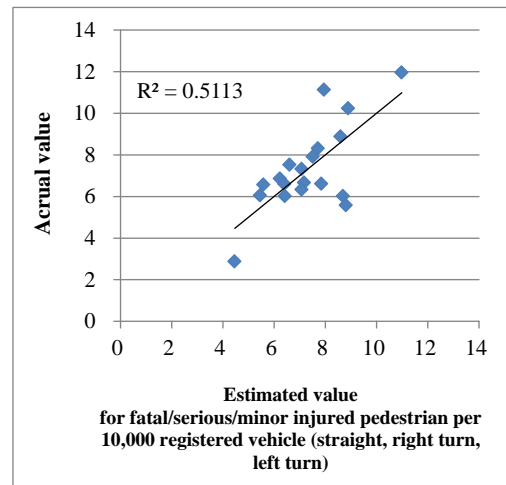


Figure10. Relationship between actual values and estimated values for the number of fatal/serious/minor injured pedestrians per 10,000 registered vehicles, which are estimated by combination of angle of hindrance at driver's side and angle of view at the passenger's side.

Combination of Visibility and Pedestrian Head Protection Performance

The combination of the visibility and the pedestrian head protection score in the JNCAP test was scrutinized in order to estimate the number of fatal/serious/minor injured pedestrian accidents including three vehicle maneuvers: straight-going, right-turn and left-turn. Out of 19 vehicle models, both of the visibility parameter and the pedestrian head protection score in the JNCAP test were available only for 14 vehicle models. The result of multiple regression analysis showed that the combination of angle of hindrance at driver's side and the pedestrian head protection score in the JNCAP test (PHPS) was the best one.

The effect of angle of hindrance at driver's side on the number of all injured pedestrians was illustrated (See Figure 11).

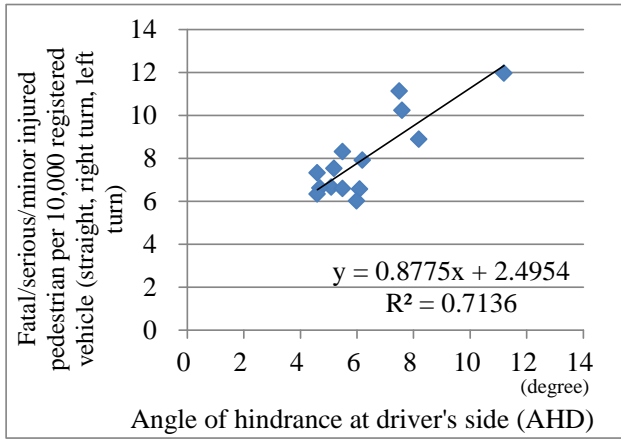


Figure 11. Relationship between the number of fatal/serious/minor injured pedestrians per 10,000 registered vehicles and angle of hindrance at driver's side in straight-going, right-turn, left- turn.

The good relationship between the pedestrian head protection score in the JNCAP test and the number of injured pedestrians by vehicle models was clearly shown in Figure 12.

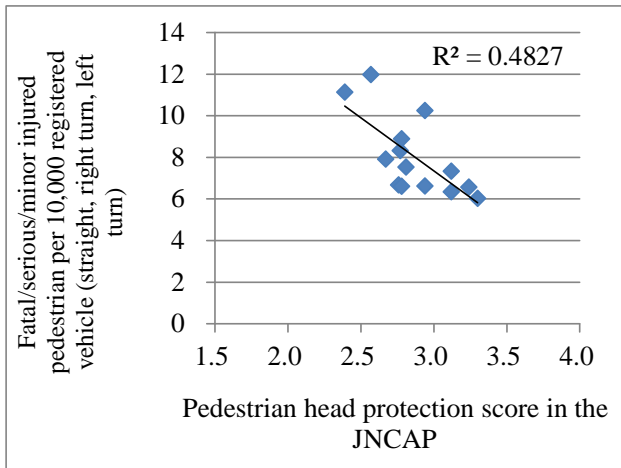


Figure 12. Relationship between the pedestrian head protection score in the JNCAP test and the number of fatal/serious/minor injured pedestrian per 10,000 registered vehicles.

The multiple regression equation was obtained as follow (Equation 2):

Estimated values

$$= 0.6900 \cdot \text{AHD} - 2.7692 \cdot \text{PHPS} + 11.6231 \quad (2).$$

It was successfully captured that the combination of visibility and pedestrian head protection performance, which were in different areas, could estimate the number of the real-life pedestrian accidents at high accuracy. Relationship between actual values and estimated values was shown in Figure 13.

From the viewpoint of statistics, P values were 0.0008, 0.0248 for AHD, PHPS respectively, which were less than 0.05. F value of the equation was 7.44E-05. Hence, this analysis could be said to be significant. Standard regression coefficients for AHD, AVP were 0.66, -0.38, respectively. AHD had a little greater effect than PHPS.

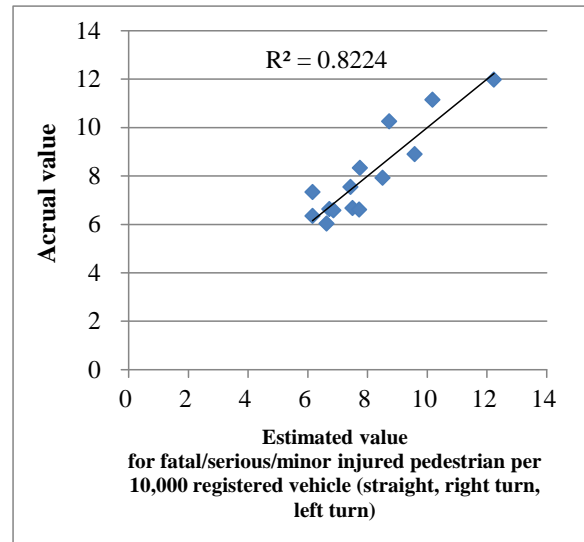


Figure 13. Relationship between actual values and estimated values for the number of fatal/serious/minor injured pedestrians per 10,000 registered vehicles, which are estimated with use of angle of hindrance at driver's side and the pedestrian head protection score in the JNCAP test.

Although the multiple regression analysis here cannot be said to be absolutely excellent because of the limited number of vehicle models, it should be stressed that the concept and procedure could be very useful for improving real-world safety for pedestrian from the viewpoint of vehicle.

Detailed Analysis for Pedestrian Accidents

Pedestrian accidents were analyzed in more detail for each danger-cognitive velocity: 0-20, 20-40, over 40km/h and the injuring objects on pedestrian: vehicle body, tires, road, others. The accident data of 39 vehicle models during four years: 2008-2011 were utilized.

Danger-cognitive velocity In fatal injured cases, the situations of straight-going and higher velocity had the majority of the accidents (See Figure 14). In serious cases, the situations of right turn and lower velocity increased (See Figure 15).

As to minor injured cases, the situation of "20km/h or less" occupied a large part of the pedestrian accidents (See Figure 16).

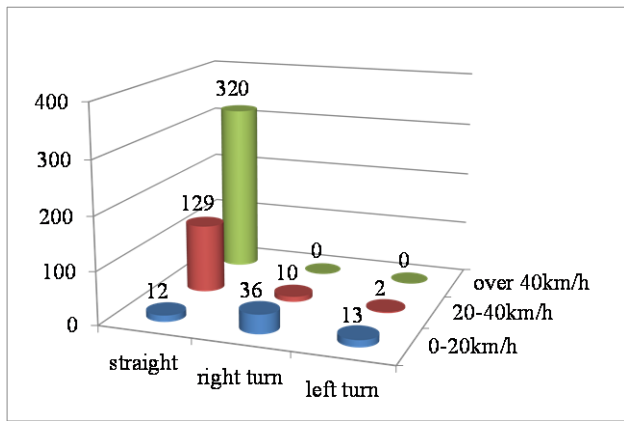


Figure14. The number of **fatal** injured pedestrian for each of vehicle maneuvers and danger- cognitive velocity.

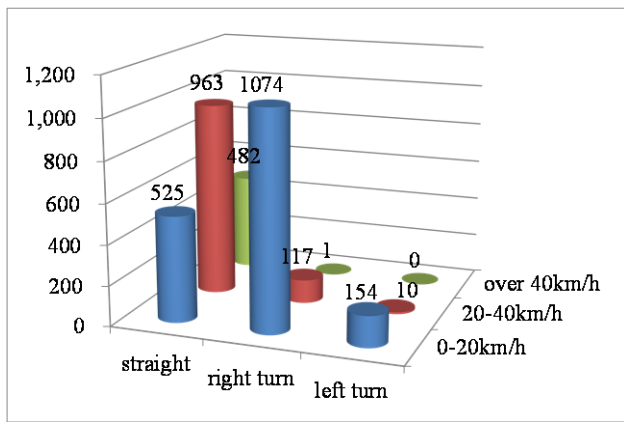


Figure15. The number of **serious** injured pedestrian for each of vehicle maneuvers and danger- cognitive velocity.

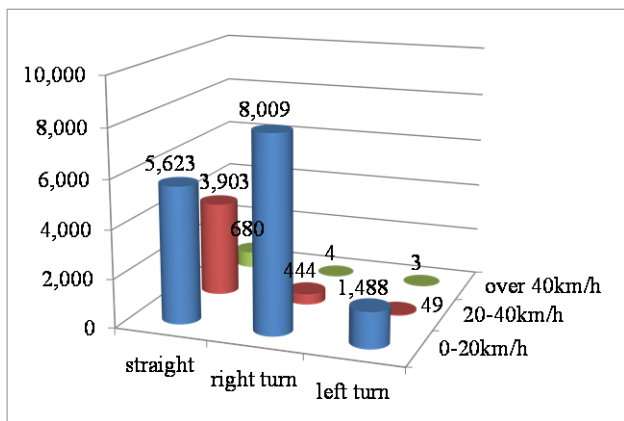


Figure16. The number of **minor** injured pedestrian for each of vehicle maneuvers and danger-cognitive velocity.

Injuring objects on pedestrians Although macro accident data had only four categories about injuring objects injury on pedestrians: vehicle body, tires, road, others, the percentages of injuring objects were studied. In fatal cases, the percentage of vehicle body was as high as 75% and the percentage of road around 20% in the straight-going maneuver (See Figure 17). On the other hand, the percentages of tires and road were higher in right-turn maneuver and left-turn maneuver because it was presumed that vehicles would roll up a pedestrian with a tire or push down and made a pedestrian hit road surface in many cases.

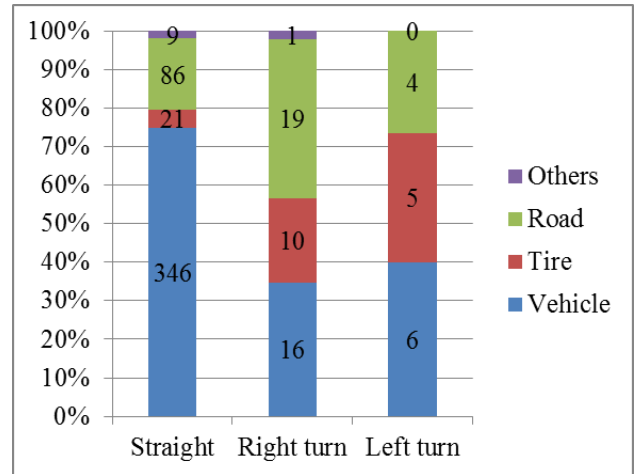


Figure17. The number of **fatal** injured pedestrian for each of vehicle maneuvers and injuring object.

In serious injured cases, the percentage of vehicle body in straight-going maneuver was lower than in fatal cases, while the percentage of road was around 30% (See Figure 18).

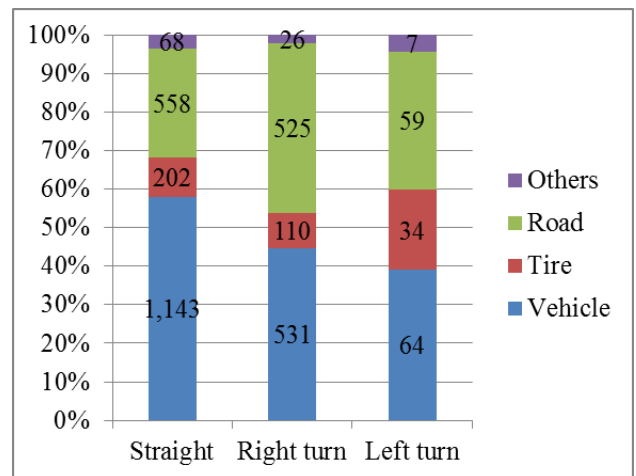


Figure18. The number of **serious** injured pedestrian for each driver's maneuver and injuring object.

In minor injured cases, the percentages of four kinds of injuring objects were not so different among three types of vehicle maneuvers (See Figure 19).

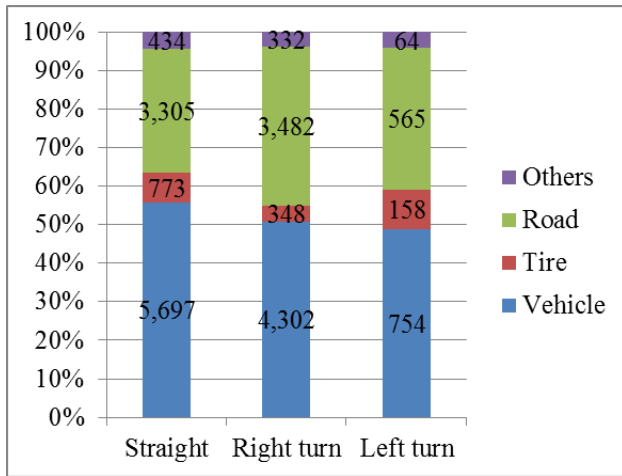


Figure19. The number of **minor** injured pedestrian for each of vehicle maneuvers and injuring object.

Detailed Analysis for Effect of NCAP Performance on Pedestrian Accidents

The effects of the pedestrian head protection score in the JNCAP test on the number of injured pedestrian were scrutinized by danger-cognitive velocity and injuring objects on a pedestrian.

Out of 39 vehicle models, 29 vehicle models which the pedestrian head protection score in the JNCAP test is available for, and had the vehicle registered volume more than 300,000 during four years, were evaluated for the purpose.

The correlation between the pedestrian head protection score in the JNCAP test and the number of fatal injured pedestrians in the collisions at danger-cognitive velocity of over 40km/h colliding with all objects was analyzed (See Figure 20). Focusing on vehicles body as the injuring object, the coefficient of determination increased from 0.1957 to 0.269 (See Figure 21).

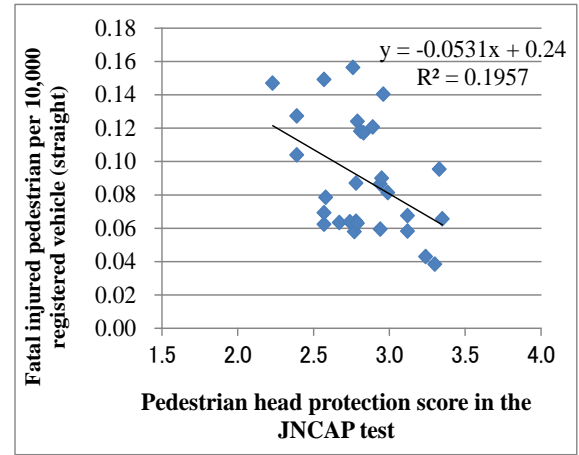


Figure20. Relationship between “the pedestrian head protection score in the JNCAP test” and “the number of **fatal** injured pedestrian per 10,000 registered vehicles“ under the condition of danger- cognitive velocity that is **over 40km/h**, in cases where a human body collided with any injuring object (**vehicle body, tires, road, others**).

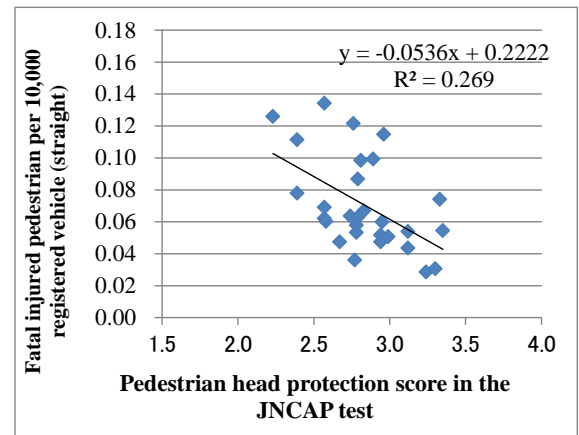


Figure21. Relationship between “JNCAP score for pedestrian head protection performance” and “the number of **fatal** injured pedestrian per 10,000 registered vehicles“ under the condition of danger- cognitive velocity that is **over 40km/h**, in cases where a human body collided with **vehicle body**.

In fatal/serious and fatal/serious/minor injured cases as well as fatal ones, this study was conducted and summarized (See Figure 22). Focusing on vehicle body as the injuring object, i.e. excluding tires, road and others, the effect of the pedestrian head protection score in the JNCAP test was made clearer in fatal/serious cases.

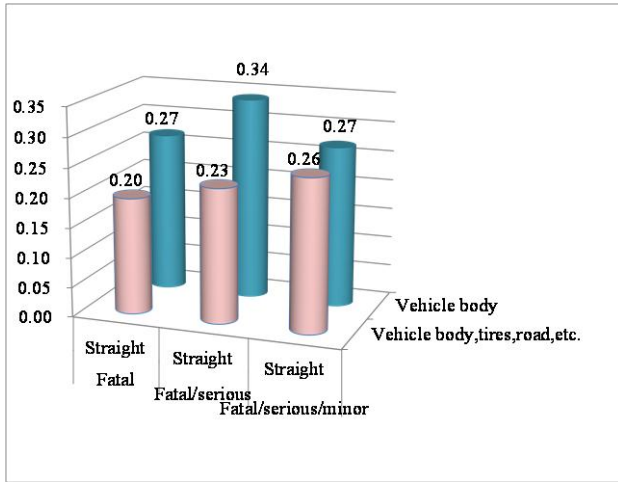


Figure 22. Coefficients of determination for relationships between “the number of injured pedestrian per 10,000 registered vehicles” and “the pedestrian head protection score in the JNCAP test” under the condition of danger-cognitive velocity that is over 40km/h in the straight-going maneuver.

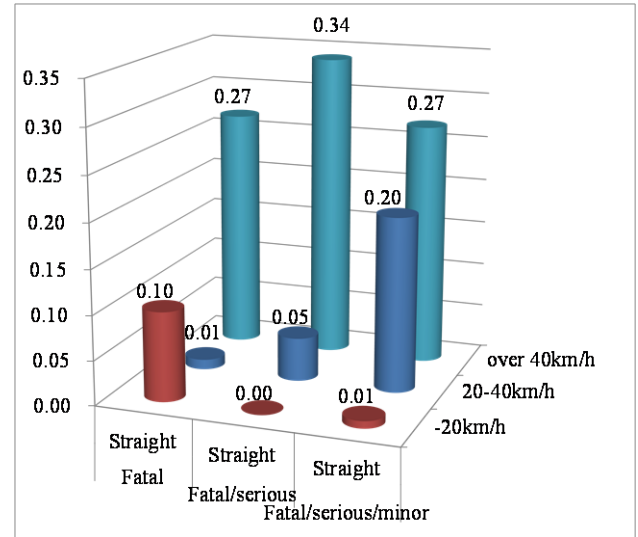


Figure 23. Coefficients of determination between “the number of injured pedestrians per 10,000 registered vehicles” and “the pedestrian head protection score in the JNCAP test” in cases where a human body collided with vehicle body.

The correlation between the pedestrian head protection score in the JNCAP test and the number of fatal injured pedestrians was analyzed for each danger-cognitive velocity: 20km/h or less, 20-40km/h, over 40km/h in the cases where a vehicle body was the injuring object in the straight-going maneuver. The summarized figure showed that the higher the velocity was, the more the effect of the pedestrian head protection score in the JNCAP test on the number of injured pedestrians was (See Figure 23).

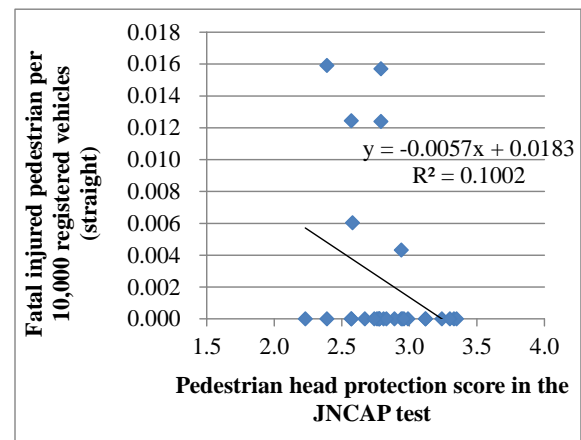


Figure 24. Relationship between “the pedestrian head protection score in the JNCAP test” and “the number of fatal injured pedestrian per 10,000 registered vehicles” under the condition of danger-cognitive velocity that is 20km/h or less.

The scatter chart under the situation of fatal injury and at the danger-cognitive velocity of 20km/h or less, depicted the coefficient of determination i.e.0.10 as meaningless (See Figure 24).

Two scatter charts under the situation of fatal/serious injury at the danger-cognitive velocity of “20-40km/h” and “over 40km/h” exemplified that the higher the velocity was, the more

the effects of the pedestrian head protection score in the JNCAP test was (See Figure 25, 26).

velocity range is dominant while 60km/h velocity range accounts for only 1% of total accidents.

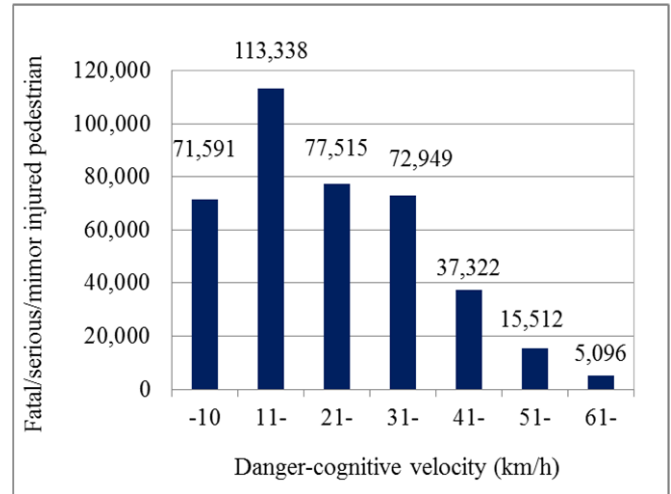
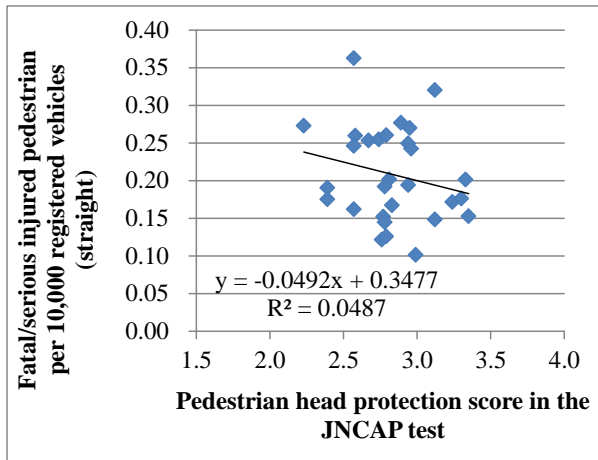


Figure 25. Relationship between “the pedestrian head protection score in the JNCAP test” and “the number of **fatal/serious** injured pedestrians per 10,000 registered vehicles“ under the condition of danger-cognitive velocity that is **20-40km/h**.

Figure 27. Distribution of danger-cognitive velocity of pedestrian accidents in Japan.

CIDAS data was analyzed using PC-Crash. The resultant velocity distribution of 115 cases is shown in Figure 28. The peak is in 31-40km/h velocity range, which is higher than that of Figure 27 by 20km/h. The velocity range over 60km/h accounts for 23% or 1/4 of total cases.

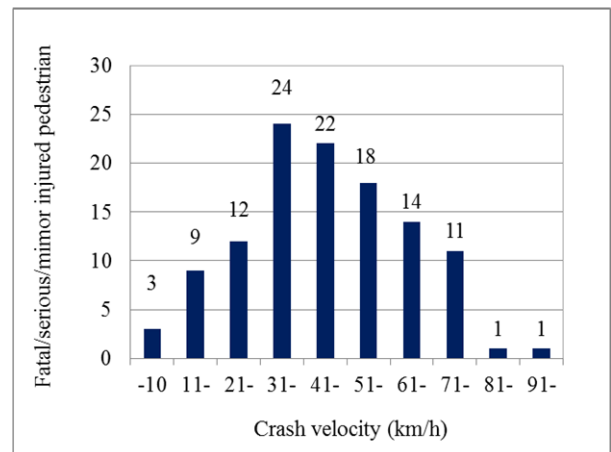
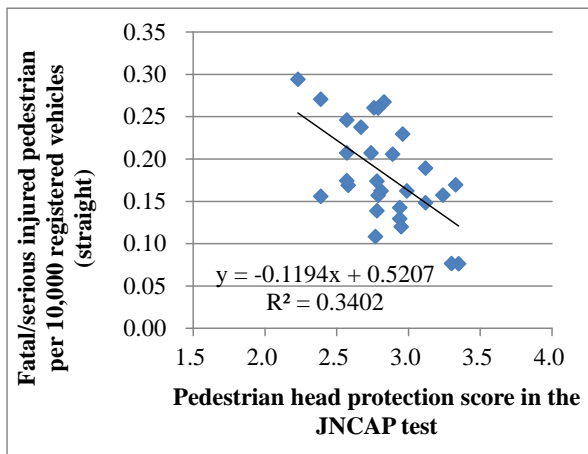


Figure 26. Relationship between “the pedestrian head protection score in the JNCAP test” and “the number of **fatal/serious** injured pedestrian per 10,000 registered vehicles“ under the condition of danger-cognitive velocity that is **over 40km/h**.

Figure 28. Velocity distribution of pedestrian accidents in China calculated by PC-Crash.

Comparison between Japan and China for Velocity Distribution of Pedestrian Accidents

Figure 27 shows danger-cognitive velocity in pedestrian accidents that occurred with passenger vehicles, freight vehicles, and minivans in 18 years from 1990 through 2007. In total, 390,000 cases were analyzed. In Japan, 11-20km/h

As shown in the previous section, the more the velocity, the more the effects of the pedestrian head protection score in the JNCAP test on the number of injured pedestrian. Therefore it follows that JNCAP would be effective especially in the crash velocity range of 31-50km/h, which account for 40% of total 115 in China.

In-Depth Analysis

In-Depth accident analysis was performed for pedestrian accidents. The purpose of the analysis is to analyze pedestrian accidents in Japan and China and identify the similarities and differences so as to extract challenges in the efforts to reduce pedestrian accidents in China by utilizing CIDAS data. Table 1 shows the data used for the analysis and the number of cases. For Japan, the data collected by ITARDA through investigation on accidents in Tsukuba City, Ibaraki Prefecture are shown. This data includes three body types: sedans, SUVs, and station wagons, and three driving maneuvers: straight-ahead driving, turning right or turning left. The data was collected for about 19 years from 1993 through 2011. The number of injury in the accidents amounts to 1129 cases. On the other hand, for China, the data collected by CIDAS through investigation on pedestrian accidents in Beijing, Ningbo, Changsha, Weihai and Foshan. The same body types and driving maneuvers as these of ITARDA's are covered. The data was collected for about 2 years from 2011 to 2012. The number of injury in the accidents amounts to 452 cases. The objects that hit and injured pedestrians are categorized into body, tire, road surface, and others. As we did for comparison with JNCAP, the objects that belong to vehicles were extracted. The number of accidents with sedans, SUVs, or station wagons during straight-going, turning right or turning left was 670 in Japan and 313 in China. For the reasons of sample size, the number of accidents were narrowed down to cases with sedans during straight-going: 391 in Japan and 203 in China respectively. Out of them, the number of accidents where a head, which is tested in JNCAP, hits a vehicle is 124 in Japan and 95 in China respectively.

Table 1.
The number of injury

	Japan	China
All injury data	1,129	452
Impacted by vehicle	670	313
Vehicle Type : sedan Accident Type : straight	391	203
Contact area : Head	124	95

Comparison of Pedestrian Accident Velocity

As a great contributor to the reduction of fatal accidents, pedestrians' crash velocity was compared between Japan and China. The results are shown in Figure 29. The crash velocity was calculated based on danger-cognitive velocity in case of Japan and by PC-Crash in case of China. The analysis included accidents with station wagons, SUVs, and sedans during straight-going, turning left, or turning right. Accidents at a crash velocity over 40km/h are dominant: accounting for 60% of total 670 cases in Japan and 80% of total 313 cases in China respectively. The proportion of accidents at a velocity over 40km/h is higher in China.

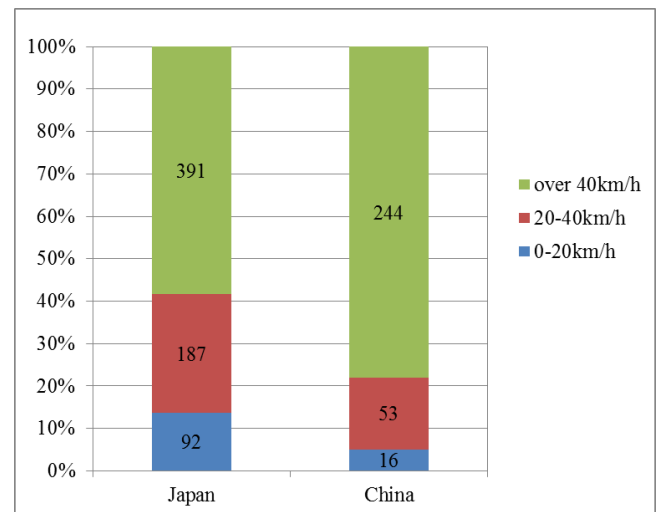


Figure 29. Proportion of pedestrian crash velocity station wagon, SUV, and sedan during straight-going, turning left, or turning right.

Pedestrian crash velocity was further analyzed by the types of vehicles. As the sample size was too small for station wagons and SUVs, the data on accidents with sedans during straight-going was focused in the analysis. Accidents at a velocity over 40km/h shown in Figure 30 accounts for 65% of total 391 cases in Japan and for 85% of total 203 cases in China: 5% higher respectively.

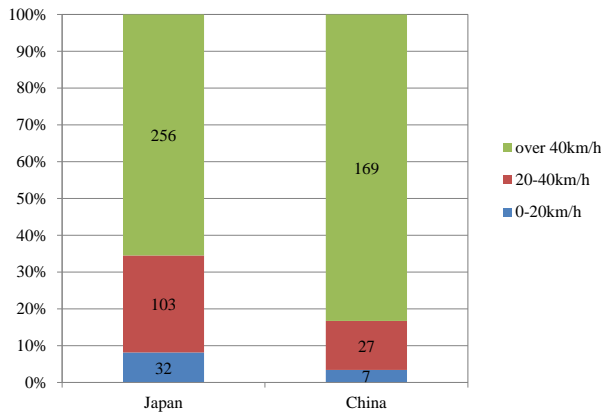


Figure 30. Proportion of pedestrian accident velocity with sedans during straight-going.

Distribution of velocity range was compared focusing on accidents in which a head hits a vehicle body and leads to fatal injury. The results are shown in Figure 31. The proportion is similar to that of Figure 30. This means that a head tends to hit a vehicle body in an accident at a speed over 40km/h.

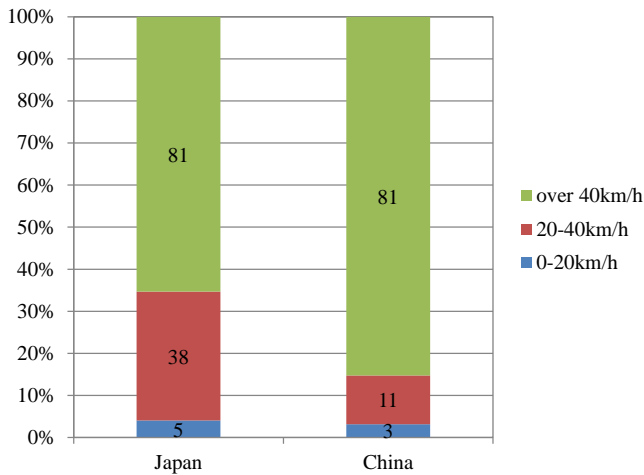


Figure 31. Proportion of pedestrian accident velocity (a head hits a body of sedan vehicle during straight-going).

Impacted Area of Vehicle

Impacted areas of vehicle were analyzed next. Figure 32 shows distribution of impacted areas for each AIS. The more severe the AIS injury is, the more likely the pedestrian hits the cowl or A-pillar. For all AISs, cases where the pedestrian hits the hood account for 30%.

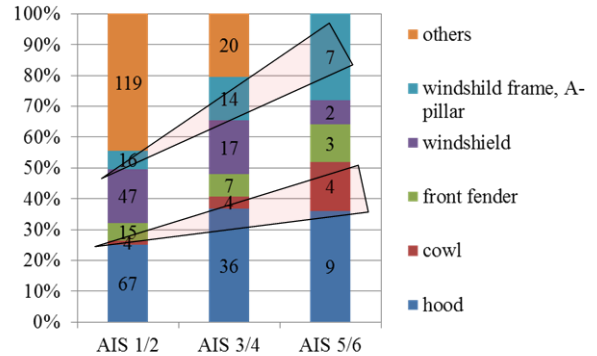


Figure 32. Injury level and impacted areas of vehicle body (Japan).

Figure 33 shows the relation between injury level and impacted areas in China. The more severe the AIS injury level is, the more likely the pedestrian hits the windshield and less likely it hits the hood. Presumably, the higher the crash velocity is, the more likely pedestrian bounces and hits the windshield and head injury leads to fatal injury because of a high velocity.

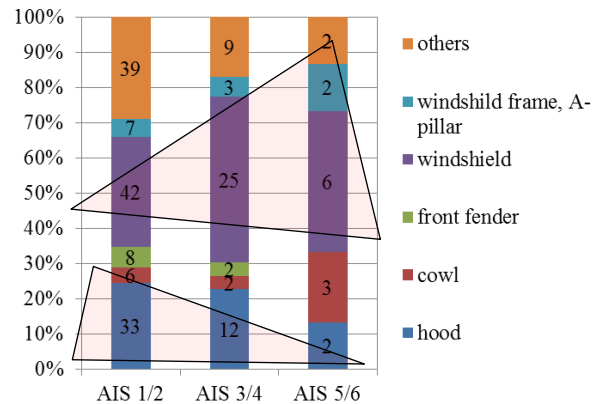


Figure 33. Injury level and impacted areas of vehicle body (China).

Injured Parts of Pedestrian

To exemplify the above assumption, injured areas of pedestrians were compared between Japan and China. Figure 34 shows the data on whole velocity range and Figure 35 shows the data at a velocity over 40km/h. Head accounts for 30% in Japan while it accounts for 50% in China. Figure 35 shows the distribution of injured areas in accidents at a velocity over 40km/h. The distribution is similar to that of Figure 34. In Japan, since the cases at a velocity below 40km/h are dominant, the velocity range over 40km/h is not so influential.

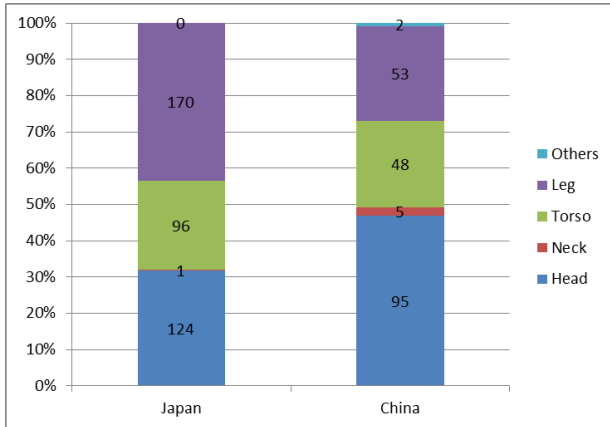


Figure 34. Comparison of injured areas over whole velocity range (Japan vs china).

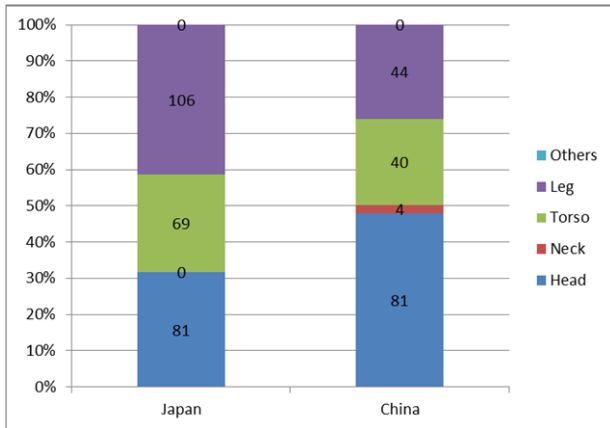


Figure 35. Comparison of injured areas at a velocity over 40km/h (Japan vs china).

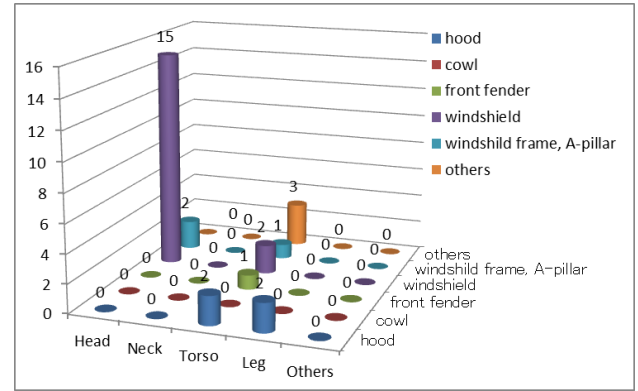


Figure 36. Injured areas and impacted areas of vehicle over 60km/h in China.

DISCUSSION AND LIMITATION

Visibility

With regard to visibility, a lot of factors except for the ones discussed in this study could be considered such as gradual section change of A-pillar according to change of height, size of structure around the lower part of A-pillar, size of gap between A-pillar and door mirror. Also, visibility would depend on whether a driver is long-waisted or short-waisted. Nevertheless, it is clear, to some extent, that angles of hindrance and angles of view have statistically significant effects on the number of fatal or injured pedestrian accidents.

Pedestrian Head Protection Performance

Pedestrian head protection performance test in the JNCAP is designed to simulate a crash at the collision velocity of 44km/h. With utilizing the danger-cognitive velocity in the current study which seems to be lower than the collision velocity, the effect of the pedestrian head protection score in the JNCAP test on the number of pedestrian accidents was more significant in higher speed zone. It was presumed that a lot of minor collisions in the danger-cognitive velocity of 20km/h or less could not depend on the pedestrian head protection score in the JNCAP test. On the other hand, pedestrian injury outcome at severe collisions with higher impact energy at the higher collision velocity could be much more affected by the pedestrian head protection performance.

The pedestrian head protection score in the JNCAP test was studied here, while the accident data of pedestrian include not only head, but also chest, abdomen, lower extremity, etc. In spite of the fact, the good correlation between the pedestrian head protection score in the JNCAP test and the number of injured pedestrians would mean that the better energy absorption for head could be also effective for injuries on other part of human body.

Figure 36 shows the relationship between injured areas and impacted areas of vehicle over 60km/h in China. It was found that over 60km/h in China a head dominantly hits windshield.

Another Measure to Reduce Fatal or Injured Pedestrian Accidents

In an additional study, it was confirmed that the less the danger-cognitive velocity was, the less the fatality rate was (See Figure 37.) The fatality rate was defined here as the number of fatal injured pedestrians divided by the number of all fatal or injured pedestrians in each danger-cognitive velocity zone. The fatality rate was 24.8% in the danger-cognitive velocity zone of over 40km/h, 3.1% in the velocity zone of 20-40km/h, and 0.2% in the velocity zone of 20km/h or less. It was ascertained that the danger-cognitive velocity is another significant factor which could affect the severity of injury. Consequently, the systems such as automatic emergency braking systems against pedestrian have a big potential to avoid a collision with a pedestrian or to decrease a collision speed, leading to the decrease in the number of injured pedestrians. Under the circumstances, Although such a system would lessen the effect of visibility and pedestrian protection performance on the number of pedestrian accidents, the spread of such a system would be highly desirable for the real-world safety improvement.

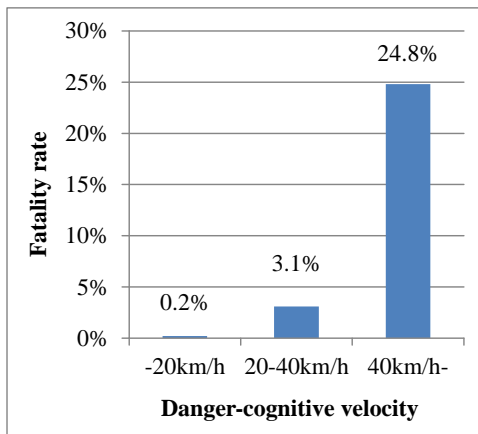


Figure 37. Fatality rates in the three ranges of danger-cognitive velocity in cases where a human body collided with vehicle body in the straight-going maneuver.

Vehicle Models

The vehicle models scrutinized in the current study were the ones which had undergone full model changes during the period of 1999 through 2007. Although those models seemed to be little old, enough volumes of registered vehicles for each vehicle model was needed for statistical accident research. Hence, most of the vehicle models studied here are no longer sold in the market and have undergone full model changes improving visibility performance and pedestrian protection performance.

Method of Accident Research

It can be ascertained that the method of macro accident data analysis utilized in this study, which is based on the number of accidents per 10,000 registered vehicles for each vehicle model, is capable of studying relationships among the number of accidents and explanatory variables. This can be conducted because all accidents with injuries reported to police are compiled and connected to the vehicle models and types in Japan.

Number of In-depth Accident Data

As for in-depth accident data analysis both in China and Japan, although it cannot be said that the number of accident data was enough, the idea of distribution of injured part of human body and the injuring parts of vehicle body were captured. More data would be necessary for improving the accuracy. Two years have passed since the CIDAS project started. We would like to analyze accidents in more detail so as to contribute to the reduction of pedestrian accidents.

CONCLUSIONS

It was ascertained that the pedestrian accident would be more likely to occur when the angle of hindrance due to A-pillar was larger, and when the horizontal angle of view through the windshield was smaller.

Furthermore, it was clarified that the influence of visibility on the occurrence of pedestrian accident was different among the straight going maneuver, the right-turn maneuver.

It was possible to predict the number of fatality or injured in the pedestrian accidents to a certain degree of probability, with use of the combination of visibility indices.

The better pedestrian head protection score in the JNCAP test would lead to the decrease in the number of pedestrian accidents with the fatality or the injured.

The combination of visibility index and pedestrian head protection score in the JNCAP test successfully provided much better prediction of the number of fatality or injured in the pedestrian accidents. In other words, it was clarified that the optimization of parameters in visibility indices and pedestrian head protection could lead to the decrease in the number of pedestrian accident.

The effects of the pedestrian head protection score in the JNCAP test on the number of pedestrian accidents with the fatality or the injured were elaborately scrutinized from the viewpoint of danger-cognitive velocity and vehicle maneuver, i.e., straight-going, right-turn and left-turn. The results demonstrated that the pedestrian head protection score in the JNCAP test was highly correlated with the pedestrian accident especially in the case where a pedestrian was impacted by the

vehicle body, but not a tire nor road, furthermore in the straight-going maneuver at the danger-cognitive velocity of over 40km/h.

In-depth accident analysis with data of ITARDA and CIDAS was conducted in Japan and China. The result showed that JNCAP would be effective especially in the crash velocity range of 31-50km/h, which accounts for as much as 40% of total 115 occurred in five major cities in China.

REFERENCES

- [1] IRTAD. 2012. "Road Safety Annual Report 2011." 5. Crash trends, P.203. Table 2. Reported fatalities by road user group 1990, 2000, 2009 and 2010. P.204.
<http://www.internationaltransportforum.org/irtadpublic/pdf/111rtadReport.pdf>
- [2] The Ministry of Public Security of the People's Republic of China, 2012.6. "Annual Statistical Report of Road Traffic Accidents in the P.R. of China (2011)." 2012.6, P.8
- [3] National Agency for Automotive Safety & Victims Aid, 2012. "Car Safety Performance Guidebook Detailed Edition." 2012.3.
http://www.nasva.go.jp/mamoru/en/panf_2012_en.pdf
- [4] Liers, H. 2009. "Benefit Estimation of the Euro NCAP Pedestrian Rating Concerning Real-World Pedestrian Safety". ESV2009, No.09-387.
- [5] Liers, H. and Hannawald, L. 2011. "Benefit Estimation of Secondary Safety Measures in Real-world Pedestrian Accidents." ESV 2011, No.11-0300.
- [6] Strandroth, J., Rizzi, M., Sternlund, S., Lie, A. and Tingvall, C. 2011. "The correlation between pedestrian injury severity in real-life crashes and Euro NCAP pedestrian test results." ESV 2011, No. 11-0188.

- [7] Takeuchi, K. and Ikari, T. 2007. "Correlation between JNCAP Pedestrian Head Protection Performance Tests and Real-world Accidents." ESV2007, No.07-0203.
- [8] Hamacher, M., Eckstein, L., Kuhn, M. and Hummel, T. 2011. "Assessment of Active and Passive Technical Measures for Pedestrian Protection at the Vehicle Front." ESV 2011, No.11-0057.
- [9] Hasegawa, Y., Fujita, H., Endo, T., Fujimoto, M., Tanabe, J. and Yoshida, M. 2008. "Development of Front Pillar for Visibility Enhancement." Honda R&D Technical Review: October 2008.
- [10] Huipeng, C., Lianxue, F. and Heyue, Z. 2009. "A Comparative Study between China and IHRA for the Vehicle-Pedestrian Impact." SAE paper No. 2009-01-1205.

DEFINITIONS, ACRONYMS, ABBREVIATIONS

ITARDA: Institute for Traffic Accident Research and Data Analysis, a Japanese organization

CATARC: China Automotive Technology & Research Center

CIDAS: China In-depth Accident Study

AHD: Angle of Hindrance at Driver's side

AHP: Angle of Hindrance at Passenger's side

AVD: Angle of View at Driver's side

AVP: Angle of View at Passenger's side

PHPS: Pedestrian Head Protection Score in the JNCAP test

THE NEW EU I-SIZE REGULATION – KEY ELEMENTS OF THE SIDE IMPACT TEST PROCEDURE

Farid Bendjellal

Britax Group, Germany

Paper Number 13-0488.

ABSTRACT

Background

The Informal Group of UN GRSP* has developed a new standard for approving child restraint systems in Europe, called *I-Size* regulation. Key objectives for developing this regulation were 1/reducing misuse rate through promoting ISOFIX restraint and 2/enhancing compatibility between cars and child restraint systems and 3/introducing a side impact test procedure.

The latter is the focus of this paper. The aim of the procedure is to reproduce – with an intruding door concept – the door relative velocity between the door and the struck vehicle. The objective of this study is to investigate the key features of this test procedure.

*GRSP: Working Party on Passive Safety, World Forum for Harmonization of Vehicle Regulations, UN Economic Commission for Europe.

INTRODUCTION

The i-Size regulation is described in details in documents (1) and (2). It is based on 5 key pillars:

- Universal Integral Isofix restraint
- Seat classification based on occupant size
- Mandatory extended rear facing installation up to 15 months of age
- New anthropomorphic test dummies
- Side impact test procedure with intruding door in addition to the frontal and rear impact.

Universal integral Isofix

The Universal integral Isofix restraint means that only Isofix seats with integral occupant restraint system are specified by this regulation. In addition to Isofix attachment, the CRS is secured with an anti-rotation device, i.e. a top tether or a support leg. To allow for universal approval, vehicle regulations ECE R16 (3) – seat-belts & vehicle space for Isofix restraints and ECE R14 (4 and 5) – safety-belt and Isofix anchorages – were updated. In particular the geometry and strength of the

vehicle floor must fulfill new requirements to ensure adequate compatibility, as shown in Figure 1.

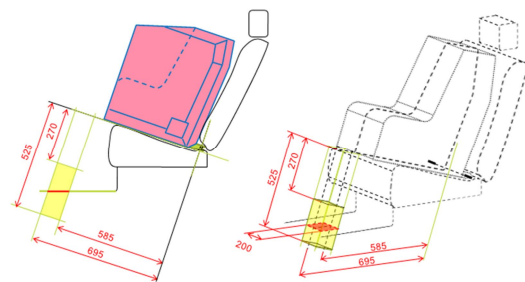


Figure 1. Vehicle floor contact surface with the support leg - Geometrical specifications (3).

In addition to the geometrical requirements the vehicle floor shall meet strength demands to ensure that a stable interaction between the floor and the support leg. Figure 2 describes the test procedure that will be applied to the vehicle structure to fulfill these requirements.

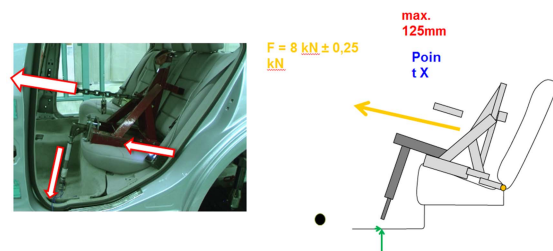
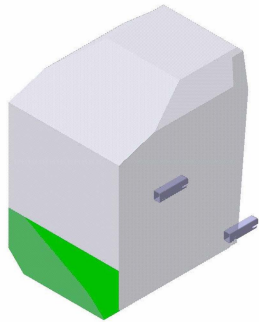


Figure 2. Test method used in i-Size regulation for testing the floor strength (4), (5).

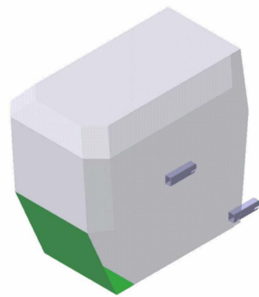
To ensure child restraint to vehicle compatibility the Universal Integral Isofix comprises the following features:

- ISOFIX
 - 2 lower anchorages + 1 anti-rotation device:
 - Top Tether or
 - Support leg

- No use of the adult safety belt for the restraint of the child seat
- Universal
 - F2X ISO fixture for forward facing seats and R2 ISO fixture for rear facing seats as shown in Figure 3
 - With top tether or support leg
 - Integral
 - Child is restrained only by the CRS restraint system



a)



b)

Figure 3. F2X (a) and R2 (b) ISOFIX envelopes.

For the vehicle the i-Size will require the following demands:

- F2X and R2 envelopes
- Geometrical and strength requirements for vehicle floor in contact with the support leg of the child seat
- Top tether anchorages

The seat classification refers to the stature of the child to help the consumers in their purchasing choice. A seat will be classified according to the stature of the child that will be accommodated. The seat internal dimensions must meet defined values which are checked using a dedicated device.

Rear facing installation has been extended to an age of 15 months and this is why the i-Size regulation requires that both the vehicle and the child seat meet the R2 ISOFIX envelop.

The i-Size Side Impact Test Procedure

It is based on a test bench that is oriented 90° with respect to the sled displacement direction. The test bench is equipped with sliding Isofix anchorages that allow a 200 mm of free movement of the seat. During the test the bench and the child seat are accelerated to reach a velocity of 7 m/s. Then the child seat impacts a door which is fixed with respect to the laboratory. The door is covered with a 35 mm rubber cell and 20 mm Styrodur foam. The test procedure may be realized either with a deceleration sled or an acceleration sled. In the later case specific requirements shall be satisfied (6). Figure illustrates the main components of the procedure.

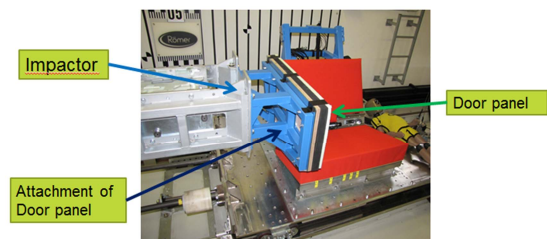
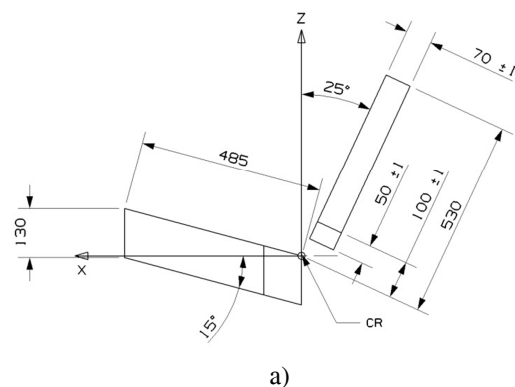


Figure 4. Overview of the i-Size side impact test method.

The test bench is described in Annex 6 of the regulation (1), (2). One of the main differences compared to the ECE R44 test bench is the back rest angle which is 25° (20° in the R44 case). Side and top views of the bench are shown in Figure 5.



a)

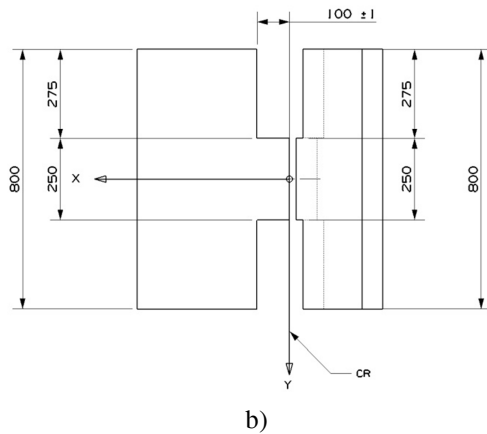


Figure 5. Side (a) and top (b) views of the test bench with corresponding dimensions.

The test bench cushion shall meet density requirements as well as mechanical characteristics.

Adjustment of Top Tether or Support Leg

Top Tether – The top tether in the side impact test must be adjusted to its shortest length.

Support Leg – This must be adjusted so that it reaches the floor plane.

Tests and dummy sizes

The child restraint is to be tested with the smallest and largest dummy in relation to the size that was indicated by the child seat manufacturer, as shown in Table 1.

Table 1.
Size range of the child seat and dummy size to be used for its testing

size range indication	≤ 60	$60 < x \leq 75$	$75 < x \leq 87$	$87 < x \leq 105$
Dummy	Q0	Q1	Q1.5	Q3

Sled Pulse In order to reproduce an intruding door effect, the Informal Group has defined a specification for the relative velocity between the door and the test bench. The corresponding velocity-time corridor is shown in Figure 6.

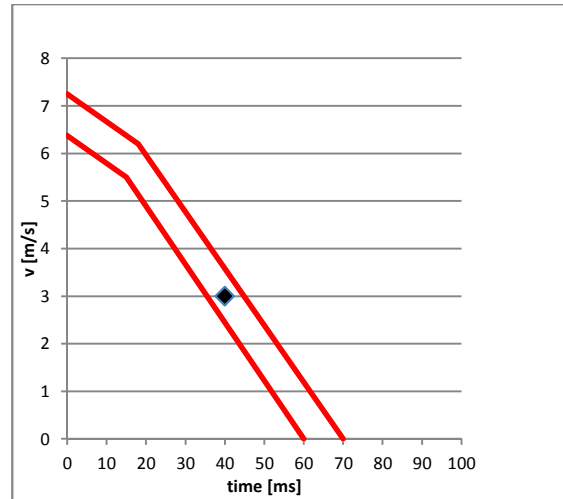


Figure 6. Relative velocity between the door and the test bench.

Dummy installation and Positioning

The dummy is installed in such a way that its position is stable at t_0 . The CRS is installed with the upright position.

Installation should be done as follows:

- The unoccupied CRS shall be attached to the ISOFIX anchorage system
- Adjustment of the top tether
- The dummy shall be placed in the CRS separate from the seat-back of the chair by a flexible spacer
- Adjustment of the belt
- After the installation the dummy centre line and the CRS center line shall be aligned exactly with the centre line of the test bench

In Figure 7 a Group I seat with a Q3 dummy is shown.

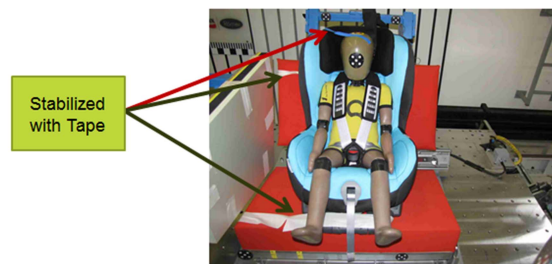


Figure 7. Test set up.

This procedure was used to evaluate the responses of Q1 and Q3 dummies when using ECE R44 approved rear facing as well as forward facing Isofix seats.

Findings

The i-Size regulation requires a number of performance requirements. These are:

- Head containment, which is defined by the following parameters:
 - (a) No head contact with the door panel.
 - (b) Head shall not exceed a vertical plane identified by a red line on top of the door (top view camera). This vertical plane is identified by a line on the impacted door as defined in Annex 6 Appendix 3 Figure 1 of the i-Size regulation
- Head protection criterion HPC 15ms: 600 and 800 resp. for Q0, Q1, Q1.5 and Q3
- Head resultant 3ms acceleration: 75G and 80 G resp. for Q0, Q1, Q1.5 and Q3

Other parameters are considered in the i-Size regulation such as chest deflection and neck loads (tension and flexion moment) but only for monitoring purpose.

Three ISOFIX child seats were tested using the set up described previously in the paper. These were R44 approved seats, 2 forward facing, one with a support leg and one with a top tether. The 3rd seat was an infant carrier.

Head containment was analysed using high speed videos. In all 3 tests the head did not go beyond the vertical plane and therefore the head containment was met. It must be mentioned that all 3 seats were designed to meet an internal test procedure – with a fixed door – which required energy absorption in the seat lateral structure.

In Figure 9, Q1 and Q3 dummies' maximum head 3ms accelerations and HPC are presented as a percentage of regulatory limits. It can be seen that Q3 head accelerations are just below the limit with values ranging from 86% to 90%. For Q1 dummy the values are higher ranging from 112% to 120%. If we consider the HPC 15ms parameter, Q3 responses are between 50% and 55% while Q1 responses range from 88% to 90%.

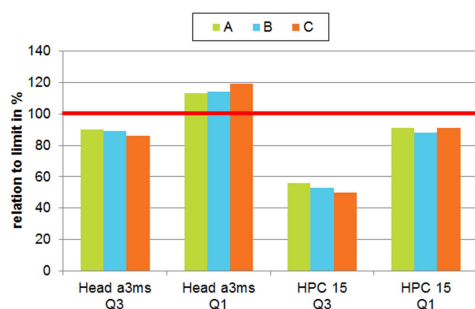


Figure 8. Head accelerations and HPC values obtained with Q1 and Q3 dummies.

As a first indication it appears that the test procedure defined in the i-Size regulation is a demanding one. In order to reduce the loads on occupant there will be a need for additional energy absorption. However we have to keep in mind that the design of the CRS must meet both internal and external dimensions (Isofix fixture) and this is where we see one of the key challenges of this regulation.

CONCLUSIONS

It is shown that the test procedure proposed is a severe one when considering the requirements for internal and external child seat dimensions. In particular the Q1 dummy head acceleration shows peak responses that will represent a significant challenge in terms of design for next generation of child restraint systems.

Limitation - The present study does not cover other key characteristics of the test procedure such as repeatability and reproducibility. Further investigations are needed to comprehend the full impact of this demanding procedure.

REFERENCES

- [1] Proposal for a new regulation on child restraint systems: UN Economic Commission for Europe. World Forum for Harmonization of vehicle regulations, 157th Session – document ECE-TRANS-WP29-2012-53e. Geneva 26-29 June 2012.
- [2] Proposal for a new regulation on child restraint systems: UN Economic Commission for Europe. World Forum for Harmonization of vehicle regulations, 158th Session – document ECE-TRANS-WP29-2012-53e coor1. Geneva 13-16 November 2012
- [3] Proposal for Supplement 3 to the 06 series of amendments to regulation Nb 16 (Safety Belts): UN Economic Commission for Europe. World Forum for Harmonization of vehicle regulations, 157th Session – document ECE-TRANS-WP29-2012-43e. Geneva 26-29 June 2012.
- [4] Proposal for Supplement 4 to the 07 series of amendments to regulation Nb 14 (seat-belt anchorages): UN Economic Commission for Europe. World Forum for Harmonization of vehicle regulations, 157th Session – document ECE-TRANS-WP29-2012-42 e. Geneva 26-29 June 2012.
- [5] Proposal for Supplement 4 to the 07 series of amendments to regulation Nb 14 (seat-belt anchorages): UN Economic Commission for Europe. World Forum for Harmonization of vehicle

regulations, 158th Session – document ECE-TRANS-WP29-2012-97 e. Geneva 13-16 November 2012

[6] Proposal for Supplement 1 to the draft new Regulation on child restraint systems: World Forum for Harmonization of vehicle regulations, Working Party for Passive Safety GRSP -52nd Session – document ECE-TRANS-WP29-GRSP- 2012-18 e. Geneva 11-14 December 2012.

CHILD ADVANCED SAFETY PROJECT FOR EUROPEAN ROADS (CASPER), BETTER KNOWLEDGE AND BETTER TOOLS TO IMPROVE THE REAL PROTECTION OF CHILDREN IN CARS

Philippe Lesire

LAB PSA Peugeot-Citroën/Renault, France

Heiko Johannsen

TU Berlin, ILS Kfz, Germany

Rémy Willinger

Université de Strasbourg, France

Alejandro Longton

IDIADA, Spain

Alan Kirk

Loughborough University, UK

Philippe Beillas

Université de Lyon1, IFSTTAR LBMC, France

Anita FIORENTINO

Fiat Automobiles Group

Paper Number 13-0426

ABSTRACT

This paper is a synthesis of the results obtained in the different parts of the EC CASPER project and considers sociological approaches, technical works, and field and accident data. From parent's behaviour and wishes that show cultural differences, to human modelling works, this project widely covers the topic of child safety in cars.

The CASPER project has brought a significant amount of field data that have been useful for a better understanding of the situation and used as basis for all the other tasks of the project.

Consequent steps forward have been made in the development and improvement of tools usable for the approval of Child Restraint Systems (CRS) and in this aim a large collaboration with the GRSP Informal Group on CRS took place. Results have been presented and discussed in workshops with main participants and stakeholders of the child safety area.

INTRODUCTION

Considering the whole region of Europe, the World Health Organisation (WHO) reported that in 2008 the number of children 0 to 14 years old that died because of road traffic accidents was 4,408. Focussing on 20 EU countries, in 2009, 747 road traffic fatalities of children 0 to 14 years old were counted in the International Road Traffic and Accident Database (IRTAD). Based on these accident data, it is obvious that in spite of the

significant improvements in recent years in vehicle safety, the current number of deaths and casualties added to the social and economic costs is still unacceptable. Fatalities and injuries should be reduced by all the available ways: public regulation, prevention/education of road users, road infrastructure, compatibility between vehicles, active, passive and tertiary safety devices. The CASPER project has been based on these approaches with the aim to improve the global protection of children in cars, using the research results obtained both in previous European projects financed by the European Commission (such as CREST and CHILD), and also the knowledge acquired through the collaboration with other European organizations such as EEVC WG 18, ISO/TC22/SC12/WG1 and NPACS. The activities have been supported by research addressing many fields such as in depth road accidents data collection and analysis, the influence of the impact of societal behaviour of adults in transport situations and technological based solutions to improve the safety of children.

CASPER addresses two main aspects:

- The analysis of the reasons and consequences of misuse of CRS's and of the influence of the conditions of transportation of children, as compared to the certification test procedures.
- The improvement of the efficiency of child protection through the development of innovative tools in order to provide to CRS manufacturers the possibility to develop and test their products at a lower cost, with new methods, and at a same guarantee efficiency.

The first point has been treated in reports on the conditions of use of CRS and related consequences in accidents. They include messages to be forwarded through information campaigns. Positive effects on the protection of children derived from these reports could be seen in a short time. This would solve a large part of the issue of child occupant safety. The improvement of the behaviour of dummies, associated to new sensors, as well as dummies and child human numerical models are necessary to propose improved test procedures, based on road reality issues. Here, the effect on the protection of children will be realised in the longer term but complementary to the improvement of rate of correct use of children.

The project has mobilised a large part of the European scientific and business expertise in the field of passive safety related to children: 7 European countries are involved, with 15 partners who have a long experience in child safety with complementary profiles. The consortium of CASPER did not involve any CRS manufacturer as the preferred solution was to disseminate results in existing working groups in which a large number of CRS suppliers are involved, to organize regular workshops and to disseminate results in international conferences.

ORGANISATION OF THE WORK

The work plan of the CASPER project is to use as much as possible existing data related to injuries of children and to collect the missing information, which can help to find reliable solutions for improved protection of children in road accidents. Dummy modifications and modelling, creation of tools of new generation such as human models, analyse the possible solutions both on the side of vehicles and CRS. For this, the work has been organized around five technical work packages (WPs) with specific objectives and deliverables.

WP1 has been considering the protection of children based on the use of crash test dummies. First at the hardware level (enhancement of biofidelity, improvement of measurement capabilities), with the aim of proposing new protection criteria usable in test procedures for the evaluation of CRS performance. Secondly with the completion of the Q series FEM models family.

WP2 has defined, developed and validated child human body segments corresponding to 5 different sizes (ages). Whole-body child human models have been created by assembling the previously described body segments, although the validation process needs to be continued.

WP3 aimed to understand the travelling conditions of children in cars and the main issues in terms of

lack of protection in accidents. A large amount of field and accident data have been collected and analysed. The results have been used as the basis of determining the issues to be solved, and to highlight priorities for the actions to be taken for a rapid improvement of the situation. They have led to proposed evolutions of child dummies and the definition of human models characteristics.

WP4 has evaluated possible solutions based on the real traveling conditions of children, the previous information and enforcement campaigns. It has also defined possible actions of communication and education, and evaluated the proposals of test procedures for a new regulation of CRS approval.

WP5 has been organizing the dissemination and the exploitation of the project results as well as networking with other organisations involved in the field of child protection in road transport such as the GRSP informal group on CRS, in charge of writing a new text for CRS approval.

RESULTS

As CASPER has been considering child safety issues with a global approach, it has been necessary to base all research activities on field data in the different areas of car child safety. For this, data from previous projects and results available in the literature were used, and they were completed with the collection of data specific to the different task topics. For some studies, existing collection methodology used in the past have been adapted, in some other areas, such as a sociological approach, it has been necessary to set up the methodology, and to validate it before starting to collect data. The data collected were mainly focussed around two topics: accident data (from different types and sources) and misuse data (descriptive, quantitative, etc.). Each set of data have been analysed and results are reported in public deliverables.

ACCIDENT DATA

One of the priorities of this task was to make a status point on child fatalities in cars [1]. Then in depth investigations of accident cases (fatal or not) were necessary to provide accident cases for the establishment of injury criteria using car passenger accidents [2] and other accident types [3].

Report on fatality studies

According to WHO, an estimated 122,571 children in the age group of 0 to 14 years old died because of road traffic accidents in 2008. This represents 1.3% of children dying before the age of 15 and approximately 10% of road traffic accident fatalities world-wide. In these figures all kinds of transport modes and pedestrians are included. For some countries no data exist, and for many

countries underreporting is known, thus the WHO includes some best estimates. The database screening and literature review shows clear limitations referring to the focus on children fatalities as car passengers. No current numbers on child fatalities as car passengers for the whole world can be found in published data from WHO or the IRTAD database. As a more detailed study was available for the French situation, CASPER has been looking at what could be the priorities to limit child in car fatalities, knowing that the study results are representative of the French situation but generalisation of results to other countries should be done with some caution. For frontal impact fatalities in France, the priority is to improve the quality of use of restraint systems. When the child is correctly restrained, very few fatal cases are observed in conditions similar to the frontal test of the current regulation. In side impact, the current level of protection does not seem sufficient, the level of intrusion and the direct impacts with intruding objects are important for children on the struck side. For roll-overs the priority is to protect children from being ejected from the car and from projection inside of the car. The rate of correctly restrained children in this type of fatal accident is very low in France, which indicates that existing systems when correctly used could be preventing these fatalities. Rear impact remains rare in the French fatality study.

Looking now at European figures, and focussing on children from 0 to 13 years old, there are 392 fatalities recorded as car or taxi passengers in EU-23 for 2008, involved in 337 accidents. Just under one third were killed in single vehicle accidents, half in 2 vehicle accidents and one fifth in 3 or more vehicle accidents. Of the 2 vehicle accidents, 55% of fatalities are in accidents involving 2 cars, followed by 23% in accidents involving a heavy goods vehicle (HGV). Car passengers account for 44% of all child fatalities, closely followed by 37% for pedestrians. Child car passenger fatalities (0 to 13 years old) account for 1.1% of all road accident fatalities (37,265) in EU-23 for 2008 and 7% of all car passenger fatalities. Over a 10 year period the reduction in child car passenger fatalities is estimated to be 50% for the EU-19 countries with data available, higher than the improvement of 32% for all fatalities. For fatality rates by population, the EU-23 rate is 0.55 per 100,000. National level data in Europe has no information on restraint use and therefore, of course, no detail on misuse, which has been shown in detailed studies such as the CREST, CHILD and CASPER projects to have an effect on injury outcome. Large efforts are made in road accident investigation in the CASPER project as little detailed information is available to the level of detail required.

Focussed car accidents in depth investigations

Real world accident cases are collected to ensure that information on child kinematics, injury causation, injury criteria and CRS performance (including misuse where understood) is available to the project in order to support further activities in injury criteria, dummy/model development and the understanding of misuse. This has an implication for how the analysis should be interpreted as the database is not representative of the overall child car passenger crash population. However, the database does give an indication of which body regions are being injured in different CRS types or for different ages of children and gives insights into restraint conditions that lead to injury. The combined dataset, including the number of data available from the three EC child occupant safety projects (CREST, CHILD and CASPER) is one of the largest collections of in-depth road accident data focused on restrained child occupants. Overall there are 1301 restrained children in the combined database, 954 in frontal impacts, 341 in lateral impacts and 6 in rear impacts. Of these restrained children, 30% have a maximum abbreviated injury score (MAIS) of 3 or above. The consideration of misuse remains a challenge and the knowledge continues to grow with the collection of further accident cases, experiences from field surveys and sled testing

An analysis for frontal impacts is carried out using the more recent CHILD and CASPER cases, considering 483 restrained children, 37% using the adult seat belt only and 63% in additional CRS. Injury severity levels by body region for each CRS type are examined. Head injuries are important to consider for all CRS types in frontal impacts but the relative importance decreases from rear facing CRS through to children using just the adult seat belt. Neck injuries feature in this dataset only for forward facing harness systems, especially at the AIS ≥ 3 level. Thoracic and abdominal injuries are present for all forward facing restraints but particularly for booster systems, followed by just using the adult seat belt. Likewise extremity injuries follow a similar pattern although upper extremity injuries fall away at the AIS ≥ 3 level. A relationship is observed between cases where misuse has been identified and higher rates of serious injury.

Similar analysis for lateral impacts is carried out, also using the combined CHILD and CASPER database, considering 148 restrained children, 35% using the adult seat belt only and 65% in additional CRS. When injuries are known, 46% have a MAIS ≥ 2 and 34% have a MAIS ≥ 3 . Struck side children have greater proportions of serious injury or fatality than non-struck side children. For these struck side children the rates of higher injury levels

are much higher when there is direct intrusion to the area in which they are seated. At over 300 mm of maximum intrusion, 68% of the 41 restrained children on the struck side are MAIS ≥ 2 , 44% are MAIS ≥ 4 or have fatal injuries. Injury severity levels by body region for each CRS type are examined. For struck side children the head is the most important body region for all restraint types. At the AIS ≥ 3 level thoracic and lower extremity injury also feature for all restraint types except lower extremity for rear facing CRS. For the non-struck side the number of injured children is low but a similar pattern to struck side children is evident with head, thoracic and lower extremity injuries.

Focussed accidents from other types (domestic, cyclists, pedestrians)

This kind of accident, often offers more simple configurations than car accidents. The aim was to collect some of them and to check that they can contribute to the validation of the models built in the CASPER project and to further develop injury risk functions, as the method chosen is the reproduction through physical or virtual reconstructions of loads sustained by children during real car accidents. The involved project partners looked for interesting paediatric domestic, pedestrian and cyclist accidents to reconstruct, with the aim of getting more information about injury mechanisms and injury risk functions.

The database contains 25 domestic accidents, 16 pedestrian cases and 6 cyclist accident cases. As there was no experience with the simulation with dummy models of domestic accident cases, a validation of the method was necessary. Selected cases involved children of approximately 3 years of age, which is the age that corresponded at that time of the project to the only validated LS-Dyna FE Q dummy model. The simulation results show that the head a3ms and HIC values do not correlate in the same way as observed from car occupant tests. The data points from the simulation do not help for the development of injury risk functions for the head. The possible reasons are that the loading conditions are different for analysed domestic and car occupant accidents or that the dummy model is not suitable for reconstruction of this kind of accident or that the dummy, and the associated dummy model, are not validated for this type of loading condition. In a next step, drop tests with the physical dummy and dummy model were executed and compared. This comparison showed that the results were comparable.

Domestic cases were used with human body FEM head and neck models, not to validate these cases but to use them in addition with road cases in order to derive some head tolerance limits to specific

head injuries observed. That means that they used developed head neck finite element models to reconstruct numerically domestic and road accident cases and to extract some mechanical parameters like intra-cerebral pressure, von mises stress, energy etc. in order to correlate these parameters with the observed injuries.

FIELD DATA COLLECTION

Activities in this area are all based on a common subject: the quality of CRS use. Two aspects were considered in the CASPER project, the first one focusing on sociological aspects of CRS use [4] in order to have a better understanding of parameters leading to situations not being the optimum in terms of protection of children, the second one on technical aspects of the restraint system use and misuse to see how could solutions be applied to enhance the situation [5]. These activities are completed by a dynamic testing program of misuse situations (described in the section Applications).

Report on social approach to child safety:

The CASPER approach was to use different sociological methodologies in order to rapidly get information about the way parents behave with their children during car travel and about their belief and knowledge regarding road safety. First a questionnaire was developed to gather data on demographics, travel patterns, CRS use, child position in the car, but also information regarding how parents perceive the way they secure their children, the way they drive, how they choose the systems and what kind of improvement they expect. This questionnaire, distributed on-line, collected 998 answers throughout Europe. The survey gives trends about parents' behaviour and beliefs concerning road child safety. This approach by a questionnaire was completed by the focus group method. It is a technique involving the use of in-depth group interviews to gather detailed data and to understand how people construct their reality. In addition to the classical methods used, an electronic survey on a larger scale has been undertaken. For this, the form used for the field data collection was modified and translated into 5 languages to be used for a large scale electronic survey in Europe. Results were analysed focusing on Italian and French data for which both types of survey were available. As a summary of results it can be said that people generally over-estimate their driving capacities and their ability to correctly use restraint systems. ISOFIX is not known by a large majority of parents and better information on the right moment to switch from one system to the next one is necessary. Globally parents also find that CRS are complicated to use and they may allow their children to use only the seatbelt for short journeys, or if traveling in somebody else's

car. Due to the co-operativeness and behaviour of the children in the car, 72% of parents answered that the presence of children can cause an accident. The focus group study insisted on the fact that external pressures such as time constraints can influence this behaviour of the parents. The focus group study also showed that though most of the parents answered in the survey that safety was a key factor, the comfort of the child was in fact paramount for the parents. CASPER has established a methodology to effectively conduct such focus groups regarding traveling with children. This approach could also be very efficiently completed by the observation of the real behaviour of parents in the everyday life through naturalistic studies.

Misuse studies

Misuse of child seats is still a widespread and serious problem. This is true for all three studied regions (Berlin, Lyon and Naples) even if there were also significant regional differences, for example, a very high rate of non-use cases in Naples compared to other places. The main problem with the use of CRS is the correct belt path of the vehicle belt and the general installation of the child seat in the vehicle. Both problems could be prevented by the use of ISOFIX. Field studies have shown that less than 4% of the CRS were fixed with ISOFIX in the vehicle. The market penetration of this system is extremely low considering that the vehicle fleet equipment of ISOFIX anchorages was around 50% in 2011. External factors, such as the available time and the trip purpose, have influence on the securing quality. Parents want to secure their child correctly, but there is still a great need for the simplification of the usability of child seats.

Results collected in Lyon during the CHILD and CASPER surveys were compared with the aim to estimate the evolution in CRS usage and misuse. No significant difference was found in terms of appropriate use: more than 80% of appropriate use according to the weight of the children, the rate of inappropriate use being mainly due to a change of CRS too early for the child with similar patterns in 2003 and 2011. The average rate of misuse found was about 65% in 2011 (71% in 2003) which confirms that many children are still incorrectly secured in cars. The main differences between the two surveys concern forward facing systems with harness: installations of the children in this CRS group were better in 2011 than in 2003 with a decrease of some serious misuse, such as incorrect harness use. Regarding booster seats, the most frequent misuse situations were the same in 2011 and 2003, with the lower belt guides often not used and the chest part of the seatbelt under the arm (instead of having it on the clavicle). Most of these

misuse situations could probably be reduced by giving better information on the safety effect of misuse to parents.

Collaboration between CASPER and the Safety Road Institute of Belgium (IBSR) has resulted in an additional data collection conducted in different areas of Belgium. It took place in September 2011, with a complete study of the restraint conditions for 1500 children. Results at a global level show the same tendencies as in the other studies: many children are not correctly restrained, the use of CRS decreases a lot for children older than 6 years, and too many parents are not aware that the situation is not correct. For the first time the number of ISOFIX systems was large enough to compare “classical attachment CRS” and “ISOFIX systems”. The use of ISOFIX is more common in big cities than in the countryside. The global rate of misuse with ISOFIX systems compared to the “classical” ones is 2.3 times lower. Considering only forward facing CRS with harness, the rate of misuse is nearly divided by 3 compared to the systems fixed by the seatbelt. The reduction of the proportion of misused systems is smaller but still visible on booster seats equipped with rigid ISOFIX anchorages compared to standard booster systems.

IMPROVEMENT AND DEVELOPMENT OF TOOLS

Initial investigations for hardware and numerical tools

Prior to any new development or improvement of the tools used for the evaluation of the performance of CRS, it was necessary to define the state of the art based on the knowledge from previous EC projects and to determine what were the priorities in terms of protection for children of different ages [6]. The objective of this work was to identify the various child injury mechanisms in frontal and lateral collisions and to determine the associated physical parameters, in order to provide injury risk curves or at least to recommend limits. Priorities are given in terms of injury mechanisms necessary to be reproduced in accident reconstructions and simulations both by child dummies, child dummy models and child human models. They are given for each dummy corresponding age and for the following body regions: head, neck, thorax and abdomen. As result of this analysis, a focus has been defined in the CASPER project on limits to be found on the head-neck segments for youngest children (6 weeks, 6 months, 1 year and 3 years) and on the abdomen and thorax for older children (3 and 6 years). Consequently, injury criteria are needed on these areas and corresponding injury mechanisms are integrated in the specification of child models.

Dummy improvements

Following the analysis of relevant injuries, it was found necessary to identify the shortcomings of the dummies then a prioritization was made and an estimation of the necessary work on the different items. Works were then focussed on the 3 main priorities [7,8]:

Abdomen sensor system The objective was to progress on the development of an abdominal sensor system that could be used to assess the risk of abdominal injury for the Q dummies. Of the three available solutions, one was selected by the project partners based on availability, forecasted acceptability and cost, and likelihood to be able to solve the identified shortcomings of these systems. The Abdominal Pressure Twin Sensors (APTS), originally developed and prototyped within the CHILD project were selected and further development work towards an industrialization of the sensor was conducted. The new work conducted in CASPER includes the characterization of the APTS in multiple loading scenarios, and the development of possible solutions to solve a number of shortcomings that were identified. Finite Element models of the sensors that were developed outside of the CASPER project were also used to support the sensor development phase. Candidate injury criteria were then evaluated based on the results from 17 accident reconstructions involving 19 instrumented dummies restrained by a three point belt. Injury risk curves were built for maximum pressure and pressure rate based criteria. The confidence intervals were found to be sensitive to the scaling approach, especially since injury and non-injury points were almost without overlap. Further work on the improvement of the risk curves is needed. It could include a study of the scaling assumptions between dummies and the addition of points based on further testing or comparison with PMHS data. Other perspectives include the quantification of the repeatability and reproducibility of the system, and the definition of in-dummy calibration procedures. The sensors were also implanted in the Q10 dummy and additional Q3 testing with shields and harness systems were performed.

Evaluation of the lumbar spine stiffness The stiffness of the lumbar spine is one of the parameters influencing the rotation of the pelvis under the lap strap and its subsequent penetration into the abdominal cavity. Physicians and physiotherapists think that the lumbar stiffness is too high. It is interesting to note that the lumbar spine stiffness is much lower in the P series than in the Q series. Overall, the spine stiffness (lumbar and thoracic) could affect the kinematics. Tests were performed on the Q3 dummy to evaluate its lumbar spine stiffness in flexion. The stiffness was

found to be similar to the stiffness of the HIII 3 Y.O. dummy. In the absence of better biomechanical reference, it was decided to take no further action on this issue and focus on the gap at the groin.

Auxiliary equipment for Q dummies to improve belt interaction response Several proposals were made to reduce the risk for the belt to lock itself into the gap at the groin of the Q3. Two proposals were selected for the current task: creation of a soft abdominal insert to fill the gap made of silicon, and reinforcement of the dummy suit realised with additional patches to be positioned as a prototype solution. Two prototypes were built. The prototypes can be used independently or together. These solutions are relatively generic and could be adapted to the Q6 or the Q10 if needed. An evaluation of the prototypes in sled tests was performed. It confirmed the interest of the solution to prevent the penetration of the belt in the gap at the groin. While it is believed that the gap issue should be tackled for the dummy used in future regulation, it must however be noted that even in the case of a successful and complete evaluation, more work will be needed to transform the prototypes into an industrial solution. It should be noted that ultimately, the influence of any dummy modifications proposed in this report should be investigated for repeatability and reproducibility. However, this is beyond the scope of the current task.

SIMULATION TOOLS

LS-DYNA dummy models

In order to complete the Q-dummy FE model family Q, Q1,5 and Q6 dummy models were generated on the basis of the Q series physical dummies using information from the existing Q3 dummy model (e.g., material data) [9,10]. Component level and full dummy level's validations were performed to evaluate the FE model performance. The test conditions assumed are standard dummy certification tests. Compared with these physical test data generated, the model responses are satisfactory. For future model updates it is suggested to validate the performance in conditions that are closer to real crash configurations. Sled test data generated in CASPER might be used for this purpose if models of the sled set-up, including seats, are available. Prior to the development of the CASPER Q dummy models, model quality requirements were discussed at the beginning of the project with experts from the industry. It was decided to include in the development of the models suggestions from these discussions. The model has to be representative of the latest hardware level, and include correct implementation geometry, mass, inertia and

material properties. The model has to be able to give response similar to the dummy sensors, and the required time step is approximately 1 microsecond without mass scaling. Once developed, it has to go through a detailed report of validation process based on dummy certification tests and simplified loading tests representing relevant loading conditions. In addition the modelling of a Q10 model was started.

Q1 and Q1.5 FEM The Q1 and Q1.5 models were created on the basis of the physical Q1 Dummy Rev B Dec 2008 and the physical Q1.5 dummy Rev B July 2009. The Q1 model was developed first and the Q1.5 was obtained by scaling and local remeshing from Q1. For both sizes a Beta V1.0 release model has been prepared. The model has been used by project partners in virtual testing procedures. More validation works are needed to improve the performance of the models and bring them to a tool usable by the industry.

Q6 dummy model The Q6 model was created on the basis of the physical Q6 Dummy Rev A Dec 2008. All the requirements were considered when developing the models as far as possible. On the simplified loading conditions it has to be remarked that no test data were available for the Q dummies. As CASPER did not have the budgets for generating such data this recommendation could not be fulfilled and validation is done only on the certification tests. It should be noted that they do include full scale dummy tests, assuming impacts on the thorax. A Beta V1.0 release model has been prepared. The model has been used for the determination of accident reconstruction scenarios prior to perform a physical test with dummy. It has also been used in the validation of side impact test procedure in combination with models of generic CRS and using the virtual test environment developed in CASPER.

Q10 modelling works At the end of the CASPER project, Q10 prototypes were recently delivered by the EU EPOCH project and the first Q10 CAD data were made available. During the 2 month extension of the project, works was initiated in CASPER with the aim to complete the Q dummy family. The development of the model of the Q10 mesh and assembly was started. This work has been based on the prototype version of the dummy, and characteristics used for this work are based on the Q6 material.

At the end, the following parts of Q10 models have been meshed and assembled: head, neck, neck shield, shoulder, chest, lumbar spine, chest deflection sensor (IR-TRACC) in frontal and lateral, upper and lower arms and upper and lower legs. The pelvis abdomen area was not meshed

during the CASPER project as last minute hardware changes did not allow sufficient time for completion. However, this work will be finished outside of the frame of the CASPER project. Then the model validation can be started with the first component tests such as certification tests are available. This work can only be finalized once the dummy becomes an industrial version.

Human body modelling

The development of finite element models (FEM) of children was one of the aims of the CASPER project. Such models can be used as complementary tools to dummies in order to simulate the response of a child subjected to impact loading. One possible application for such models is the development of model based injury criteria and tolerance values by simulating the child response in accident configurations. It is similar in principle to the work performed using dummies and accident reconstructions in the CASPER project. The Consortium decided to focus on the models of the head-neck for youngest children (6 weeks, and 6 months, 1 year and 3 years) and on the abdomen and thorax for older children (3 and 6 years). Partners from different institutes were developing models of body segments that have to be merged to have complete human body models of different sizes. It was necessary to proceed step by step in order to ensure that all parts would be compatible, that the interface between parts would allow them to be meshed and that in the end different full body models would be able to be run. Once the size of the mathematical models for each body segment in terms of the anatomical structures have been defined, detailed anatomical [11] and mechanical properties [12] for development of the specified mathematical models were investigated.

Child geometry for modelling purposes This task aims to provide essential information related to children for external data but also for data on the geometry of bones and internal organs. Data were collected both from literature and by collecting missing data. The external geometry of 71 children have been measured and 29 anthropometric dimensions were taken for each leading to a total of more than 2800 measurements. This work is based on a measurement survey which allowed acquiring anthropometric data in two approaches: classical (sitting and standing measurements) and in a car, with different restraint systems. These data can be used to develop the corresponding numerical child body model. In particular, they could be used to develop the 6 years old numerical model using scaling technique. Results from this work could be considered for improvement of test procedures, dummies (and associated models), cars and CRS designs. Internal geometrical data of different ages were obtained from whole body CT scans. From

anonym medical images of two subjects, the 3D geometry of the skin, bones, and the main soft organs has been reconstructed and transmitted to other CASPER partners in order to develop the corresponding numerical model.

Report on child mechanical parameters The objective was to provide data on the mechanical properties of children and validation data contributing to the development of specific human segments and whole body models per age. An in-depth literature review has been performed and reported. Even if it is obvious that lots of data are missing, no experimental work on this item has been conducted in the CASPER project. Scaling methods have been used as far as possible to fill the lack of data. Starting points for a mechanical definition as well as sources of experimental data for validation of the segment model and human body models were listed. Mechanical properties for child body segments at different ages have been synthesized from the literature. It can be concluded that there is a lack of data and that biomechanical researches to characterize the child human body have to be strongly encouraged. It can also be stated that the data that exist has been helpful to proceed to a first generation of children body models for safety research purposes.

Finite Element Models (FEM) of children

The objective was first to set child segment models based on the geometrical and mechanical properties for each child age under consideration. So partners have shared the work and body segments to be developed were head, neck, thorax, abdomen and lower legs. The coupling of the segment models has been organised as well by attributing to each institution a specific coupling issue. Finally the methodology for accident simulation has been set.

Mainly due to the late arrival of the complete bodies of child human models, and to their levels of validation, it has not been possible to propose numerical injury limits using complete child models on the different body segments to be protected per age groups as first planned. So partners have essentially worked with the body segments they have developed in order first to improve the response of the models and validate them against different scenarios. Loadings similar to the one of real accidents were used and applied on a model of a given body segment (head, abdomen, etc.). This allowed to show the sensitivity of the different parts of the child human body models to loading conditions and for some of them give an overview of what injury criteria could be achievable in future works. Some positioning tools for models have been developed in the project.

6 week old human model For this child's age, it was proposed to limit the development of FEM to the meshing of the head neck system of the six week old child (6 W.O.C.) [13]. The model developed in this project includes the main anatomical features of a newborn head. Concerning the neck, a simplified model was developed just to reproduce a global behaviour of this structure and to allow a good kinematics of the head. The developed 6 W.O.C. finite element head-neck model was based on the geometrical 3D reconstruction of slices obtained by CT scanners.

6 month old human model As for the 6 week old FEM, it was decided to focus on head and neck only for the development of a 6 month old child FEM (6 M.O.C.) [14]. The new finite element head model simulates closely the main anatomical features: skull, sutures, fontanel, falx, tentorium, subarachnoid space, scalp, cerebrum, cerebellum and brainstem. The neck model integrates the first thoracic vertebra, the seven cervical vertebrae, intervertebral discs and the upper and lower ligament system.

1 year old human model Body segments constituting this 1 year old child FEM have been developed separately by different partners and meshed after validation of the different parts. The starting point of the 1 Y.O.C. model is the DICOM data coming from an 11months 21 days old child. [14]. The new finite element head model simulates closely the main anatomical features: skull, falx, tentorium, subarachnoid space, scalp, cerebrum, cerebellum and brainstem. Based on a scan of a 1 YOC, the surfaces of each of the cervical vertebrae were reconstructed. The cervical vertebrae were modelled using shell elements, the intervertebral discs with brick elements and the ligaments with spring elements. The FE model of the 1 YOC upper and lower bodies was developed following the anatomical image as stated in the general description of this model. It includes a complete skeleton of the chest rib cage, the spine, and other bones such as humerus, ulna, radius, clavicle, pelvis, femurs, tibias, fibulas, foot bones. The main anatomical features of soft tissues and internal organs were represented with certain simplifications, especially for internal organs. The validity of the thorax model was evaluated by simulation of thorax frontal impact. Response of the thorax model is rather stiff, and there is needs for adjustments of soft tissue material properties. Meshing works have been conducted in order to obtain a complete body of 1YOC FEM. The developed model of the whole 1YOC body totals 99,168 elements, and the node number is 110,753. Mechanical properties have been implemented and complete body validations were initiated, to first check the robustness of the model. When possible,

real world accident cases physically reconstructed were used as input for the model for further validation.

3 year old human model As for the 1 YOC FEM, body segments of the 3 year old child FEM have been developed by different partners in the aim of merging them to obtain a complete body 3YOC FEM after the validation of the different parts. The starting point of this model is the geometry coming from DICOM data of a 3.25 years old child [15]. The complete model is composed about 170 000 elements. Concerning the 3 YOC head-neck FEM, 21 accident cases have been reconstructed (13 domestic accidents and 8 road accidents). For all reconstructed accidents global parameters have been calculated like HIC (using a dummy head FEM) and specific parameters like brain Von mises strain stress, pressure. Focussing on road accident cases reconstructed, the same conclusions can be done which can demonstrate the usefulness of finite element model to extract more specific mechanical parameters. The neck model integrates the first thoracic vertebra, the seven cervical vertebrae, intervertebral discs and the upper and lower ligament system. A detailed thorax and abdomen including lungs, kidneys, spleen, heart, liver, abdominal area, combined muscle, inner soft tissue, ribcage and thoracic vertebrae have been modelled. To define injury criteria for the abdominal area of the 3 year old child, the approach chosen was to compare the numerical dummy loads, measured in accident reconstruction cases taken from the CASPER database with the loads on the 3 YOC model. The correlating injuries occurred in the real accident would therefore be the basis for the injury criteria definition. The simulations with 3YOC model should show that the model is capable of estimating the abdominal injury risk. For the reconstruction with the 3yoc model, appropriate cases were chosen from the CASPER database with loads measured with the APTS and MFS systems. An attempt was undertaken to compare these both readings with the conclusion that no valid comparison is possible due to the complete different load sensing principles. The lower limbs model includes, femur, tibia, fibula, foot, pelvis, ligament system and flesh. After the validation work, the model has been coupled to the Head/Neck and to the Pelvis model. Simulation and validation work for the combined model were limited due to the late delivery of the body segments by the partners.

6 year old human model The objective was to develop a six years old child finite element model developed in this project in terms of meshing segment per segment [16]. The boundaries of the model (near the neck and the lower extremity) were

shared with the groups working on the neighbouring models. For simulation and validation work that purpose, the neighbouring segments have been simplified. The validation of the 6 YOC FEM has only been performed on the different body segments using simplified neighbouring body segments when a full body setup is needed for the simulation. No simulation test has been performed in the frame of the CASPER project with a 6 YOC fully FE complete body model. The development of a 6 Y.O.C has been done by scaling down existing adult FE head-neck model. With the 6 YOC head-neck FEM 15 accident cases have been reconstructed, 3 domestic accidents and 12 road accidents. The neck model integrates the first thoracic vertebra, the seven cervical vertebrae, intervertebral discs and the upper and lower ligament system and has been established by scaling down the adult neck model developed previously. A finite element model of the abdomen and thorax of the 6 Y.O.C. was developed for the current project. It includes skeletal structures and major organs meshed using surface or solid elements. Its geometry was developed based on a combination of CT-scan data, average literature data and positioning data from a previous study. In particular, the spine was modified to account for the seated posture. Using material parameters from the literature, the model was run against 6 validation setups. These setups correspond to published datasets collected in two recent studies using child PMHS, and one study based on porcine testing. The setups include loading to the thorax and abdomen using various belts and one impactor. After adjustment of some of the material properties, the model was found able to approximate all test responses. A finite element model of the lower limbs of a 6 YOC was developed; It includes all bones, muscles and skin. Hip, knee, and ankle are modelled with the help of 6 DOF mathematical joints.

Multi-body full body human models (MBM)

Multi-body human models are simpler to create and to use than the FEM. Their robustness is easier to achieve and the time needed to run a simulation is far lower than with FEM. For this reason it seemed interesting to develop child human MBM. The automotive industry can use such tools for a first validation of scenarios. Then FEM and physical tests can be useful to validate a chosen option, but the number of these tests can significantly be reduced by first using MBM.

2 sizes of MBM have been created in CASPER using for each similar techniques: a 6 Week old [13] and a 6 month old children [14]. As base model for the baby model the TNO's facet 50th percentile human occupant model was used and scaled down towards baby dimensions using the

MADYMO/Scaler. Since scaling from adult to children is not straightforward, a literature survey was performed to the mechanical properties (stiffness or force-displacement curves) and injury criteria for the body segments that are most vulnerable for babies in a car crash. Next, validation data were sought in order to validate the model's responses to impact. And finally, the robustness of the model was checked by performing simulations with the baby model in a group 0 seat. It was concluded that 2 robust and calculation time efficient baby models have been created. Mechanical properties and injury limits of the head, neck and thorax of babies between 0 and 3 months old are available. However, validation data of babies of this age are very limited. Scaling of validation tests of other age children would be needed to extensively validate this baby model.

APPLICATIONS

Test procedures

Within the CASPER project existing test procedures were reviewed with respect to their relevance and ability for improving safety taking into account accident data [17]. For frontal impact it was concluded that the test set-up as defined for the new European Regulation UN-ECE R129 sufficiently reflects the passive safety needs to maintain high levels of occupant protection. However, future activities should analyse modification of the seat cushion angle for booster type CRS. While the chosen seat cushion angle reflects average car conditions it might be worthwhile for booster type CRS to take into account worst case conditions which is expected to be more flat.

For rear impact no modifications are proposed as the current standard seems to offer appropriate safety performance. Regarding roll-over it is proposed to add an additional requirement for the head displacement. While the current criteria is just analysing the relative head displacement during roll it seems relevant to apply the same absolute limit as done for frontal impact regarding the head excursion limit in Z direction above CR point. It is proposed that a new threshold for maximum head excursion for all impact types should be negotiated between CRS and car manufacturers.

Finally CASPER supported the GRSP Informal Group on CRS while developing and validating a new side impact test procedure. This test procedure consists of a flat intruding panel and an accelerated test bench. Within the CASPER consortium two deceleration sled facilities and one acceleration sled facility were used to implement the test procedure. The new test procedure is sufficiently repeatable and reproducible. In addition it is adequately

challenging for products being on the market today, especially regarding dummy readings for the smallest dummy of the CRS age group and head containment for the largest dummy of the CRS age group. Especially the validation of the side impact test procedure was supported by simulations in addition to the testing. Furthermore the new frontal and lateral impact test procedures of the new ECE Regulation were implemented as FE models.

Injury risk functions for dummy approach

Test procedures can be fully efficient only if some injury criteria are available. Once the CASPER accident reconstruction database was developed, available data from previous accident reconstruction programmes were imported. Quality checks for the input data were performed and when necessary, corrections took place. Then, 36 new full-scale reconstructions and 2 sled tests performed in the CASPER project were regularly uploaded. 70 datasets of dummy readings are available for frontal impact, distributed across all dummy sizes, and 23 for lateral impact with very few cases for small dummies, as the focus was made on Q3 and Q6. First draft of injury risk curves for Q dummies for frontal impact were presented in 2007 based on the results of the CHILD project. However, the risk curves for the neck were based on scaling of adult data. In addition risk curves for the abdomen and chest were missing. Based on accident reconstructions from the CREST, CHILD and CASPER projects, injury severity levels were paired with dummy reading results [18]. For the head in frontal impact conditions, reliable numbers of data points are available to derive injury risk curve with a high confidence using the survival method. For the neck in frontal impact conditions a trend for Q1 and Q1.5 dummies can be observed that scaled data from adult seems to describe the injury risk quite well. For the chest neither resultant acceleration nor the chest deflection seem to be injury risk predictive. For the chest compression this is likely caused by belt interaction problems of the Q dummies for 3-point belts and/or issues in the test with respect to the use of the chest compression sensor (e.g., wrong installation, wrong treatment of data).. The further developed APTS abdominal sensor shows good prediction of injury risk although the number of cases is still low. For lateral impact only an injury risk curve for head a3ms was derived. For the other body regions the number of cases with injuries is too low.

It is important to state that the developed injury risk limits are based on comparing Q dummy readings with injury severity and are therefore only applicable for Q dummies. However, the advantage

of this approach is that no scaling between human and dummy is necessary because the curves were already derived using the tools they should be applied to.

The table below shows the proposed CASPER injury criteria. It has to be noticed that for the head injury limit, the value available was only applicable in case of head contact which is not the case with the new proposed one as it is based on injury cases that were almost equally distributed amongst contact and non-contact cases. The neck load limits

proposed by EEVC were based on the scaling of adult data, with the CASPER data it is possible to confirm the scaled data at least for Q1 and Q1.5. For Q3 and Q6 it is recommended to define limits based on the state of the art CRS performance in order not to allow worsening of the situation compared to today.

	Head a3ms	HIC	Neck FZ	Neck MY	Chest a3ms	Chest deflect.	Abdomen	Head lateral a3ms
Reference Dummy	Q3	Q3	Q1	Q1	Q3	Q3	Q3	Q3
Unit	g	-	kN	Nm	g	mm	bar	G
CASPER 20% risk	75	NR*	1 (no injuries below)	No sufficient data	NR* but necessity of limit for chest	No sufficient data	0.9	55
CASPER 50% risk	120	NR*	1.3 (only AIS 3+ above)	No sufficient data	NR* but necessity of limit for chest	No sufficient data	1.3	85

* NR= Not recommended

Chest measurements remain an issue: biomechanically, a chest deflection based metrics is considered to deliver correlation with injury risks but the reconstruction results to date do not allow the collection of usable deflection data with confidence. Except for the head in frontal impact conditions the risk curves still suffer from a lack of data points. That means that further research is necessary to improve the confidence. This is particularly true for lateral impact.

Development of relevant parts for virtual test procedures

Virtual modelling and testing will become more and more important for child safety development. Therefore all relevant parts for virtual frontal and lateral test procedures were developed in the CASPER project [17].

Virtual test procedure The virtual test procedure consists of separate parts. Therefore the parts for the simulation are also included in separate files. The benefit of this approach is that the main simulation file is easier to use. Changes in the separate files can be made simple; the files can

be easily exchanged and also be used for other simulations. The specific included files are the test bench, the belt anchorage, the ISOFIX anchorage, the sled belt system, the sled pulse, the Q dummy models, the CRS models and the impactor shape used for side impact. They can be easily included or excluded in the main file to analyse differences or to change between frontal and lateral impact. During the CASPER project the parts for the sled test environment were configured and now are available in the LS-Dyna code. First analyses with frontal, lateral and 30 degrees impact showed that they are useable. Also the comparisons between experimental and virtual test results under different test conditions are acceptable. Problems with the simulation stability mostly occur from solid material definitions in the dummy or CRS which are deformed too much under high severity impact conditions. Important for good virtual test results are well validated models, especially the dummy and CRS parts.

Models of CRS 3 sizes of generic models of CRS have been created in order to validate the different sizes of dummy and human models developed in the CASPER project: Group 0+, Group 1 and Group 2/3. All of them went through a validation

process in combination with virtual test environment models. For each CRS the separate parts were meshed and assembled together and defined with basic materials. The basic seat parts such as cushion, backrest, head rest and covers were defined as elastic material. Sets with moveable parts are pre-defined to make a simple transformation and/or rotation possible, for example for the backrest and headrest adjustment. The dummy model is defined in the release posture and had to be positioned in the CRS model. The internal dummy positioning definition allows a simple positioning with a pre-processor. Similar to the dummy positioning via pre-simulations another pre-simulation is necessary for belt positioning.

Misuse test program

The performance of a CRS is strictly influenced by the quality of its use. During the CASPER project misuse of CRS has been observed in the field and tested dynamically, in order to evaluate the effect of these misuses on the protection of children. The study of the influence of 3 different types of misuse has been undertaken in CASPER: use of CRS not in accordance with the user manual instructions, dummy postural changes, and appropriateness of the restraint system. Each situation always being compared to results obtained in similar test conditions with a correctly used appropriate restraint system. The experience in CASPER has also shown the difficulties in running comparable field studies in different locations: it is necessary to define clear parameters for the assessment of misuse severity [5]. All subjective influences should be excluded as much as possible. It has to be remembered that results are only applicable to the tested configurations (CRS, dummy, type and severity of impact), but global tendencies can be outlined:

Dummy behaviour: dummies are not able to measure the full range of injury risks (e.g. effect of having the seatbelt twisted for children using a booster seat, excessive slack in harness, etc.).

Dummy instrumentation: in many cases, differentiating events using standard dummy readings is not an easy task. Films are helpful to see differences in global kinematics. Abdominal sensors are also good predictors to prevent injuries in this area. For the moment these sensors are not part of the standard equipment of Q series dummies but are at an advanced stage of prototypes.

Inappropriate use: The use of inappropriate CRS for children too young can lead to the ejection of the upper part (escape at the level of shoulders) or of the complete body from the CRS that can lead to serious injuries. This statement is mainly based on films combined with the knowledge that children

and child dummies behave differently in these conditions due to a difference of shoulder rigidity. When used with a larger dummy than it has been designed for, a CRS can show additional injury risks because of a higher head excursion (risk of head impact with vehicle interior), additionally there can be a risk of CRS structural integrity issues due to the overloading (depending on the CRS characteristics, only high quality products were tested in this series) leading to the risk of projection or ejection of the child and the CRS together. Tests conducted with a Q6 without CRS led to a dramatic increase in the abdominal pressure with a high risk of submarining compared to the same test performed with a CRS.

Wrong use of practical functionalities: can lead to misuse for which the effect varies from no visible effect to the total destruction of the CRS. The non-use of ISOFIX connectors on a booster seat does not decrease the level of protection considering dummy readings. On shell systems, misuse of ISOFIX connection or anti-rotation device lead to a higher global excursion and therefore a higher risk of impact of the child with the vehicle interior. In some cases, failure of the CRS base has been observed. It is important to remember that if tested CRS had been of a lower quality some integrity issues may have occurred.

Postural effect: when the child dummies are positioned in more relaxed (and more realistic) postures, the risk of sustaining serious injuries is higher for the head and for the abdomen. Some head impacts and seatbelt penetrations into the abdominal areas have been observed on films and dummy readings. In some postures, only the film is able to indicate that the dummy behaved differently than in the reference tests.

Wrong seatbelt route on boosters: is a critical misuse that leads to not restraining the upper part of the child dummy or to strong forces applied onto the lower rib cage and abdominal areas. When combined with postural situations, these misuse situations become even more critical for the safety of the considered children.

Possible solutions for CRS in terms of use

The purpose of this report [19] is to provide applications and research results for the improvement of child protection systems. As well as considering the effect any CRS improvements would have on policies or any legislation that would need to be created or improved. The issue of cost and subsidies for child restraints is considered. Research on the effectiveness of interventions is reported and recommendations on future policies are made.

Results from the sociological survey carried out as part of the CASPER project proved to be an extremely valuable resource, as many of the proposed solutions are based on information gathered in the survey. Recent statistics show that a large percentage of CRS are misused, this project aims to reduce this figure by implementing innovative designs and creating new legislation. To list some of the ways CRS are being misused: they are being incorrectly installed i.e. putting a rearward facing device in a forward facing position or incorrectly fastening the seatbelt to the device. Parents play a key role in child safety and this is researched in great depth within this project. Research was carried out in two ways: preventing these types of CRS misuse as well as researching other problems with CRS such as transporting children with disabilities. The proposed solutions are presented alongside any issues that might occur. One of the key areas of CRS improvement is Car-to-CRS communication, this ties in with integrated CRS as the idea is to make CRS fully homologated for the car. ISOFIX involves having anchors built into the car which CRS can fix onto. The next step is to develop Car-to-CRS communication so that the CRS can benefit from the cars safety features. Car manufacturers can also build CRS directly into the car creating integrated CRS which are also considered in this document.

At the moment CRS are predominantly used in cars, however they could also be used in aeroplanes, trains and buses. Results would have then to be optimised for each of the different situations. During this project the CASPER consortium investigated and evaluated the systems which are currently available or currently being developed. This was done by analysing the demands and applications in terms of research, development and approval of CRS for child protection.

Communication

It is very important to communicate to children that the correct use of the seatbelt is crucial for their safety and that it has to be combined with the use of a booster seat until their size is close to the one of adults. Messages for parents should start with the fact that children always need to be restrained while travelling in cars. The choice of an appropriate CRS, its installation in the vehicle and the correct seatbelt route for children on boosters are essential requirements to guarantee the highest level protection for children. Some systems are easier to use than others, equipped with indicators telling if installation and adjustments of different parts are correct (such as ISOFIX). Of course, they still require a minimum of attention to be correctly installed and it's important to check their

compatibility with the vehicles in use before purchasing them.

Dummy and human models: accident simulation methodology

The objective was to use virtual reconstructions of real road traffic accidents as well as domestic accidents in order to calculate mechanical parameters for some relevant segments and to correlate these parameters with observed injuries. The methodology is applicable to investigate various injury mechanisms of child body segments, including the head, neck, thorax and abdominal injuries in different restraints, loading conditions, various age and size of children. The validity of the child segment models was expected to be evaluated by using available experimental data and accident data. Concerning road accidents reconstruction methodology with whole human body models, guidelines are provided for MBM of children.

For FEM child models, methodologies to define criteria for different body segments have been proposed, based on road accident case replications (loading conditions based on measurement from child dummy crash test were used to assess FEM and injury related parameters can be calculated from simulations) or on domestic accidents (fall cases simulation). Finally guidelines for whole body model reconstructions have been proposed in case of road accident reconstructions.

Numerical and experimental injury criteria

Modelling children is not an easy task. Firstly, there is little data on the mechanical properties of the different anatomical structures for evident ethical reasons, which poses a real biofidelity problem for FEM. Furthermore, there is no available validation to date for the different body segment models and different children's ages. One of the only ways to overcome this lack of data is through the reconstruction of a large number of accidents. During the CASPER project some accidents were collected both domestic and road accidents per age. But even with a consequent effort of partners, the number of physical reconstructions is still too low to establish clear tolerance limits to specific injury mechanisms for all ages and all body segments. However several mechanical parameters were extracted from these finite element models, with the aim of identifying the mean criterion able to predict, for example, loss of consciousness and bone fractures.

The report "Synthesis on numerical and experimental injury criteria" [20] reports mechanical properties used and validations per segment and per age as used to determine as a first attempt injury criteria by reconstructing

numerically with the developed finite element models selected accidents (domestic and road accident cases).

Three focused analyses are proposed. The first concerns the 1YOC finite element model. It presents mechanical properties implemented under Ls-dyna code as well as road and domestic accident reconstructions results in order to establish some tolerance limits to specific head injury criteria. Then validation of the thorax, abdomen and lower limb are presented separately. Work undertaken with the complete meshed model are also presented in this report. The second part of this document aims to describe 3YOC FEM. It shows the validation performed on isolated body segments by partners. The last part focuses on the 6YOC FEM mechanical properties, validations and first attempt to tolerance limits. It ends with the presentation of the coupling of all segments that should lead to a whole 6YOC FEM.

CONCLUSION

The growing demand for greater mobility in Europe has made individual transportation an essential feature of modern living. Children are more and more often transported in cars, even daily from home to school, and so the risk of becoming involved in an accident has consequently increased. Consequently, there is a big interest to encourage the deployment of innovative technologies that should lead to the introduction of safer products on the market. All available strategies should be applied in order to reduce the number of injured and killed children on the roads.

Thanks to increased knowledge in the field of injury mechanisms, the development of new designs for more efficient restraint systems and a better ease of use will become a high priority for the car and CRS manufacturers.

The CASPER project has defined the priorities to enable progress in this field of child occupant protection. The prevention of injuries resulting in a major permanent disability has important social implications, and more for children, but more generally the reduction of injury severity is correlated with lower cost of medical care and hence a lower social cost of accidents. CASPER is contributing to better protection of children by enhancing the development of designs, methods, tests, and tools that will reduce the risk of injuries. It was clear since the beginning of the project that CRS manufacturers and organisations such as ISO, IHRA, EEVC and all standards organisations were waiting for this information. With expectations being rather large it has been necessary to cover a lot of subjects. Globally, significant progress has been made during the CASPER project and most of the new knowledge acquired has already been

taken on board by the relative working groups. The establishing of an International working group for the revision of the standards for CRS approval has been a very good opportunity to have results from research projects integrated as soon as validated in the new proposals. The rather long process of improvement of the situation by the presence on the market of new protective devices has been shortened due to the rapid availability of results. The first CRSs answering all the new requirements could be already on the market only one year after the end of the project. Of course it will take time before these CRS represent a large proportion of CRS sales but having them developed and available is the first and necessary step for the improvement of the situation. This new generation of CRS will also improve the rate of correct use of systems as one of the requirements is to make them easier to install with clear indications of the correct use on the systems themselves. In parallel, requirements for the car manufacturers have also been introduced in the concept of these new CRS in order to ensure a better compatibility between CRS and vehicles.

This project has contributed to the harmonisation of passive safety research on child safety worldwide, and it has underlined that some of the issues such as abdominal injuries could be addressed. The methodology to do so is not only applicable in Europe, even if adaptations of the sensor to other dummies could be required. The harmonisation of the research methods and tools would enable the comparison of the situation in the different areas of the World. Effectively, it is well understood in developed countries that children when travelling in cars have to be restrained and how it has to be done. What is necessary here is to enhance the safety culture of parents so they do things in a better way. But what is also important (more important in terms of potential number of children to be saved) is to spread child safety worldwide and particularly in the emerging economies where motorization is growing at the greatest rate. This could also improve the cost effectiveness of regulations because the necessity for the car industry to comply with different regulations in various countries, as it is the case often now, can be avoided.

The short-term exploitation of the outputs of CASPER has to be communication and educational programs. It should be implemented by the application of methodologies and procedures for the development of improved child restraint systems, providing better protection for children in cars. In the medium and long term, the number of children killed or injured in cars should be considerably reduced if both communication/education and improvement of systems are conducted in parallel, so parents will

learn what is important to do while the CRS and car manufacturers will improve their restraint systems quality and compatibility.

ACKNOWLEDGMENTS

The paper is written on behalf of the members of the CASPER project. The CASPER project is co-funded by the European Commission under the 7th Framework Programme (Grant Agreement no. 218564). The members of the CASPER consortium are: GIE RE PR - PSA/RENAULT, Technische Universität Berlin, Université de Strasbourg, APPLUS IDIADA Automotive SA, IFSTTAR, Loughborough University (UK), FIAT Group Automobiles Spa, Medizinische Hochschule Hannover, Chalmers tekniska högskola AB, Bundesanstalt für Straßenwesen, TNO, Verein für Fahrzeugsicherheit Berlin e.V., Ludwigs Maximilian Universität, Centre Européen d'Etudes de Sécurité et d'Analyse des Risques, Humanetics Europe GmbH. Further information is available at the CASPER web site www.childincarsafety.eu.

UK Loughborough cases, collected during the EC CREST/CHILD projects, include accident data from the United Kingdom Co-operative Crash Injury Study, collected up to 2006. CCIS was managed by TRL Ltd on behalf of the Department for Transport (Transport Technology and Standards Division) who funded the project with Autoliv, Ford Motor Company, Nissan Motor Europe and Toyota Motor Europe. The data were collected by teams from the Birmingham Automotive Safety Centre of the University of Birmingham, the Vehicle Safety Research Centre at Loughborough University, and the Vehicle & Operator Services Agency of the Department for Transport. The views expressed in this work are those of the authors and not necessarily those of the UK CCIS sponsors.

Data on the CRS-to-car interface was provided by CSC Car Safety Consulting UG in Berlin based on car assessment of current cars and old cars, mainly offering ISOFIX.

REFERENCES

- [1] CASPER deliverable - D3.2.1
- [2] CASPER deliverable - D3.2.3
- [3] CASPER deliverable - D3.3.1
- [4] CASPER deliverable - D3.1.1
- [5] CASPER deliverable - D3.1.2
- [6] CASPER deliverable - D2.1.1
- [7] Abdominal Pressure Twin Sensors for the Q dummies: from Q3 to Q10 - P. Beillas & al. – ICRASH conference 2012 - Milano, I
- [8] CASPER deliverable - D1.2
- [9] CASPER mid-term workshop - presentation „CASPER_10_Dummy_Modelling“ – Johannsen & al – 2010, Munich
- [10] CASPER final workshop - presentation „Overview of CASPER dummy models“ – Lehmann & al – 2012, Berlin
- [11] CASPER deliverable - D2.2.1
- [12] CASPER deliverable - D2.2.2
- [13] CASPER final workshop - presentation „TNO 6w and 6m old child human body model“ – Rodarius & al – 2012, Berlin
- [14] CASPER deliverable - D2.3.2
- [15] CASPER deliverable - D2.3.3
- [16] CASPER deliverable - D2.3.4
- [17] CASPER deliverable - D4.1
- [18] CASPER deliverable – D1.6
- [19] CASPER deliverable - D4.6
- [20] CASPER deliverable - D2.5.5

All public deliverables and presentations from mid-term and final workshops are available on the CASPER project website www.casper-project.eu